

**Source Contributions to Atmospheric Organic Compound  
Concentrations: Emissions Measurements and Model Predictions**

Thesis by  
James Jay Schauer

In Partial Fulfillment of the Requirements  
for the Degree of  
Doctor of Philosophy

California Institute of Technology  
Pasadena, California

1998  
(Submitted March 12, 1998)

© 1998

James Jay Schauer

All rights reserved

to Diane

## Acknowledgments

I would like to first thank my advisor, Professor Glen R. Cass, for giving me the opportunity to undertake such a challenging and rewarding research project. Glen's continued enthusiasm for research and his insight into virtually all aspects of air pollution has made a significant impact on me over the past few years.

I also wish to thank Professor Bernd R. T. Simoneit for sharing his insight and experience with analytical organic chemistry, fundamental interpretation of mass spectra, and the use of molecular markers as tracers in the environment. In addition, I would like to acknowledge the other members of my advisory committee: Professor Michael Hoffmann, Professor John Seinfeld, and Professor Rick Flagan, for their time participating in my committee, but even more importantly for their efforts to build the environment at Caltech where important environmental engineering research is conducted.

Mike Kleeman and Lynn Salmon provided significant assistance with the logistical aspects of the source tests conducted as part of this work. Mike worked with me from the early hours through the late nights during the source testing efforts, always providing a helping hand and helping to maintain the momentum to push forward. Lynn's knowledge of air pollution sampling techniques was a tremendous resource. In addition, Lynn completed the inorganic ion analyses of the source test samples and helped with many other aspects of sample handling.

The analytical work conducted as part of this thesis required significant effort and expertise. I thank Jay Odum for the time that he spent with me discussing GC/MS analysis. In addition, collaboration with Mike Hannigan and Matt Fraser during the preparation of standards and tabulation of a mass

spectral database assisted the analytical work conducted as part of my research efforts.

There are also those who helped with the small things that are far too numerous to list but are not forgotten: Christos Christoforou, Chris Nolte, Phil Fine, Peter Green, Yaniv Dubowski, Ann Miguel, and Pat Chuang.

I thank Rapheal Susnowitz, Thu Vo, Pons Lazo, and the staff at the California Air Resources Board's Haagen-Smit Laboratory in El Monte, California, for their assistance and cooperation in conducting the motor vehicle source tests. I thank Lee Reavis, Debbie Walker, and Chef Jorge Amador (Total Food Management) for their assistance and cooperation in conducting the food cooking tests; Eric Grosjean and Daniel Grosjean (DGA, Inc.) for preparation and analysis of the C<sub>18</sub> cartridges used for carbonyls; Rei Rasmussen (Oregon Graduate Institute) for preparation and analysis of the SUMA canisters used for measurement of C<sub>10</sub> and smaller vapor-phase hydrocarbons; Judy Chow and Cliff Frazier at the Desert Research Institute for X-ray fluorescence measurements; Bob Cary at Sunset Labs for EC/OC measurements, and the California Air Resources Board for supporting this work under agreement number A93-329 and agreement number 97-6PM.

Finally, I wish to thank my wife, Diane, for her love, support and encouragement, and my daughter, Emily, for helping me find the simple but meaningful purposes in life. I also wish to thank my parents and brothers, David and Andy, who have had a profound influence on my entire life.

## Abstract

A dilution source sampling system is used to quantify the air pollutant emissions from major urban air pollution sources. The emissions from catalyst-equipped gasoline-powered motor vehicles, noncatalyst gasoline-powered motor vehicles, diesel trucks, meat charbroiling, the cooking of vegetables with seed oils, fireplace combustion of softwood and hardwood, cigarette combustion, and paint spray coating operations are characterized. Semi-volatile and particle-phase organic compounds in the diluted source emissions are collected simultaneously by both a traditional filter/PUF (polyurethane foam) sampling train and by an advanced organic compound-based denuder/filter/PUF sampling train to provide information on the gas/particle phase distribution of the semi-volatile organic compounds. Emission rates of hundreds of organic compounds, spanning carbon numbers from C<sub>1</sub> to C<sub>29</sub> are determined by gas chromatography/mass spectrometry and gas chromatography with flame ionization detection including n-alkanes, isoprenoids and other branched alkanes, cycloalkanes, aromatics, polycyclic aromatic hydrocarbons, olefins, n-alkanoic acids, n-alkenoic acids, carbonyls, lactones, petroleum biomarkers, levoglucosan and other wood smoke markers, steroids, and synthetic chemicals. Fine particle mass emission rates and fine particle elemental chemical composition are measured as well.

The emissions profiles collected by use of the dilution source sampler are used to develop receptor-based air quality models that use organic compounds as tracers to determine source contributions to gas-phase and particle-phase air pollutant concentrations in the atmosphere. These models are applied to study source contributions to the existing particulate and gas-phase organic air pollution problems in Southern California and in California's San Joaquin Valley. In the Los Angeles area, diesel engine exhaust, fine particle paved road dust, food cooking operations and wood smoke are the largest contributors to annual average fine particle concentrations in the atmosphere, accompanied by smaller

amounts of gasoline-powered vehicle exhaust aerosol, cigarette smoke, tire dust, plant fragments and natural gas combustion aerosol. In the San Joaquin Valley, wood smoke, background aerosol are found to be major contributors to the elevated fine particle concentrations experienced during the winter months.

## Table of Contents

### Chapter 1

<b>Introduction</b>	<b>1</b>
1.1 Motivation	1
1.2 Research Objectives	3
1.3 Approach	5
1.4 References	10

### Chapter 2

<b>Organic Compounds from Meat Charbroiling</b>	<b>13</b>
2.1 Introduction	13
2.2 Experimental Methods	15
2.2.1 Comprehensive Source Sampler	15
2.2.2 Dilution Sampler Preparation and Evaluation	23
2.2.3 Source Testing Procedure	25
2.2.4 Organic Chemical Analysis	26
2.3 Results and Discussion	30
2.3.1 Fine Particle Mass and Chemical Composition	30
2.3.2 Non-Methane Organic Compounds	31
2.3.3 Volatile Organic Compounds	33



2.3.4 Semi-Volatile and Particle Phase Organic Compounds	39
2.3.5 Comparison Between Measurement Methods for Semi-Volatile Organics	43
2.3.6 Gas/Particle Partitioning: Experiment Versus Theory	47
2.4 References	51

### **Chapter 3**

<b>Organic Compounds from Cooking with Seed Oils</b>	<b>55</b>
3.1 Introduction	55
3.2 Experimental Methods	56
3.2.1 Comprehensive Source Sampling	56
3.2.2 Source Testing Procedure	58
3.2.3 Organic Chemical Analysis	59
3.3 Results	61
3.3.1 Fine Particle Mass and Chemical Composition	64
3.3.2 Organic Compound Emissions	67
3.3.3 Gas/Particle Partitioning: Experiment Versus Theory	77
3.3.4 Contribution to Concentrations of Alkanoic Acids in the Los Angeles Atmosphere	80
3.4 References	83

**Chapter 4**

<b>Organic Compounds from Medium Duty Diesel Trucks</b>	<b>85</b>
4.1 Introduction	85
4.2 Experimental Methods	87
4.2.1 Comprehensive Source Sampling	87
4.2.2 Source Testing Procedure	89
4.2.3 Organic Chemical Analysis	90
4.3 Results	93
4.3.1 Fine Particle Mass and Chemical Composition	93
4.3.2 Distribution of Organic Compounds	95
4.4 References	115

**Chapter 5**

<b>Organic Compounds from Gasoline-Powered Motor Vehicles</b>	<b>117</b>
5.1 Introduction	117
5.2 Experimental Methods	119
5.2.1 Comprehensive Source Sampling	119
5.2.2 Vehicle Selection	121
5.2.3 Source Testing Procedure	121
5.2.4 Organic Chemical Analysis	126
5.3 Results	127

5.3.1 Comparison of Speciated Volatile Hydrocarbon Emissions Measurements	127
5.3.2 Fine Particle Mass and Chemical Composition	129
5.3.3 Distribution of Carbon Emissions	132
5.3.4 Organic Compound Tracers for Gasoline-Powered Motor Vehicle Exhaust	150
5.4 References	152
<b>Chapter 6</b>	
<b>Organic Compounds from Fireplace Combustion of Wood</b>	<b>155</b>
6.1 Introduction	155
6.2 Experimental Methods	158
6.2.1 Comprehensive Source Sampling	158
6.2.2 Source Test Procedure	162
6.2.3 Organic Chemical Analysis	164
6.3 Results	167
6.3.1 Fine Particle Emission Rates and Elemental Compositions	167
6.3.2 Mass Balance on Organic Compound Emissions	170
6.3.3 Emission Rates of Individual Organic Compounds	176
6.3.4 Gas/Particle Partitioning: Experiment Versus Theory	187
6.3.5 Determination of the Contribution of Wood Smoke to Ambient VOC Concentrations	189

6.4 References	194
----------------	-----

## **Chapter 7**

### **Organic Compounds in Cigarette Smoke** **197**

7.1 Introduction	197
7.2 Experimental Methods	199
7.2.1 Comprehensive Source Sampling	199
7.2.2 Source Testing Procedure	202
7.2.3 Organic Chemical Analysis	203
7.3 Results	206
7.3.1 Fine Particle Emissions Rates and Composition	206
7.3.2 Emissions of CO and CO <sub>2</sub>	213
7.3.3 Mass Balance on Organic Compound Emissions	213
7.3.4 Emission Rates of Individual Organic Compounds	216
7.4 References	224

## **Chapter 8**

### **Organic Compounds from Industrial Spray Painting Operations** **226**

8.1 Introduction	226
8.2 Experimental Methods	228
8.2.1 Source Sampling	228

8.2.2 Source Testing Procedure	230
8.2.3 Organic Chemical Analysis	230
8.3 Results	232
8.3.1 Fine Particle Emissions Rates and Chemical Compositions	232
8.3.2 Mass Balance on Organic Compound Emissions	234
8.3.3 Emission Rates of Individual Organic Compounds	237
8.3.4 Texanol as a Tracer for Water-Based Spray Coating Operations	241
8.4 References	244
<b>Chapter 9</b>	
<b>Source Apportionment of Airborne Particulate Matter Using Organic Compounds as Tracers</b>	<b>245</b>
9.1 Introduction	245
9.2 Experimental Section	248
9.2.1 Ambient Samples	248
9.2.2 Source Samples	250
9.2.3 Organic Compound Identification and Quantification	255
9.3 Source/Receptor Reconciliation	260
9.3.1 Chemical Mass Balance Approach	260
9.3.2 Selection of Sources and Organic Compounds: An Emissions Inventory Assisted Approach	262

9.3.2.1 A Test for Apparent Chemical Stability	263
9.3.2.2 Elimination of Colinearity Between Source Profiles	272
9.3.2.3 Completeness of the Source Profile Library	274
9.4 Results	276
9.4.1 Total Fine Particulate Mass Apportionment	284
9.5 References	290
<b>Chapter 10</b>	
<b>Source Apportionment of Wintertime Gas-phase and Particle-Phase Air Pollutants Using Organic Compounds as Tracers</b>	<b>299</b>
10.1 Introduction	299
10.2 Experimental Methods	301
10.2.1 Ambient Samples	301
10.2.2 Source Samples	304
10.2.3 Organic Chemical Analysis	308
10.3 Source/Receptor Reconciliation	310
10.3.1 Chemical Mass Balance Approach	310
10.4 Results	315
10.4.1 Characterization of Fine Organic Compound Mass Present in Ambient samples	315
10.4.2 Fine Particle Organic Compound and Fine Particle Mass Apportionment	323
10.4.3 Non-Methane Organic Gas Apportionment	332

10.5 References	338
-----------------	-----

## Chapter 11

### **Source Reconciliation of Atmospheric Gas-Phase and Particle-Phase Pollutants Using Organic Compounds as Tracers** 342

11.1 Introduction	342
11.2 Experimental Methods	343
11.2.1 Ambient Samples	343
11.2.2 Source Samples	346
11.3 Source/Receptor Reconciliation	351
11.3.1 Chemical Mass Balance Approach	351
11.3.2 Selection of Sources and Organic Compounds	352
11.4 Results	354
11.4.1 Comprehensive Apportionment of Organic Compounds in the Atmosphere	354
11.4.2 Apportionment of Volatile Organic Compound Concentrations	356
11.4.3 Apportionment of Fine Particulate Organic Compound Mass and Fine Particulate Mass	362
11.4.4 Apportionment of Semi-Volatile Organic Compounds	368
11.4.5 Apportionment of Individual Organic Compounds	370
11.4.6 Comparison of Unapportioned Organic Compound Mass to Organic Acid Tracers	370

11.5 References	374
<b>Chapter 12</b>	
<b>Conclusion</b>	<b>379</b>
12.1 Summary	379
12.1.1 Meat Charboiling	380
12.1.2 Cooking Vegetables in Seed Oils	381
12.1.3 Diesel Trucks	382
12.1.4 Gasoline-Powered Motor Vehicles	383
12.1.5 Fireplace Combustion of Wood	384
12.1.6 Cigarette Smoke	386
12.1.7 Spray Coating Operations	387
12.1.8 Source Contributions to Atmospheric Fine Particle Concentrations	388
12.1.9 Source Contributions to Wintertime Gaseous and Particulate Pollutant Concentrations	389
12.1.10 A Comprehensive Source Apportionment Model for Organic Compounds	391
12.2 Suggestions for Future Research	392
<b>Appendix A. Whole Gasoline Vapor and Gasoline Headspace Vapor Emissions Profiles</b>	<b>394</b>
<b>Appendix B. Paved Road Dust Emissions Profiles</b>	<b>398</b>



## List of Figures

- Figure 2.1. Sampling equipment connected to the comprehensive dilution source sampler for the measurement of gas-phase, semi-volatile, and particle-phase organic compounds, and fine particle mass and chemical composition. 17
- Figure 2.2. Material balance on the gas-phase, semi-volatile, and particle-phase organic compound emissions from meat charbroiling measured by the comprehensive source sampler. 34
- Figure 2.3. Emission rates of fatty acids and carbonyls from meat charbroiling operations. 41
- Figure 2.4. Comparison of the total mass of individual organic compounds collected by the denuder/filter/PUF and filter/PUF sampling trains during the charbroiled meat cooking source tests. 44
- Figure 2.5. The distribution of organic compounds between the gas-phase and particle-phase in the diluted exhaust from meat charbroiling as measured by the denuder/filter/PUF and filter/PUF sampling trains. 45
- Figure 2.6. Partitioning coefficient,  $K_{p,opm}$ , for the n-alkanoic acids in the diluted exhaust from meat charbroiling operations as measured by the denuder/filter/PUF and filter/PUF sampling train plotted as a function of the vapor pressure of the pure compounds. 49
- Figure 3.1. Material balance on the gas-phase, semi-volatile, and particle phase organic compounds emitted from stir frying vegetables in soybean oil. 62
- Figure 3.2. Formation of free fatty acids from glycerol esters of fatty acids. 68
- Figure 3.3. Emission rates and phase distributions of n-alkanoic acids emitted from cooking vegetables in seed oil. 73

Figure 3.4. Emission rates of selected aldehydes emitted from cooking vegetables in seed oil.	75
Figure 3.5. Partitioning of n-alkanoic acids in the diluted exhaust from cooking with seed oils as a function of the vapor pressure of the pure compound as measured by a denuder/filter/PUF sampling train.	79
Figure 4.1. Dynamometer cycle used for medium duty diesel truck emissions testing.	91
Figure 4.2. Comparison of fine particle organic and elemental carbon emitted from the diesel trucks tested as measured by a traditional filter sampler and a denuder/filter/PUF sampler.	96
Figure 4.3. Material balance on the gas-phase, semi-volatile, and particle-phase organic compounds emitted from medium duty diesel trucks driven over the hot start Federal Test Procedure urban driving cycle on a chassis dynamometer.	103
Figure 4.4. Chemical structures of isoprenoids and tricyclic terpanes present in diesel fuel and emitted from diesel trucks.	107
Figure 4.5. Comparison of the distribution n-alkanes and isoprenoids in medium-duty diesel truck exhaust and present in the diesel fuel supplied to those trucks.	108
Figure 4.6. Polycyclic aromatic hydrocarbons (PAH) emitted from medium-duty diesel trucks and present in diesel fuel.	110
Figure 4.7. Semi-volatile n-alkane, isoprenoid, and tricyclic terpane ambient concentrations measured in Azusa, California, in the summer of 1993 compared to the tailpipe emission rates of these compounds from medium-duty diesel trucks on the FTP hot start driving cycle.	113
Figure 5.1. Federal Test Procedure (FTP) Urban Driving Cycle.	124

- Figure 5.2. Individual hydrocarbon compounds emitted from a composite of 3 light-duty vehicles tested on the FTP Urban Driving Cycle as measured by the FTP/CVS sampler compared to measurements made for the same species and vehicles using the 2-stage dilution sampler. 128
- Figure 5.3. Mass balance on the non-methane organic compounds and elemental carbon emitted from catalyst-equipped and noncatalyst equipped gasoline-powered light-duty motor vehicles. 134
- Figure 5.4. Mass balance on the semi-volatile and particle-phase organic compounds and elemental carbon emitted from catalyst-equipped gasoline-powered light-duty motor vehicles. 143
- Figure 5.5. Mass balance on the semi-volatile and particle-phase organic compounds and elemental carbon emitted from noncatalyst-equipped gasoline-powered light-duty motor vehicles. 144
- Figure 5.6. Emissions of n-alkanes and isoprenoids from gasoline-powered light-duty motor vehicles and the concentration of these compounds in gasoline. 147
- Figure 5.7. Emissions of PAH and alkyl-PAH from gasoline-powered light-duty motor vehicles and the concentration of these compounds in gasoline. 148
- Figure 6.1. Mass balance on the non-methane organic compounds emitted from the fireplace combustion of pine wood. 171
- Figure 6.2. Mass balance on the carbonyl, semi-volatile, and particulate organic compounds emitted from the fireplace combustion of oak wood. 174
- Figure 6.3. Mass balance on the carbonyl, semi-volatile, and particulate organic compounds emitted from the fireplace combustion of eucalyptus wood. 175

Figure 6.4. Chemical structure of levoglucosan, guaiacol, substituted guaiacols, syringol, and substituted syringols emitted from the fireplace combustion of wood.	184
Figure 6.5. Emission rates of organic compounds from wood combustion and their gas/particle phase distributions in the diluted exhaust from a residential fireplace.	185
Figure 6.6. Gas/particle partitioning of PAH in the diluted exhaust from wood burned in a residential fireplace as a function of the vapor pressure of the pure compound.	190
Figure 7.1. Mass balance on the non-methane organic mass emitted from the cigarette smoking.	214
Figure 7.2. Mass emission rates of C <sub>2</sub> through C <sub>8</sub> hydrocarbons emitted from cigarette smoking, meat charbroiling, and fireplace combustion of wood.	218
Figure 7.3. Mass emission rates of light gas-phase carbonyls emitted from cigarette smoking, meat charbroiling, and fireplace combustion of wood.	220
Figure 7.4. Chemical structures of selected semi-volatile organic compounds emitted from cigarette smoke.	221
Figure 7.5. Gas and particle phase emission rate of semi-volatile organic compounds emitted from cigarette smoking.	222
Figure 8.1. Mass balance on the non-methane organic compounds measured in the emissions from oil-based paint spray coating and water-based paint spray coating operations conducted in an industrial-scale paint spray booth.	235
Figure 8.2. Mass emission rates for selected individual organic compounds emitted from oil-based paint spray coating and water-based paint spray coating operations.	240
Figure 8.3. Chemical structures of the organic compounds present in technical grade Texanol.	242

Figure 9.1. Air quality monitoring sites in Southern California used in the present study.	249
Figure 9.2. Central basin 1982 annual average ambient compound concentrations divided by compound emissions within the 80X80 km emissions inventory area centered over Downtown Los Angeles (Hildemann et al., 1991). Solid lines represent the average $\pm$ two standard deviations of the ratio of concentration to emission rate observed for the conserved reference materials: elemental carbon, fine particle aluminum, and fine particle silicon. Central basin average ambient concentrations include all data from within the emissions inventory area: Pasadena, West Los Angeles, and Downtown Los Angeles. Values shown at $10^3$ are greater than or equal to $10^3$ .	266
Figure 9.3. Distribution of particulate organic compound emissions by source type within the Los Angeles basin, 1982.	275
Figure 9.4. Comparison of model predictions to measured ambient concentrations for the mass balance compounds - Downtown Los Angeles, 1982 annual average.	278
Figure 9.5. Source apportionment of ambient fine organic aerosol mass concentration - 1982 annual average.	282
Figure 9.6. Relative source contribution to modeled ambient concentrations of organic compounds used in the mass balance at Downtown Los Angeles - 1982 annual average.	285
Figure 9.7. Source apportionment of fine particle mass concentrations - 1982 annual average.	287
Figure 10.1. Mass balance on the fine particle organic compounds measured at Bakersfield, California, between December 26-28, 1995.	319

## List of Figures

- Figure 2.1. Sampling equipment connected to the comprehensive dilution source sampler for the measurement of gas-phase, semi-volatile, and particle-phase organic compounds, and fine particle mass and chemical composition. 17
- Figure 2.2. Material balance on the gas-phase, semi-volatile, and particle-phase organic compound emissions from meat charbroiling measured by the comprehensive source sampler. 34
- Figure 2.3. Emission rates of fatty acids and carbonyls from meat charbroiling operations. 41
- Figure 2.4. Comparison of the total mass of individual organic compounds collected by the denuder/filter/PUF and filter/PUF sampling trains during the charbroiled meat cooking source tests. 44
- Figure 2.5. The distribution of organic compounds between the gas-phase and particle-phase in the diluted exhaust from meat charbroiling as measured by the denuder/filter/PUF and filter/PUF sampling trains. 45
- Figure 2.6. Partitioning coefficient,  $K_{p,opm}$ , for the *n*-alkanoic acids in the diluted exhaust from meat charbroiling operations as measured by the denuder/filter/PUF and filter/PUF sampling train plotted as a function of the vapor pressure of the pure compounds. 49
- Figure 3.1. Material balance on the gas-phase, semi-volatile, and particle phase organic compounds emitted from stir frying vegetables in soybean oil. 62
- Figure 3.2. Formation of free fatty acids from glycerol esters of fatty acids. 68
- Figure 3.3. Emission rates and phase distributions of *n*-alkanoic acids emitted from cooking vegetables in seed oil. 73

Figure 11.2. Source contributions to non-methane organic gases concentrations, September 8-9, 1993.	360
Figure 11.3. Source contributions to fine particulate organic carbon concentrations, September 8-9, 1993.	363
Figure 11.4. Source contributions to fine particle mass concentrations, September 8-9, 1993.	366
Figure 11.5. Source contributions to the atmospheric concentrations of the mass balance species used in the CMB model at Azusa, September 8-9, 1993.	371
Figure 11.6. Comparison of the calculated "other" organics from the CMB model results and the fine particle 1,2-benzenedicarboxylic acid concentrations for the present summer study and from a fine particle source apportionment study of the wintertime aerosol in California's San Joaquin Valley (Chapter 10).	372

**List of Tables**

Table 2.1. Average Fine Particle Emission Rate and Fine Particle Chemical Composition From Meat Charbroiling.	32
Table 2.2. Organic Compound Emission Rates from Hamburger Meat Charbroiling Over a Natural Gas-Fired Grill.	35
Table 3.1. Average Fine Particle Mass Emission Rate and Fine Particle Chemical Composition Emitted From Cooking Vegetables in Seed Oils.	65
Table 3.2. Organic Compound Emission Rates from Frying Vegetables in Seed Oils.	69
Table 4.1. Average Fine Particle Emission Rate and Fine Particle Chemical Composition for Medium-Duty Diesel Truck Exhaust.	94
Table 4.2. Organic Compounds Present in Diesel Fuel and in Medium Duty Diesel Truck Exhaust.	97
Table 5.1. Fine Particle Tailpipe Emissions from the Gasoline-Powered Motor Vehicles Tested.	122
Table 5.2. Average Fine Particle Emission Rate and Fine Particle Chemical Composition of Tailpipe Exhaust from Gasoline-Powered Motor Vehicles.	133
Table 5.3. Organic Compounds Present in Gasoline and in Gasoline-Powered Motor Vehicle Tailpipe Emissions.	136
Table 6.1. Average Fine Particle Emission Rate and Fine Particle Chemical Composition of Emissions from Fireplace Combustion of Wood.	168
Table 6.2. Organic Compound Emission Rates from Fireplace Combustion of Wood.	177



Table 6.3. Estimate of the Contribution from Wood Smoke to the Ambient Concentrations of Benzene, Ethene, and Ethyne in Fresno, California, During Two Winter Episodes Using Levoglucosan as a Tracer for Wood Smoke.	192
Table 7.1. Cigarettes Smoked in Present Study.	204
Table 7.2. Average Fine Particle Emission Rate and Fine Particle Chemical Composition for Cigarette Smoking.	207
Table 7.3. Organic Compounds Measured in Cigarette Smoke.	208
Table 8.1. Average Fine Particle Emission Rate and Fine Particle Chemical Composition from Architectural Spray Coating Operations.	233
Table 8.2. Organic Compounds Present in the Emissions from an Industrial-Scale Paint Spray Coating Booth.	238
Table 9.1. Estimate of Fine Aerosol Organic Carbon (OC) Emissions within 80 x 80 km square Study Area Centered Over Los Angeles for 1982.	251
Table 9.2. List of Compounds Available for Possible Use in the Receptor Model- 1982, Los Angeles.	256
Table 9.3. Source Apportionment of Primary Fine Organic Aerosol: 1982 Annual Average Determined by Chemical Mass Balance.	280
Table 9.4. Source Apportionment of Fine Particulate Mass Concentration: 1982 Annual Average Determined by Chemical Mass Balance.	288
Table 10.1. Atmospheric Concentrations of Fine Particle-Phase Organic Compounds During the IMS95 Experiments.	316
Table 10.2. Source Apportionment Of Fine Primary Organic Carbon: Determined By Chemical Mass Balance.	325
Table 10.3. Source Apportionment Of Fine Particulate Mass Concentrations: Determined By Chemical Mass Balance.	329

Table 10.4. Source Apportionment Of Non-Methane Organic Gases: Determined By Chemical Mass Balance.	335
Table 11.1. Source Apportionment Of Non-Methane Organic Gas (TO-12) Concentrations During The Severe Photochemical Smog Episode Of September 8-9, 1993: Determined By Chemical Mass Balance.	361
Table 11.2. Source Apportionment Of Fine Particulate Organic Compound Concentrations During The Severe Photochemical Smog Episode Of September 8-9, 1993: Determined By Chemical Mass Balance.	364
Table 11.3. Source Apportionment Of Fine Particle Mass Concentrations During The Severe Photochemical Smog Episode Of September 8-9, 1993: Determined By Chemical Mass Balance.	367
Table 11.4. Source Apportionment Of Gas-Phase Semi-Volatile Organic Compound Concentrations During The Severe Photochemical Smog Episode Of September 8-9, 1993: Determined By Chemical Mass Balance.	369
Table A.1. Whole Gasoline Vapor And Headspace Gasoline Vapor Emissions Profiles.	395
Table B.1. Emissions Profiles For Paved Road Dust Fine Particulate Mass	399

## Chapter 1

### Introduction

#### 1.1 Motivation

Organic compounds play an important role in urban air pollution. Low molecular weight gas-phase organic compounds, often called volatile organic compounds (VOCs), react with oxides of nitrogen to form ozone in photochemical smog. Emissions of these compounds from specific sources, such as gasoline-powered motor vehicles (1-3), have been extensively characterized. In addition, air pollution transport and receptor models have been used to understand the chemistry, transport, and origin of the VOCs in the urban atmosphere (4-7). As these gas-phase air pollution models continue to advance, they are limited by the quality and quantity of the emissions data available to drive the models. For example, very little speciated emissions data exist for the highly reactive carbonyls, which have been shown to make up a significant portion of the chemical reactivity of the urban atmosphere (8).

In addition to the VOCs, the urban atmosphere also contains higher molecular weight organic compounds that are present in the particle phase in the atmosphere, and semi-volatile organic compounds which are present simultaneously in both the gas-phase and the particle-phase. Recent studies have begun the process of characterizing non-volatile and semi-volatile organic

compounds that are present in the particle-phase in the urban atmosphere and in the emissions from air pollution sources (9-18). This information has been used in conjunction with atmospheric dispersion models (19, 20) to predict air pollutant source contributions to ambient fine particulate organic compound concentrations, but such data have not previously been incorporated into receptor-based air pollution models that use chemical substances in the source emissions as tracers to compute the relationship between the direct primary emissions of organic compounds and their concentrations in atmospheric fine particles.

In contrast to the VOC's and the heavy particle-phase organic compounds, very little is known about the emissions of semi-volatile organic compounds from air pollution sources. This is mainly due to the difficulty of collecting semi-volatile organic compounds, which are too volatile to be effectively collected on particle filters and are not volatile enough to be sampled using gas canisters. The previously collected data on the emissions of semi-volatile organic compounds from air pollution sources have been limited to specific classes of compounds such as methoxyphenols in wood smoke (21, 22) and polycyclic aromatic hydrocarbons (PAH) emitted from diesel trucks (23).

Historically, the gas-phase air pollution models and the particle-phase air pollution models have been developed in parallel with very little interaction. These models, however, are being merged into comprehensive air pollution models that can simultaneously track the transport and chemical reaction of gas-

and particle-phase organic compounds in the atmosphere. These developments have laid the foundation to study aspects of air pollution that could not be addressed in the past, including (1) the role of semi-volatile organic compounds in gas-phase chemistry and ozone formation and (2) secondary aerosol formation from VOCs and semi-volatile organic compounds. However, these modeling efforts are limited by the availability of comprehensive emissions data that simultaneously describe volatile organic gases, semi-volatile organic compounds, and particle-phase organic compounds. Further progress in the study of this aspect of air pollution, therefore, requires that measurements of these compounds from air pollution sources be made in a manner that is consistent with the atmospheric measurements against which the air pollution model results will be compared. In addition, once such emissions data have been acquired, it will be possible to explore the design of new receptor-based air quality models that use organic compounds as tracers for the effluent from specific emissions sources in order to better understand the relationship between direct primary emissions from air pollution sources and ambient pollutant concentrations.

## **1.2 Research Objectives**

The principal objectives of this research are to quantify the emissions of volatile gas-phase, semi-volatile, and particle-phase organic compounds from air

pollution sources and to develop receptor-based air pollution models which use these emissions data to quantify the primary contributions of air pollution sources to atmospheric pollutant concentrations.

Air pollutant emissions data are sought which are collected and analyzed by sampling techniques which are the same as those used for the quantification of individual organic compounds in the ambient atmosphere. This requires the use of a dilution source sampler which can dilute hot exhaust emissions from combustion sources to near ambient temperatures and pressure prior to sampling, such that the organic compounds in the cooled diluted exhaust are present at near their atmospheric equilibrium distribution between the gas- and particle-phases. In addition, the sampler must be specifically configured for the simultaneous collection and quantification of gas-phase, semi-volatile and particle-phase organic compounds, a development which has not been reported previously. Sampling and analytical techniques for the collection and quantification of a broad range of semi-volatile organic compounds are needed, and a desired characteristic of the sampling technique is that it should achieve an accurate determination of the particle/gas phase partitioning of the semi-volatile organic compounds present in the diluted source emissions.

In this work, the major sources of organic compounds emissions to the urban atmosphere first are tested to quantify the emissions of volatile gas-phase hydrocarbons, carbonyls, semi-volatile organic compounds, and particle-phase organic compounds along with fine particle mass and elemental composition.

Then receptor-based air quality models are developed that utilize these emissions source data to understand the relationship between the direct primary emissions from air pollution sources and the atmospheric concentrations of these pollutants. This is done by using unusual organic compounds that are present in the emissions from some sources but not others as tracers for the effluent from particular sources in the atmosphere. Receptor models which can elucidate the relationships between the emissions and ambient concentrations of fine organic particle mass, fine particle mass, volatile organic compound mass, semi-volatile organic compound mass, and individual organic compounds are sought.

### **1.3 Approach**

This section provides an overview of the research presented in the following chapters. Chapters 2 through 9 describe the collection of the source emissions data and discuss the significance of the emissions from each source tested. In Chapter 2, the design of the comprehensive source sampling system for organic compounds is described, and the results of performance tests of the sampler are presented along with measurements of the emissions from meat charbroiling. Little, if any, data have existed previously that describe the emissions of gas-phase and semi-volatile carbonyls and organic acids from meat charbroiling. In addition, the distribution of n-alkanoic acids between the gas-

and particle-phases in the diluted meat smoke is discussed, and it is shown that these compounds do not follow the distribution predicted by gas/particle partitioning theory, in all likelihood because semi-volatile organic compounds become trapped within solid meat-fat containing particles where they cannot easily repartition into the vapor phase.

Chapter 3 discusses the emissions from cooking with seed oils. Organic compound fingerprints that describe the emissions from these cooking operations, using different seed oils, are presented along with a discussion of the gas/particle partitioning of n-alkanoic acids in the diluted exhaust from cooking with seed oils. The n-alkanoic acids in the diluted exhaust from these sources follow gas/particle partitioning theory, which differs from the distribution of the same compounds in the diluted meat charbroiling exhaust. The emissions of n-alkanoic acids and carbonyls from cooking with seed oils are shown to be significant contributors to the urban atmospheric concentrations of these compounds.

Chapter 4 reports the emissions from medium-duty diesel trucks operated over the hot-start portion of the Federal Test Procedure (FTP) urban driving cycle on a chassis dynamometer. Gas-phase carbonyls and diesel fuel components are found in large quantities in the exhaust emissions from diesel engines. The distribution of the organic compounds present in diesel fuel is compared to the distribution of these compounds in the tailpipe emissions from the diesel trucks, showing a significant change in the ratio of alkylated-PAH to



unsubstituted PAH following combustion. In addition, the distribution of specific n-alkanes, isoprenoids, and tricyclic terpanes in the emissions from diesel trucks is shown to be the same as previously reported in the Los Angeles area atmosphere, indicating that these compounds are likely to be useful to help trace diesel engine exhaust in the atmosphere.

Chapter 5 details the measurement and emissions from both gasoline-powered catalyst-equipped motor vehicles and noncatalyst gasoline-powered motor vehicles operated over the cold-start FTP dynamometer cycle. Significant differences are seen in the total mass emissions and in the distribution of organic compounds between the catalyst-equipped vehicles and the non-catalyst equipped vehicles. A comparison of the composition of the gasoline used during the source tests and emissions from the gasoline-powered motor vehicles shows a significant decrease in the ratio of alkylated-PAH to unsubstituted PAH present in the vehicle exhaust as compared to the fuel, a transformation similar to that observed for the diesel engines.

In Chapter 6, the emissions from fireplace combustion of two types of hardwood and one softwood are presented. Levoglucosan is found to be a major constituent in the fine particulate matter emitted from all three types of wood burned, and it is shown that the distribution of syringol- and guaiacol- type compounds can be used to distinguish between the emissions from hardwood and softwood combustion. Gas-phase emissions of acetylene, ethene, and benzene from wood combustion are shown to be important to the ambient

concentrations of these compounds during a period of high wood burning. This result is significant since acetylene, ethene and benzene are often used by other investigators to differentiate between the contributions from whole gasoline evaporation versus gasoline-powered motor vehicle exhaust in the atmosphere; interference from the effects of wood combustion could introduce significant uncertainties into such calculations.

The emissions of organic compounds present in cigarette smoke are quantified in Chapter 7. Of particular significance is the measurement of the phase distributions of semi-volatile organic compounds which may have been used incorrectly as cigarette smoke tracers in the past while only tracking the particle-phase concentrations of these compounds.

Chapter 8 covers the emissions from spray paint coating operations using both water-based paint and oil-based paint. Texanol, a semi-volatile organic compound, is found to be emitted in significant quantities from spray coating with water-based paints.

In Chapter 9, a receptor-based air quality model for computing source contributions to atmospheric fine particulate matter concentrations using organic compounds as tracers is developed and is tested using a fine particle data set collected in the south coast region of southern California. The contributions to annual average fine particulate matter concentrations from nine primary sources are quantified. These primary sources along with inorganic ions contributed by gas-to-particle conversion processes in the atmosphere are shown to account

for virtually all of the annual average fine particle mass concentrations in the atmosphere at four urban locations in the greater Los Angeles area.

In Chapter 10, the chemical mass balance (CMB) model that uses organic compounds as tracers developed in Chapter 9 is extended to determine source contributions to ambient pollutant concentrations during two wintertime high-pollution episodes in California's San Joaquin Valley. The contributions to ambient fine particle concentrations from the combustion of hardwood and softwood can be distinguished separately along with emissions from gasoline-powered motor vehicles, diesel engines, meat cooking operations, natural-gas combustion, and fine particle paved road dust. In addition, source contributions to ambient volatile organic compound (VOC) concentrations are studied using a model that employs both gas- and particle-phase organic compounds as tracers.

In Chapter 11, a comprehensive receptor-based air quality model is developed that simultaneously tracks source contributions to volatile organic compounds, semi-volatile organic compounds and particle-phase organic compounds by using individual organic compounds as tracers for the relevant emissions sources. The model is applied to study the south coast region of southern California during a severe summertime air pollution episode.

Finally, in Chapter 12 the major results of this research are summarized and suggestions are provided for future extensions of this work.

## 1.4 References

1. Burns, V. R.; Benson, J. D.; Hochhauser, A. M.; Koehl, W. J.; Kreucher, W. M.; Reuter, R. M. *SAE Tech. Pap. Ser.* **1991**, No. 912320.
2. Sigsby, J. E.; Tejada, S.; Ray, W.; Lang, J. M.; Duncan, J. W. *Environ. Sci. Technol.* **1987**, 21, 466-475.
3. Stump, F.; Tejada, S.; Ray, W.; Dropkin, D.; Black, F.; Crews, W.; Snow, R.; Siudak, P.; Davis, C. O.; Baker, L.; Perry, N. *Atmos Environ.* **1989**, 23, 307-320.
4. Harley, R. A.; Cass, G. R. *Atmos. Environ.* **1995**, 29, 905-922.
5. Harley, R. A.; Hannigan, M. P.; Cass, G. R. *Environ. Sci. Technol.* **1992**, 26, 2395-2408.
6. Fujita, E. M.; Watson, J. G.; Chow, J. C.; Zhiqiang, L. *Environ. Sci. Technol.* **1994**, 28, 1633-1649.
7. Scheff, P. A.; Wadden, R. A. *Environ. Sci. Technol.* **1993**, 27, 617-625.
8. Grosjean, E.; Grosjean, D.; Fraser M. P.; Cass G. R. *Environ. Sci. Technol.* **1996**, 30, 2687-2703.
9. Rogge, W. F.; Mazurek, M. A.; Hildemann, L. M.; Cass, G. R.; Simoneit, B. R. T. *Atmos. Environ.* **1993**, 27, 1309-1330.
10. Rogge, W. F., Hildemann, L. M.; Mazurek, M. A.; Cass, G. R.; Simoneit, B. R. T. *Environ. Sci. Technol.* **1991**, 25, 1112-1125.

11. Rogge, W. F., Hildemann, L. M.; Mazurek, M. A.; Cass, G. R.; Simoneit, B. R. T. *Environ. Sci. Technol.* **1993**, 27, 636-651.
12. Rogge, W. F., Hildemann, L. M.; Mazurek, M. A.; Cass, G. R.; Simoneit, B. R. T. *Environ. Sci. Technol.* **1993**, 27, 1892-1904.
13. Rogge, W. F., Hildemann, L. M.; Mazurek, M. A.; Cass, G. R.; Simoneit, B. R. T. *Environ. Sci. Technol.* **1993**, 27, 2700-2711.
14. Rogge, W. F., Hildemann, L. M.; Mazurek, M. A.; Cass, G. R.; Simoneit, B. R. T. *Environ. Sci. Technol.* **1993**, 27, 2736-2744.
15. Rogge, W. F., Hildemann, L. M.; Mazurek, M. A.; Cass, G. R.; Simoneit, B. R. T. *Environ. Sci. Technol.* **1994**, 28, 1375-1388.
16. Rogge, W. F., Hildemann, L. M.; Mazurek, M. A.; Cass, G. R.; Simoneit, B. R. T. *Environ. Sci. Technol.* **1997**, 31, 2726-2730.
17. Rogge, W. F., Hildemann, L. M.; Mazurek, M. A.; Cass, G. R.; Simoneit, B. R. T. *Environ. Sci. Technol.* **1997**, 31, 2731-2737.
18. Rogge, W. F., Hildemann, L. M.; Mazurek, M. A.; Cass, G. R.; Simoneit, B. R. T. *Environ. Sci. Technol.* **1998**, 32, 13-22.
19. Rogge, W. F.; Hildemann, L. M.; Mazurek, M. A.; Cass, G. R.; Simoneit, B. R. T. *J. Geophys. Res.* **1996**, 101, 19379-19394.
20. Hildemann, L. M.; Cass, G. R.; Mazurek, M. A.; Simoneit, B. R. T. *Environ. Sci. Technol.* **1993**, 27, 2405-2055.

21. Hawthorne, S. B.; Krieger, M. S.; Miller, D. J.; Mathiason, M. B. *Environ. Sci. Technol.* **1989**, 23, 470-475.
22. Hawthorne, S. B.; Miller, D. J.; Langenfeld, J. J.; Krieger, M. S. *Environ. Sci. Technol.* **1992**, 26, 2251-2262.
23. Lowenthal, D. H.; Zielinska, B.; Chow, J. C.; Watson, J. G.; Gautum, M.; Ferguson, D. H.; Neuroth, G. R.; Stevens, K. D. *Atmos. Environ.* **1994**, 28, 731-743.

## Chapter 2

# Organic Compounds from Meat Charbroiling

## 2.1 Introduction

Atmospheric dispersion models (1, 2) and an atmospheric receptor model that uses organic compounds as tracers (3) have been used to understand the relationship between fine particulate matter emitted from meat cooking operations and atmospheric fine particle concentrations. In the Los Angeles area, meat cooking operations were found to contribute up to approximately 20% of the annual average fine organic particle concentrations in the atmosphere at four air quality monitoring sites in 1982. Although the relationship between ambient fine particle concentrations and primary particle emissions from meat cooking operations is relatively well characterized, little is known about the relationship between the emissions from meat cooking operations and other aspects of air pollution such as photochemical smog formation, secondary organic aerosol formation, and the ambient concentrations of air toxics. The lack of understanding of the effect of meat cooking emissions on these aspects of air quality is largely due to two reasons: 1) the lack of data on the emissions of gas-phase and semi-volatile organic compounds from meat cooking operations, and 2) the previous inability of air pollution models to address the

role of semi-volatile organic compounds in secondary aerosol formation and photochemical smog.

Significant progress has been made in recent years toward understanding the atmospheric behavior of semi-volatile organic compounds (4, 5). In addition, air pollution models are now capable of better addressing the role of secondary organic aerosol formation from reactive organic gases (6). These two developments have laid the foundation for the development of comprehensive air pollution models which will be able to simultaneously track the gas-phase and particle-phase organic compound concentrations and the chemistry and physics of the interaction of gas-phase organic compounds with the associated particulate matter. A limiting factor in the application of these models to studying specific air pollution problems is the scarcity of emissions inventory data for the semi-volatile organic compounds covering virtually all major urban air pollution sources. To this end, a series of air pollution source tests is being conducted to obtain comprehensive emissions source profiles covering gas-phase, semi-volatile, and particle-phase organic compounds, including hydrocarbons, carbonyls, and organic acids, plus fine particle emission rates and fine particle elemental composition. The current paper addresses the measurement of such emissions from meat charbroiling operations.



## 2.2 Experimental Methods

### 2.2.1 Comprehensive Source Sampler

An advanced source sampling system has been developed which facilitates the simultaneous measurement of gas-phase, semi-volatile and particle-phase organic compound emission rates; fine particle mass emission rates and fine particle elemental composition. The portable dilution tunnel was originally developed for fine particulate measurements by Hildemann et al. (7) and has been extended with additional equipment that allows single compound quantification of gas-phase and semi-volatile organic compound emissions. In this dilution source sampler, which can operate as a single-stage dilution tunnel or a two-stage dilution tunnel, hot exhaust emissions are mixed with a 10 to 100 fold excess of activated carbon-filtered and HEPA-filtered air which in the presence of sufficient residence time causes those organic vapors that will form particulate matter upon cooling in the atmosphere instead to condense onto pre-existing particles in the source exhaust within the dilution sampler itself. The emissions thus can be sampled at near atmospheric temperature and pressure in order to obtain data on the partitioning of organic compounds between the gas and particle phases.

A diagram of the front portion of the dilution source sampler used here is shown in Figure 1 of Hildemann et al. (7). Modification of that sampler begins as

the diluted mixture of particles and gases is withdrawn from the residence time chamber located at the far downstream side of the sampling system. As shown in Figure 2.1 of the present work, samples are withdrawn through AIHL-design cyclone separators (8) which are operated at a flowrate of 30 lpm such that fine particles with aerodynamic diameters smaller than 1.8  $\mu\text{m}$  in diameter pass through the cyclones along with all gas-phase species. Semi-volatile organic and fine particle-phase compounds then are collected with two different sampling trains that operate in parallel. The first sampling train begins with a XAD-coated annular denuder (URG, Inc.; 400 mm long, 4 channel denuder), shown on the right side of Figure 2.1. The flow next is divided between three quartz fiber filters (47 mm diameter, Pallflex Tissuequartz 2500 QAO) operated in parallel at a flowrate of 10 lpm each. The flow out of each of the three quartz fiber filters is then combined and is passed through two polyurethane foam (PUF) cartridges (Atlas Foam; density = 0.022  $\text{g cm}^{-3}$ , ILD = 30; 5.7 cm diameter by 7.6 cm long) operated in series. The gas-phase semi-volatile organic compounds are collected by the annular denuder while particles and particle-phase organic compounds pass through the denuder and are collected on the filters downstream of the denuder. The PUFs downstream of the filters collect any semi-volatile organics that blow off the filters.

The XAD coated annular denuders are prepared by a modified version of the procedure originally developed by Gundel et al. (9) and are operated at a

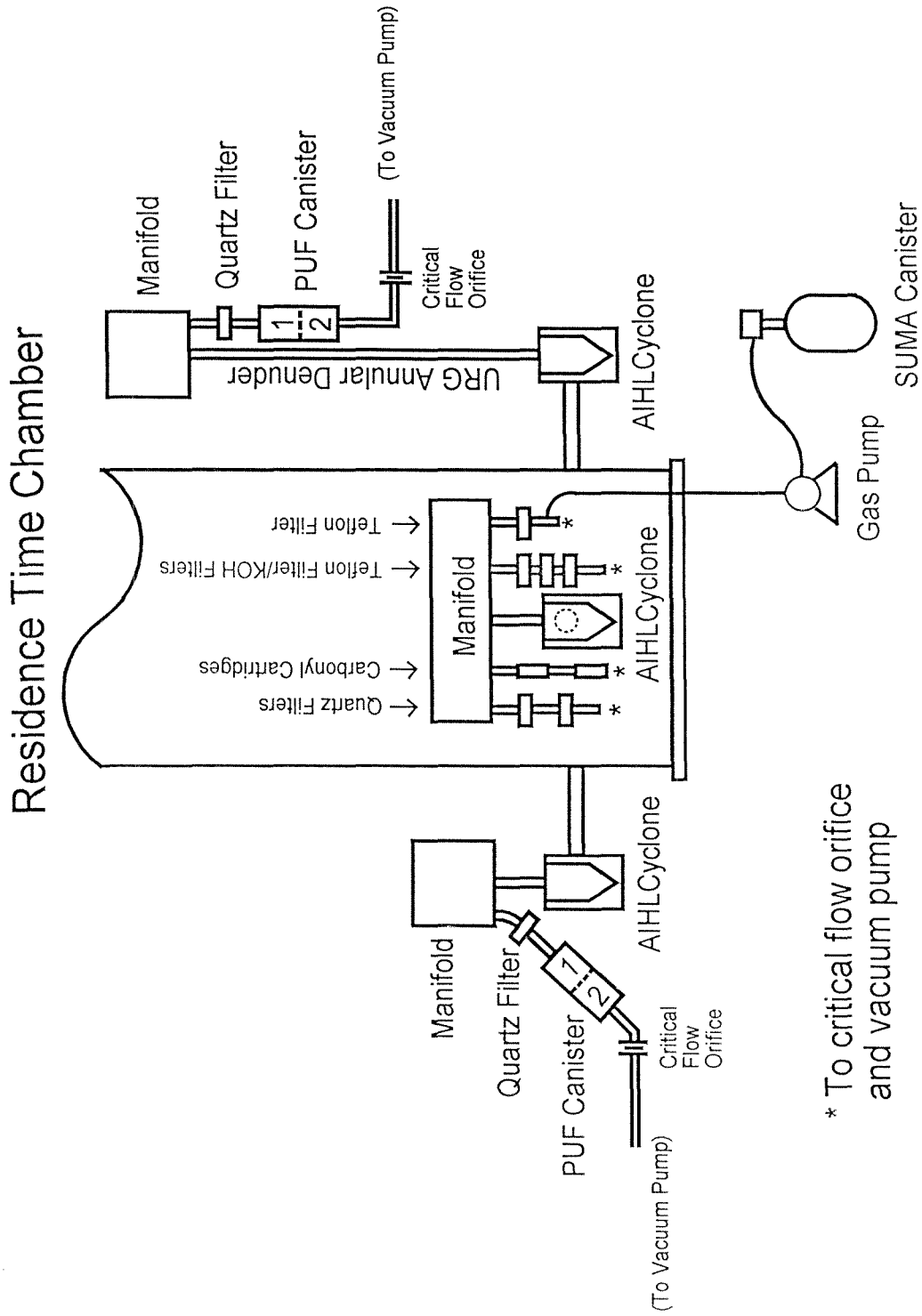


Figure 2.1. Sampling equipment connected to the comprehensive dilution source sampler for the measurement of gas-phase, semi-volatile, and particle-phase organic compounds, and fine particle mass and chemical composition.

flowrate of 30 lpm. Briefly, the XAD coated annular denuders are coated with a slurry of XAD-4 (Sigma Amberlite XAD-4). The XAD-4 is ground with a mortar and pestle to pass through a 400 mesh sieve, cleaned, then slurried into a solvent mixture of dichloromethane/acetone/hexane (2:3:5) (Fisher Optima Grade). The internal walls of the denuder are wetted with an aliquot of the XAD slurry and then rinsed with four successive batches of a clean XAD-free dichloromethane/acetone/hexane mixture (denuder solvent). The denuder is then dried with high purity nitrogen. The slurry application is repeated five more times. The XAD-4 adheres directly to the etched glass denuder walls and no adhesive is required (9). Within 12 hours prior to being used in a source test, the denuder is cleaned by four successive extractions with the denuder solvent in the presence of mild shaking of the solvent-filled denuder assembly. The denuder is then dried with high purity nitrogen. Denuders are sealed with Teflon-lined end caps from the time of preparation until use.

Particle losses in a similar URG annular denuder have been evaluated at operating conditions similar to those used in the current study, and it has been shown that electrically neutral fine particle losses are less than 5% for particles with diameters between 0.015 and 0.75  $\mu\text{m}$  (10). Experimental results reported by Gundel et al. (9) and experiments conducted in the course of the present project also demonstrate low fine particle losses in the denuders. Typically only one denuder/filter/PUF sampling unit is placed in operation during

a source test. A single denuder is used for a sampling time of up to approximately 30 minutes. The denuders are changed during source tests lasting longer than 30 minutes to assure that sampling is almost continuous throughout the source test cycle.

Prior to the current project, the use of XAD-coated denuder technology has only been reported for the collection of PAH (9) and nitro-PAH (11). The current research requires that the technology be applicable to many classes of organic compounds. For this reason, tests were conducted to demonstrate the ability to extract and recover a broad range of organic compounds from these denuders. A denuder was spiked with a standard suite containing over 100 compounds including series of n-alkanes, n-alkanoic acids, n-alcohols, PAH, fatty acid methyl esters, phenol, and benzaldehyde. All of these compounds were found to be quantitatively extracted from the denuders by four successive extractions with denuder solvent as described above, with no residual compounds remaining as measured by a second round of this extraction procedure. In addition, results will be presented in the current study showing good agreement between the total mass emission rates (but not necessarily phase separation) measured by the denuder/filter/PUF sampling train and a less complex filter/PUF sampling train.

A second type of semi-volatile and particle-phase organic compound sampling train is operated simultaneously in parallel with the denuder/filter/PUF

system. In this second system, an AIHL-design cyclone separator operated at 30 lpm is followed by three filter/PUF units in parallel each operated continuously at a flowrate of 10 lpm throughout the source test cycle. Each of the filter/PUF units consists of a quartz fiber filter (47 mm diameter, Pallflex Tissuequartz 2500 QAO) followed by two PUF cartridges (Atlas Foam) operated in series as shown on the left side of Figure 2.1. Each PUF cartridge consists of a 5.7 cm diameter by 7.6 cm long cylinder of polyurethane foam which is sized to retain 95% of the gas-phase naphthalene entering the PUF cartridge when operated at 10 lpm over the entire source test (12). Less volatile, heavier organic compounds are collected with even higher efficiencies than seen for naphthalene. During a typical source test, one cyclone/denuder/filter/PUF sampling train and four cyclones each with 3 filter/PUF assemblies are connected to the residence time chamber of the dilution tunnel; the extra filter/PUF units are intended for collection of excess sample to be used in further method development efforts.

In addition to the above sampling trains, a third type of cyclone-based filter sampler combined with VOC canisters and cartridges is operated for the collection of fine particulate matter, carbonyls, organic acids, and gas-phase organic compounds. A schematic of this system is shown in the center of Figure 2.1, pictured with the dilution tunnel's residence time chamber located behind the cyclone. Three stacked filter units and one carbonyl sampling line are connected to the outlet of an AIHL cyclone that draws air at a flowrate of 31 lpm

from the residence time chamber of the source sampler. The first stacked filter unit consists of two quartz fiber filters (47 mm diameter, Pallflex Tissuequartz 2500 QAO) in series which are used for elemental and organic carbon (EC/OC) analysis by thermal evolution and combustion analysis as described by Birch and Cary (13). The OC measured on the backup quartz fiber filter is used to help understand the adsorption of semi-volatile organic compounds onto the front filter (14, 15). The second filter stack contains three filters, a Teflon membrane filter (47 mm diameter, Gelman Teflo, 2  $\mu\text{m}$  pore size) followed by two KOH impregnated quartz fiber filters in series. This Teflon membrane filter is used for gravimetric determination of the fine particle mass emissions rate and is analyzed by X-ray fluorescence for 35 trace elements (16). The tandem KOH-impregnated quartz fiber filters are used to collect vapor-phase organic acids which will be analyzed in association with other research activities and will not be reported here. The third filter holder assembly contains one Teflon membrane filter which is used for a duplicate fine particle mass emissions measurement and for inorganic ion measurements by ion chromatography (17), atomic absorption spectroscopy and colorimetry (18). Downstream of that single Teflon filter the sample flow is divided, and a small portion of the flow is used to fill a 6 liter polished stainless steel SUMA canister for the collection of non-methane volatile hydrocarbons ranging from  $\text{C}_2$  to  $\text{C}_{10}$ . The 6 liter SUMA canister is filled continuously at a constant flowrate set to fill the canister over the entire source test cycle. Carbonyls are collected at the outlet of the AIHL cyclone separator

by two C<sub>18</sub> cartridges impregnated with dinitrophenylhydrazine (DNPH) that are operated in series (19). The air flowrates through the DNPH impregnated cartridges are typically in the range 0.3 to 0.5 lpm.

The flowrates through each of the sampling substrates are controlled with the use of critical orifices and are measured before and after each source test with rotameters that have been calibrated using an electronic bubble flowmeter (Gilian Instrument Corporation Model # 800268). The sample and the dilution air flowrates into the dilution tunnel are monitored throughout the source tests with a venturi meter and an orifice meter, respectively. The venturi meter and the orifice meter have been calibrated using dry gas meters. From these sample and dilution air flowrates and the analytical measurements described above, quantitative emissions rates can be determined for chemically speciated fine particulate matter, as well as for individual gas-phase, semi-volatile and particle-phase organic compounds.

Electronic particle sizing instruments and a pair of MOUDI impactors also were connected to the residence time chamber during the meat charbroiling source tests to obtain particle size distributions and particle chemical composition as a function of size. The size distributions and the results obtained from the impactors will be reported elsewhere.



### 2.2.2 Dilution Sampler Preparation and Evaluation

Prior to the meat charbroiling source tests, the dilution source sampler was completely disassembled and cleaned by vapor degreasing. Directly after degreasing, the sampler pieces were immediately wrapped with clean aluminum foil which had been baked at 550 °C for 12 hours. After the dilution sampler was reassembled, clean dilution air was passed through the sampler as the sampler was heated to approximately 95 °C by wrapping the stainless steel sections with electrical heating tape. The sampler was maintained at 95 °C for a minimum of four hours to remove any residual light hydrocarbons remaining after vapor degreasing. All of the small sampler pieces, including the filter holders and cyclones, were thoroughly cleaned with a detergent solution, next rinsed with deionized water, and then cleaned by sonication with hexane, methanol, and dichloromethane.

The dilution air supply to the dilution tunnel consists of ambient air that has been cleaned by passage through a HEPA filter and an activated carbon bed (7). A comprehensive blank test was conducted at the onset of the source sampling program to determine the ability of the dilution air cleaning system to remove particles, semi-volatile organic compounds, carbonyls, and VOCs. The dilution air cleaning system was found to have very high removal efficiencies for particulate matter, semi-volatile organic compounds, and all carbonyls. As expected, the lightest VOCs were not completely removed by the activated

carbon bed, so a system for measuring the residual VOC's in the dilution air was added to the source sampler. Dilution air is sampled and analyzed by the same procedures as used for the diluted sample gas stream described above, and source test results are then corrected by subtraction of any VOC background concentration present in the dilution air.

Particle losses in the comprehensive dilution sampler were evaluated by extracting a section of the dilution tunnel walls immediately following the completion of a cigarette source test in our laboratory. The extract was handled by the same procedures that will soon be discussed for the sample extracts, and compounds deposited per  $\text{cm}^2$  of dilution sampler interior wall area were quantified by GC/MS. The mass of individual organic compounds that were deposited onto the entire sampler internal surface area was calculated by scaling up the mass deposited onto the extracted area of the sampler walls to represent the entire interior surface area of the sampling system. The semi-volatile organic compounds that are predominantly present in the gas phase showed no detectable losses to the walls, while the predominately particle-phase organic compounds showed losses of approximately 7%, which is consistent with earlier particle loss experiments reported by Hildemann et al. (7). The compounds which were partitioned between both the gas-phase and the particle-phase were found to have losses in between the pure particle-phase compounds and the pure gas-phase organic compounds. These results indicate

that there are no preferential losses of semi-volatile organic compounds in the comprehensive dilution source sampler and that those losses that do occur affect primarily particulate matter, accounting for approximately 7% of the fine particle mass emissions.

### **2.2.3 Source Testing Procedure**

The meat charbroiling source tests were conducted in the field at a large institutional-scale natural gas-fired charbroiler that is in current commercial use. Emissions were sampled downstream from the filter and grease extractor that exist in the charbroiler exhaust ventilation system, which was operated at flowrate of  $400 \text{ m}^3 \text{ min}^{-1}$ . The source effluents were diluted by a second stage of dilution within the dilution sampler to bring the organic vapor/particle mixture to ambient conditions at  $29 \text{ }^\circ\text{C}$ . Two charbroiler tests were conducted using commercially distributed pre-formed hamburger patties (Kraft Premier, 114 grams of meat per patty, 20% fat); one test was conducted with defrosted hamburgers and the second test was conducted using hamburgers that were still frozen when placed on the grill as is the common practice at the facility tested. In batches of eight at one time, 80 hamburger patties were cooked over a period of 85 minutes during the test in which the frozen hamburgers were not defrosted prior to cooking. In batches of eight at one time, 112 hamburger patties were

cooked over a period of 72 minutes during the test where the hamburger patties were completely defrosted prior to cooking.

#### **2.2.4 Organic Chemical Analysis**

Extraction of particle-phase organic compounds collected on quartz fiber filters during the source tests is based on the previous work by Mazurek et al. (20) and Rogge et al. (21-27) and Rogge (28). Prior to sampling, the quartz fiber filters were baked at 550 °C for a minimum of 12 hours to reduce residual carbon levels associated with new filters. Immediately after sampling, the filters were stored in a freezer at -21 °C until the samples were extracted. The filters were typically extracted within one to two weeks following sample collection. Before the quartz fiber filters were extracted, they were spiked with a mixture of seven deuterated internal recovery standards: n-decane-d<sub>12</sub>, n-pentadecane-d<sub>32</sub>, n-tetracosane-d<sub>50</sub>, n-hexanoic acid-d<sub>11</sub>, n-decanoic acid-d<sub>19</sub>, phenol-d<sub>5</sub>, benzoic acid-d<sub>5</sub>, and benzaldehyde-d<sub>6</sub>. The samples were extracted twice with hexane (Fisher Optima Grade), followed by three successive benzene/isopropanol (2:1) extractions (benzene: high purity lots of E&M Scientific benzene; isopropanol: Burdick & Jackson). Extracts were filtered, combined, and reduced in volume to approximately 250 ml, and were split into two separate fractions. One fraction was then derivatized with diazomethane to convert organic acids to their methyl ester analogs which are amenable to GC/MS identification and quantification.

The procedures developed for the identification and quantification of organic compounds collected on the XAD-coated annular denuders and the PUF plugs were based on the methods previously developed for the analysis of air pollution samples collected on the quartz fiber filters. The analytical methods developed for the XAD-coated annular denuders and the PUF plugs can be used to quantify vapor-phase semi-volatile organic compounds that are as heavy as particle-phase organic compounds or which are as volatile as dodecane for alkanes, heptanoic acid for n-alkanoic acids, and naphthalene for polycyclic aromatic hydrocarbons under appropriate sampling conditions.

After the completion of each source test, the denuders used for sampling were extracted within 12 hours. During sample extraction, the denuder is first spiked with the same deuterated internal standard mix used for the filter extraction, and is then extracted with the use of four aliquots of 40 ml each of denuder solvent by pouring each aliquot into the denuder and shaking the Teflon capped denuder for approximately 30 seconds per aliquot. The four aliquots are composited and reduced to a volume of approximately 250 ml and then split into two separate fractions. One fraction is derivatized with diazomethane.

Prior to source sampling, the PUF plugs are cleaned by four successive extractions with a solvent mixture of dichloromethane/acetone/hexane (2:3:5) (Fisher Optima Grade). The foam plugs are repetitively compressed during the extraction. After the cleaning procedure, the PUF cartridges are air dried in the

dark in an organics clean room and are then stored in annealed borosilicate jars with solvent-washed Teflon lid liners in the freezer at -21 °C. After sampling, the PUF plugs are spiked with the same internal standard mix used for the filter and denuder extractions, and then are extracted with four successive aliquots of a mixture of dichloromethane/acetone/hexane (2:3:5). The extracts are filtered, combined, reduced in volume to approximately 250 ml and then split into two separate fractions. One fraction is derivatized with diazomethane as is done with the filter extracts and the denuder extracts.

Filter, PUF, and denuder field blanks are analyzed with each set of source samples. The field blanks are prepared, stored and handled by exactly the same procedures as used for the source samples.

Both the derivatized and underivatized sample fractions are analyzed by GC/MS on a Hewlett-Packard GC/MSD (GC Model 5890, MSD Model 5972) using a 30 meter by 0.25 mm diameter HP-1701 capillary column (Hewlett-Packard). 1-Phenyldodecane is used as a co-injection standard for all sample extracts and standard runs. The deuterated n-alkanes in the internal standard are used to determine extraction recovery for the compounds quantified in the underivatized samples. The deuterated acids are used to verify that the diazomethane reactions are driven to completion. In addition, the deuterated n-alkanoic acid recoveries are used in conjunction with the recovery of

deuterated tetracosane to determine the recovery of the compounds quantified in the derivatized fraction.

Semi-volatile and particle-phase organic compounds collected during the source test program are identified and quantified by gas chromatography/mass spectrometry (GC/MS). Although not all organic compounds emitted from air pollution sources are solvent extractable nor are they all elutable from a GC column, hundreds of compounds can be identified and quantified in source emissions (21, 23-28). Hundreds of authentic standards have been prepared for the positive identification and quantification of the organic compounds found in the current source test program. When quantitative standards could not be obtained for a given compound or compound class, significant effort was made to obtain a non-quantitative secondary standard that could be used for unique identification of the organic compounds. An example of such a secondary standard is the use of petroleum candle wax as a source of *iso*-alkanes and *anteiso*-alkanes that can then be used to help identify their presence when found in cigarette smoke particulate matter. Quantification of compounds identified using secondary standards has been estimated from the response factors for compounds having similar retention times and chemical structure. When neither quantitative nor secondary standards could be obtained, compound identification is classified as either 1) *probable*: when the sample mass spectrum is identical to the library spectrum but no standard was available, and 2) *possible*: same as

probable except that the spectrum contained additional information due to coelution with another compound. Compounds having probable and possible identifications are noted but their emission rates are not quantified.

Total non-methane organic gases (NMOG, EPA method TO12) and individual organic vapor-phase hydrocarbons ranging from C<sub>1</sub> to C<sub>10</sub> were analyzed from the SUMA canisters by gas chromatography/flame ion detection (GC/FID) as described by Fraser et al. (29). Carbonyls collected by the C<sub>18</sub> cartridges were analyzed by liquid chromatography/UV detection as described by Grosjean et al. (30).

## **2.3 Results and Discussion**

### **2.3.1 Fine Particle Mass and Chemical Composition**

Fine particle emission rates and bulk chemical composition were found to be very similar in both meat charbroiling source tests in this study with an average fine particle mass emission rate of  $18.8 \pm 2.0$  grams per kilogram of meat cooked and an aerosol organic carbon content of  $56.6 \pm 3.3$  percent. The average emission rate is approximately half the 39.8 grams per kilogram of meat cooked reported by Hildemann et al. (31) when cooking hamburgers on the same charbroiler at longer cooking times, 7-8 minutes per burger patty as compared to the approximate 5 minute cooking duration in the current study for comparable defrosted hamburgers. The emission rate per unit of meat



charbroiled thus seems to scale approximately in proportion to cooking time on the grill, which seems logical. The fraction of organic carbon in the particle emissions in the present test is not statistically different from that measured by Hildemann et al. (31). Table 2.1 shows the average fine particle emission rate and fine particle elemental and inorganic ion composition obtained during the present meat charbroiling tests. Fine particulate matter emitted from meat charbroiling contains virtually no elemental carbon and very little inorganic matter. Potassium was measured at a level of 0.34 percent of the fine particle mass, much less than organic carbon but in a higher concentration than any of the other inorganic species which were measured. Knowledge of the potassium content of meat smoke is important because non-soil potassium has been used in the past as if it were a nearly unique tracer for woodsmoke (32). In some cases, the potassium content of meat smoke should be considered as well. Smaller quantities of nitrogen as nitrite, aluminum, silicon, phosphorus, sulfur, and chloride also were detected in meat smoke, as shown in Table 2.1.

### **2.3.2 Non-Methane Organic Compounds**

Single compound quantification of the gas-phase, semi-volatile, and particle-phase organic compound emissions was performed only on the source test which utilized defrosted hamburgers for cooking. A material balance on gas-phase and fine particulate organic compounds measured by the comprehensive dilution source sampling system during the defrosted hamburger

Table 2.1. Average Fine Particle Emission Rate and Fine Particle Chemical Composition From Meat Charbroiling. (Values shown in boldface are greater than zero by at least two standard errors).

Fine Particle Mass Emissions Rate (AVG $\pm$ STD): <b>18.8 <math>\pm</math> 2.0</b> g kg <sup>-1</sup> of Meat Cooked			
X-ray Fluorescence (Wt % of Fine Particle Mass)			
Aluminum	<b>0.039 <math>\pm</math> 0.019</b>	Selenium	0.00 $\pm$ 0.01
Silicon	<b>0.082 <math>\pm</math> 0.018</b>	Bromine	0.00 $\pm$ 0.01
Phosphorus	<b>0.066 <math>\pm</math> 0.018</b>	Rubidium	0.00 $\pm$ 0.01
Sulfur	<b>0.19 <math>\pm</math> 0.012</b>	Strontium	0.00 $\pm$ 0.01
Chlorine	<b>0.16 <math>\pm</math> 0.030</b>	Yttrium	0.00 $\pm$ 0.01
Potassium	<b>0.34 <math>\pm</math> 0.030</b>	Zirconium	0.00 $\pm$ 0.01
Calcium	0.01 $\pm$ 0.03	Molybdenum	0.00 $\pm$ 0.02
Titanium	0.02 $\pm$ 0.12	Palladium	0.00 $\pm$ 0.04
Vanadium	0.00 $\pm$ 0.05	Silver	0.01 $\pm$ 0.05
Chromium	0.00 $\pm$ 0.01	Cadmium	0.00 $\pm$ 0.05
Manganese	0.00 $\pm$ 0.01	Indium	0.00 $\pm$ 0.06
Iron	0.01 $\pm$ 0.01	Tin	0.00 $\pm$ 0.08
Nickel	0.01 $\pm$ 0.01	Antimony	0.00 $\pm$ 0.09
Copper	0.00 $\pm$ 0.01	Barium	0.02 $\pm$ 0.33
Zinc	0.00 $\pm$ 0.01	Lanthanum	0.01 $\pm$ 0.44
Gallium	0.00 $\pm$ 0.01	Mercury	0.00 $\pm$ 0.01
Arsenic	0.00 $\pm$ 0.01	Lead	0.00 $\pm$ 0.02
Elemental and Organic Carbon (Wt % of Fine Particle Mass)			
Organic Carbon	<b>33.8 <math>\pm</math> 2.0</b>	Elemental Carbon	<b>0.0 <math>\pm</math> 0.5</b>
Ionic Species by Ion Chromatography (Wt % of Fine Particle Mass)			
Chloride	<b>0.17 <math>\pm</math> 0.08</b>	Ammonium	0.00 $\pm$ 0.15
Nitrite	0.00 $\pm$ 0.06	Sodium	<b>0.37 <math>\pm</math> 0.11</b>
Nitrate	<b>0.38 <math>\pm</math> 0.01</b>	Calcium	0.00 $\pm$ 0.59
Sulfate	0.00 $\pm$ 0.10	Magnesium	0.00 $\pm$ 0.06

Notes: (a) measured by downstream of the organics denuder. Organic carbon measured on undenuded filter is 56.6 percent of fine particle mass.

charbroiling test is shown in Figure 2.2. These emissions include 14.9 grams of fine particulate organic compound mass per kg of meat cooked, 8.67 g kg<sup>-1</sup> of C<sub>2</sub>-C<sub>10</sub> volatile hydrocarbon gases, 1.0 g kg<sup>-1</sup> of higher molecular weight vapor-phase organics collected by the XAD-coated denuders, and 5.48 g kg<sup>-1</sup> of C<sub>1</sub>-C<sub>10</sub> carbonyls.

### 2.3.3 Volatile Organic Compounds

The emissions rate of non-methane C<sub>1</sub>-C<sub>10</sub> volatile organic compounds (VOC) from meat charbroiling was measured to be 13.6 grams per kilogram of meat cooked. Although the VOC emissions from charbroiling are relatively small on a mass basis compared to other urban sources, the emissions contain noticeable amounts of several very reactive light olefinic hydrocarbons. The VOC emissions were found to consist of 2.0 percent propene, 1.6 percent butenes, and 0.8 percent 1,3-butadiene by mass, accompanied by less reactive unsaturated organics including 10.5 percent ethylene and 2.4 percent acetylene. It is unclear if these olefinic compounds are formed from the meat that is being charbroiled or are formed directly from the natural gas combustion used in the charbroiler. Table 2.2 lists the contribution of 41 volatile organic compounds to the non-methane C<sub>1</sub>-C<sub>10</sub> VOC emissions from charbroiling. The quantified volatile hydrocarbons make up 30 percent of the VOC emissions and another 36 percent of the VOC emissions consist of C<sub>1</sub>-C<sub>10</sub> aldehydes.

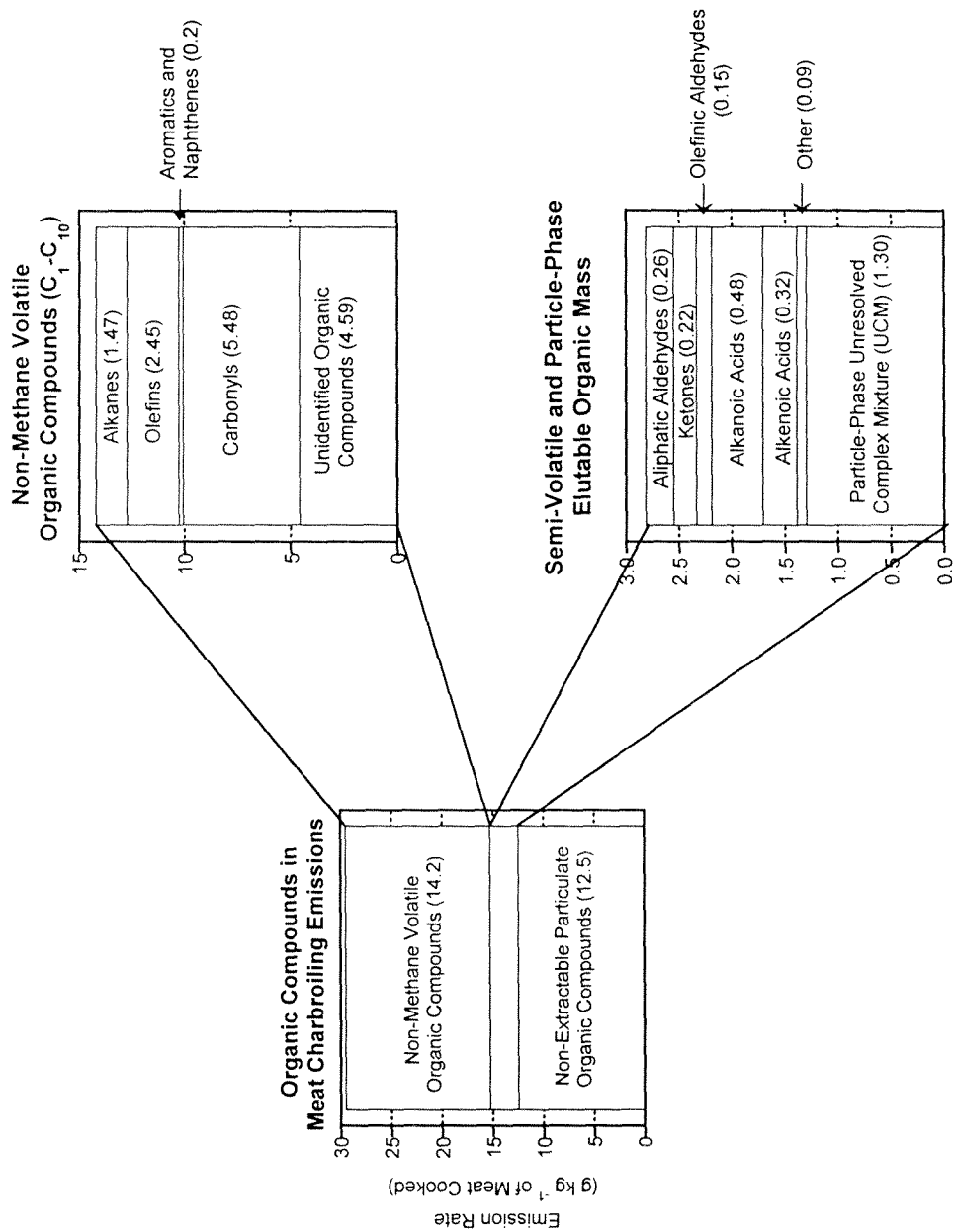


Figure 2.2. Material balance on the gas-phase, semi-volatile, and particle-phase organic compound emissions from meat charbroiling measured by the comprehensive source sampler.

Table 2.2. Organic Compound Emission Rates from Hamburger Meat Charbroiling Over a Natural Gas-Fired Grill

Compound	Gas Phase ( $\mu\text{g kg}^{-1}$ of meat cooked)			Fine Particle ( $\mu\text{g kg}^{-1}$ of meat cooked)			Total	Notes
	VOC	DNPH	XAD	Filter	PUF1	PUF2		
	Canister	Cartridge	Denuder					
n-Alkanes								
Methane	18000000						18000000	a
Ethane	663000						663000	a
Propane	190000						190000	a
n-Butane	107000						107000	a
n-Pentane	87000						87000	a
n-Hexane	44000						44000	a
n-Heptane	46000						46000	a
n-Octane	38000						38000	a
n-Nonane	13000						13000	a
n-Decane							< 5000	a
n-Tridecane			3100	330			3430	b
n-Tetradecane			3110	580	1320		5000	a
n-Pentadecane			4490	520	1240		6240	b
n-Hexadecane			3110	135			3240	a
n-Heptadecane							< 400	b
n-Octadecane			1290	160			1450	a
n-Nonadecane			400		320		720	b
n-Eicosane			1020		170		1190	a
n-Heneicosane			390	130	360		880	b
n-Docosane			450	160			610	a
n-Tricosane			500	60			560	b
n-Tetracosane			430	260			690	a
n-Pentacosane			110	380	290		780	b
n-Hexacosane				260			260	a
n-Heptacosane				650			650	b
n-Octacosane				1140			1140	a
n-Nonacosane				770			770	b
Branched alkanes								
i-Butane	54000						54000	a
i-Pentane	74000						74000	a
2,3-Dimethylbutane	5000						5000	a
2-Methylpentane	22000						22000	a
2,4-Dimethylpentane	5000						5000	a
2-Methylheptane	5000						5000	a
2,2,4-Trimethylpentane	11300						11300	a
Alkenes								
Ethene	1485000						1485000	a
Propene	289000						289000	a
1-Butene	73000						73000	a

Identification notes: a) authentic quantitative standard. b) authentic quantitative standard for similar compound in series. c) secondary standard. d) probable identification. e) analyzed as a methyl ester. +) detected but not quantified. Additional Notes: <sup>†</sup> Naphthalene and nonan-2-one are too volatile for complete collection by denuder. Mass of these compounds collected on PUF is from the gas-phase. <sup>‡</sup> Emissions shown are for two parallel sampling techniques; total is taken from denuder/filter/PUF.

Table 2.2 (continued - page 2)

Compound	Gas Phase ( $\mu\text{g kg}^{-1}$ of meat cooked)			Fine Particle ( $\mu\text{g kg}^{-1}$ of meat cooked)			Total	Notes
	VOC	DNPH	XAD	Filter	PUF1	PUF2		
	Canister	Cartridge	Denuder					
Branched alkenes								
i-Butene	159000						159000	a
Diolefins								
1,3-Butadiene	105000						105000	a
Alkynes								
Ethyne(Acetylene)	336000						336000	a
Saturated Cyclic Hydrocarbons								
Cyclopentane	5000						5000	a
Methylcyclopentane	9000						9000	a
Cyclohexane							< 5000	a
Methylcyclohexane	13000						13000	a
Biogenic hydrocarbons								
Isoprene	3000						300	a
Squalene				342			342	a
Aromatic hydrocarbons								
Benzene	83000						83000	a
Toluene	40000						40000	a
Ethylbenzene	11000						11000	a
m-Xylene + p-Xylene	12000						12000	a
Styrene							< 5000	a
o-Xylene	11000						11000	a
1,3,5-Trimethylbenzene							< 5000	a
1,2,4-Trimethylbenzene	24000						24000	a
Naphthalene †			5860		1690	1440	8990	a
Phenanthrene			1120	34	90		1220	a
Anthracene			110	51			160	a
Fluoranthene			400	120			520	a
Pyrene			570	100			670	a
Chrysene/Triphenylene			330	270			600	a
Aliphatic aldehydes								
Formaldehyde		1382000					1382000	a
Acetaldehyde		1092000					1092000	a
Propanal		504000					504000	a
Butanal/Isobutanal		373000					373000	a
Hexanal		203000					203000	a
Heptanal		125000					125000	a
Octanal		146000					146000	a
Nonanal ‡		141000	115000	32700			148000	a
Decanal ‡		70000	29500	4060			33600	a

Identification notes: a) authentic quantitative standard. b) authentic quantitative standard for similar compound in series. c) secondary standard. d) probable identification. e) analyzed as a methyl ester. +) detected but not quantified. Additional Notes: † Naphthalene and nonan-2-one are too volatile for complete collection by denuder. Mass of these compounds collected on PUF is from the gas-phase. ‡ Emissions shown are for two parallel sampling techniques; total is taken from denuder/filter/PUF.

Table 2.2 (continued - page 3)

Compound	Gas Phase ( $\mu\text{g kg}^{-1}$ of meat cooked)			Fine Particle ( $\mu\text{g kg}^{-1}$ of meat cooked)			Total	Notes
	VOC	DNPH	XAD	Filter	PUF1	PUF2		
	Canister	Cartridge	Denuder					
Aliphatic aldehydes								
Undecanal †		35000	13600	3550			17200	a
Dodecanal †		38000	26200	3830			30000	a
Tridecanal			15300	2680			18000	a
Tetradecanal			14400	3580			18000	a
Pentadecanal			12850	1570			14400	b
Hexadecanal			3490				3490	b
Heptadecanal			2510				2510	b
Dicarbonyls								
Glyoxal		550000					550000	a
Methylglyoxal		334000					334000	a
Biacetyl		28000					28000	a
Ketones								
Nonan-2-one †			55700		15400	6200	77300	c
Decan-2-one			65500	10000			75500	c
Undecan-2-one			107000	3430			107000	c
Tridecan-2-one			39000	3250			42300	c
Tetradecan-2-one			61900	3400			65300	c
Pentadecan-2-one			64500	5200			69700	c
Heptadecan-2-one			21300	1680			23000	c
Unsaturated carbonyls								
Crotonaldehyde		495000					495000	a
Methacrolein		52000					52000	a
2-Decenal			98200	5950			104000	a
2-Undecenal			80600	5530			86100	a
n-Alkanoic acids								
Heptanoic acid			26000	6190			32200	a,c
Octanoic acid			29400	9290			38700	a,c
Nonanoic acid			42400	6030			48400	a,e
Decanoic acid			8890	2220			11100	a,e
Dodecanoic acid			4610	1850			6460	a,c
Tetradecanoic acid			4040	17700			21700	a,e
Pentadecanoic acid			220	5750			5970	a,e
Hexadecanoic acid			11400	163000			174000	a,e
Heptadecanoic acid				10300			10300	a,e
Octadecanoic acid			2150	96900			96100	a,e
Nonadecanoic acid				600			600	a,e
Eicosanoic acid				860			860	a,e
Docosanoic acid				350			350	a,e

Identification notes: a) authentic quantitative standard. b) authentic quantitative standard for similar compound in series. c) secondary standard. d) probable identification. e) analyzed as a methyl ester. +) detected but not quantified. Additional Notes: † Naphthalene and nonan-2-one are too volatile for complete collection by denuder. Mass of these compounds collected on PUF is from the gas-phase. ‡ Emissions shown are for two parallel sampling techniques; total is taken from denuder/filter/PUF.

Table 2.2 (continued - page 4)

Compound	Gas Phase ( $\mu\text{g kg}^{-1}$ of meat cooked)			Fine Particle ( $\mu\text{g kg}^{-1}$ of meat cooked)			Total	Notes
	VOC	DNPH	XAD	Filter	PUF1	PUF2		
	Canister	Cartridge	Denuder					
n-Alkenoic acids								
9-Hexadecenoic acid				18400			18400	b,e
9-Octadecenoic acid				214000			214000	a,e
9,12-Octadecadienoic acid				32000			32000	a,e
Alkanedioic acids								
Hexanedioic acid				1990			1990	a,e
Octanedioic acid				3900			3900	a,e
Furanones ( $\gamma$ -Lactones)								
5-Ethylidihydro-2(3H)-furanone			6490	2850			9370	a
5-Propylidihydro-2(3H)-furanone			7020	1800			8820	b
5-Butylidihydro-2(3H)-furanone			9540	1420			11000	a
5-Pentylidihydro-2(3H)-furanone			4770	1290			6060	b
5-Hexylidihydro-2(3H)-furanone			3120	920			4040	a
5-Heptyldihydro-2(3H)-furanone				390			390	b
5-Octylidihydro-2(3H)-furanone				480			480	b
5-Nonyldihydro-2(3H)-furanone				800			800	b
5-Decylidihydro-2(3H)-furanone				1750			1750	b
5-Undecylidihydro-2(3H)-furanone				780			780	b
5-Dodecylidihydro-2(3H)-furanone				670			670	b
Other Compounds								
Cholesterol				3970			3970	a
Hexadecanamide				+				d
Octadecanamide				+				d
9-Octadecenamide				+				d
Unresolved Complex Mixture				1300000			1300000	

Identification notes: a) authentic quantitative standard. b) authentic quantitative standard for similar compound in series. c) secondary standard. d) probable identification. e) analyzed as a methyl ester. +) detected but not quantified. Additional Notes: <sup>†</sup> Naphthalene and nonan-2-one are too volatile for complete collection by denuder. Mass of these compounds collected on PUF is from the gas-phase. <sup>‡</sup> Emissions shown are for two parallel sampling techniques; total is taken from denuder/filter/PUF.



Formaldehyde and acetaldehyde are emitted from meat cooking operations at 1.38 and 1.09 grams per kg of meat cooked which is higher than all other emissions rates for individual VOC's except ethylene. Propanal, crotonaldehyde, and glyoxal are also emitted in significant quantities at 0.50, 0.50 and 0.55 grams  $\text{kg}^{-1}$  of meat cooked. The emissions of these carbonyls adds significantly to the reactivity of the VOCs emitted from meat cooking operations.

#### **2.3.4 Semi-Volatile and Particle Phase Organic Compounds**

Seventy-one vapor-phase semi-volatile and particle-phase organic compounds have been quantified in samples collected on the denuders, filters, and PUFs during the charbroiled meat cooking test as shown in Table 2.2. n-Alkanoic acids, n-alkenoic acids, and carbonyls make up a significant fraction of the semi-volatile and particle-phase organic compounds emitted from meat charbroiling that are extractable and elutable. 9-Octadecenoic acid (oleic acid) and n-hexadecanoic acid (palmitic acid) are emitted at by far the largest rates, with average emissions of 214,000 and 174,000  $\mu\text{g kg}^{-1}$  of meat cooked, respectively. n-Alkanoic acids as light as n-heptanoic acid and as heavy as n-docosanoic acid have been identified and quantified.

Significant quantities of heavy aliphatic n-aldehydes and alkan-2-ones also are found in the meat cooking exhaust, spanning the range from nonanal to heptadecanal and nonan-2-one to heptadecan-2-one. In addition, two semi-

volatile olefinic aldehydes have been identified and quantified, 2-decenal and 2-undecenal. 2-Decenal and 2-undecenal have been previously identified in the head space vapor of heated peanut oil (33). Grosjean et al. (30) measured the atmospheric concentration of aliphatic aldehydes spanning the range from formaldehyde through tetradecanal in the South Coast Air Basin of California during a period of poor air quality and found noticeable quantities of the high molecular weight aliphatic aldehydes. They also showed that the chemical reactivity of the high molecular weight aldehydes taken as a group was comparable to that of formaldehyde or acetaldehyde separately. Although low molecular weight aldehydes are known to be both emitted by primary sources of air pollution as well as formed by chemical reaction in photochemical smog (34), the origin of the high molecular weight aliphatic aldehydes in the urban atmosphere has been unknown. We now know from the present study that the high molecular weight aldehydes are emitted in large quantities from meat charbroiling. Food preparation could be a significant contributor to the high molecular weight aldehydes and hence to the photochemical reactivity of the urban atmosphere. Other sources (e.g., the cooking oil fumes mentioned above) should be sought as well through further source testing. Figure 2.3 shows the distribution of emissions for semi-volatile and particle-phase fatty acids (n-alkanoic acids and alkenoic acids) and carbonyls, as well as the low molecular weight gas-phase carbonyls measured by the DNPH impregnated C<sub>18</sub> cartridges.

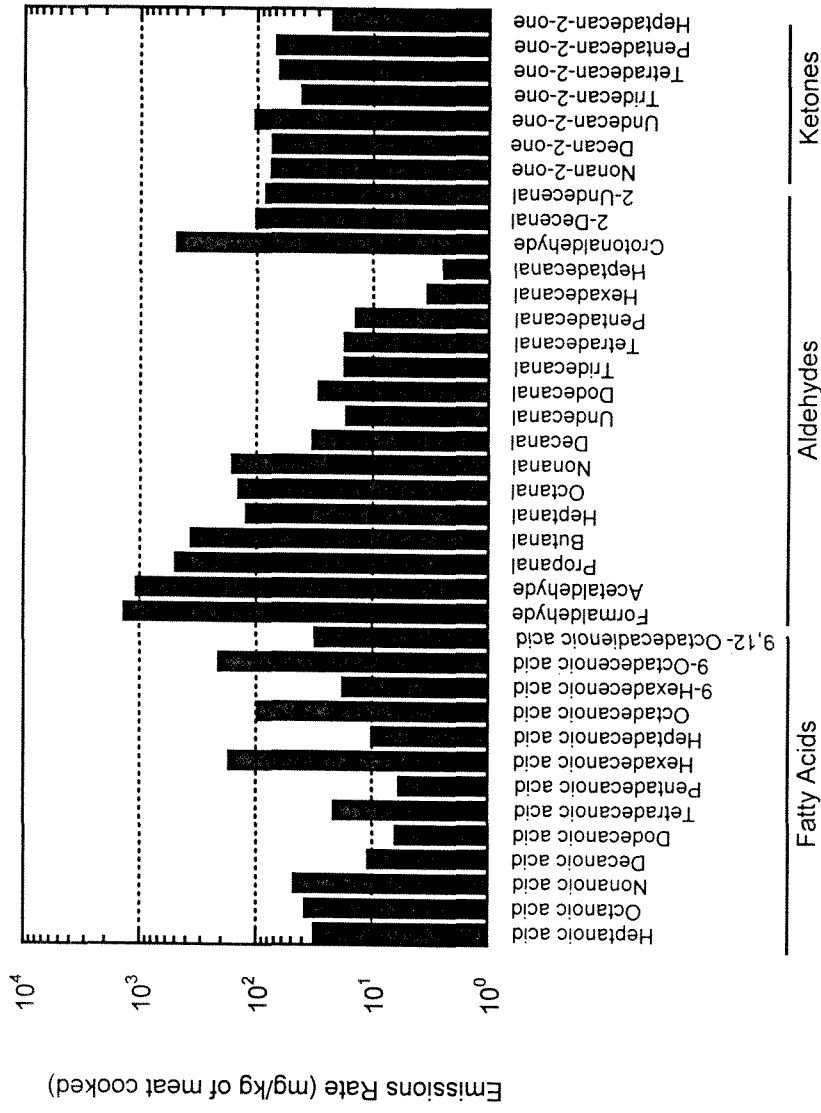


Figure 2.3. Emission rates of fatty acids and carbonyls from meat charbroiling operations.

n-Alkanes, low molecular weight PAH, and alkanedioic acids also are present in the meat charbroiling emissions. In addition, squalene and cholesterol were found at levels of approximately 342 and 3970  $\mu\text{g kg}^{-1}$  of meat cooked, respectively.

As previously indicated, the fine particle mass emission rate per unit of meat cooked as measured by Hildemann et al. (31) when charbroiling meat for approximately twice the cooking time used here, was reported to be approximately twice the emission rate per hamburger patty cooked in the current study. The individual organic compounds present in the particle phase during the meat charbroiling source tests conducted by Hildemann et al. (31) were reported by Rogge et al. (21). The individual organic compound emission rates normalized to fine particle organic carbon emissions for the test conducted by Hildemann et al. (31) averaged  $1.12 \pm 0.21$  (mean  $\pm$  standard deviation of the mean) times those observed in the current study. Thus the relative chemical composition of the particulate organic compounds measured in the two sets of tests are found to be quite similar. The earlier tests of Hildemann et al. (31) lack vapor phase and semi-volatile compound emissions data so no comparison is possible in these cases.

### 2.3.5 Comparison Between Measurement Methods for Semi-Volatile Organics

The total mass emission rate of each individual organic compound determined from the denuder/filter/PUF sampling train showed good agreement with the total mass emission rate determined from the filter/PUF sampling train. Figure 2.4 provides a comparison of the total measured emission rates obtained by the two sampling methods for individual compounds within the following compound classes: alkanolic acids, alkenolic acids, aldehydes, ketones, PAH, lactones, and alkanes.

The distribution between the gas- and particle-phase of each of the 71 organic semi-volatile and particle-phase organic compounds which were identified and quantified by the denuder/filter/PUF sampling train is given in Table 2.2. The phase distribution of the lactones, the carbonyls, and the n-alkanoic acids as measured by the denuder/filter/PUF sampling train is compared to the filter/PUF sampling train in Figure 2.5. The compounds that are quantified in Table 2.2 but not shown in Figure 2.5 are either completely in one phase or are not measured at concentrations high enough to obtain a good description of their phase distributions by either method. For the denuder/filter/PUF sampling train the gas-phase fraction of each compound is taken as the fraction of that compound collected on the XAD-coated denuder, while the particle-phase fraction is the fraction collected on the combined filter plus PUF samples. In the case of the filter/PUF sampling train, the fraction of the

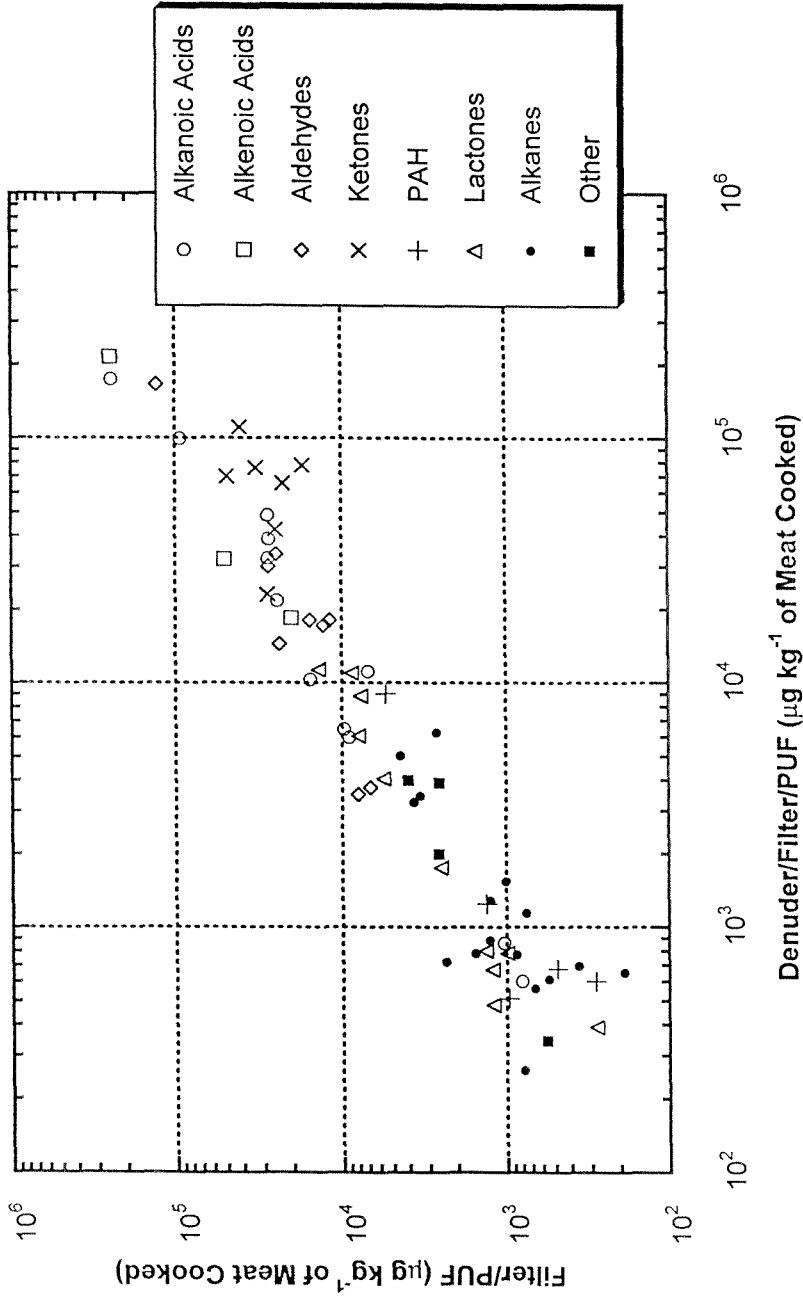


Figure 2.4. Comparison of the total mass of individual organic compounds collected by the denuder/filter/PUF and filter/PUF sampling trains during the charbroiled meat cooking source tests.

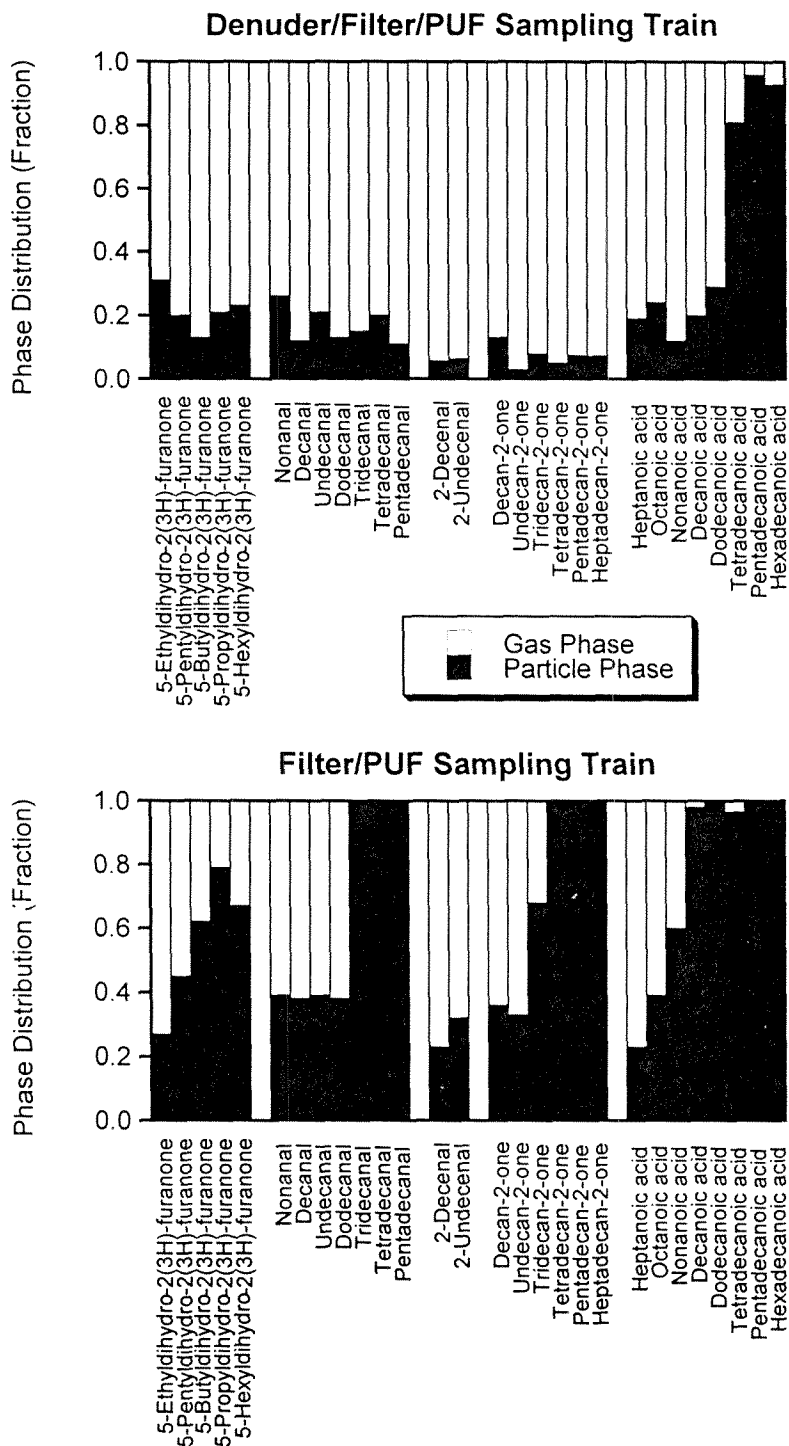


Figure 2.5. The distribution of organic compounds between the gas-phase and particle-phase in the diluted exhaust from meat charbroiling as measured by the denuder/filter/PUF and filter/PUF sampling trains.

mass collected on the filter is taken as the particle-phase portion and the gas-phase fraction is the fraction collected on the two PUFs in series located downstream of the filter.

Although the total compound masses collected by the two sampling trains show good agreement, there are significant differences in the phase distributions measured by the two sampling methods when operated simultaneously in parallel. As seen in Figure 2.5, the fraction of compound mass measured to be in the particle phase by the filter/PUF sampling system is much greater than observed by the denuder/filter/PUF sampling system for the higher molecular weight compounds in each of the compound classes. The likely explanation for this observation is that adsorption of vapor-phase semi-volatile organic compounds occurs on the filter as those vapors first pass over the filter in the filter/PUF sampling train. As seen in Figure 2.5, virtually complete sorption of the vapor-phase semi-volatile organic compounds onto the filter in the filter/PUF system occurs for the highest molecular weight species in each group. This finding has significant implications for the interpretation of the low OC loading that was found on the back-up quartz fiber filter of the tandem EC/OC filter stack. The back-up filter only contained 2.0 percent of the organic carbon found on the front filter. Traditionally, this might have been interpreted to mean that the potential for sampling artifacts was low since there was little vapor phase material collected on the back-up filter. Instead just the opposite was true: the



artifact is so great that certain vapor phase species do not pass through the filter at all. This suggests that the use of the back-up filter as a measure of the adsorption to the front filter may not be applicable when taking source samples from sources similar to meat smoke exhaust.

### 2.3.6 Gas/Particle Partitioning: Experiment Versus Theory

Gas/particle partitioning theory (3, 35, 36) holds that the phase distribution of a semi-volatile organic compound is determined by its absorption into the particle phase matrix, and that this phase distribution can be described by a partitioning coefficient,  $K_{p,opm}$ , defined as:

$$K_{p,opm} = \frac{F/OPM}{A} \quad (1)$$

where  $K_{p,opm}$  is the gas/particle partitioning coefficient based on organic particulate matter as the receiving particle phase substrate in units of  $\text{m}^3 \mu\text{g}^{-1}$ .  $F$  is the particle-associated mass concentration of the semi-volatile organic compound of interest in  $\mu\text{g}/\text{m}^3$ ,  $OPM$  is the total organic particulate matter concentration into which the compound can partition in  $\mu\text{g}/\text{m}^3$ , and  $A$  is the gas-phase mass concentration of the compound of interest in  $\mu\text{g}/\text{m}^3$ . It is expected that the gas/particle partitioning coefficient,  $K_{p,opm}$ , will depend on the vapor pressure of the various organic compounds (36):

$$\text{Log}(K_{p, \text{opm}}) = m_{r, \text{opm}} \text{Log}(p_L^0) + b_{r, \text{opm}} \quad (2)$$

where  $p_L^0$  is the vapor pressure over a liquid pool of the semi-volatile organic compound of interest in torr, and  $m_{r, \text{opm}}$  and  $b_{r, \text{opm}}$  are coefficients that can be estimated by regressing a series of experimentally measured values of  $K_{p, \text{opm}}$  on the corresponding liquid vapor pressure values,  $p_L^0$ , for the members of a given organic compound class. If the compounds have similar activity coefficients when present in the particulate organic matrix and the partitioning process has reached equilibrium, then  $-m_{r, \text{opm}}$  should be close to unity. Under this condition,  $b_{r, \text{opm}}$  is a constant characteristic of the partitioning for that class of compounds with the specific particle matrix.

Figure 2.6 shows the gas/particle partitioning of the alkanolic acids during these source tests as a function of the vapor pressure of each of the organic acids as measured by the filter/PUF and the denuder/filter/PUF sampling trains. The best fit curve through the denuder/filter/PUF data has a slope of -0.62, suggesting that the partitioning is not at equilibrium as described by Pankow and Bidleman (4). This suggests that the semi-volatile organic compounds have not equilibrated between the gas and particle phases either because of insufficient residence time or because the mass transfer between phases is inhibited. In similar measurements made while testing the emissions from cooking with lighter

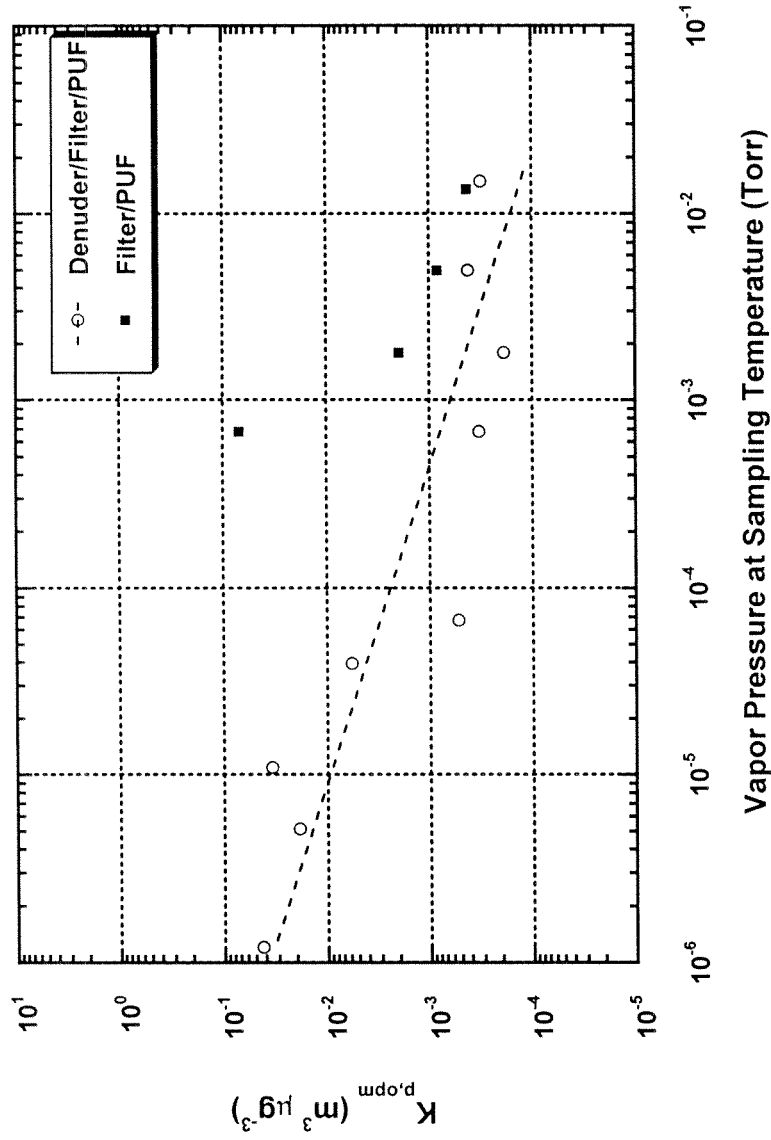


Figure 2.6. Partitioning coefficient,  $K_{p,opm}$ , for the n-alkanoic acids in the diluted exhaust from meat charbroiling operations as measured by the denuder/filter/PUF and filter/PUF sampling train plotted as a function of the vapor pressure of the pure compounds.

seed oils, the n-alkanoic acids were found to be partitioned as would be predicted at equilibrium (see Chapter 3). In those tests, the seed oil cooking samples had significantly less time to equilibrate than did the charbroiled meat cooking exhaust prior to sampling. For this reason it seems likely that the semi-volatile organic compounds in the charbroiled meat exhaust are inhibited from transferring to the gas phase from the particle phase or into the particle phase from the gas phase. The fact that the mass transfer to and from the meat smoke particles may be inhibited is consistent with the possibly solid character of meat fat at room temperature; meat fat is a major constituent in the diluted particle mass emissions from meat charbroiling.

The phase distribution of the n-alkanoic acids measured by the filter/PUF sampling train during the meat charbroiling test is also shown in Figure 2.6. The phase distribution measured by the filter/PUF system is significantly shifted as compared to the phase distribution measured by the denuder/filter/PUF system. All of the n-alkanoic acids have been found in much higher percentages on the filter when sampled by the filter/PUF method. In fact, all of the n-alkanoic acids with vapor pressures less than n-decanoic acid are not even detected on the PUF downstream of the particle filter in the filter/PUF system. This again suggests that a strong filter adsorption artifact exists for the n-alkanoic acids within a meat smoke matrix when sampled by the filter/PUF method.

## 2.4 References

1. Rogge, W. R.; Hildemann, L. M.; Mazurek, M. A.; Cass, G. R.; Simoneit, B. R. T. *J. Geophys. Res.* **1996**, 101, 19379-19394.
2. Gray, H. A.; Cass, G. R. *Atmos. Environ.* **1998**, in press.
3. Schauer, J. J.; Rogge, W. R.; Hildemann, L. M.; Mazurek, M. A.; Cass, G. R.; Simoneit, B. R. T. *Atmos. Environ.* **1996**, 30, 3837-3855.
4. Pankow, J. F.; Bidleman, T. F. *Atmos. Environ.* **1992**, 26A, 1071-1080.
5. Odum, J. R.; Hoffmann, T.; Bowman, F.; Collins, D.; Flagan, R. C.; Seinfeld, J. H. *Environ. Sci. Technol.* **1996**, 30, 2580-2585.
6. Pandis, S. N.; Harley, R. A.; Cass, G. R.; Seinfeld, J. H. *Atmos. Environ.* **1992**, 26A, 2269-2282.
7. Hildemann, L. M.; Cass, G. R.; Markowski, G. R. *Aerosol Sci. Technol.* **1989**, 10, 193-204.
8. John, W.; Reischl, G. *JAPCA* **1980**, 30, 872-876.
9. Gundel, L. A.; Lee, V. C.; Mahanama K. R. R.; Stevens R. K.; Daisey J. M. *Atmos. Environ.* **1995**, 29, 1719-1733.

10. Ye, Y.; Tsai, C.; Pui, D. Y. H. *Aerosol Sci. Technol.* **1991**, 14, 102-111.
11. Kamens, R. M.; Zhi-Hua, F.; Yao, Y.; Chen, D.; Chen, S.; Vartianen, M. *Chemosphere* **1994**, 28, 1623-1632.
12. Bidleman, T. F.; Simon, G. C.; Burdick, N. F.; You, F. *J. Chromat.* **1984**, 301, 448-453.
13. Birch, M. E.; Cary, R. A. *Aerosol Sci. Technol.* **1996**, 25, 221-241.
14. Gray, H. A.; Cass, G. R.; Hunzicker, J. J.; Heyerdahl, E. K.; Rau, J. A. *Environ. Sci. Technol.* **1986**, 20, 580-589.
15. Hart, K. M.; Pankow, J. F. *Environ. Sci. Technol.* **1994**, 28, 655-661.
16. Dzubay, T. G. *X-ray Analysis of Environmental Samples*, **1977**, Ann Arbor Science, Ann Arbor, MI.
17. Mueller, P. K.; Mendoza, B. V.; Collins, J. C.; Wilgus, E. A. "Application of Ion Chromatography to the Analysis of Anions Extracted from Airborne Particulate Matter," In *Ion Chromatographic Analysis of Environmental Pollutants*, **1978**, Sawicki, E.; Mulik, J. D.; Wittgenstein, E. Eds.; Ann Arbor Science, Ann Arbor, MI, pp. 77-86.
18. Solorzano, L. *Limnol. Oceanogr.* 1969, 14, pp. 799-801.

19. Grosjean, E.; Grosjean, D. *Int. J. Envir. Anal. Chem.* **1995**, 61, 343-360.
20. Mazurek, M. A., Simoneit, B. R. T.; Cass, G. R.; Gray, H. A. *Int. J. Envir. Anal. Chem.* **1987**, 29, 119-139.
21. Rogge, W. R.; Hildemann, L. M.; Mazurek, M. A.; Cass, G. R.; Simoneit, B. R. T. *Environ. Sci. Technol.* **1991**, 25, 1112-1125.
22. Rogge, W. R.; Mazurek, M. A.; Hildemann, L. M.; Cass, G. R.; Simoneit, B. R. T. *Atmos. Environ.* **1993**, 27, 1309-1330.
23. Rogge, W. R.; Hildemann, L. M.; Mazurek, M. A.; Cass, G. R.; Simoneit, B. R. T. *Environ. Sci. Technol.* **1993**, 27, 636-651.
24. Rogge, W. R.; Hildemann, L. M.; Mazurek, M. A.; Cass, G. R.; Simoneit, B. R. T. *Environ. Sci. Technol.* **1993**, 27, 1892-1904.
25. Rogge, W. R.; Hildemann, L. M.; Mazurek, M. A.; Cass, G. R.; Simoneit, B. R. T. *Environ. Sci. Technol.* **1993**, 27, 2700-2711.
26. Rogge, W. R.; Hildemann, L. M.; Mazurek, M. A.; Cass, G. R.; Simoneit, B. R. T. *Environ. Sci. Technol.* **1993**, 27, 2736-2744.
27. Rogge, W. R.; Hildemann, L. M.; Mazurek, M. A.; Cass, G. R.; Simoneit, B. R. T. *Environ. Sci. Technol.* **1994**, 28, 1375-1388.

28. Rogge, W. R. Ph.D. Thesis, California Institute of Technology, Pasadena, CA, **1993**.
29. Fraser, M. P.; Cass G. R.; Simoneit B. R. T.; Rasmussen R. A. *Environ. Sci. Technol.* **1997**, 31, 2356-2367.
30. Grosjean, E.; Grosjean, D.; Fraser M. P.; Cass G. R. *Environ. Sci. Technol.* **1996**, 30, 2687-2703.
31. Hildemann, L. M.; Markowski, G. R.; Cass, G. R. *Environ. Sci. Technol.* **1991**, 25, 744-759.
32. Sheffield, A. E.; Gordon, G. E.; Currie, L. A.; Riedder, G. E. *Atmos. Environ.* **1994**, 28, 1371-1384.
33. Chung, T. Y.; Eiserich, J. P.; Shibamoto, T. *J. Agric. Food Chem.* **1993**, 1467-1470.
34. Harley, R. A.; Cass, G. R. *Atmos. Environ.* **1995**, 29, 905-922.
35. Pankow, J. F. *Atmos. Environ.* **1994**, 28, 185-188.
36. Liang, C.; Pankow, J. F. *Environ. Sci. Technol.* **1996**, 30, 2800-2805.



## Chapter 3

# Organic Compounds from Cooking with Seed Oils

### 3.1 Introduction

The C<sub>16</sub> and C<sub>18</sub> fatty acids (n-alkanoic acids and n-alkenoic acids) are among the most prominent single organic compounds found in the urban atmospheric fine particulate mixture (1). These particle phase acids are known to be emitted from many sources such as meat cooking operations, wood combustion, motor vehicle exhaust, and road dust (2), but air pollution modeling results for the Los Angeles Basin indicate that there must be additional as yet unquantified sources of these compounds (3, 4). Seed oils are comprised largely of esters of n-alkanoic acids (5) and fatty acids have been identified in the exhaust from heated seed oils (6). Thus, they are a likely source of the missing fatty acids emissions which could arise from food cooking operations employing seed oils. In addition, the role of the gas phase, semi-volatile and particle phase organic compounds from food frying operations in photochemical smog and secondary aerosol formation has not been evaluated largely due the lack of emissions data for sources of this type. To this end, the emissions from cooking with seed oils are investigated in the present study.

## 3.2 Experimental Methods

### 3.2.1 Comprehensive Source Sampling

The seed oil cooking emissions tests reported here were conducted using a large institutional-scale deep fryer and a large industrial-scale electric grill operated by professional chefs as they prepared commercially distributed food products. Emissions were sampled downstream from the filters and grease extractors located in the ventilation system above the appliances. The overall exhaust system was operated at an air flowrate of  $400 \text{ m}^3 \text{ min}^{-1}$  and provided sufficient dilution with ambient air to bring the food cooking effluents to ambient temperature prior to collection of source samples. The diluted source effluent was withdrawn from the kitchen vent stack through AIHL-design cyclone separators (7) which were operated at flowrates such that coarse particles with aerodynamic diameters greater than  $1.8 \text{ }\mu\text{m}$  were trapped while fine particles and gases passed through the cyclone separator. Fine particle emissions data are emphasized in the present study, because such data are needed for use in the development of urban and regional emissions control strategies for fine particles that will be required under the newly adopted National Ambient Air Quality Standard for fine particulate matter in the United States (8).

Semi-volatile and fine particle-phase organic compounds were collected directly from the exhaust vent using both a denuder/filter/PUF sampling train and a filter/PUF sampling train. The details of these sampling configurations are described in Chapter 2. The filter/PUF samples collected during the seed oil cooking tests were not analyzed as part of this study and have been stored for use in future research projects. Fine particulate matter, carbonyls, organic acids, and gas phase hydrocarbons were also collected during these tests by the same cyclone-based unit as described in Chapter 2.

The ambient air entrained into the exhaust hood above the appliances contained low concentrations of background contaminants that must be subtracted from the source effluent. These background semi-volatile and particle phase organic compound concentrations were sampled from the ambient air in the kitchen by a filter/PUF sampling train. As discussed in Chapter 2, the total mass of each individual organic compound collected by the denuder/filter/PUF sampling train agreed well with the total mass collected by the filter/PUF sampling train. Fine particle mass, fine particle bulk elemental composition, carbonyls, organic acids, and gas phase hydrocarbons present in the background air were measured by use of a sampling train that duplicates the measurements made in the stack above the cooking appliances.

### 3.2.2 Source Testing Procedure

The vegetable stir frying source tests were conducted on an industrial-size electric grill using a commercially distributed mixture of precut broccoli, red and green peppers, celery, and onions (Ingardia Brothers Produce Inc., Costa Mesa, CA). Soybean oil (Vons Company Inc., Los Angeles, CA) was used for one test and canola oil (Cargill Foods, Minneapolis, MN) was used for the other vegetable stir fry source test. Both the soybean oil and the canola oil tests were conducted while stir frying 22.6 kg of vegetables using approximately 1.5 liters of seed oil and 3 kg of stir fry sauce (Chef Mate, Nestles; main ingredients: water, soy sauce, high fructose corn syrup, sherry, vegetable oil, and modified food starch) over a period of one hour. The denuder/filter/PUF sampling train was operated throughout the stir fry source tests except for the approximately 1 minute required to replace the denuder in the middle of the test. The full suite of chemical measurements described above was made during the soybean oil source test while all measurements except for gas-phase volatile hydrocarbons and fine particle trace elements and ionic species were made during the canola oil stir fry source test.

The deep fried potatoes source test was conducted using an industrial scale deep fryer at 175 °C which was filled with commercial hydrogenated soybean oil (Creamy Liquid Shortening, Kraft Food Service, Preferred). The

hydrogenated soybean oil in the deep fryer during the source test had been in use for several days of cooking prior to the tests and was considered relatively fresh by the cooking staff. Sixty-eight kilograms of deep frying potatoes (Kraft 3/8 inch Grade A fancy, Frozen) were cooked in 1.13 kg batches in two parallel fryers operating simultaneously over a period of 75 minutes by placing the frozen potatoes directly in the hot cooking oil. The denuder/filter/PUF sampling train was operated for two 30-minute time periods during the cooking test, while all other sampling equipment was operated continuously throughout the test. Gas-phase volatile hydrocarbons and fine particle trace elements and ionic species measurements were not made during the deep fried potatoes cooking source test.

### **3.2.3 Organic Chemical Analysis**

The extraction procedure employed for semi-volatile organic compounds collected on XAD-coated annular denuders and PUF cartridges, as well as particle-phase organic compounds collected on quartz fiber filters, are discussed in Chapter 2. The extracts collected on these substrates were reduced in volume to approximately 250  $\mu$ l and were then split into two fractions. One fraction was derivatized with diazomethane to convert organic acids to their methyl ester analogs.

Filter, PUF, and denuder field blanks were analyzed with each set of source samples. The field blanks were prepared, stored and handled by exactly the same procedures as used for the source samples.

Both the derivatized and underivatized sample fractions are analyzed by GC/MS on a Hewlett-Packard GC/MSD (GC Model 5890, MSD Model 5972) using a 30 m by 0.25 mm diameter HP-1701 capillary column (Hewlett-Packard). 1-Phenyldodecane was used as a co-injection standard for all sample extracts and standard runs. The deuterated internal standards were used to determine extraction recovery for the compounds quantified in the underivatized samples, and the deuterated acids were used to verify that the diazomethane reactions were driven to completion. In addition, the deuterated n-alkanoic acid recoveries were used in conjunction with the recovery of deuterated tetracosane to determine the recovery of the compounds quantified in the derivatized fraction.

Hundreds of authentic standards have been prepared for the positive identification and quantification of the organic compounds found in the current source test program. When quantitative standards could not be obtained for a given compound or compound class, significant effort was made to obtain a non-quantitative secondary standard that could be used for unique identification of the organic compounds. Quantification of compounds identified using

secondary standards has been estimated based on the response factors for compounds having similar retention times and chemical structures.

Total non-methane organic gases (NMOG, EPA method TO12) and individual organic vapor phase hydrocarbons ranging from C<sub>1</sub> to C<sub>10</sub> were analyzed from the SUMA canisters by gas chromatography/flame ionization detection (GC/FID). Carbonyls collected by the C<sub>18</sub> impregnated cartridges were analyzed by liquid chromatography/UV detection.

### **3.3 Results and Discussion**

A material balance for the gas-phase and fine particle-phase organic compounds emitted from stir frying vegetables in soybean oil is shown in Figure 3.1. The total mass of organic carbon in the particle phase was measured from one of the quartz fiber filters located downstream of the XAD coated denuder. Organic compound mass was obtained by assuming a ratio of 1.4 between organic compound mass and organic carbon. Of the 15.7 mg of fine particle-phase organic compound mass emitted per kg of vegetables cooked during the soybean oil-based vegetable stir fry test, 82% of the mass is composed of free fatty acids (n-alkanoic acids and n-alkenoic acids). n-Alkanes and olefinic n-aldehydes make up smaller but noticeable portions of the mass emitted. It should be noted that virtually all of the fine particle mass can be identified at the single compound level. A similar mass balance can be constructed for the

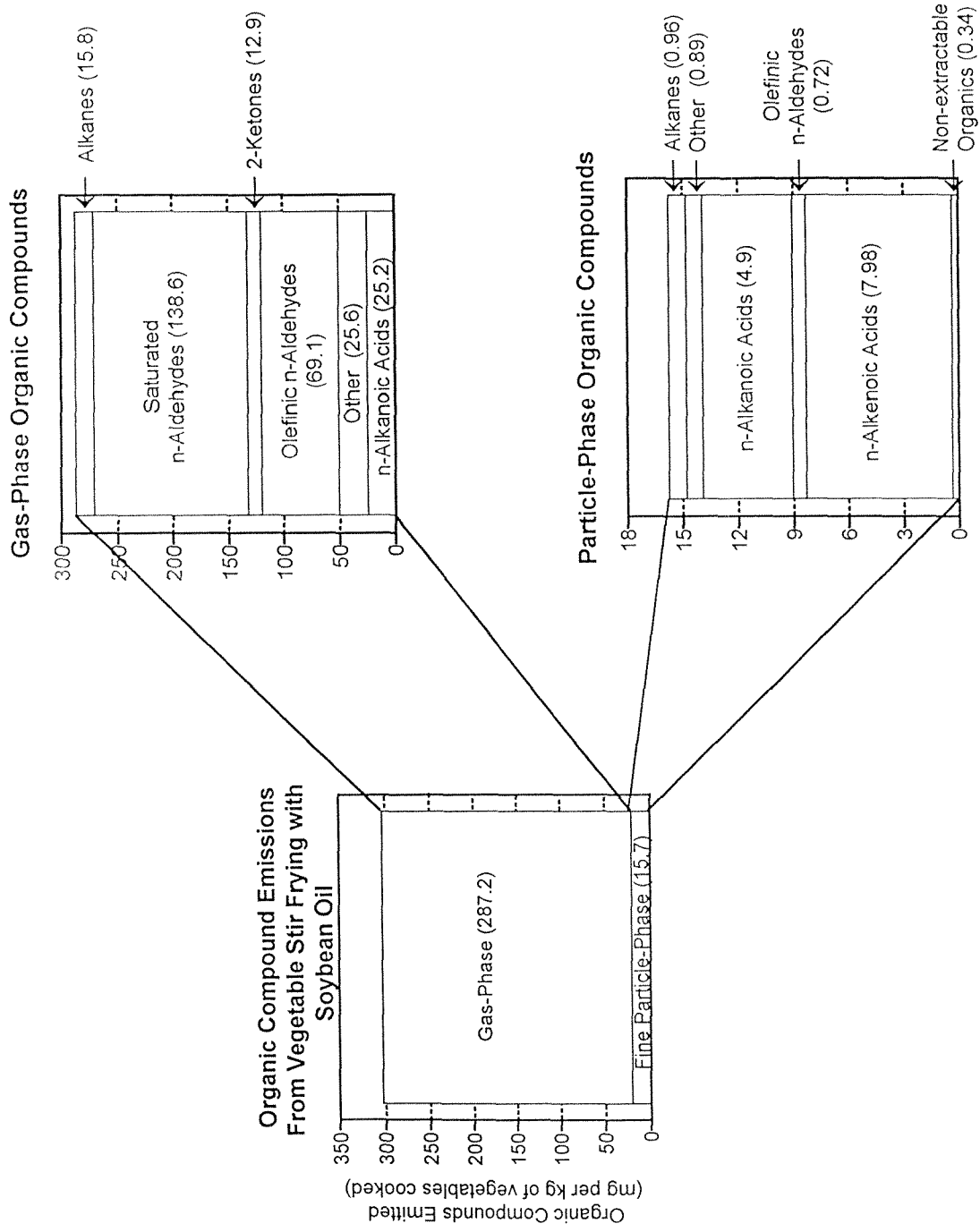


Figure 3.1. Material balance on the gas-phase, semi-volatile, and particle phase organic compounds emitted from stir frying vegetables in soybean oil.



fine particulate matter emitted during the canola oil based stir fry and the deep fried potatoes source tests, and one finds that the free fatty acids also make up a major portion of the particle mass. The total fraction of the fine particle organic compound mass that can be identified on a single compound level for the canola oil based stir fry test and the deep frying of potatoes test are 83% and 73%, respectively.

The gas-phase organic compound emissions from stir frying vegetables in soybean oil are dominated by carbonyls, as shown in Figure 3.1. A total of 242 mg of carbonyls are emitted per kg of vegetables cooked, which accounts for 84 percent of the mass of quantified gas-phase organic compound emissions. Gas-phase n-alkanoic acids contribute the next largest fraction of the gas-phase emissions, accounting for 25.2 mg per kg of vegetables cooked. Although the  $C_7^+$  gas-phase n-alkanoic acids measured make up only 9.5% of the gas phase organic compound emissions, these gas-phase n-alkanoic acids emissions are more than 5 times greater than the emissions of higher molecular weight fine particulate n-alkanoic acids.

Gas-phase carbonyl emissions were measured at 252 and 108 mg per kg of vegetables cooked for stir frying in canola oil and deep frying in hydrogenated soybean oil, respectively. The total mass of  $C_7^+$  gas-phase emissions of n-alkanoic acids is known based on analysis of the denuder samples, and is found to account for 18.8 and 5.5 mg per kg of vegetables cooked for stir frying

in canola oil and deep frying potatoes in hydrogenated soybean oil, respectively. Since gas-phase hydrocarbon emissions were found to be small during the soybean oil frying experiment, the hydrocarbons were not measured during the canola oil based stir frying and the potatoes frying experiments.

### **3.3.1 Fine Particle Mass and Chemical Composition**

Fine particulate matter was collected for mass emissions rate determination and inorganic chemical analysis by directly drawing the diluted cooled cooking exhaust through a Teflon membrane filter. Fine particle mass emissions rates were measured to be  $21.5 \pm 1.2$  and  $29.5 \pm 1.3$  mg per kilogram of vegetables cooked for the soybean oil and canola oil stir fry tests, respectively. The average fine particle emission rate for these two tests on a seed oil use basis is 190 mg of fine particle mass per liter of seed oil used in stir frying. The composition the fine particulate matter generated from the soybean oil stir fry test is shown in Table 3.1. As expected the aerosol is predominately organic matter consisting of  $69.6 \pm 5.5$  percent organic carbon. Several ionic species also were measured in the fine particle emissions at lower but noticeable percentages. Nitrate ion was found to contribute 2.2% of the fine particle mass. Sodium, ammonium, and sulfate each made up about 1.0% of the fine particle mass. Potassium and chloride both contributed approximately 0.27% to the fine particle mass. These ionic species are believed to be derived from the vegetables and the stir fry sauce. The fine particle mass emitted during

Table 3.1. Average Fine Particle Mass Emission Rate and Fine Particle Chemical Composition Emitted From Cooking Vegetables in Seed Oils

	Vegetables Stir Fried in Soybean Oil	Vegetables Stir Fried in Canola Oil	Deep Frying of Potatoes
Mass Emission Rate (mg kg <sup>-1</sup> of vegetables cooked)	21.5 ± 1.2	29.5 ± 1.3	13.1 ± 1.2
Particle Composition:			
Organic Carbon (wt %) <sup>b</sup>	69.6 ± 5.50	58.3 ± 4.7	62.7 ± 5.1
Elemental Carbon (wt %)	< 4.0	< 3.4	< 4.0
Na <sup>+</sup> (wt % by IC)	1.0 ± 0.1	a	a
NH <sub>4</sub> <sup>+</sup> (wt % by IC)	0.94 ± 0.06	a	a
Cl <sup>-</sup> (wt % by IC)	0.27 ± 0.06	a	a
NO <sub>3</sub> <sup>-</sup> (wt % by IC)	2.2 ± 0.06	a	a
SO <sub>4</sub> <sup>-</sup> (wt % by IC)	1.08 ± 0.08	a	a
Potassium (wt% by XRF)	0.27 ± 0.10	a	a
Sulfur (wt% by XRF)	0.28 ± 0.06	a	a

Notes: (a) not measured

(b) measured downstream of the organics denuder

the canola oil stir frying experiment was measured to be  $58.3 \pm 4.7$  percent organic carbon.

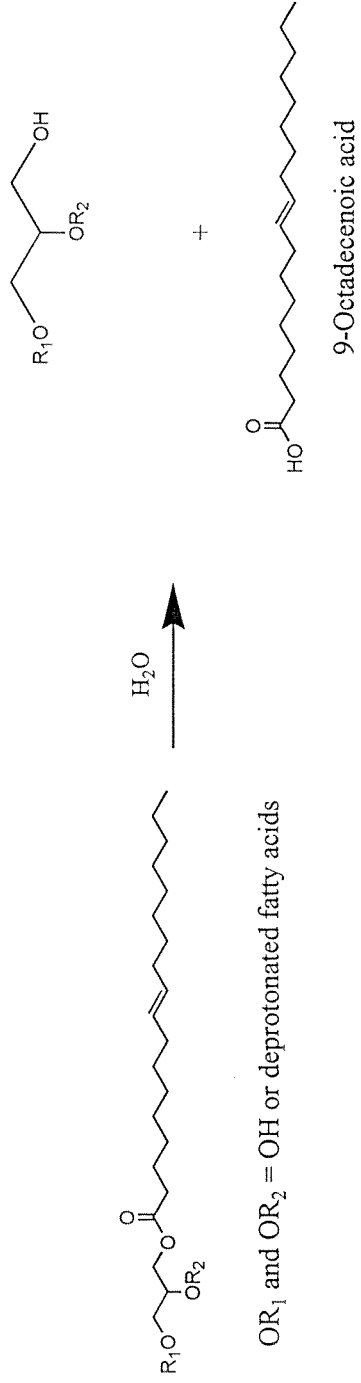
The emission rate of fine particle mass was measured to be  $13.1 \pm 1.2$  mg per kg of potatoes cooked from the potatoes deep frying process. If these deep fryers were operated for 8 hours per day then the emission rate of fine particle mass would be 5.7 grams per day for both fryers while processing a total of 435 kg of fried potatoes. The fine particle mass was determined to be comprised of  $62.7 \pm 5.1$  percent organic carbon.

Total organic carbon mass was also measured for each of the seed oil cooking tests on the quartz fiber filters located downstream of the organics denuder and on undenuded quartz fiber filters. Previous work has shown that certain gas-phase semi-volatile organic compounds can sorb to undenuded quartz fiber filters or to the particulate matter collected on the filters causing the addition of a positive artifact to the organic compound mass and the total mass collected on the filter. The emission rate of fine particle organic carbon measured downstream of the denuder averaged over all three tests was  $80.6 \pm 3.5\%$  of the fine particle organic carbon measured from the undenuded samples collected on quartz fiber filters. This result is consistent with the strong sorption artifact for gas-phase fatty acids when passed through a quartz fiber filter as observed in Chapter 2 when sampling meat smoke.

### 3.3.2 Organic Compound Emissions

Refined seed oils used for cooking are largely comprised of fatty acid esters of glycerol (1,2,3-propanetriol) (5) with typically less than a few percent of hydrocarbons and other organic compounds (9). Samples of the seed oils used in the current experiments were derivatized with diazomethane to convert any free fatty acids to their methyl ester analogs. Analysis by GC/MS showed that virtually no free fatty acids were present in these refined seed oils. The n-alkanoic acids and the n-alkenoic acids present in the emissions from the seed oil cooking operations are likely due to the hydrolysis of glycerides present in the seed oils as shown in Figure 3.2.

As previously indicated the organic compound emissions from the seed oil cooking operations tested in this study are dominated by carbonyls and fatty acids. Table 3.2 lists the emission rate and gas/particle phase distribution of 99 organic compounds identified and quantified in the emissions from these seed oil cooking tests. Low molecular weight volatile hydrocarbons were only measured for the soybean oil stir fry test and were found to be very low except for methane and ethane, which are believed to be due to a small amount of unburned natural gas present in the atmosphere of the cooking facility. Methane and ethane are not expected to be emitted in any noticeable quantities from the seed oil cooking operation studied and since natural gas leakage from the cooking appliances is the likely source of the methane and ethane.



When  $\text{OR}_1$  and  $\text{OR}_2$  are both deprotonated fatty acids, then a triglyceride is converted to a diglyceride and a free fatty acid.

When  $\text{OR}_1$  and  $\text{OR}_2$  represent one  $\text{OH}$  and one deprotonated fatty acid, then a diglyceride is converted to a monoglyceride and a free fatty acid.

When  $\text{OR}_1$  and  $\text{OR}_2$  are both  $\text{OH}$ , then a monoglyceride is converted to glycerin and a free fatty acid.

Figure 3.2. Formation of free fatty acids from glycerol esters of fatty acids.

Table 3.2. Organic Compound Emission Rates from Frying Vegetables in Seed Oils

Compound	Stir Frying of Vegetables in Soybean Oil ( $\mu\text{g kg}^{-1}$ of Vegetables Cooked)		Stir Frying of Vegetables in Canola Oil ( $\mu\text{g kg}^{-1}$ of Vegetables Cooked)		Deep Frying of Potatoes in Hydrogenated Oil ( $\mu\text{g kg}^{-1}$ of Potatoes Cooked)		Notes
	Gas	Particle	Gas	Particle	Gas	Particle	
	Phase	Phase	Phase	Phase	Phase	Phase	
n-Alkanes							
Methane	168000 <sup>Δ</sup>		*		*		a, e
Ethane	8690 <sup>Δ</sup>		*		*		a, e
Propane	550		*		*		a, e
n-Butane	750		*		*		a, e
n-Pentane	800		*		*		a, e
n-Hexane	100		*		*		a, e
n-Heptane	110		*		*		a, e
n-Octane	110		*		*		a, e
n-Nonane	490		*		*		a, e
n-Decane	650		*		*		a, e
n-Tridecane	830		380		230		b, f
n-Tetradecane	930		530	25	340	5	a, f
n-Pentadecane	690		660	35	430	37	b, f
n-Hexadecane	720	150	450	33	230	18	a, f
n-Heptadecane	170	34	650	95	310	33	b, f
n-Octadecane	77	28	180	16	96	11	a, f
n-Nonadecane	82	14	97	22	49	9	b, f
n-Eicosane	38	26	100	14	37	6	a, f
n-Heneicosane	26	38	46	15	26	3	b, f
n-Docosane	19	10	36	10	20	1	b, f
n-Tricosane	25	18	36	5	19	1	b, f
n-Tetracosane	18	18	15	18	12		a, f
n-Pentacosane			7	13	9		b, f
n-Hexacosane		18		17			b, f
n-Heptacosane		340		470			a, f
Branched alkanes							
i-Butane	420		*		*		a, e
i-Pentane	280		*		*		a, e
n-Alkenes							
Ethene	760		*		*		a, e
Branched alkenes							
i-Butene	750		*		*		a, e
Alkynes							
Ethyne(Acetylene)	550		*		*		a, e
Aromatic hydrocarbons							
m-Xylene + p-Xylene	190		*		*		a, e
p-Ethyltoluene	150		*		*		a, e

Identification notes: (a) authentic quantitative standard. (b) authentic quantitative standard for similar compound in series. (c) secondary standard. (d) detected as a methyl ester.

Sample collection notes: (e) collected in SUMA canister (f) collected on denuder/filter/PUF sampling train. (g) collected on DNPH impregnated C<sub>18</sub> cartridges. \* not measured. See text for details.

Additional Notes: † Compound is too volatile for complete collection by denuder at sampling conditions; mass of this compound reported in the gas-phase includes mass collected on PUF cartridge. <sup>Δ</sup> Believed to be from natural gas and not from stir fry materials.

Table 3.2. (continued - page 2)

Compound	Stir Frying of Vegetables in Soybean Oil ( $\mu\text{g kg}^{-1}$ of Vegetables Cooked)		Stir Frying of Vegetables in Canola Oil ( $\mu\text{g kg}^{-1}$ of Vegetables Cooked)		Deep Frying of Potatoes in Hydrogenated Oil ( $\mu\text{g kg}^{-1}$ of Potatoes Cooked)		Notes
	Gas	Particle	Gas	Particle	Gas	Particle	
	Phase	Phase	Phase	Phase	Phase	Phase	
Aromatic hydrocarbons							
Naphthalene <sup>†</sup>	645		588		338		a, f
Acenaphthylene	38		37		19		a, f
Phenanthrene	138	7	120	8	83	2	a, f
Anthracene	11	1	8	2	6	2	a, f
Fluoranthene	40	7	24	5	19	1	a, f
Pyrene	28	4	15	5	19	1	a, f
Chrysene/Triphenylene	5	9		13	5	9	a, f
Aliphatic aldehydes							
Formaldehyde	20100		18600		12400		a, g
Acetaldehyde	50100		42200		20900		a, g
Propanal	12200		17000		7000		a, g
Butanal/Isobutanal	19700		17400		4500		a, g
Hexanal	4100		6400		6700		a, g
Heptanal	4300		8000		5200		a, g
Octanal	7900		9700		5700		a, g
Nonanal	12400		14800		13500		a, g
Decanal	5200		1090		2900		a, g
Undecanal	3000		200		1200		a, g
Dodecanal	1260		920				a, f
Tridecanal	550		180				a, f
Tetradecanal	410						a, f
Pentadecanal	440		411				a, f
Dicarbonyls							
Glyoxal	9400		9600		6400		a, g
Methylglyoxal	7400		10000		5500		a, g
Biacetyl	4200		2800		1400		a, g
Ketones							
2-Nonanone	3300				78		c, f
2-Decanone	2670		3130		590		c, f
2-Undecanone	2310				145		c, f
2-Tridecanone					84		c, f
2-Tetradecanone					180		c, f
2-Pentadecanone	3900	170	8050	120	1100	30	c, f
2-Heptadecanone	720	60	860	75	300		c, f
Unsaturated carbonyls							
Crotonaldehyde	29100		24100		5200		a, g
Methacrolein	5500		1100		800		a, g

Identification notes: (a) authentic quantitative standard. (b) authentic quantitative standard for similar compound in series. (c) secondary standard. (d) detected as a methyl ester.

Sample collection notes: (e) collected in SUMA canister (f) collected on denuder/filter/PUF sampling train. (g) collected on DNPH impregnated C<sub>18</sub> cartridges. \* not measured. See text for details.

Additional Notes: <sup>†</sup> Compound is too volatile for complete collection by denuder at sampling conditions; mass of this compound reported in the gas-phase includes mass collected on PUF cartridge. <sup>Δ</sup> Believed to be from natural gas and not from stir fry materials.



Table 3.2. (continued - page 3)

Compound	Stir Frying of Vegetables in Soybean Oil ( $\mu\text{g kg}^{-1}$ of Vegetables Cooked)		Stir Frying of Vegetables in Canola Oil ( $\mu\text{g kg}^{-1}$ of Vegetables Cooked)		Deep Frying of Potatoes in Hydrogenated Oil ( $\mu\text{g kg}^{-1}$ of Potatoes Cooked)		Notes
	Gas	Particle	Gas	Particle	Gas	Particle	
	Phase	Phase	Phase	Phase	Phase	Phase	
Unsaturated carbonyls							
2-Decenal	16100	400	26400	650	2630		a, f
2-Undecenal	18400	420	29400	550	2880		a, f
n-Alkanoic acids							
Heptanoic acid	5940		530	162	370	2	a, d, f
Octanoic acid	5930	160	4330	170	640	27	a, d, f
Nonanoic acid	11890	180	12200	180	3270	51	a, d, f
Decanoic acid	780	28	700		190	9	a, d, f
Dodecanoic acid	320	59	210	20	100	4	a, d, f
Tetradecanoic acid	130	93	87	42	60	52	a, d, f
Pentadecanoic acid		58		59		12	a, d, f
Hexadecanoic acid (palmitic)	238	2980	690	2280	800	1760	a, d, f
Heptadecanoic acid				50		23	a, d, f
Octadecanoic acid (stearic)	15	1250	65	1040	37	848	a, d, f
Nonadecanoic acid				7			a, d, f
Eicosanoic acid		38		65		48	a, d, f
Docosanoic acid		29		35		7	a, d, f
n-Alkenoic acids							
9-Hexadecenoic acid		174		36		18	b, d, f
9-Octadecenoic acid (oleic)		3250		6310		1940	a, d, f
9,12-Octadecadienoic acid (linoleic)		4190		3030		1750	a, d, f
9,12,15-Octadecatrienoic acid (linolenic)		310		270		77	a, d, f
Alkadiolic acids							
Hexanedioic acid				33			a, d, f
Octanedioic acid		58		165		3	a, d, f
Furanones ( $\gamma$ -Lactones)							
5-Ethylidihydro-2(3H)-furanone <sup>†</sup>	470		370		41		a, f
5-Propylidihydro-2(3H)-furanone <sup>†</sup>	170		170		11		b, f
5-Butylidihydro-2(3H)-furanone	430	17	670	30	240	10	a, f
5-Pentylidihydro-2(3H)-furanone	280	30	470	38	75	7	b, f
5-Hexylidihydro-2(3H)-furanone	74	45	130	40	49	9	a, f
5-Heptyldihydro-2(3H)-furanone	33	5		5		3	b, f
5-Octylidihydro-2(3H)-furanone		43		53		1	b, f
5-Nonyldihydro-2(3H)-furanone		29		33		2	b, f
5-Decylidihydro-2(3H)-furanone		3		4		1	b, f
5-Undecylidihydro-2(3H)-furanone		41		30		2	b, f
5-Dodecylidihydro-2(3H)-furanone		12		10		1	b, f
Other Compounds							
Chlorpyrifos		54		76	23	33	a, f

Identification notes: (a) authentic quantitative standard. (b) authentic quantitative standard for similar compound in series. (c) secondary standard. (d) detected as a methyl ester.

Sample collection notes: (e) collected in SUMA canister (f) collected on denuder/filter/PUF sampling train. (g) collected on DNPH impregnated  $\text{C}_{18}$  cartridges. \* not measured. See text for details.

Additional Notes: <sup>†</sup> Compound is too volatile for complete collection by denuder at sampling conditions; mass of this compound reported in the gas-phase includes mass collected on PUF cartridge. <sup>Δ</sup> Believed to be from natural gas and not from stir fry materials.

The emission rates and phase distributions of the fatty acids for all three seed oil cooking tests are shown in Figure 3.3. The distributions of C<sub>18</sub> fatty acids (octadecanoic acid, 9-octadecenoic acid, 9,12-octadecadienoic acid, and 9,12,15-octadecatrienoic acid) in the emissions are consistent with the compositions of the seed oils used for cooking. Refined soybean oil contains the highest relative content of octadecadienoic esters compared to the other seed oils used (10). Since octadecadienoic acid contains two double bonds, it is expected to break down more readily during the cooking process than the other more saturated fatty acids. For this reason we do not expect that the ratio of this fatty acid to other n-alkanoic acids will be the same within the emissions as the ratio of the parent esters in the original seed oils used. Nevertheless, the octadecadienoic acid emissions from cooking with soybean oil are the highest among the three oils used in the tests. In canola oil, oleic acid (9-octadecenoic acid) makes up a higher fraction of the acids present as esters than in any other commercial edible seed oil (10). As can be seen in Figure 3.3, the largest monounsaturated C<sub>18</sub> acid (9-octadecenoic acid) emissions are observed when using canola oil. Hydrogenated soybean oil has been processed to remove the tri-olefinic C<sub>18</sub> acid (linolenic acid) present as esters and to convert some of the linoleic acid (9,12-octadecadienoic acid) esters to the monounsaturated (9-octadecenoic acid) and the saturated fatty acid (stearic acid) esters (5). Consistent with this operation, the smallest linolenic acid emissions are seen when deep frying with hydrogenated soybean oil. In addition, stearic acid

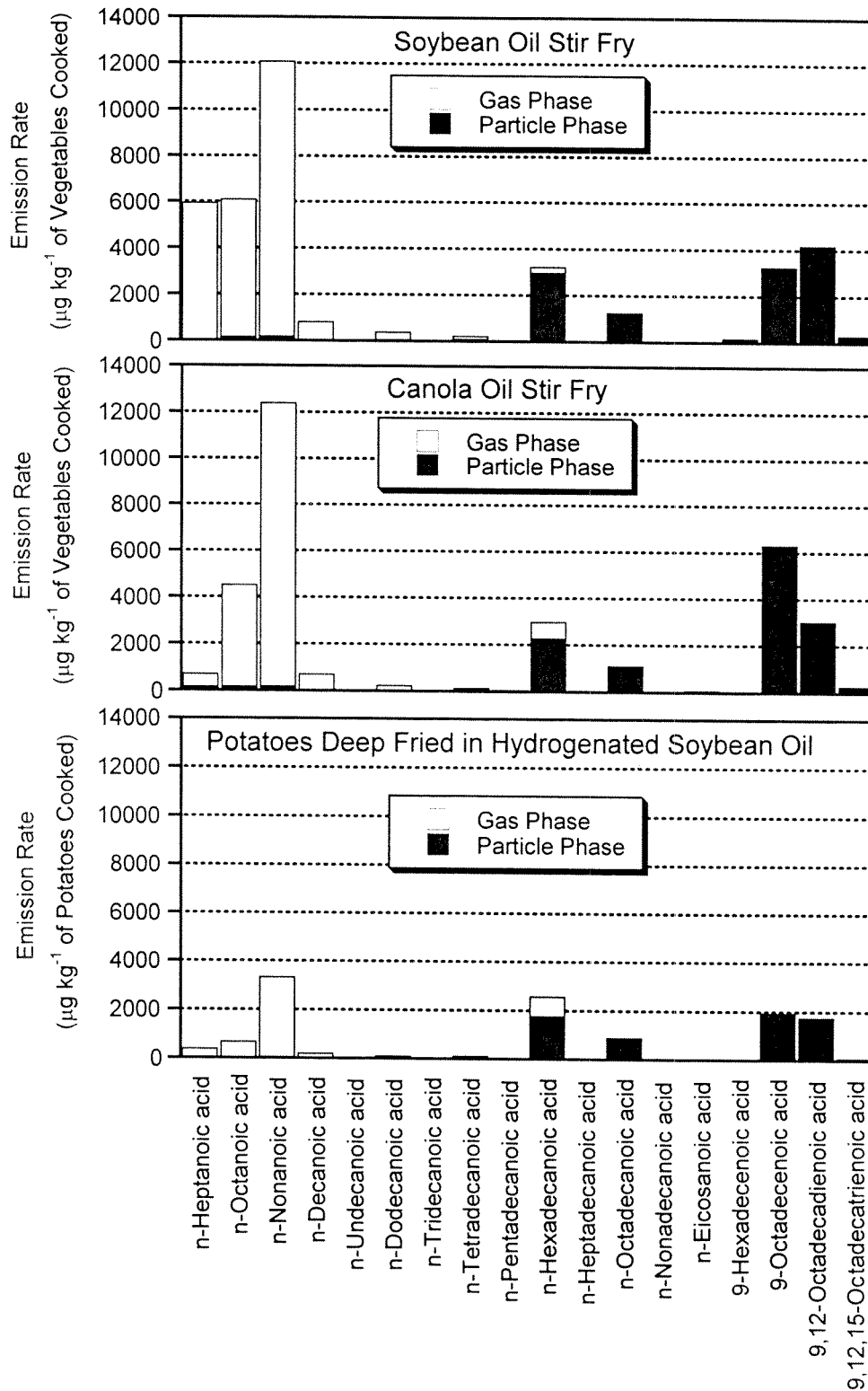


Figure 3.3. Emission rates and phase distributions of n-alkanoic acids emitted from cooking vegetables in seed oil.

makes up a higher percentage of the C<sub>18</sub> fatty acids in the exhaust from deep frying than from either of the seed oils used for stir frying.

Nonanoic acid is emitted at the highest rate of all the C<sub>7</sub> and greater n-alkanoic acids from all of the food cooking operations tested. Nonanoic acid is expected to be formed from the breakdown of oleic acid present in the seed oils. The distributions of the C<sub>14</sub>, C<sub>16</sub>, and C<sub>18</sub> saturated fatty acids are consistent with the compositions of the seed oils (5, 10), indicating that these acids are likely formed directly from the hydrolysis of their glycerol ester precursor analogs.

Acetaldehyde is emitted at the highest rate of any of the carbonyls for all three cooking operations. Figure 3.4 shows the emission rates of the paraffinic aldehydes, the olefinic aldehydes, and glyoxals for all three of the seed oil cooking tests. Significant quantities of crotonaldehyde, 2-decenal, and 2-undecenal were emitted from the stir fry cooking with soybean oil and canola oil. 2-decenal and 2-undecenal have been previously identified in the exhaust of heated seed oil (6). It should also be noted that the relative abundance of the C<sub>5</sub> through C<sub>10</sub> aldehydes peaks at nonanal, which is consistent with the relative distribution of the alkanolic acid emissions which peak at nonanoic acid. Again, nonanal formation from the decomposition of the unsaturated fatty acid, 9-octadecenoic acid (oleic acid), is a likely cause of the elevated emissions observed.

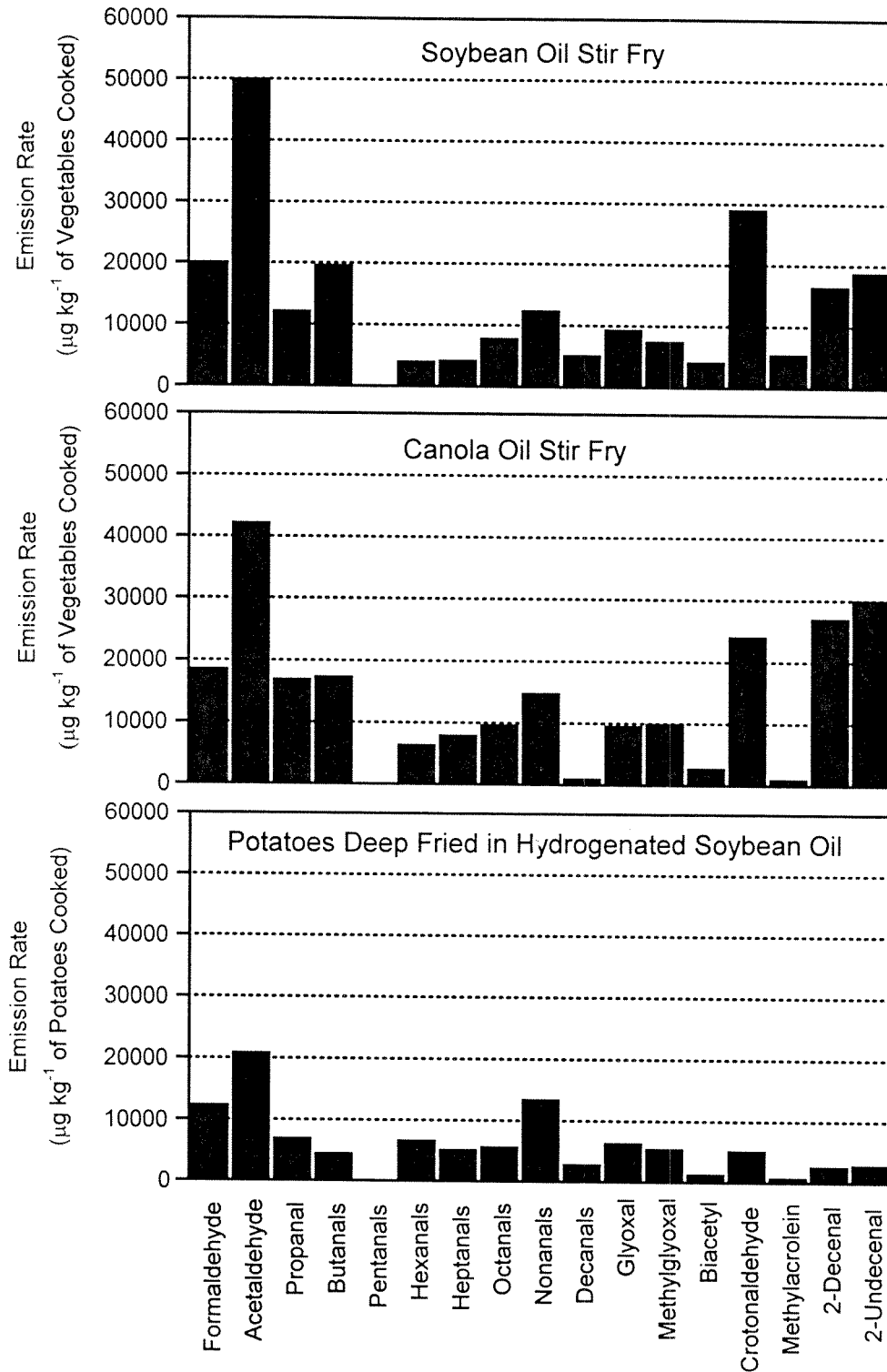


Figure 3.4. Emission rates of selected aldehydes emitted from cooking vegetables in seed oil.

In addition to the aldehyde emissions, noticeable amounts of 2-ketones also are emitted from the seed oil cooking operations. 2-Pentadecanone is emitted in the highest amount from all three cooking processes at much greater levels than pentadecanal. 2-Nonanone, 2-decanone and 2-undecanone are all emitted in relatively large quantities from the soybean oil-based stir frying experiment.

$\gamma$ -Lactones spanning the range from gas-phase 5-ethylidihydro-2(3H)-furanone to particle-phase 5-dodecyldihydro-2(3H)-furanone are quantified in the emissions from the seed oil cooking operations. These compounds are not emitted in great quantities but may serve as tracers for food cooking exhaust in some cases. These compounds are also emitted from meat charbroiling operations.

A chlorinated insecticide, chlorpyrifos, was found in the exhaust of all three seed oil cooking processes. An analysis of the seed oils used for the cooking tests indicated that this compound was not present in the oils. It is unclear if the chlorpyrifos found in the cooking exhaust originated from the vegetables that were stir fried or if it was present in the cleaning materials used in the kitchen. In addition relatively small emissions of polycyclic aromatic hydrocarbons (PAH) and alkanes were quantified. Significantly more n-heptacosane is emitted than the other high molecular weight n-alkanes from

vegetable stir frying; however, the emission rate of this compound is very minor compared to other urban sources of this compound (2).

### 3.3.3 Gas/Particle Partitioning: Experiment Versus Theory

According to gas/particle partitioning theory (11, 12), the phase distribution of a semi-volatile organic compound is determined by its absorption into the particle phase matrix. This phase distribution can be described by a partitioning coefficient,  $K_{p, opm}$ , defined as:

$$K_{p, opm} = \frac{F/OPM}{A} \quad (1)$$

where  $K_{p, opm}$  is the gas/particle partitioning coefficient based on organic particulate matter as the receiving particle phase substrate in units of  $\text{m}^3 \mu\text{g}^{-1}$ . OPM is the total organic particulate matter concentration into which the compound can partition ( $\mu\text{g m}^{-3}$ ). A is the gas-phase mass concentration of the compound of interest ( $\mu\text{g m}^{-3}$ ), F is the particle-associated mass concentration of the semi-volatile organic compound of interest ( $\mu\text{g m}^{-3}$ ). It is expected that the gas/particle partitioning coefficient,  $K_{p, opm}$ , will depend on the vapor pressure of the various organic compounds (12):

$$\text{Log}(K_{p, opm}) = m_{r, opm} \text{Log}(p_L^0) + b_{r, opm} \quad (2)$$

where  $p_L^0$  is the vapor pressure over a liquid pool of the semi-volatile organic compound of interest in torr, and  $m_{r,opm}$  and  $b_{r,opm}$  are coefficients that can be estimated by regressing a series of experimentally measured values of  $K_{p,opm}$  on the corresponding liquid vapor pressure values,  $p_L^0$ , for the members of a given organic compound class. The coefficient  $-m_{r,opm}$  should be close to unity if the compounds have similar activity coefficients when present in the particulate organic matrix and the partitioning process has reached equilibrium. The coefficient  $b_{r,opm}$  is a constant characteristic of the partitioning for that class of compounds with the specific particle matrix.

Figure 3.5 shows a partitioning plot for n-alkanoic acids emitted during the seed oil cooking experiments based on the relationship proposed by Pankow (12) as measured during the present experiments using the denuder/filter/PUF sampling train. Good agreement with the model is observed. All three data sets have  $R^2$  values of greater than 0.96, and have slopes of  $-0.97 \pm 0.10$ ,  $-1.01 \pm 0.12$ , and  $-1.13 \pm 0.13$  for the deep frying of potatoes, the canola oil vegetable stir fry and the the soybean oil vegetable stir fry, respectively. Partitioning coefficients,  $b_{r,opm}$ , for the n-alkanoic acids in the exhaust from the deep frying of potatoes, stir frying vegetables in canola oil, and stir frying vegetables in soybean oil are  $6.5 \pm 0.3$ ,  $6.7 \pm 0.5$ , and  $7.1 \pm 0.5$ , respectively. This result is very different than the phase distribution of these same compounds observed in meat smoke exhaust (Chapter 2), where the alkanolic acids did not



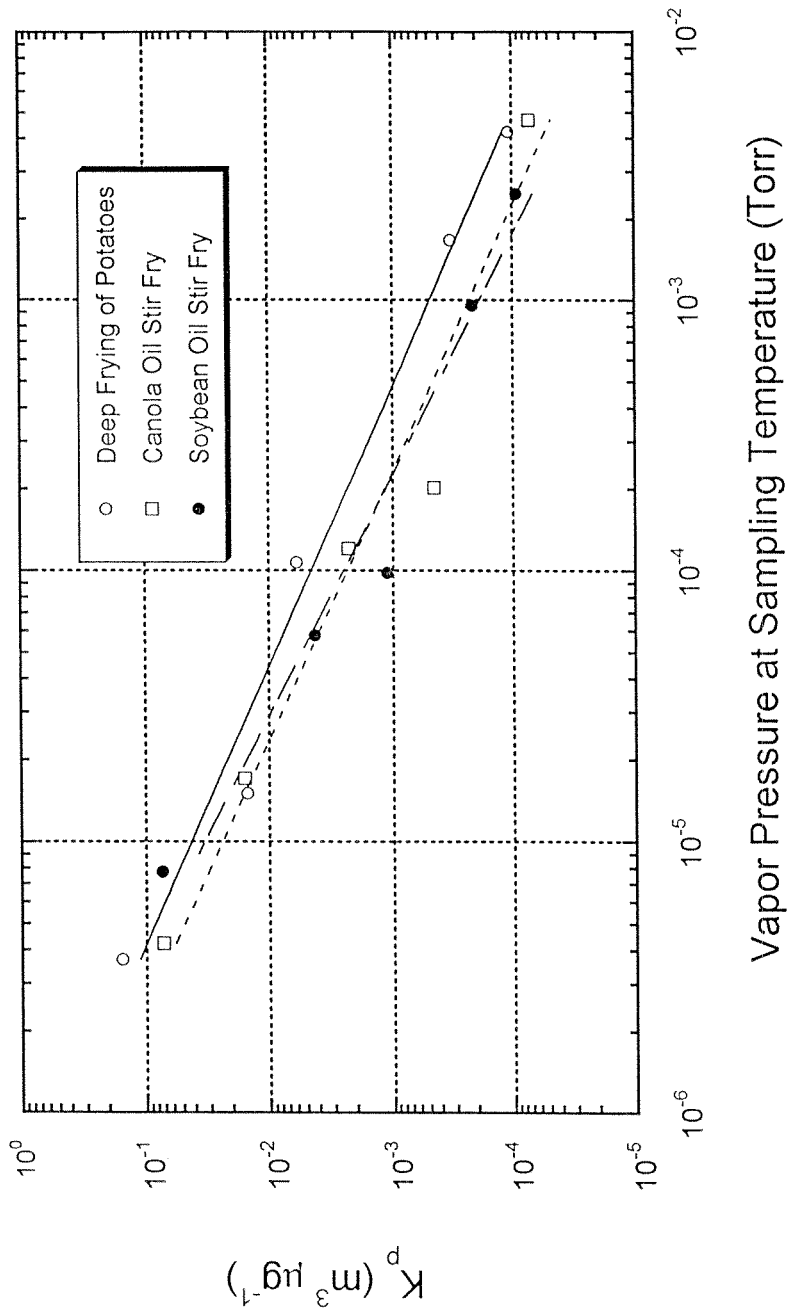


Figure 3.5. Partitioning of n-alkanoic acids in the diluted exhaust from cooking in seed oil as a function of the vapor pressure of the pure compound as measured by a denuder/filter/PUF sampling train.

follow the above partitioning theory, most likely because they were to some degree trapped within solidified meat fat particles.

### **3.3.4 Contribution to Concentrations of Alkanoic Acids in the Los Angeles Atmosphere**

An analysis of the source contributions to atmospheric fine particle mass concentrations and fine organic aerosol concentrations in Southern California has been presented by Schauer et al. (2) using particulate organic tracers for the sources studied. In that study, nine sources of organic compounds accounted for most of the ambient fine aerosol concentrations in the Los Angeles Basin during the year 1982. It was found that the sources studied could not completely account for the n-alkanoic acids concentrations measured in the fine particles, and it was suggested that emissions from cooking with seed oils might constitute a missing primary source of n-alkanoic acids. Based on the results of the present source testing program, the seed oil cooking contribution to the n-alkanoic acids in the atmospheric fine particles during the 1982 time period studied by Schauer et al. (2) can be estimated.

The California Air Resources Board estimates that one commercial deep fryer is operated seven days per week for each 252 people living in an urban area (13). If the deep fryers tested in this study are considered to be typical of commercial deep fryers and if we assume that a typical commercial deep fryer is operated an average of 8 hours per day, then the emission rate of hexadecanoic

acid and octadecanoic acid for the study 1982 period from deep fryers would be 11.1 and 5.3 kg per day, respectively, for the South Coast Air Basin that surrounds Los Angeles.

The emissions from stir frying and grill frying with seed oils can be estimated from the consumption of the oils used for these cooking operations. The United States Census Bureau reported that the consumption of salad and cooking oils in the U. S., which does not include baking and frying fats, was 3.0 million kilograms in 1994. Additionally, 0.91 million kilograms of margarine were consumed (14). The estimated consumption of these edible oils can be back-calculated to 1982 using an annual growth factor which is extrapolated from the seed oil consumption increase of 32% in the United States that occurred from 1981 to 1992 (10). If we assume that 75% of the salad and cooking oils were consumed for frying, and 25% of the margarine was consumed for frying and that the per capita consumption of cooking oils is similar for the entire United States and Southern California, then the emissions from stir frying and grill frying with seed oils can be estimated in the South Coast Air Basin to be 11.2 and 4.2 kg per day of n-hexadecanoic acid and n-octadecanoic acid emitted by commercial establishments. These combined emissions from both types of seed oil cooking account for approximately a 9% increase in these alkanic acids emissions when compared to the primary sources previously assessed (2).

As mentioned previously, nonanoic acid is emitted in relatively large quantities from cooking with seed oils. The nonanoic acid emission rate is only 28% of the hexadecanoic acid emission rate in meat smoke, but the ratio for the same compounds in the emissions when cooking with seed oils is approximately 400%. Therefore, if seed oil cooking accounts for 9% of the C<sub>16</sub> and C<sub>18</sub> alkanolic acid emissions and meat cooking accounts for approximately 45% of the C<sub>16</sub> and C<sub>18</sub> alkanolic acid emissions in this study area, then seed oil cooking emissions of nonanoic acid from cooking with seed oils should dominate over the emissions of nonanoic acid from meat charbroiling operations. It is uncertain whether there are other major primary sources of nonanoic acid emissions to the atmosphere, but clearly an investigation of these lighter organic acids is warranted. If cooking with seed oils is shown to dominate the primary emissions of nonanoic acid to the atmosphere, then the differences in the relative distribution of organic acids in source emissions and in the atmosphere discussed above may help to distinguish the effluent of seed oil use from the effluent from meat cooking operations when measured in the atmosphere.

### 3.4 References

1. Rogge, W. R.; Mazurek, M. A.; Hildemann, L. M.; Cass, G. R.; Simoneit, B. R. T. *Atmos. Environ.* **1993a**, 27, 1309-1330.
2. Schauer, J. J.; Rogge, W. R.; Hildemann, L. M.; Mazurek, M. A.; Cass, G. R.; Simoneit, B. R. T. *Atmos. Environ.* **1996**, 30, 3837-3855.
3. Rogge, W. R.; Hildemann, L. M.; Mazurek, M. A.; Cass, G. R.; Simoneit, B. R. T. *J. Geophys. Res.* **1996**, 101, 19379-19394.
4. Hildemann, L. M.; Klinedinst, D. B.; Klouda, G. A.; Currie, L. A.; Cass, G. R. *Environ. Sci. Technol.* **1994**, 28, 1565-1576.
5. Eckery, E. W. *Vegetable Fats and Oils*; Reinhold: New York, 1954, pp. 25-50.
6. Chung, T. Y.; Eiserich, J. P.; Shibamoto, T. *J. Agric. Food Chem.* **1993**, 41, 1467-1470.
7. John, W.; Reischl, G. *JAPCA* **1980**, 30, 872-876.
8. Code of Federal Registry, Vol. 41, 1997
9. Kuksis, A. *Biochemistry.* **1964**, 3, 1086-1093.

10. Morgan, N. *Food Review* **1993**, 16, 26-30.
11. Pankow, J. F.; Bidleman, T. F. *Atmos. Environ.* **1992**, 26A, 1071-1080.
12. Pankow, J. F. *Atmos. Environ.* **1994**, 28, 185-188.
13. Personal Correspondence from Randy Pasek, California Air Resources Board, May, 30, 1997.
14. *Fats and Oils, Production, Consumption, and Stocks-May, 1995*, Census Bureau On-Line Information Service, Census-BEA Electronic Bulletin Board, **1995**.

## Chapter 4

### Organic Compounds from Medium Duty Diesel Trucks

#### 4.1 Introduction

Since diesel fuel consists largely of aliphatic hydrocarbons containing 10 to 25 carbon atoms, it is expected that these components and their thermally-altered breakdown products also will be present in diesel exhaust. The inorganic and organic composition of fine particulate matter emitted in the exhaust from diesel-powered motor vehicles has been characterized in the past (1, 2) at a level sufficient to determine the contribution of primary emissions from diesel engines to atmospheric fine particle mass concentrations via transport modeling and organic chemical tracer techniques (3, 4). Specific volatile and semi-volatile gas-phase polycyclic aromatic hydrocarbons (PAH) emitted from diesel-powered motor vehicles also have been examined (5-7). However, a detailed analysis of the remaining semi-volatile gas-phase emissions from contemporary diesel trucks has not been reported. These semi-volatile organic compounds (SVOC) can play a role in photochemical smog formation and are likely candidates to become the precursors of secondary organic aerosol (SOA) that is produced from the low vapor pressure products of atmospheric chemical reactions. The

lack of emissions data for these compounds from diesel engines, however, has prevented current air quality models from assessing their importance in urban air pollution. In the present work, new measurements of diesel engine exhaust emissions have been undertaken with an emphasis on defining the mixture of semi-volatile organic compounds emitted and their distribution between the gas and particle phases.

The ratio of methyl-substituted PAH to unsubstituted PAH has been used previously to help determine the origin of hydrocarbon contamination in aquatic environments (8) and in the atmosphere (9). Crude oils and many refined petroleum products have a higher ratio of methyl-substituted PAH to unsubstituted PAH than is found in engine exhaust emissions due to thermal dealkylation within the engine (10). In the present study, the composition of the commercial diesel fuel burned in the diesel trucks tested is compared to the composition of the organic compounds emitted from the diesel trucks during the source tests. The change in the degree of methyl-substitution of the PAH in the exhaust emissions when compared to the fuel as well as other selective changes in the relative distribution of organic compounds is assessed, with an emphasis on quantifying those features that show potential for distinguishing diesel fuel vapors in the atmosphere from the organic compounds emitted from diesel truck exhaust as well as distinguishing diesel truck exhaust from gasoline-powered motor vehicle exhaust.



## 4.2 Experimental Methods

### 4.2.1 Comprehensive Source Sampling

A two-stage dilution sampler is used in the present study. It consists of two sections, a pre-dilution tunnel followed by the primary sampling system. The pre-dilution tunnel is connected directly to the tailpipe of the diesel truck being tested on the dynamometer via a stainless steel hose. At the entrance of the pre-dilution tunnel, HEPA-filtered and activated carbon-filtered dilution air is turbulently mixed with the vehicle exhaust. The pre-dilution tunnel is operated at a fixed combined flowrate of 9910 lpm, such that the exhaust concentration in this tunnel is always proportional to the total emission rate from the tailpipe. At the downstream end of the pre-dilution tunnel, a small portion of the total flow is drawn through a cyclone separator which removes particles larger than a nominal 10  $\mu\text{m}$  in aerodynamic diameter. The gas-phase and particulate species that exit the cyclone pass through a venturi meter into the primary sampling system where they are diluted a second time. Stages 1 plus 2 of this system dilute the vehicle exhaust by a total average dilution factor of approximately 140 fold.

The primary sampling system is a modified version of the portable dilution sampler originally developed by Hildemann et al. (11). The modified sampling system has been previously described in Chapter 2, but briefly

consists of a dilution tunnel, which in the current study provides the second stage of dilution, followed by a residence time chamber that retains the diluted source sample while further condensation of organic gases onto the particles takes place. A diagram of the original dilution sampler as used in a motor vehicle test configuration is shown in Figure 1b of Hildemann et al. (1) and the added details of the particulate and gas-phase measurement systems now placed at the downstream end of the source sampler are shown in Figure 2.1 in Chapter 2. At the downstream end of the dilution sampler, instruments for measuring fine particulate and gas-phase species concentrations and chemical composition are attached to the residence time chamber from which samples are withdrawn for chemical analysis. Samples are drawn through AIHL-design cyclone separators (12) which are operated at flowrates such that fine particles with aerodynamic diameters smaller than 1.8  $\mu\text{m}$  pass through the cyclone separator along with gas-phase species. Gas-phase, semi-volatile and fine particle-phase organic compounds are collected downstream of the cyclones using three types of sampling trains that are operated simultaneously in parallel at this location. Semi-volatile and particulate organic compounds are collected by both a denuder/filter/PUF sampling train and filter/PUF sampling trains. A description of these sampling units is included in Chapter 2. Fine particle emission rates and chemical composition, as well as the emissions rates of carbonyls, organic acids, and gas-phase hydrocarbons are collected with the third type of cyclone based sampling train discussed in Chapter 2.

The internally exposed area of the entire two-stage dilution sampler is constructed only of aluminum, Teflon, and stainless steel. The entire sampler is assembled with Teflon o-rings and is completely free of grease coatings and rubber gaskets.

Electronic particle sizing instruments and a pair of MOUDI impactors are also connected to the residence time chamber during the diesel vehicle source tests to obtain particle size distributions and particle chemical composition as a function of particle size. The size distributions and the results obtained from the MOUDI impactors will be reported elsewhere.

#### **4.2.2 Source Testing Procedure**

The two medium duty diesel trucks tested in the present study were both sampled during 1996 from the current in-use vehicle fleet in southern California and were fueled with commercially-obtained California reformulated diesel fuel. The first vehicle tested was a 1995 model year Isuzu intercooled turbo diesel truck with a 3.8 liter, 4 cylinder engine. The second vehicle was a GMC Vandura 3500 full-sized commercial van with a 6.5 liter, 8 cylinder diesel engine. The Isuzu truck and the GMC van had accumulated 39,993 miles and 30,560 miles of driving, respectively, prior to being tested.

Due to vehicle testing facility operating procedures, the diesel trucks could not be moved onto the dynamometer directly from cold storage. The truck has to be driven onto the dynamometer, which entails first starting the engine, so the diesel trucks had to be tested with a hot start FTP cycle. Prior to the start of each source test, the truck tested was warmed up on the dynamometer for approximately ten minutes. The engine was then shut off and the truck tailpipe was connected to the source sampler. The flows through the source samplers were established and the truck was started and driven over the dynamometer cycle shown in Figure 4.1. For both vehicle tests the two roller hydraulic dynamometers were operated at a load of 7500 pounds and an actual horsepower (AHP) of 17.5. The second diesel truck was tested directly after the first truck was finished. The filters used for fine particle mass and bulk chemical composition determination and the denuder were changed between tests, and all other samples destined for detailed analysis of individual organic compounds were collected as a composite sample of the exhaust from the two trucks.

#### **4.2.3 Organic Chemical Analysis**

The sample extraction and GC/MS techniques used to quantify the emissions of semi-volatile and particle-phase organic compounds from diesel trucks are the same as was used for the meat charbroiling source tests and are described in Chapter 2.

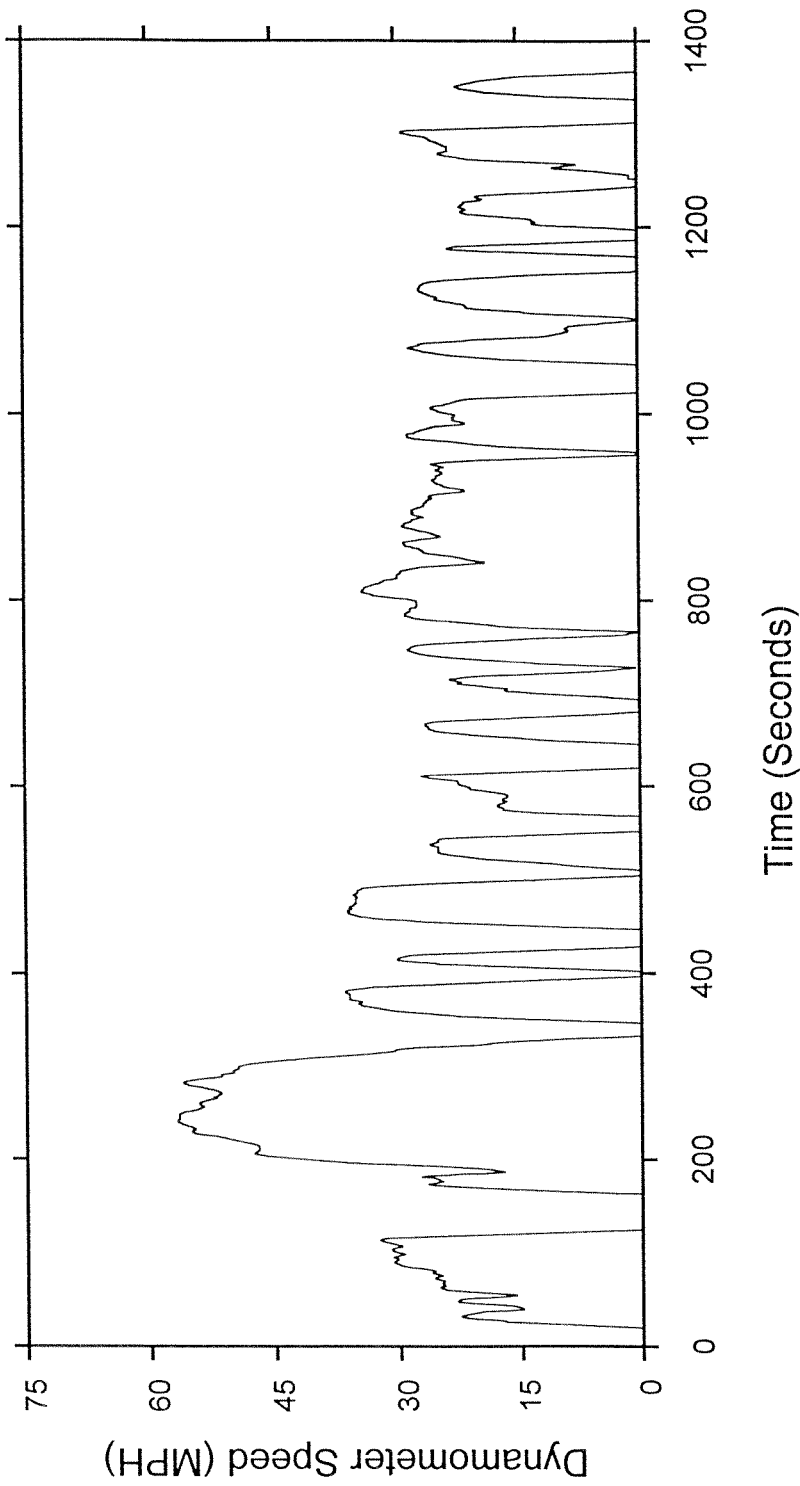


Figure 4.1. Dynamometer cycle used for medium duty diesel truck emissions testing.

Filter, PUF, and denuder field blanks were analyzed in conjunction with the diesel truck source test. The field blanks were prepared, stored and handled by exactly the same procedures as used for the source samples.

Hundreds of authentic standards have been prepared for the positive identification and quantification of the organic compounds found in the current source test program. When quantitative standards could not be obtained for a given compound or compound class, significant effort was made to obtain a non-quantitative secondary standard that could be used for unique identification of the organic compounds. An example of such a secondary standard is the use of motor oil as a source of hopanes and steranes that was used to help identify these compounds in the fine particle diesel exhaust. Quantification of compounds identified using secondary standards has been estimated from the response factors for compounds having similar retention times and chemical structure. In the case of the hopanes and steranes an authentic standard of cholestane was used to estimate the response factors of the remaining hopanes and steranes that were quantified.

Total non-methane organic gases (NMOG, EPA method TO12) and individual organic vapor-phase hydrocarbons ranging from  $C_1$  to  $C_{10}$  were analyzed from the SUMA canisters by gas chromatography/flame ionization detection (GC/FID). Carbonyls collected using the DNPH-impregnated  $C_{18}$  cartridges were analyzed by liquid chromatography/UV detection.

## 4.3 Results and Discussion

### 4.3.1 Fine Particle Mass and Chemical Composition

Fine particle mass and chemical composition measurements made by directly filtering a known volume of the diluted cooled vehicle exhaust without the use of the semi-volatile organic vapor denuder system are shown in Table 4.1. Chemical species for which the emissions rates are significantly greater than zero are shown in bold-face type. Fine particle mass emission rates for the medium-duty diesel trucks tested averaged  $185 \pm 22$  mg per kilometer driven on the FTP urban driving cycle ( $195.6 \pm 3.1$  mg per kilometer for the Isuzu truck and  $173.7 \pm 16.1$  mg per kilometer for the GMC van). The fine particle mass collected in this fashion consisted of 30.4 percent organic carbon and 30.8 percent elemental carbon. Sulfate and ammonium ion were found to compose 1.0 percent and 0.73 percent of the mass, respectively, accompanied by detectable amounts of silicon, iron, and zinc.

Organic and elemental carbon also were measured on the quartz fiber filters located downstream of the XAD-coated denuders. The emission rate of fine particle elemental carbon as measured on the filter downstream of the denuder showed good agreement with the undenuded filter sample at 56 mg of elemental carbon per kilometer driven. Significantly less organic carbon was collected on filters located downstream of the denuders than was the case for

Table 4.1. Average Fine Particle Emission Rate and Fine Particle Chemical Composition for Medium-Duty Diesel Truck Exhaust. (Values shown in boldface are greater than zero by at least two standard errors.)

Fine Particle Mass Emissions Rate (AVG $\pm$ STD)		<b>185 <math>\pm</math> 22 mg km<sup>-1</sup></b>	
Elemental and Organic Carbon (Wt % of Fine Particle Mass)			
Organic Carbon <sup>a</sup>	<b>19.7 <math>\pm</math> 1.6</b>	Elemental Carbon	<b>30.8 <math>\pm</math> 2.6</b>
Ionic Species (Wt % of Fine Particle Mass)			
Chloride	0.00 $\pm$ 0.18	Sulfate	<b>1.00 <math>\pm</math> 0.25</b>
Nitrite	0.01 $\pm$ 0.01	Ammonium	<b>0.73 <math>\pm</math> 0.11</b>
Nitrate	0.23 $\pm$ 0.38		
X-ray Fluorescence (Wt % of Fine Particle Mass)			
Aluminum	0.08 $\pm$ 0.14	Selenium	0.00 $\pm$ 0.01
Silicon	<b>0.63 <math>\pm</math> 0.04</b>	Bromine	0.00 $\pm$ 0.01
Phosphorus	0.01 $\pm$ 0.06	Rubidium	0.00 $\pm$ 0.01
Sulfur	<b>0.22 <math>\pm</math> 0.02</b>	Strontium	0.00 $\pm$ 0.01
Chlorine	0.00 $\pm$ 0.06	Yttrium	0.00 $\pm$ 0.02
Potassium	0.00 $\pm$ 0.09	Zirconium	0.00 $\pm$ 0.02
Calcium	0.03 $\pm$ 0.08	Molybdenum	0.00 $\pm$ 0.04
Titanium	0.00 $\pm$ 0.29	Palladium	0.01 $\pm$ 0.10
Vanadium	0.00 $\pm$ 0.12	Silver	0.01 $\pm$ 0.11
Chromium	0.01 $\pm$ 0.03	Cadmium	0.06 $\pm$ 0.12
Manganese	0.01 $\pm$ 0.02	Indium	0.06 $\pm$ 0.14
Cobalt	0.01 $\pm$ 0.01	Tin	0.00 $\pm$ 0.18
Iron	<b>0.05 <math>\pm</math> 0.01</b>	Antimony	0.00 $\pm$ 0.21
Nickel	0.00 $\pm$ 0.01	Barium	0.00 $\pm$ 0.79
Copper	0.01 $\pm$ 0.01	Lanthanum	0.00 $\pm$ 1.04
Zinc	<b>0.07 <math>\pm</math> 0.01</b>	Mercury	0.00 $\pm$ 0.03
Gallium	0.01 $\pm$ 0.02	Lead	0.01 $\pm$ 0.04
Arsenic	0.00 $\pm$ 0.03		

Notes: (a) measured by downstream of the organics denuder. Organic carbon measured on undened filter is 30.4 percent of fine particle mass.



the undenuded filter sample taken in parallel. Figure 4.2 shows the emission rates of organic and elemental carbon measured by the two sampling techniques. A detailed analysis of the organic carbon distribution between the collection substrates of the denuder/filter/PUF sampling system indicated that there was very little organics mass on the two PUF plugs located downstream of the XAD-coated denuder/filter combination as compared to the difference between the undenuded filter and the denuded filter measurement of the fine particle organic carbon concentration. This indicates that the lower particulate organic carbon mass on the filter in the denuder/filter/PUF system could not be due to organic carbon volatilizing off that filter as the volatilization of organic aerosol would have resulted in higher concentrations measured on the PUF located downstream. These facts indicate that the larger quantity of organic carbon collected on the undenuded filter was due mainly to sorption of semi-volatile gas-phase organic compounds to the undenuded filter and not due to vaporization of particulate matter from the filter located downstream of the denuder.

#### **4.3.2 Distribution of Organic Compounds**

The quantities of individual gas-phase plus particle-phase organic compounds and elemental carbon emitted from the medium-duty diesel trucks are shown in Table 4.2 and are summarized in Figure 4.3. The composition of diesel fuel also is given in Table 4.2, as measured by diluting diesel fuel with

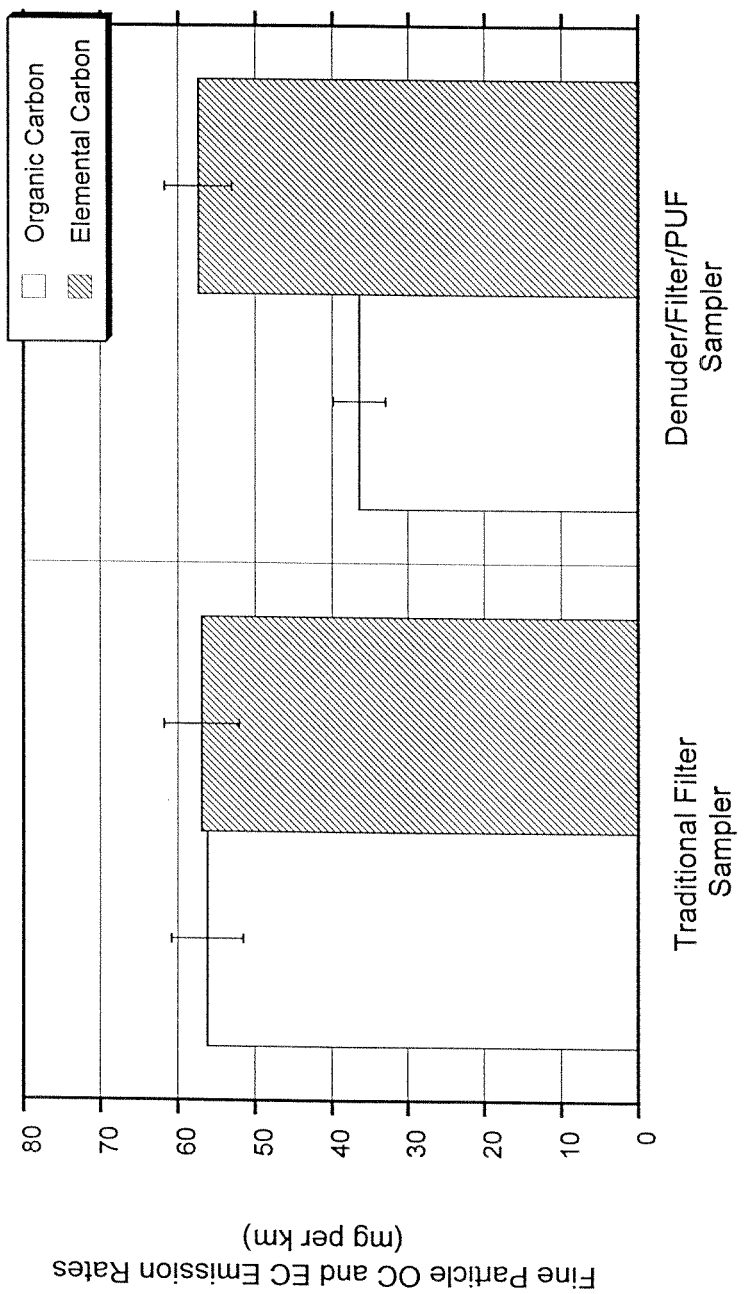


Figure 4.2. Comparison of fine particle organic and elemental carbon emitted from the diesel trucks tested as measured by a traditional filter sampler and a denuder/filter/PUF sampler.

Table 4.2. Organic Compounds Present in Diesel Fuel and in Medium Duty Diesel Truck Exhaust

Compound	Diesel Powered Medium Duty Truck Emissions ( $\mu\text{g km}^{-1}$ )		Diesel Fuel Composition ( $\mu\text{g gram}^{-1}$ )	Notes
	Gas Phase	Particle Phase		
n-Alkanes				
n-Butane	3830		*	a, e
n-Pentane	1860		*	a, e
n-Heptane	470		*	a, e
n-Octane	260		*	a, e
n-Nonane	160		*	a, e
n-Undecane	*		*	
n-Dodecane <sup>†</sup>	503		15500	a, f
n-Tridecane	477		15700	b, f
n-Tetradecane	629		13500	a, f
n-Pentadecane	398	2.12	10500	b, f
n-Hexadecane	711	8.62	10100	a, f
n-Heptadecane	614	5.92	5700	b, f
n-Octadecane	601	2.84	9212	a, f
n-Nonadecane	411	3.82	7020	b, f
n-Eicosane	206	95.7	6530	a, f
n-Heneicosane	65.8	40.5	5220	b, f
n-Docosane		52.0	4340	b, f
n-Tricosane		45.5	2670	b, f
n-Tetracosane		40.7	1680	a, f
n-Pentacosane		26.1	730	b, f
n-Hexacosane		34.9	290	b, f
n-Heptacosane		25.7	180	b, f
n-Octacosane		19.7	36	a, f
n-Nonacosane		6.1		b, f
Branched alkanes				
i-Pentane	2740		*	a, e
2,2-Dimethylbutane	310		*	a, e
2,3-Dimethylbutane	570		*	a, e
2-Methylpentane	930		*	a, e
3-Methylpentane	670		*	a, e
2,4-Dimethylpentane	410		*	a, e
2-Methylhexane	570		*	a, e
2,3-Dimethylpentane	720		*	a, e
3-Methylhexane	310		*	a, e
2,2,4-Trimethylpentane	1240		*	a, e
2,5-Dimethylhexane	50		*	a, e
2,4-Dimethylhexane	50		*	a, e
2,3,4-Trimethylpentane	310		*	a, e

Identification notes: (a) authentic quantitative standard. (b) authentic quantitative standard for similar compound in series. (c) secondary standard. (d) detected as a methyl ester.

Exhaust sample collection notes: (e) collected in SUMA canister. (f) collected on denuder/filter/PUF sampling train. (g) collected on DNPH impregnated  $\text{C}_{18}$  cartridges. (\*) not measured. See text for details. Additional Notes: <sup>†</sup> Compound is too volatile for complete collection by denuder at sampling conditions; mass of this compound reported in the gas-phase includes mass collected on PUF cartridge.

Table 4.2. (continued - page 2)

Compound	Diesel Powered Medium Duty Truck Emissions ( $\mu\text{g km}^{-1}$ )		Diesel Fuel Composition ( $\mu\text{g gram}^{-1}$ )	Notes
	Gas Phase	Particle Phase		
Branched alkanes				
2,3-Dimethylhexane	160		*	a, e
2-Methylheptane	100		*	a, e
3-Ethylhexane	210		*	a, e
Norfarnesane <sup>†</sup>	360		16300	b, f
Farnesane <sup>†</sup>	434	4.1	9220	b, f
2,6,10-Trimethyltridecane	367	1.2	8830	b, f
Norpristane	566	4.9	8670	b, f
Pristane	443		5840	a, f
Phytane	439		5770	b, f
n-Alkenes				
Ethene	8560		*	a, e
Propene	780		*	a, e
<i>trans</i> -2-Butene	520		*	a, e
<i>cis</i> -2-Butene	260		*	a, e
<i>trans</i> -2-Pentene	50		*	a, e
<i>trans</i> -2-Hexene	160		*	a, e
<i>cis</i> -2-Hexene	100		*	a, e
Branched alkenes				
Isobutene	1140		*	a, e
3-Methyl-1-butene	160		*	a, e
2-Methyl-1-butene	260		*	a, e
2-Methyl-2-pentene	210		*	a, e
Diolefins				
1,3-Butadiene	310		*	a, e
Alkynes				
Ethyne	4600		*	a, e
Saturated cycloalkanes				
Cyclopentane	410		*	a, e
Methylcyclopentane	620		*	a, e
Cyclohexane	210		*	a, e
Methylcyclohexane	520		*	a, e
Pentylcyclohexane	83.9			b, f
Hexylcyclohexane	14.9		830	b, f
Heptylcyclohexane	20.0		730	b, f
Octylcyclohexane	26.2		500	b, f
Nonylcyclohexane	24.7		490	b, f
Decylcyclohexane	38.2		420	b, f
Undecylcyclohexane	23.9		430	b, f

Identification notes: (a) authentic quantitative standard. (b) authentic quantitative standard for similar compound in series. (c) secondary standard. (d) detected as a methyl ester.

Exhaust sample collection notes: (e) collected in SUMA canister. (f) collected on denuder/filter/PUF sampling train. (g) collected on DNPH impregnated C<sub>18</sub> cartridges. (\*) not measured. See text for details. Additional Notes: <sup>†</sup> Compound is too volatile for complete collection by denuder at sampling conditions; mass of this compound reported in the gas-phase includes mass collected on PUF cartridge.

Table 4.2. (continued - page 3)

Compound	Diesel Powered Medium Duty Truck Emissions ( $\mu\text{g km}^{-1}$ )		Diesel Fuel Composition ( $\mu\text{g gram}^{-1}$ )	Notes
	Gas Phase	Particle Phase		
Saturated cycloalkanes				
Dodecylcyclohexane	16.8		200	b, f
Tridecylcyclohexane	16.5	4.34	170	b, f
Tetradecylcyclohexane	15.9	3.96	160	b, f
Pentadecylcyclohexane	12.8	9.88	150	a, f
Hexadecylcyclohexane		12.9		b, f
Heptadecylcyclohexane		16.7		a, f
Octadecylcyclohexane		11.5		b, f
Nonadecylcyclohexane		9.0		b, f
Unsaturated cycloalkenes				
Cyclopentene	210		*	a, e
Aromatic hydrocarbons				
Benzene	2740		*	a, e
Toluene	3980		*	a, e
Ethylbenzene	470		*	a, e
m & p-Xylene	2330		*	a, e
o-Xylene	830		*	a, e
n-Propylbenzene	100		*	a, e
p-Ethyltoluene	520		*	a, e
m-Ethyltoluene	210		*	a, e
1,3,5-Trimethylbenzene	260		*	a, e
1,2,4-Trimethylbenzene	880		*	a, e
Naphthalene <sup>†</sup>	617		600	a, f
2-Methylnaphthalene <sup>†</sup>	611		980	a, f
1-Methylnaphthalene <sup>†</sup>	378		580	a, f
C <sub>2</sub> -Naphthalenes	542		2050	a, f
C <sub>3</sub> -Naphthalenes	240	130	1360	b, f
C <sub>4</sub> -Naphthalenes	97.3	98.6	760	b, f
Acenaphthylene	70.1			a, f
Acenaphthene	19.3			a, f
Fluorene	34.6	9.5	52	a, f
C <sub>1</sub> -Fluorene	65.2	83.0	190	b, f
Phenanthrene	93.1	47.0	57	a, f
Anthracene	12.5	10.9	5	a, f
3-Methylphenanthrene	30.3	29.4	51	b, f
2-Methylphenanthrene	42.0	35.6	45	b, f
2-Methylanthracene	10.4	10.4	6	a, f
9-Methylphenanthrene	22.9	22.0	35	b, f
1-Methylphenanthrene	17.0	17.8	28	a, f

Identification notes: (a) authentic quantitative standard. (b) authentic quantitative standard for similar compound in series. (c) secondary standard. (d) detected as a methyl ester.

Exhaust sample collection notes: (e) collected in SUMA canister. (f) collected on denuder/filter/PUF sampling train. (g) collected on DNPH impregnated C<sub>18</sub> cartridges. (\*) not measured. See text for details. Additional Notes: <sup>†</sup> Compound is too volatile for complete collection by denuder at sampling conditions; mass of this compound reported in the gas-phase includes mass collected on PUF cartridge.

Table 4.2. (continued - page 4)

Compound	Diesel Powered Medium Duty Truck Emissions ( $\mu\text{g km}^{-1}$ )		Diesel Fuel Composition ( $\mu\text{g gram}^{-1}$ )	Notes
	Gas Phase	Particle Phase		
Aromatic hydrocarbons				
C <sub>2</sub> -MW 178 PAH	196	57.2	2080	a, f
C <sub>3</sub> -MW 178 PAH	97.4	97.5	120	b, f
Fluoranthene	53.0	56.6		a, f
Acephenanthrylene	12.0	16.2		b, f
Pyrene	71.9	88.5	64	a, f
C <sub>1</sub> -MW 202 PAH	39.0	81.0	290	b, f
Benzo[ghi]fluoranthene	5.82	19.8		b, f
Cyclopenta[cd]pyrene	2.06	3.50		a, f
Benz[a]anthracene	2.98	7.76		a, f
Chrysene & Triphenylene	3.35	15.6		a, f
C <sub>1</sub> -MW 228 PAH		6.54		b, f
Tricyclic terpanes				
8 $\beta$ ,13 $\alpha$ -Dimethyl-14 $\beta$ - n-butylpodocarpane	44.0	10.6	2.1	c, f
8 $\beta$ ,13 $\alpha$ -Dimethyl-14 $\beta$ - [3'-methylbutyl]podocarpane	13.8	4.50	0.6	c, f
Diasteranes				
20S-13 $\beta$ (H),17 $\alpha$ (H)-Diacholestane		1.37		c, f
Hopanes				
18 $\alpha$ (H)-22,29,30-Trisnorneohopane		2.74		c, f
17 $\alpha$ (H)-22,29,30-Trisnorhopane		0.99		c, f
17 $\alpha$ (H),21 $\beta$ (H)-29-Norhopane		11.3		c, f
17 $\alpha$ (H),21 $\beta$ (H)-Hopane		11.4		c, f
Steranes				
20R,5 $\alpha$ (H),14 $\beta$ (H),17 $\beta$ (H)-Cholestane		0.78		c, f
20R,5 $\alpha$ (H),14 $\alpha$ (H),17 $\alpha$ (H)-Cholestane		1.19		c, f
20R&S,5 $\alpha$ (H),14 $\beta$ (H),17 $\beta$ (H)-Ergostane		3.15		c, f
20R&S,5 $\alpha$ (H),14 $\beta$ (H),17 $\beta$ (H)-Sitostane		2.61		c, f
Aliphatic aldehydes				
Formaldehyde	22300		*	a, g
Acetaldehyde	41800		*	a, g
Propanal	14000		*	a, g
Butanal	1300		*	a, g
Hexanal	2200		*	a, g
Heptanal	3200		*	a, g
Octanal	3100		*	a, g
Nonanal	4400		*	a, g

Identification notes: (a) authentic quantitative standard. (b) authentic quantitative standard for similar compound in series. (c) secondary standard. (d) detected as a methyl ester.

Exhaust sample collection notes: (e) collected in SUMA canister. (f) collected on denuder/filter/PUF sampling train. (g) collected on DNPH impregnated C<sub>18</sub> cartridges. (\*) not measured. See text for details. Additional Notes: † Compound is too volatile for complete collection by denuder at sampling conditions; mass of this compound reported in the gas-phase includes mass collected on PUF cartridge.

Table 4.2. (continued - page 5)

Compound	Diesel Powered Medium Duty Truck Emissions ( $\mu\text{g km}^{-1}$ )		Diesel Fuel Composition ( $\mu\text{g gram}^{-1}$ )	Notes
	Gas Phase	Particle Phase		
Aliphatic aldehydes				
Decanal	2800		*	a, g
Undecanal	2600		*	a, g
Dodecanal	1200		*	a, g
Tridecanal	2000		*	a, g
Olefinic aldehydes				
Crotonaldehyde	13400		*	a, g
Acrolein	3400		*	a, g
Methacrolein	4000		*	a, g
Aliphatic ketones				
Acetone	22000		*	a, g
Butanone / Methylacrolein	7500		*	a, g
Aromatic aldehydes				
Benzaldehyde	3800		*	a, g
Acetophenone	5100		*	a, g
2,5-Dimethylbenzaldehyde	4100		*	a, g
Aromatic ketones				
Indanone <sup>†</sup>	69.5			a, f
Fluorenone	34.6	9.84		a, f
Xanthone	12.4			a, f
Dicarbonyls				
Glyoxal	2100		*	a, g
Methylglyoxal	1700		*	a, g
Biacetyl	900		*	a, g
n-Alkanoic acids				
Octanoic acid	125		*	a, f, d
Nonanoic acid	240		*	b, f, d
Decanoic acid	72.9		*	a, f, d
Undecanoic acid	206		*	b, f, d
Dodecanoic acid	58.5		*	a, f, d
Tridecanoic acid	13.1		*	b, f, d
Tetradecanoic acid	5.3		*	a, f, d
Heptadecanoic acid		22.3	*	b, f, d
Octadecanoic acid		362	*	a, f, d
Nonadecanoic acid		5.7	*	b, f, d
Eicosanoic acid		14.2	*	a, f, d

Identification notes: (a) authentic quantitative standard. (b) authentic quantitative standard for similar compound in series. (c) secondary standard. (d) detected as a methyl ester.

Exhaust sample collection notes: (e) collected in SUMA canister. (f) collected on denuder/filter/PUF sampling train. (g) collected on DNPH impregnated C<sub>18</sub> cartridges. (\*) not measured. See text for details. Additional Notes: <sup>†</sup>Compound is too volatile for complete collection by denuder at sampling conditions; mass of this compound reported in the gas-phase includes mass collected on PUF cartridge.

Table 4.2. (continued - page 6)

Compound	Diesel Powered Medium Duty Truck Emissions ( $\mu\text{g km}^{-1}$ )		Diesel Fuel Composition ( $\mu\text{g gram}^{-1}$ )	Notes
	Gas Phase	Particle Phase		
Alkanedioic acids				
Octadecanedioic acid		138	*	a, f, d
Nonadecanedioic acid		176	*	a, f, d
Aromatic acids				
Benzoic acid	1260		*	b, f, d
Methylbenzoic acids	772	26.7	*	a, f, d
Other compounds				
Benzofuran	53.2			a, f
Dibenzofuran	28.7	6.0	29	a, f
Dibenzothiophene	1.98			a, f
Dibenzothiazole	251			a, f
Unresolved Complex Mixture	53800	41400	*	b, f

Identification notes: (a) authentic quantitative standard. (b) authentic quantitative standard for similar compound in series. (c) secondary standard. (d) detected as a methyl ester.  
 Exhaust sample collection notes: (e) collected in SUMA canister. (f) collected on denuder/filter/PUF sampling train. (g) collected on DNPH impregnated  $\text{C}_{18}$  cartridges. (\*) not measured. See text for details. Additional Notes: <sup>†</sup> Compound is too volatile for complete collection by denuder at sampling conditions; mass of this compound reported in the gas-phase includes mass collected on PUF cartridge.



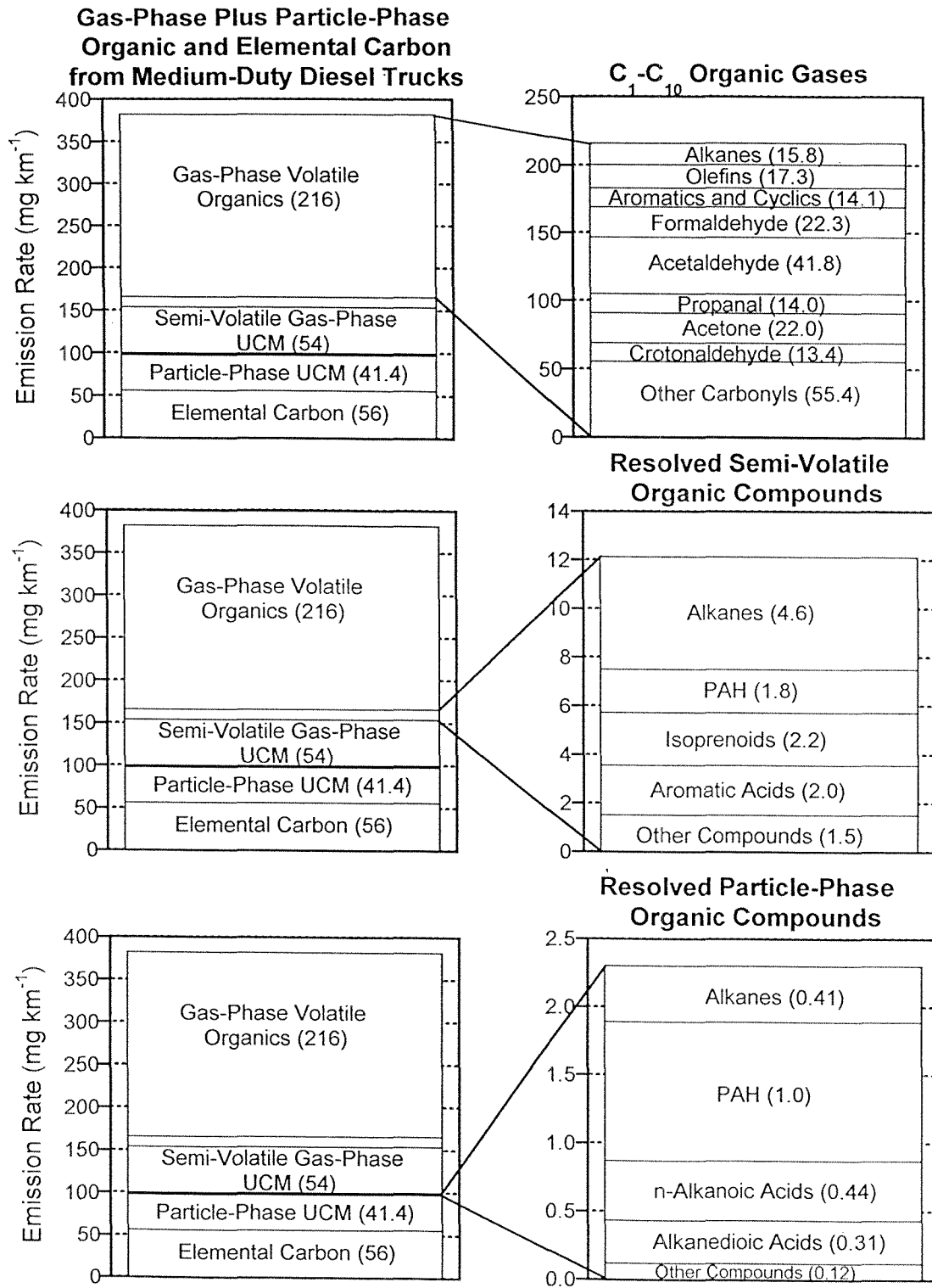


Figure 4.3. Material balance on the gas-phase, semi-volatile, and particle-phase organic compounds emitted from medium duty diesel trucks driven over the hot start Federal Test Procedure urban driving cycle on a chassis dynamometer.

extraction-grade solvents and then analyzing the diluted fuel by the same GC/MS techniques as are used for the exhaust samples in this study. Light gas-phase carbonyls make up the largest fraction of the gas-phase exhaust emissions; they are emitted at a rate of 126 mg per kilometer driven. Over half of the carbonyl emissions consist of formaldehyde plus acetaldehyde, accompanied by significant quantities of propanal, acetone, butanone, and crotonaldehyde. It is known from previous work (13, 14) that the carbonyl emissions from diesel trucks are substantial. The present study is unique because the emissions of high molecular weight carbonyls up to tridecanal are also quantified. Gas-phase alkanes are emitted at a rate of 11.2 mg per kilometer driven, accompanied by smaller quantities of aromatics, PAH, olefins and other vapor-phase organic compounds. A noticeable quantity of the gas-phase alkane mass emitted is in the carbon number range from C<sub>12</sub> through C<sub>20</sub>, which is consistent with the composition of diesel fuel.

A major part of the remaining gas-phase and particle-phase organic compound emissions is made up of an unresolved complex mixture (UCM) comprised of aliphatic branched and cyclic hydrocarbons that are not separable as individual GC peaks. The gas-phase portion of the UCM consists of high molecular weight semi-volatile organics that are in the aggregate emitted at a rate of 54 mg km<sup>-1</sup>, slightly less than half that of the total carbonyl mass emission rate, while the particle-phase UCM contributed an additional 41.4 mg km<sup>-1</sup>.

The composition of the UCM found in the particle phase was very similar to motor oil when analyzed by GC/MS. The distribution of hopanes and steranes in the fine particle exhaust emissions and in motor oil was found to be very similar as well. For these reasons, the UCM contained in the fine particulate matter emitted was quantified according to a GC/MS response factor obtained by using motor oil as a standard. Quantifying the UCM by this method closely closed a mass balance on the organic carbon collected on the quartz fiber filters as analyzed by thermal evolution and combustion analysis and by GC/MS analysis. The vapor phase semi-volatile UCM collected on the denuders and the PUF cartridge was quantified by the same procedure, because the GC/MS response factor for motor oil was close to that of n-alkanes in the carbon number range from C<sub>14</sub> to C<sub>24</sub> on a total ion current (TIC) basis.

The remaining high molecular weight carbonaceous species emitted in the diesel exhaust include resolved vapor-phase semi-volatile and particle-phase organic compounds plus elemental carbon, as summarized in Figure 4.3. Elemental carbon contributes 56 mg km<sup>-1</sup>, while an additional 14.4 mg km<sup>-1</sup> can be accounted for in terms of the individual organic compounds shown in Table 4.2. Included in the resolved organic compounds are n-alkanes, PAH, isoprenoids, saturated cycloalkanes, organic acids, hopanes and steranes.

The n-alkane emission rates are greatest in the carbon number range from C<sub>12</sub> through C<sub>20</sub>, averaging over 400 µg km<sup>-1</sup> for most individual n-alkanes in

this range. n-Butane and n-pentane also are emitted at high rates at 3830 and 1860  $\mu\text{g}$  per kilometer, respectively. As the concentration of the  $\text{C}_4$  and  $\text{C}_5$  alkanes was not analyzed in the diesel fuel, it is unclear whether these compounds are formed in the diesel engine combustion process or if they were originally present in solution in the diesel fuel. Likewise, iso-pentane and other low molecular weight branched alkanes shown in Table 4.2 are emitted at relatively high rates.

Individual organic compounds in the class of branched  $\text{C}_{14}$  through  $\text{C}_{20}$  alkanes known as the isoprenoids are emitted at rates in the range of 360 to 570  $\mu\text{g}$  per vehicle kilometer traveled. The structures of selected isoprenoid hydrocarbons are shown in Figure 4.4. These compounds are naturally present in crude oil (15) and therefore would be expected to be found in lightly processed or straight run diesel fuel cuts in the petroleum refining process. The isoprenoids, in conjunction with certain PAH, hopanes, steranes and elemental carbon as will be described shortly, have the potential to be used as tracers for diesel engine exhaust. Figure 4.5 shows the distribution of the n-alkanes and isoprenoids in the commercial California diesel fuel used in the current source tests compared to the emission rate and phase distribution of these compounds in the diesel truck exhaust. As can be seen in Figure 4.5, the tailpipe emissions are depleted in the lowest molecular weight homologues in each series of these branched and straight chain alkanes when compared to the parent fuel. It

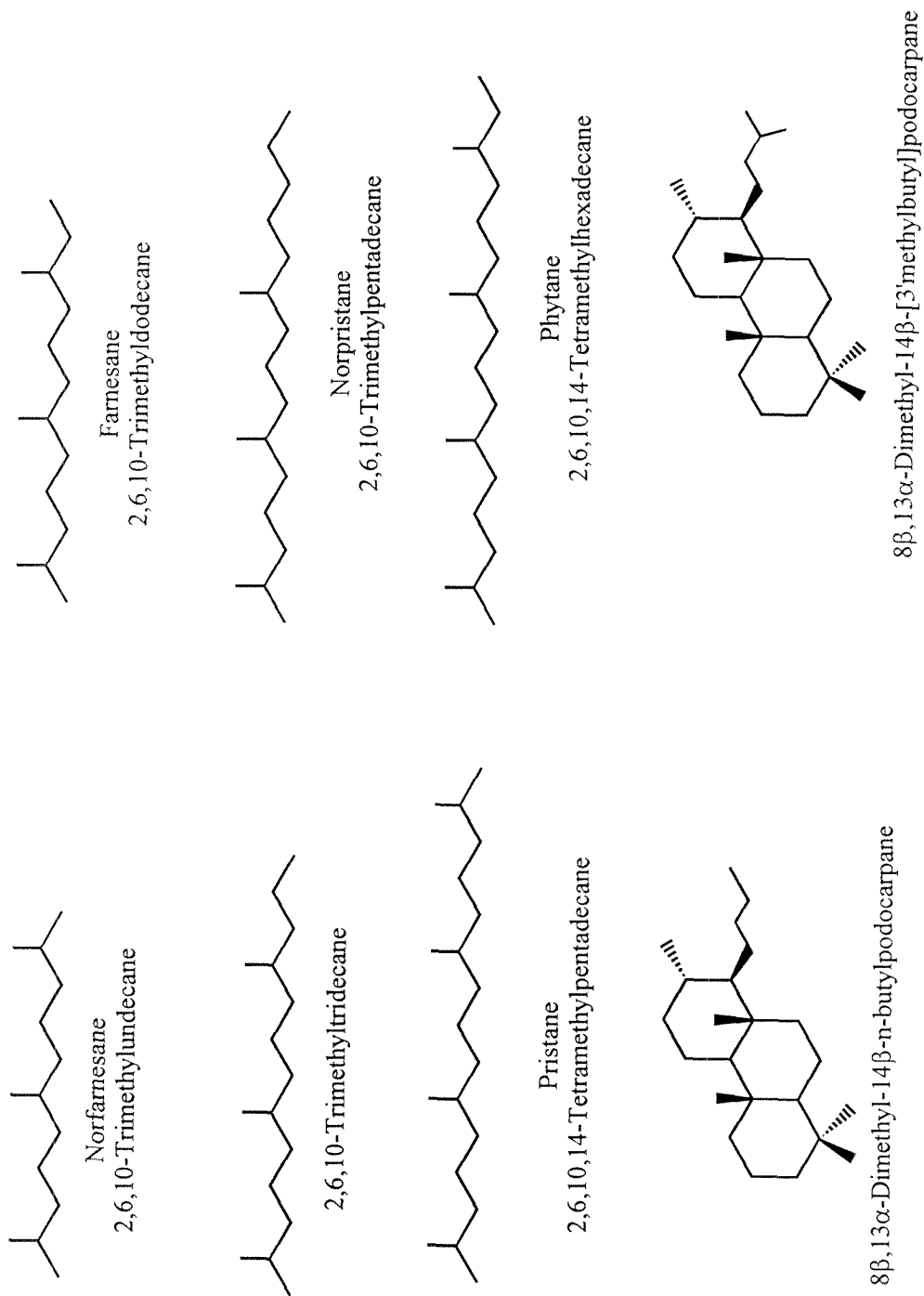


Figure 4.4. Chemical structures of isoprenoids and tricyclic terpanes present in diesel fuel and emitted from diesel trucks.

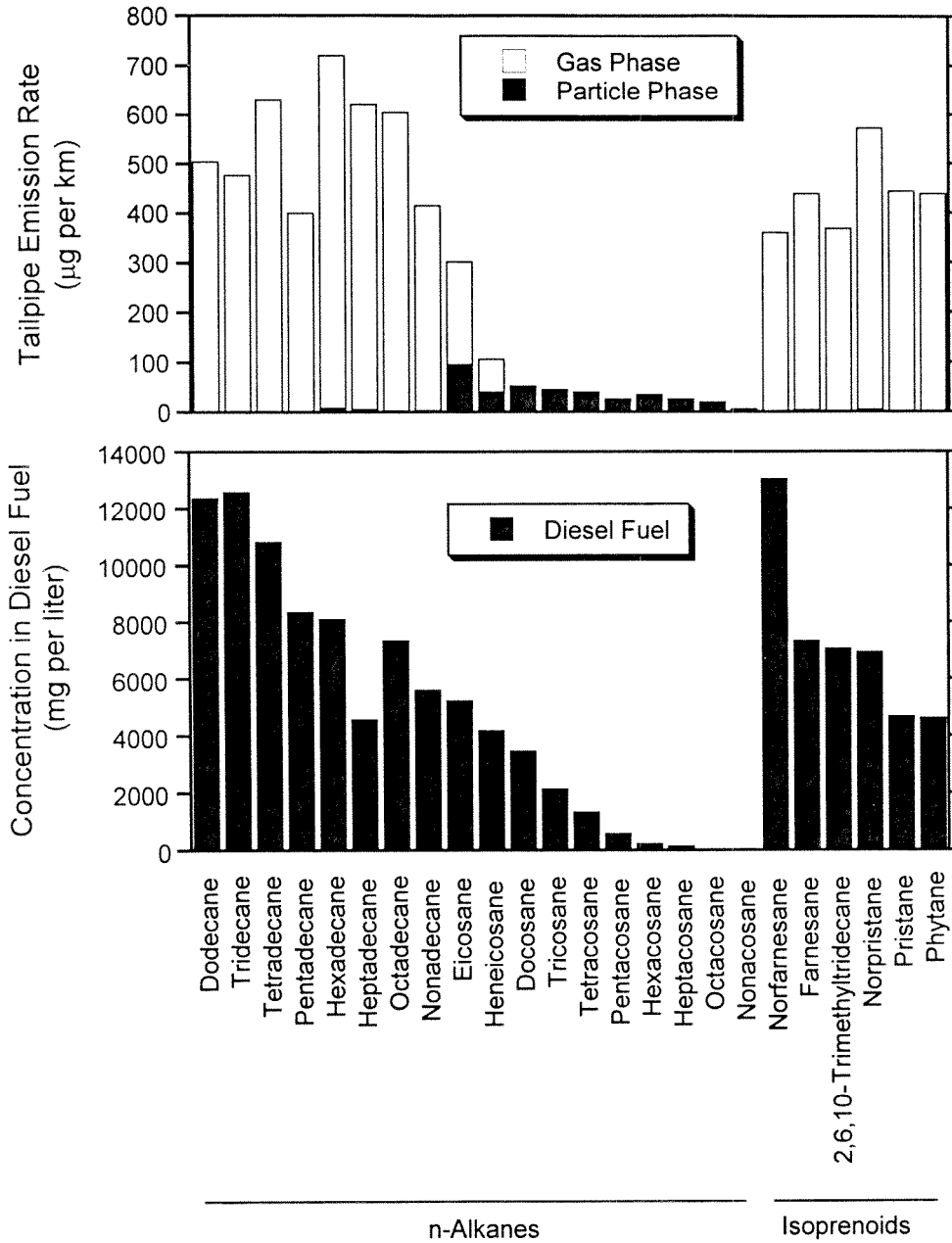


Figure 4.5. Comparison of the distribution n-alkanes and isoprenoids in medium-duty diesel truck exhaust and present in the diesel fuel supplied to those trucks.

should be noted that the overall distribution of the organic compounds between the gas and particle phases summed over the entire FTP driving cycle may not behave according to gas/particle partitioning theory (16) applied to the bulk compound emission rate data averaged over the whole test. At any given point during the FTP cycle, the organic compounds in the diluted exhaust should partition as expected by theory; however, the primary emission rates and organic compound compositions are changing continuously throughout the cycle such that the linear sum of these instantaneous equilibrated phase distributions may not add to produce gas/particle concentration ratios for the test as a whole that correspond to the equilibrium distribution at the average conditions during the test.

A similar comparison between the PAH present in the fuel and in the diesel truck emissions is shown in Figure 4.6. Significant differences can be seen in the ratio of methyl-substituted PAH to unsubstituted PAH between the fuel and the tailpipe emissions. The dimethyl phenanthrenes and anthracenes ( $C_2$ -MW 178 PAH in Table 4.2) contribute the overwhelming majority of the PAH with three or more ring structures in the diesel fuel. The ratio of these compounds to phenanthrene plus anthracene decreases from 33.5 in the diesel fuel to 1.55 in the tailpipe emissions. An analogous but less extreme difference is observed for the methyl fluoranthenes, acephenanthrylenes, and pyrenes

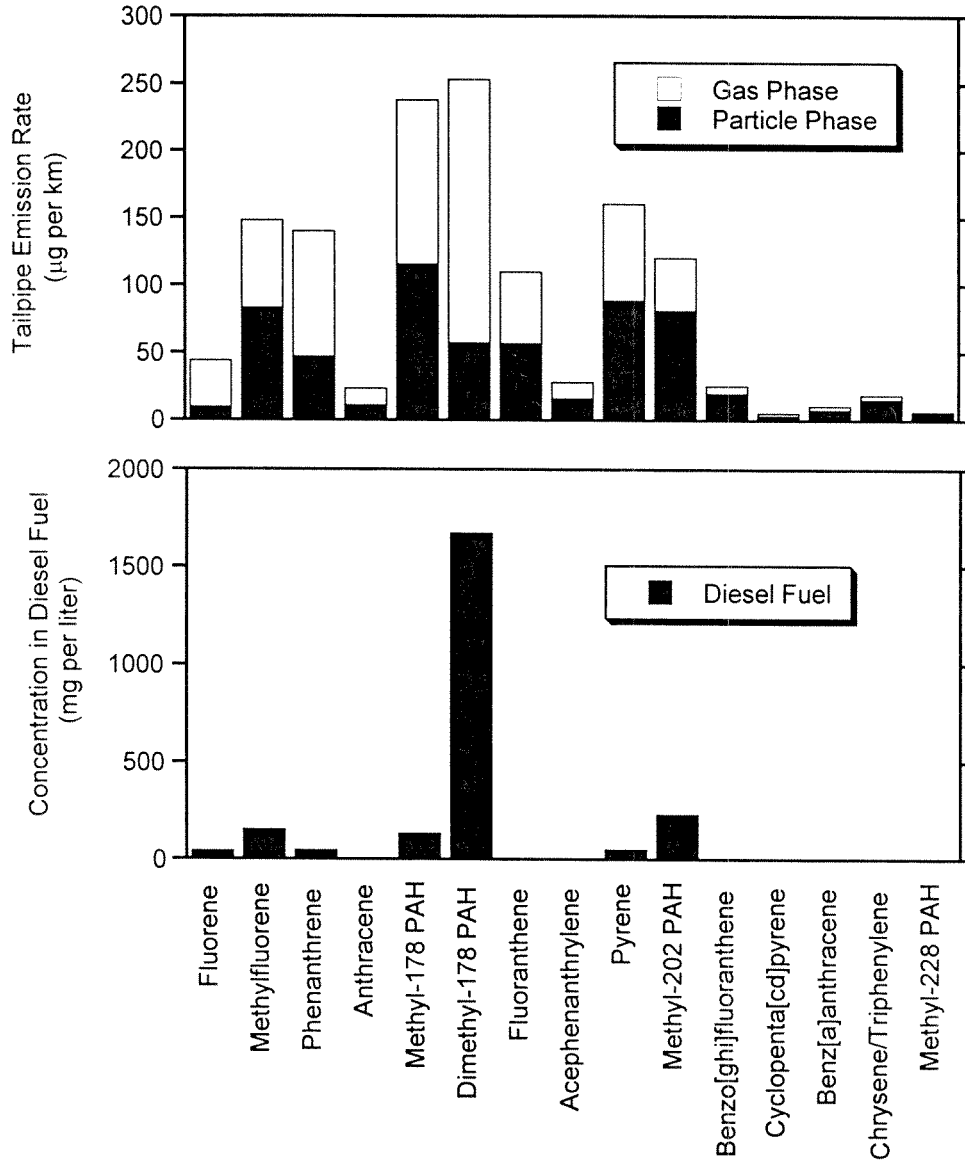


Figure 4.6. Polycyclic aromatic hydrocarbons (PAH) emitted from medium-duty diesel trucks and present in diesel fuel.



(C<sub>1</sub>-MW 202 PAH in Table 4.2) when compared to the unsubstituted PAH with molecular weights of 202.

The particle-phase hopanes and steranes present in vehicle exhaust have been used in the past as tracers for motor vehicle exhaust contributions to atmospheric fine particle samples (3, 4). To this set of particle-phase exhaust molecular tracers we can now add two semi-volatile tricyclic terpanes, 8 $\beta$ ,13 $\alpha$ -dimethyl-14 $\beta$ -n-butylpodocarpane and 8 $\beta$ ,13 $\alpha$ -dimethyl-14 $\beta$ -[3'-methylbutyl]podocarpane, which are quantified in the diesel truck exhaust and have been previously quantified in the atmosphere of Los Angeles (17). The structures of these compounds are shown in Figure 4.4. These compounds are also present in the diesel fuel used in these experiments at 2.1 and 0.6  $\mu\text{g g}^{-1}$ , respectively, as shown in Table 4.2.

The question posed at the outset of the study is now revisited, "How can diesel fuel vapors in the atmosphere be distinguished from diesel truck exhaust and how can diesel truck exhaust be distinguished from gasoline-powered motor vehicle exhaust?" Since diesel exhaust contains unburned diesel fuel, whole fuel vapors share many features in common with the tailpipe exhaust, as we have just seen. However, the diesel truck exhaust is clearly distinguished from unburned fuel by its high black elemental carbon content, by its hopanes and sterane content, by its higher ratio of unsubstituted PAH to methyl-PAH, and by its high aldehyde content (although the aldehydes are too reactive to be

considered as tracer species for diesel exhaust). The hopanes and steranes are not present in large amounts in the fuel (e.g., see Table 4.2) but are present in motor oil (see discussion of standards in text) and thus must be contributed largely by the lubricant oil used by the engines. Diesel exhaust is readily distinguished from gasoline-powered auto exhaust by its higher elemental carbon content and by the relatively high quantity of pristane and phytane in diesel exhaust. Auto exhaust in turn can be distinguished from non-tailpipe derived gasoline vapors because there is a limit placed on the atmospheric concentration of the sum of the gasoline plus diesel engine tailpipe emissions by the total quantity of hopanes and steranes in the atmosphere (3).

Ambient concentrations of semi-volatile n-alkanes, isoprenoids, and tricyclic terpanes were measured by Fraser et al. (17) in Southern California during the summer of 1993. Shown in Figure 4.7 is the 2-day average ambient concentration of n-octadecane, n-nonadecane, n-eicosane, pristane, phytane, and the tricyclic terpanes as measured by Fraser et al. (17) at Azusa, California, along with the diesel engine emission rates of these compounds from the present study. The data from Fraser et al. (17) are scaled upward across all compounds by a factor of 1.7 to correct an error in the reported air volumes sampled. Good agreement is observed between the relative distribution of these compounds measured in the atmosphere and the emission rates of these compounds from the diesel trucks tested in the present study, which further

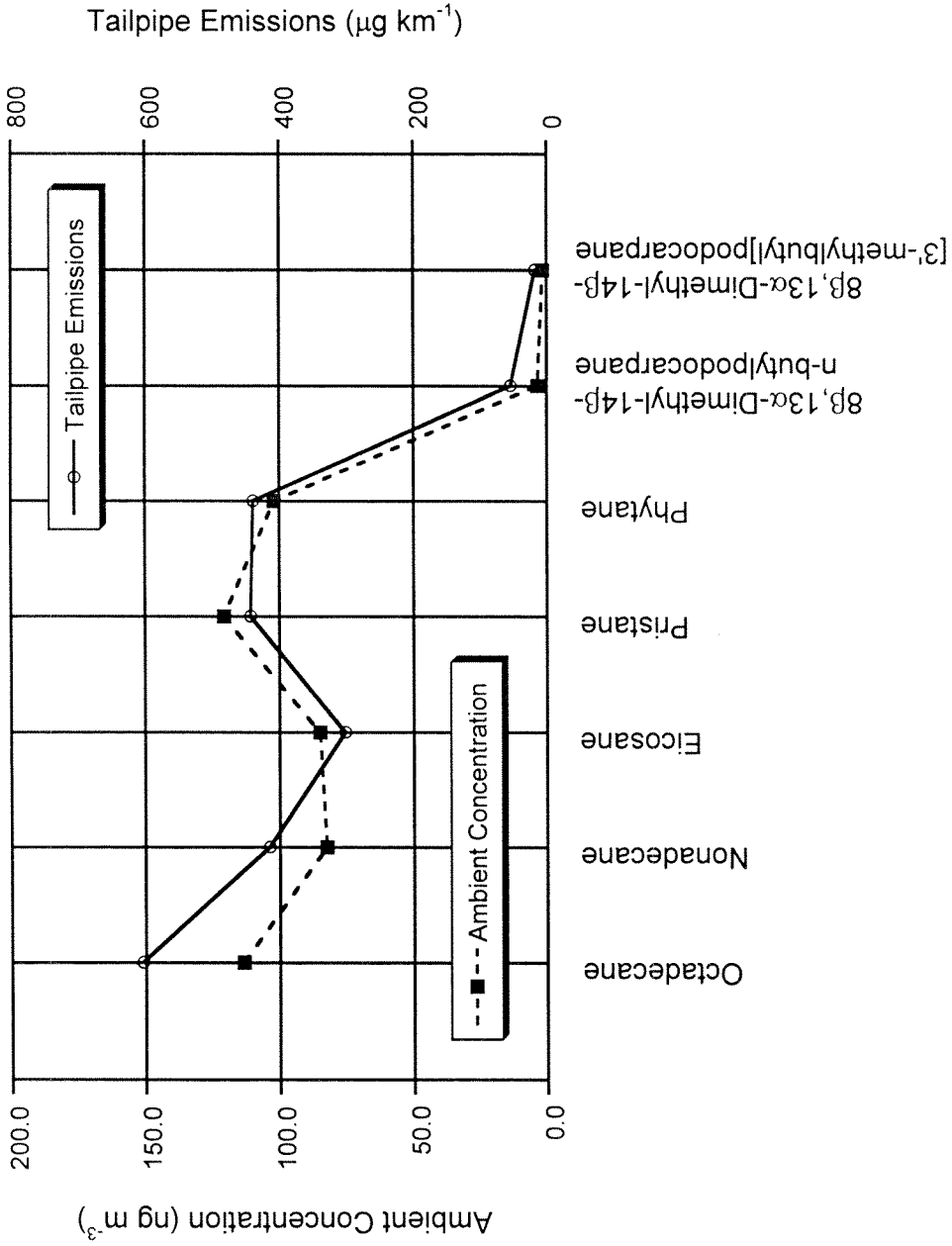


Figure 4.7. Semi-volatile n-alkane, isoprenoid, and tricyclic terpane ambient concentrations measured in Azusa, California, in the summer of 1993 compared to the tailpipe emission rates of these compounds from medium-duty diesel trucks on the FTP hot start driving cycle.

indicates that these compounds will likely be useful as part of the group of tracers for motor vehicle exhaust.

#### 4.4 References

1. Hildemann, L. M.; Markowski, G. R.; Cass, G. R. *Environ. Sci. Technol.* **1991**, 25, 744-759.
2. Rogge, W. R.; Hildemann, L. M.; Mazurek, M. A.; Cass, G. R.; Simoneit, B. R. T. *Environ. Sci. Technol.* **1993**, 27, 636-651.
3. Schauer, J. J.; Rogge, W. R.; Hildemann, L. M.; Mazurek, M. A.; Cass, G. R.; Simoneit, B. R. T. *Atmos. Environ.* **1996**, 30, 3837-3855.
4. Rogge, W. R.; Hildemann, L. M.; Mazurek, M. A.; Cass, G. R.; Simoneit, B. R. T. *J. Geophys. Res.* **1996**, 101, 19379-19394.
5. Lowenthal, D. H.; Zielinska, B.; Chow, J. C.; Watson, J. G.; Gautum, M.; Ferguson, D. H.; Neuroth, G. R.; Stevens, K. D. *Atmos. Environ.* **1994**, 28, 731-743.
6. Westerholm, R. N.; Almen, J.; Hang, L.; Rannug, J. U.; Egeback, K. E.; Gragg, K. *Environ. Sci. Technol.* **1991**, 25, 332-338.
7. Benner, B. A.; Gordon, G. E.; Wise, S. A. *Environ. Sci. Technol.* **1989**, 23, 1269-1278.
8. Fernandez, P.; Vilanova, R.; Grimalt, J. O. *Polycyclic Aromatic Hydrocarbons* **1996**, 9, 121-128.

9. Simo, R.; Grimalt, J. O.; Albaiges, J. *Environ. Sci. Technol.* **1997**, 31, 2697-2700.
10. Tancell, P. J.; Rhead, M. M.; Pemberton, R. D.; Braven, J. *Environ. Sci. Technol.* **1995**, 29, 2871-2876.
11. Hildemann, L. M.; Cass, G. R.; Markowski, G. R. *Aerosol Sci. Technol.* **1989**, 10, 193-204.
12. John, W.; Reischl, G. *JAPCA* **1980**, 30, 872-876.
13. Wagner, T.; Wyszynski, M. L. *Proc. Instn. Mech. Engrs.* **1996**, 210, 109-122.
14. Sagebiel, J. C.; Zielinska, B.; Pierson, W. R.; Gertler, A. W. *Atmos. Environ.* **1996**, 30, 2287-2296.
15. Philp, R. P. *Mass Spectra* **1985**, 4, 1-54.
16. Pankow, J. F. *Atmos. Environ.* **1994**, 28, 185-188.
17. Fraser, M. P.; Cass G. R.; Simoneit B. R. T.; Rasmussen R. A. *Environ. Sci. Technol.* **1997**, 31, 2356-2367.

## Chapter 5

# Organic Compounds from Gasoline-Powered Motor Vehicles

### 5.1 Introduction

Tailpipe emissions of volatile hydrocarbons from gasoline-powered motor vehicles have been studied extensively to determine the characteristics of the compounds emitted (1-5) and their contribution to photochemical smog formation (6-9). Likewise, a detailed analysis of the organic compounds in the particulate matter emitted in the exhaust from mid-1980's California on-road motor vehicles has been conducted (10), and this analysis has been used in air quality models to determine the direct primary contribution of motor vehicle exhaust to the fine particulate organic compounds and fine particle mass concentrations in the Southern California urban atmosphere (11,12). Very little, however, is known about the contribution of gasoline-powered motor vehicles to the urban concentrations of the high molecular weight vapor phase semi-volatile organic compounds that typically are too heavy to be analyzed by gas canister sampling and Teflon bag sampling. The role of these compounds in the atmosphere has not been addressed largely due to the lack of emissions data for these species.

Since some of the semi-volatile organic compounds are toxic air contaminants (i.e. PAH) and since the semi-volatile and heavy volatile organic compounds likely play a role in photochemical smog formation and in secondary organic aerosol formation, there is a need to understand the sources and fates of these compounds in the atmosphere. Air pollution models currently are being developed to assess the role of these compounds, and a corresponding need to measure the emissions of these compounds from urban air pollution sources exists.

In an effort to reduce the emissions of air pollutants, both motor vehicle designs and gasoline formulations have changed during the 1980's and 1990's. As a result, the composition of the emissions from gasoline-powered motor vehicles are expected to have changed as well. While considerable effort has been expended to determine the effect of reformulated fuels on the volatile organic compounds emitted from gasoline-powered vehicles (13, 14), much less is known about the effects of fuel reformulation and vehicle design changes on the semi-volatile and particulate organic compounds emitted. The most recent detailed measurements of particulate organic compound emissions from individual in-use motor vehicles in Southern California are from vehicles owned and operated in the mid 1980's (10, 15). The current study was undertaken to measure the more recent tailpipe emission rates of volatile organic compounds from gasoline-powered motor vehicles, to provide the first data on the



distribution of semi-volatile organic compounds between the gas and particle phases, and to both update and extend the carbonyl and particle-phase organic compounds emissions data.

## **5.2 Experimental Methods**

### **5.2.1 Comprehensive Source Sampling**

The dilution sampler used in the present study consists of two stages, the pre-dilution tunnel and the primary sampling system. The pre-dilution tunnel is connected via a stainless steel hose directly to the tailpipe of the gasoline-powered motor vehicle being tested on a chassis dynamometer. At the entrance of the pre-dilution tunnel, HEPA-filtered and activated carbon-filtered dilution air is turbulently mixed with the vehicle exhaust. The pre-dilution tunnel is operated at a fixed combined flowrate, such that the exhaust concentration in this tunnel is always proportional to the total emission rate from the vehicle tailpipe. Most of the exhaust from the pre-dilution tunnel is expelled through a flow orifice at the downstream end of the tunnel while a small slipstream is removed isokinetically from the pre-dilution tunnel through a cyclone separator. Particles smaller than 10  $\mu\text{m}$  in aerodynamic diameter exit the cyclone along with the gas-phase species and are passed through a venturi meter into the primary sampling system where the sample is further diluted with purified dilution air. The total dilution rate of the combined two-stage system is set at approximately 140 fold

for the noncatalyst cars and 40 fold for the catalyst-equipped cars. All of the internally exposed area of the entire two-stage dilution sampler is constructed only of aluminum, Teflon, and stainless steel. The entire sampler is assembled in a way that is completely free of grease coatings and rubber gaskets (Teflon o-rings are used as seals). The pre-dilution tunnel and the primary dilution tunnel are thoroughly cleaned prior to sampling.

The sampling system used in this experiment is a modified version of the portable dilution tunnel originally developed by Hildemann et al. (15, 16). The modifications made to this system have been previously described in Chapters 2 and 4. A diagram of the original dilution sampler is shown in Figure 1 of Hildemann et al. (16), its use with a pre-dilution tunnel to test motor vehicles is shown in Figure 1 of Hildemann et al. (15), and the new sample collection systems are shown in Figure 2.1 of Chapter 2. At the back end of the dilution sampler is the residence time chamber where the sampling trains are connected. Semi-volatile and fine particle-phase organic compounds are collected using both a denuder/filter/PUF sampling train and a filter/PUF sampling train. These sampling configurations are described in Chapter 2. In addition, a third type of cyclone-based sampling unit is operated to collect fine particulate matter, carbonyls, organic acids, and gas-phase hydrocarbons. This sampling unit is also described in detail in Chapter 2.

MOUDI impactors and electronic particle sizing instruments are also used to obtain particle size distributions and particle chemical composition as a function of size for the diluted gasoline-powered vehicle exhaust. The size distribution measurements will be reported elsewhere.

### **5.2.2 Vehicle Selection**

The vehicles tested in the current study are all sampled from the on-road vehicle fleet registered in Southern California. The catalyst-equipped motor vehicles are selected to represent the distribution of accumulated vehicle miles traveled (VMT) by automobiles and light trucks of various model years in Southern California as reported by Horie et al. (17). The nine catalyst-equipped motor vehicles tested are listed in Table 5.1. These vehicles span model years from 1981 through 1994 and consist of three light-duty trucks and six automobiles. The two noncatalyst equipped motor vehicles tested are typical vehicles of this type and are also listed in Table 5.1. No modifications or repairs were made to the vehicles; the vehicles were tested as received using the commercial gasoline fuels obtained with the vehicles.

### **5.2.3 Source Testing Procedure**

The vehicles were tested at the California Air Resources Board (CARB) Haagen-Smit Laboratory in El Monte, California. The dynamometers used for

Table 5.1. Fine Particle Tailpipe Emissions from the Gasoline-Powered Motor Vehicles Tested

Model Year	Vehicle Manufacturer and Model	Engine (Displacement and Number of Cylinders)	Vehicle Mileage (miles)	Fine Particle Emission Rate ( $\text{mg km}^{-1}$ )
Catalyst Equipped Motor Vehicles				
1994	Honda Civic	1.5 liters 4 cyl	17,458	$0.8 \pm 0.4$
1994	Ford Taurus	3.0 liters 6 cyl	26,731	$7.8 \pm 0.3$
1992	Toyota Pick-Up Truck	3.0 liters 6 cyl	41,283	$6.1 \pm 0.9$
1992	Chevy Astrovan	5.0 liters 8 cyl	49,439	$3.0 \pm 1.1$
1990	Toyota Celica	2.2 liters 4 cyl	54,911	$2.9 \pm 0.5$
1990	GMC Pick-Up Truck	5.0 liters 8 cyl	21,073	$3.2 \pm 0.5$
1986	Chrysler Reliant K	2.2 liters 4 cyl	78,656	$2.3 \pm 0.3$
1984	Toyota Tercel	1.5 liters 4 cyl	76,656	$5.4 \pm 0.6$
1981	Honda Accord	1.8 liters 4 cyl	106,722	$36.4 \pm 2.2$
Noncatalyst Equipped Motor Vehicles				
1970	Volkswagon Vancamper	1.6 liters 4 cyl	30,000 <sup>a</sup>	$200 \pm 5$
1969	Chevy Camaro	5.0 liters 8 cyl	371,780	$985 \pm 3$

<sup>a</sup> Indicated mileage since engine was rebuilt

testing were twin-roll hydraulic dynamometers. The dynamometers were loaded at settings specified by the vehicle manufacturers by the Haagen-Smit Laboratory staff, and the vehicles were driven on the dynamometers by the CARB dynamometer operations staff. The cold start Federal Test Procedure (FTP) urban driving cycle used for all of the tests is shown in Figure 5.1.

Upon receipt of each vehicle, a sample of the gasoline present in the vehicle fuel tank was withdrawn for analysis. The vehicles were warmed-up on a dynamometer and then placed in storage at 24 °C for 16 to 24 hours. After cold storage the vehicles were rolled onto the dynamometer and first were tested using the standard FTP urban driving cycle (Figure 5.1) and constant volume sampler (CVS) specified by the Federal Register for routine volatile organic compound (VOC), CO and NO<sub>x</sub> compliance testing of motor vehicles. The two stage dilution sampler was not used for these tests. At the completion of the FTP/CVS emissions test, each vehicle was returned to storage at 24 °C for an additional 16 to 24 hours. After the second storage period each vehicle was returned to the dynamometer and was tested using the same FTP urban driving cycle but with the vehicle exhaust routed to the two-stage dilution sampler.

Flows were established through the dilution sampler 1 minute prior to starting the engine on the FTP cycle. The sampler was run continuously through the first two stages of the FTP cycle, the cold start and the hot running section of

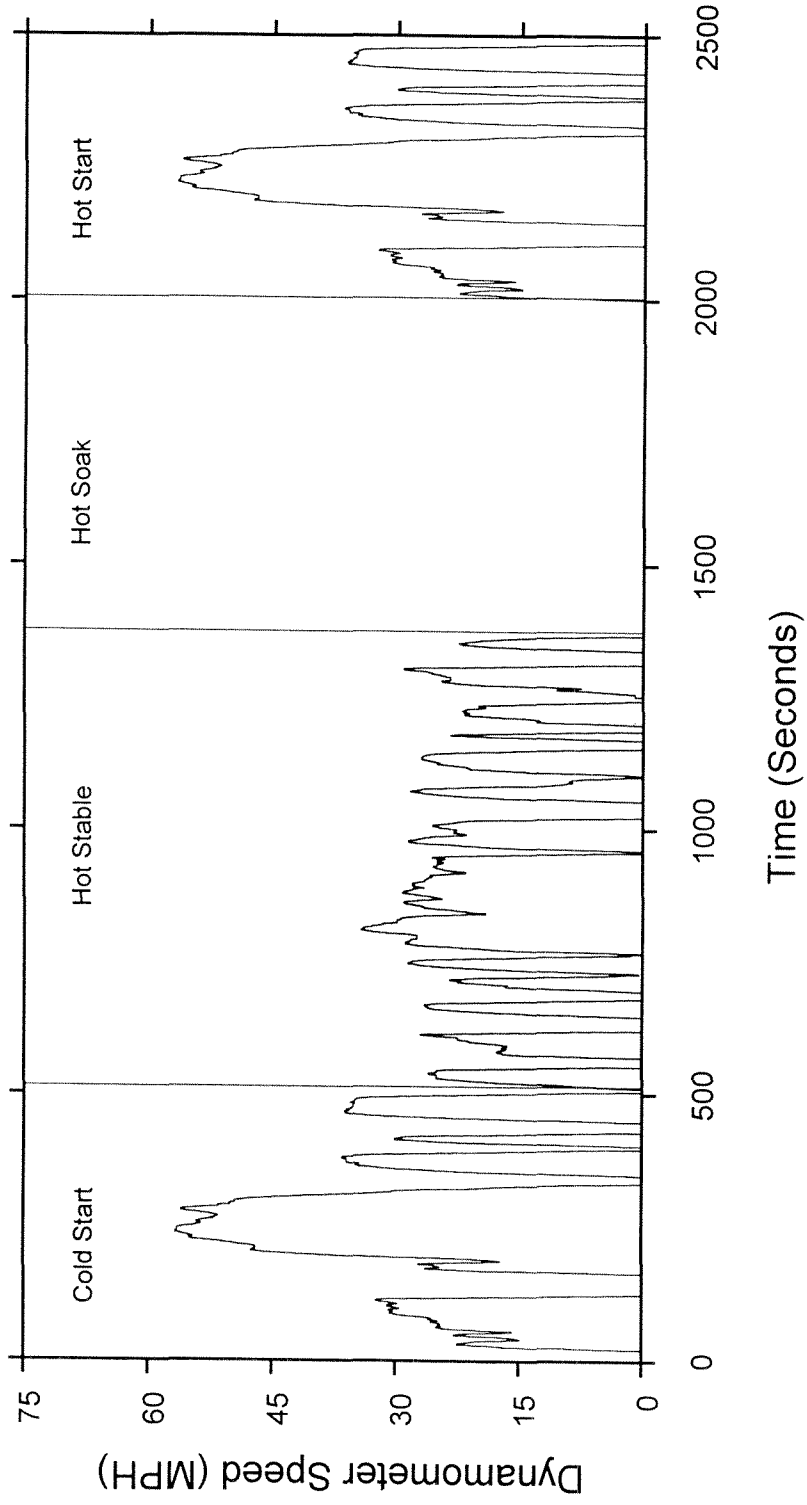


Figure 5.1. Federal Test Procedure (FTP) Urban Driving Cycle.

the cycle. One minute after the engine was turned off during the hot soak section of the FTP cycle, all of the flows through the dilution sampler were stopped. Likewise, one minute before the engine was restarted on the hot start section of the cycle, all of the flows were re-established through the dilution sampler, and the sampler was shut down one minute after the end of the FTP cycle. This protocol was employed to minimize pulling clean air over the sample collection substrates which could potentially lead to evaporation of semi-volatile organic compounds from the substrates causing sampling artifacts due to recollection on downstream substrates.

The catalyst-equipped gasoline-powered motor vehicles were tested in groups of three. Between each of the vehicles in a group, the XAD-coated denuders and one Teflon filter were replaced with new substrates. All other sample collection substrates, cartridges, and canisters were used to collect composites of the emissions from the three vehicles. This approach allowed enough mass collection for detailed organic chemical analysis while also providing for measurement of the individual fine particle mass emission rate for each vehicle tested. The same approach was used for the noncatalyst equipped motor vehicles except that only two vehicles were tested in this group.

Nitrogen oxides, carbon monoxide, methane, and total non-methane hydrocarbons were measured during the FTP/ CVS tests. In addition,

molecular weight vapor phase hydrocarbon emissions were sampled for detailed compound speciation for three vehicles, the 1992 Chevy Astrovan, the 1990 Toyota Celica, and the 1990 GMC Pick-Up Truck. These three vehicles were tested as a group using the two-stage dilution source sampler with the VOC emissions composited into one gas canister. This allows a comparison of the standard FTP hydrocarbon emissions speciation measurement to the measurements made from the canister-based sample collected by the two-stage dilution source sampler.

#### **5.2.4 Organic Chemical Analysis**

The same analytical techniques were used to quantify the semi-volatile and particulate organic compounds in the emissions from the gasoline-powered motor vehicles as was used in the diesel truck source test experiment. These procedures are described in Chapter 2.

Total non-methane organic gases (NMOG, EPA method TO12) and individual organic vapor phase hydrocarbons ranging from  $C_1$  to  $C_{10}$  are analyzed from the SUMA canisters by gas chromatography/flame ionization detection (GC/FID) (see Chapter 2). Carbonyls collected by the  $C_{18}$  impregnated cartridges are analyzed by liquid chromatography/UV detection (see Chapter 2).



## 5.3 Results

### 5.3.1 Comparison of Speciated Volatile Hydrocarbon Emissions Measurements

The speciation of the volatile non-methane hydrocarbons was determined for emissions collected by the FTP/CVS sampler from three of the vehicles in the test fleet: the 1992 Chevy Astrovan, the 1990 Toyota Celica, and the 1990 GMC Pick-Up Truck. Since these three vehicles were tested as a group by the two-stage dilution source sampler, the average emissions rates of volatile hydrocarbons for these three vehicles can be compared for the two different sampling systems. Shown in Figure 5.2 is a comparison of the emissions of 53 volatile hydrocarbons measured by gas chromatography/flame ionization detection according to the FTP/CVS hydrocarbon speciation method and according to the methods described for use with the two-stage dilution sampler. Excellent agreement is observed for volatile hydrocarbon compounds emitted at rates  $> 1.0 \text{ mg km}^{-1}$ . For hydrocarbons emitted at rates  $< 1.0 \text{ mg km}^{-1}$  there is greater scatter in the data. This scatter at lower emission rates is due to the fact that the dilution air contains small amounts of contaminants in both sampling systems. The dilution air contaminant concentrations are measured and subtracted from the emissions in both sampling systems, but this correction produces a greater relative uncertainty at low emission rates.

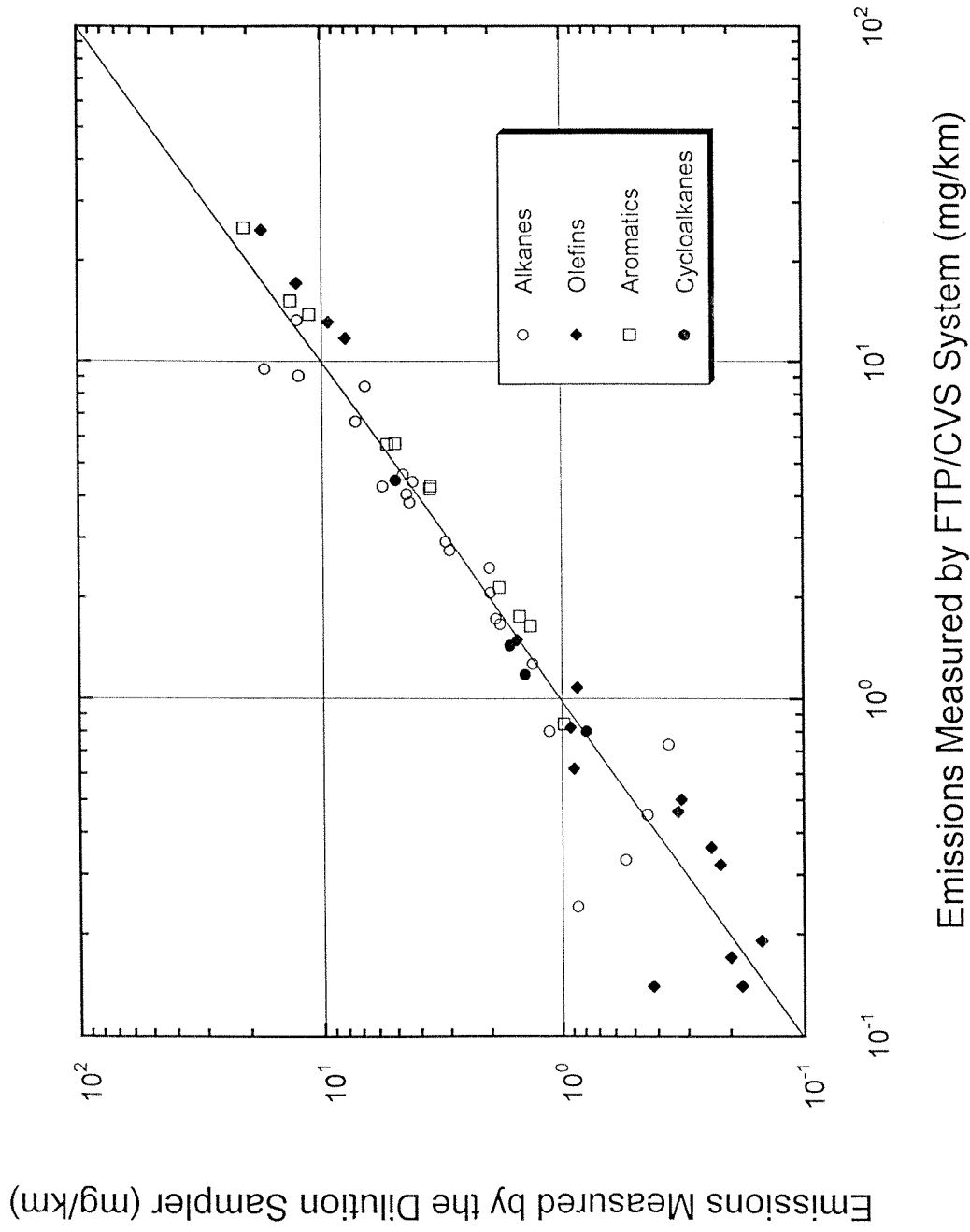


Figure 5.2. Individual hydrocarbon compounds emitted from a composite of 3 light-duty vehicles tested on the FTP Urban Driving Cycle as measured by the FTP/CVS sampler compared to measurements made for the same species and vehicles using the 2-stage dilution sampler.

The excellent agreement between the two source sampling methods is significant. Most gasoline-powered motor vehicle emissions data are collected using the FTP/ CVS Teflon bag technique, while most ambient atmospheric data are collected in stainless steel canisters like those used by the two-stage dilution sampler. Data taken by these different sampling techniques are compared whenever air pollution models driven by CVS-based emissions data are compared to ambient atmospheric data collected by canister sampling. These results indicate that there is no systematic bias inherent in these comparisons.

### **5.3.2 Fine Particle Mass and Chemical Composition**

The fine particle mass emissions rate for each of the motor vehicles tested is given in Table 5.1. Averaging over all nine of the catalyst-equipped gasoline-powered motor vehicles tested, the mean fine particle mass emission rate over the FTP driving cycle was  $7.5 \pm 2.7$  mg per kilometer. It should be noted that the 1981 Honda Accord had an emissions rate that was significantly higher than any of the other eight vehicles at  $36.4 \pm 2.2$  mg per kilometer. The average emission rate, not including the high emitter, is  $3.9 \pm 1.1$  mg per kilometer.

Hildemann et al. (15) tested a fleet of catalyst-equipped gasoline-powered vehicles in the mid 1980's and also found that one high emitting vehicle among the group tested had a significant effect on the average fine particle emission

rate from the group as a whole. The average fine particle emission rate from all catalyst-equipped cars tested by Hildemann et al. (15) was 18 mg per kilometer. Not including the high emitter, the average fine particle emission rate during the mid 1980's tests was 11 mg per kilometer. A comparison of the present emission rates to the emissions measured in the mid 1980's shows a reduction of fine particle emissions by approximately 60% over this ten year period.

The fine particle emission rates for the two noncatalyst gasoline-powered motor vehicles were 200 mg per kilometer for the 1970 Volkswagon Vancamper and 985 mg per kilometer for the 1969 Chevy Camaro. These emission rates are significantly greater than the average emission rate of  $59 \pm 25$  mg per kilometer from the noncatalyst cars tested by Hildemann et al. (15) in the mid 1980's. It should be noted that the average age of the noncatalyst equipped vehicles tested by Hildemann et al. (15) in the mid 1980's was 16 years old, and that the average age of the noncatalyst motor vehicles tested in the current study is 26 years old. This increase in average age arises from the fact that noncatalyst equipped cars were phased out in the mid-1970's. While the Volkswagon Vancamper has a rebuilt engine, the 1969 Camaro does not. With increasing age, the Camaro has accumulated 371,780 miles driven. Its fine particle emissions alone are equivalent to those of more than 130 of the in-use catalyst-equipped cars. As a result it may be that an extraordinarily small

fraction of the vehicle fleet is responsible for the majority of the fine particle emissions from gasoline-powered light-duty vehicles in Southern California.

During each group of source tests fine particle organic and elemental carbon emissions were measured from one of the quartz fiber filters located downstream of the XAD-coated annular denuder and also from one of the quartz fiber filters which did not have the gas-phase semi-volatile organic compounds removed by the denuder prior to collection on the filter. The organic carbon measured on the filters downstream of the denuder averaged 73% of the organic carbon on the undenuded filter sample for the catalyst equipped gasoline powered motor vehicles. Since very little semi-volatile organic carbon was present on the PUF cartridges of the denuder/filter/PUF sampling train, it is reasonable to assume that the higher organic carbon mass measured on the undenuded filter sample was due to sorption of gas-phase semi-volatile organic compounds to the quartz fiber filter and to the particulate matter collected on the filter.

Using the denuder/filter/PUF particulate organic carbon measurement, the fine particle mass emitted from catalyst-equipped motor vehicles was found to be comprised of  $31.8 \pm 2.1$  percent organic carbon and  $10.3 \pm 2.1$  percent elemental carbon. The next largest constituent of the fine particle mass was ammonium ion at  $2.15 \pm 0.13$  percent. Sulfate was the next largest component accounting for  $1.1 \pm 0.3$  percent of the mass. Silicon, phosphorus, chlorine,

calcium, iron, and zinc were also present in small but measurable quantities. The fine particle mass elemental and ionic composition is shown in Table 5.2.

The fine particulate organic carbon measured downstream of the denuder for the noncatalyst equipped motor vehicles was found to be 69.5% of the organic carbon on the undenuded filter sample. Using the fine particulate carbon determined by the denuder/filter/PUF sampling train, the fine particle mass emitted from the noncatalyst equipped motor vehicles tested is  $58.3 \pm 2.7$  percent organic carbon and  $1.4 \pm 0.4$  percent elemental carbon. The next largest constituent in the fine particulate mass emitted from noncatalyst equipped gasoline powered vehicles is sulfur making up 0.28% of the mass. Silicon, phosphorus, calcium, iron, zinc, and lead also contribute smaller but measurable proportions of the mass as shown in Table 5.2. The lead present in the fine particulate matter emitted is likely due to lead deposited in the engine and/or exhaust systems when the vehicles were operated with leaded gasoline in earlier years.

### **5.3.3 Distribution of Carbon Emissions**

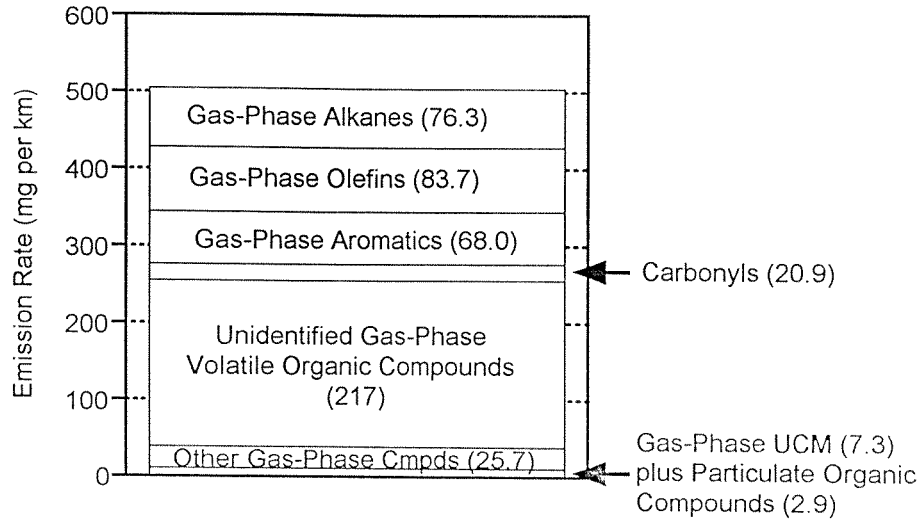
Gas-phase species dominate the organic compound emissions from both noncatalyst and catalyst-equipped motor vehicles. Figure 5.3 shows the distribution of non-methane organic compound emissions for both types of gasoline-powered motor vehicles. A detailed list of the emission rate and phase

Table 5.2. Average Fine Particle Emission Rate and Fine Particle Chemical Composition of Tailpipe Exhaust from Gasoline-Powered Motor Vehicles (Values shown in boldface are greater than zero by at least two standard errors).

	Catalyst-Equipped Gasoline-Powered Vehicles	Noncatalyst Gasoline Powered Vehicles
Fine Particle Emissions Rate (AVG ± STD)	<b>7.5 ± 2.7 mg km<sup>-1</sup></b>	<b>593 mg km<sup>-1</sup></b>
X-ray Fluorescence (Wt % of Fine Particle Mass)		
Aluminum	0.26 ± 0.23	0.00 ± 0.03
Silicon	<b>0.25 ± 0.11</b>	<b>0.12 ± 0.01</b>
Phosphorus	<b>0.31 ± 0.08</b>	<b>0.03 ± 0.01</b>
Sulfur	<b>0.48 ± 0.04</b>	<b>0.28 ± 0.01</b>
Chlorine	<b>0.44 ± 0.13</b>	0.01 ± 0.02
Potassium	0.04 ± 0.15	0.00 ± 0.01
Calcium	<b>0.35 ± 0.11</b>	<b>0.03 ± 0.01</b>
Titanium	0.01 ± 0.64	0.00 ± 0.06
Vanadium	0.00 ± 0.32	0.00 ± 0.02
Chromium	0.00 ± 0.09	0.00 ± 0.01
Manganese	0.00 ± 0.05	0.00 ± 0.00
Iron	<b>0.11 ± 0.03</b>	<b>0.01 ± 0.00</b>
Nickel	0.00 ± 0.03	0.00 ± 0.00
Copper	0.00 ± 0.03	0.00 ± 0.00
Zinc	<b>0.19 ± 0.02</b>	<b>0.03 ± 0.00</b>
Gallium	0.01 ± 0.05	0.00 ± 0.00
Arsenic	0.00 ± 0.06	0.00 ± 0.01
Selenium	0.01 ± 0.03	0.00 ± 0.00
Bromine	0.00 ± 0.03	0.00 ± 0.00
Rubidium	0.00 ± 0.03	0.00 ± 0.00
Strontium	0.01 ± 0.03	0.00 ± 0.00
Yttrium	0.00 ± 0.04	0.00 ± 0.00
Zirconium	0.00 ± 0.04	0.00 ± 0.00
Molybdenum	0.03 ± 0.09	0.00 ± 0.01
Palladium	0.00 ± 0.24	0.00 ± 0.02
Silver	0.06 ± 0.26	0.00 ± 0.02
Cadmium	0.00 ± 0.27	0.01 ± 0.03
Indium	0.12 ± 0.31	0.01 ± 0.03
Tin	0.03 ± 0.44	0.00 ± 0.04
Antimony	0.22 ± 0.52	0.02 ± 0.04
Barium	0.00 ± 1.73	0.00 ± 0.16
Lanthanum	0.31 ± 2.29	0.00 ± 0.22
Mercury	0.01 ± 0.07	0.00 ± 0.01
Lead	0.00 ± 0.09	<b>0.03 ± 0.00</b>
Elemental and Organic Carbon (Wt % of Fine Particle Mass)		
Organic Carbon	<b>23.2 ± 1.5<sup>a</sup></b>	<b>40.5 ± 1.9<sup>a</sup></b>
Elemental Carbon	<b>10.3 ± 2.1</b>	<b>1.4 ± 0.4</b>
Ionic Species (Wt % of Fine Particle Mass)		
Nitrate	0.47 ± 0.45	<b>0.07 ± 0.02</b>
Sulfate	<b>1.09 ± 0.30</b>	<b>0.05 ± 0.01</b>
Ammonium	<b>2.15 ± 0.13</b>	0.00 ± 0.01

Notes: (a) measured downstream of organics denuder. Organic carbon measured on undenuded filter is 31.8 % and 58.3 % of the fine particle mass for the catalyst-equipped and noncatalyst motor vehicle, respectively.

**Catalyst-Equipped Gasoline Powered Vehicles**



**Non-Catalyst Gasoline Powered Vehicles**

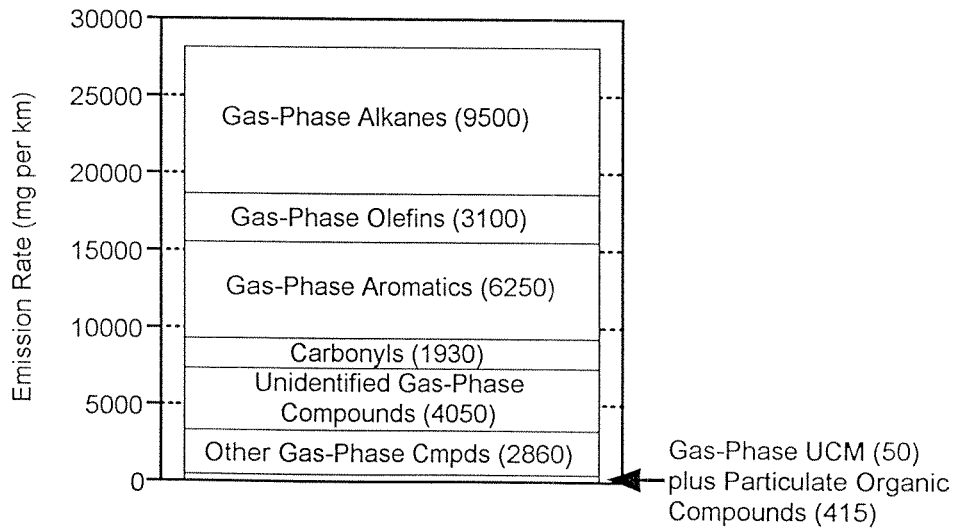


Figure 5.3. Mass balance on the non-methane organic compounds and elemental carbon emitted from catalyst-equipped and noncatalyst equipped gasoline-powered light-duty motor vehicles.



distribution of the organic compounds identified in the vehicle exhaust is given in Table 5.3. Also shown in Table 5.3 is the average composition of the commercial gasoline used by the vehicles in these source tests. n-Alkane and branched alkane gas-phase emissions are dominated by the same organic compounds which are present in noticeable quantities in gasoline. In contrast, ethene, propene, and ethyne make up a majority of the gas-phase olefinic compound emissions. These olefinic species are formed by the incomplete combustion of gasoline and are only present at trace levels in gasoline. The distribution of the monocyclic aromatic hydrocarbons emitted also is similar to the distribution of the aromatics present in the fuel, except that an enrichment in the benzene concentration is observed in the tailpipe emissions relative to the quantity of benzene in the gasoline burned.

Figures 5.4 and 5.5 show an expanded view of the semi-volatile and particle-phase organic compound emissions that form the lowest slice of the graphs in Figure 5.3 along with the elemental carbon emitted. Measurements shown are made by the denuder/filter/PUF sampling train. In this context, semi-volatile and particle-phase organic compounds are hydrocarbons with more than 11 carbons, carboxylic acids with more than 8 carbons, and all organic dicarboxylic acids. For the catalyst-equipped vehicles in Figure 5.4, the gas-phase unresolved complex mixture (UCM) of branched and cyclic hydrocarbons that appears as a wide hump that underlies the resolved peaks on

Table 5.3. Organic Compounds Present in Gasoline and in Gasoline-Powered Motor Vehicle Tailpipe Emissions

Compound	Catalyst-Equipped Gasoline-Powered Motor Vehicle Tailpipe Emissions ( $\mu\text{g km}^{-1}$ )		Noncatalyst-Equipped Gasoline-Powered Motor Vehicle Tailpipe Emissions ( $\mu\text{g km}^{-1}$ )		Gasoline Composition ( $\mu\text{g gm}^{-1}$ )	Notes
	Gas	Particle	Gas	Particle		
	<u>Phase</u>	<u>Phase</u>	<u>Phase</u>	<u>Phase</u>		
n-Alkanes						
Methane	38000		330000			a, e
Ethane	7770		36900			a, e
Propane	650		9300		100	a, e
n-Butane	1620		191000		7620	a, e
n-Pentane	4290		536000		27600	a, e
n-Hexane	2900		410000			a, e
n-Heptane	1820		268000		9700	a, e
n-Octane	1070		131000		6380	a, e
n-Nonane	430		45300		2080	a, e
n-Decane	300		42600		1120	a, e
n-Undecane	*		*		*	
n-Dodecane <sup>†</sup>	83.9		1770		136	a, f
n-Tridecane <sup>†</sup>	48.2		1280		96.4	b, f
n-Tetradecane	18.4		212		13.8	a, f
n-Pentadecane	6.2		112		14.2	b, f
n-Hexadecane	6.4	0.2	92		8.3	a, f
n-Heptadecane	4.4		130		5.6	b, f
n-Octadecane	2.0	2.2	150	13	7.8	a, f
n-Nonadecane	2.0		92	75	4.7	b, f
n-Eicosane	1.8	0.8	100	190	2.5	a, f
n-Heneicosane	1.8	0.1	32.0	214	1.9	b, f
n-Docosane		0.8	29.8	228	1.5	b, f
n-Tricosane	0.5	1.9	11.9	191	2.2	b, f
n-Tetracosane		0.9	8.9	503	1.7	a, f
n-Pentacosane		2.7	14.3	489	1.7	b, f
n-Hexacosane		0.8	9.6	764	1.0	b, f
n-Heptacosane		0.6	2.4	391		b, f
n-Octacosane			3.0	119		a, f
n-Nonacosane			2.8	95		b, f
Branched alkanes						
i-Butane	130				1040	a, e
2,2-Dimethylpropane					110	a, e
i-Pentane	11300		1720000		79200	a, e
2,2-Dimethylbutane	800		195000		5720	a, e
2,3-Dimethylbutane	2140		298000		12900	a, e
2-Methylpentane	6310		827000		36900	a, e

Identification notes: (a) authentic quantitative standard. (b) authentic quantitative standard for similar compound in series. (c) secondary standard. (d) detected as a methyl ester.

Sample collection notes: (e) collected in SUMA canister. (f) collected on denuder/filter/PUF sampling train. (g) collected on DNPH impregnated  $\text{C}_{18}$  cartridges. (\*) not measured. See text for details.

Additional Notes: <sup>†</sup> Compound is too volatile for complete collection by denuder at sampling conditions; mass of this compound reported in the gas-phase includes mass collected on PUF cartridge.

Table 5.3. (continued - page 2)

Compound	Catalyst-Equipped Gasoline-Powered Motor Vehicle Tailpipe Emissions ( $\mu\text{g km}^{-1}$ )		Noncatalyst-Equipped Gasoline-Powered Motor Vehicle Tailpipe Emissions ( $\mu\text{g km}^{-1}$ )		Gasoline Composition ( $\mu\text{g gm}^{-1}$ )	Notes
	Gas Phase	Particle Phase	Gas Phase	Particle Phase		
Branched alkanes						
3-Methylpentane	3760		512000		22700	a, e
2,4-Dimethylpentane	2920		354000		15700	a, e
2-Methylhexane	2880		372000		15300	a, e
2,3-Dimethylpentane	5340		714000		29400	a, e
3-Methylhexane	2950		415000		16200	a, e
2,2,4-Trimethylpentane	8200		1080000		34600	a, e
2,5-Dimethylhexane	1500		205000		5070	a, e
2,4-Dimethylhexane	1650		219000		6460	a, e
2,3,4-Trimethylpentane	2510		412000		13000	a, e
2,3-Dimethylhexane	1040		148000		5600	a, e
2-Methylheptane	1340		159000		6260	a, e
3-Ethylhexane	1640		205000		810	a, e
2,2,4-Trimethylhexane					190	a, e
Norfarnesane <sup>†</sup>	65.5		638		106	b, f
Farnesane <sup>†</sup>	18.8		332		22	b, f
2,6,10-Trimethyltridecane	8.8		80		15.5	b, f
Norpristane	4.6	0.3	188	19.8	4.3	b, f
Pristane	7.8		225		12.1	a, f
Phytane	3.2		252		6.9	b, f
n-Alkenes						
Ethene	29200		716000			a, e
Propene	14900		436000		10	a, e
1-Butene					170	a, e
<i>trans</i> -2-Butene	2190		69300		630	a, e
<i>cis</i> -2-Butene	900		36100		720	a, e
1-Pentene	400		51800		1480	a, e
<i>trans</i> -2-Pentene	710		77400		4120	a, e
<i>cis</i> -2-Pentene	440		42300		2290	a, e
1-Hexene	430		18400		770	a, e
<i>trans</i> -2-Hexene	300		31600		1860	a, e
<i>cis</i> -2-Hexene	170		17300		1050	a, e
Branched alkenes						
Isobutene	15600		427000		170	a, e
3-Methyl-1-butene	350		22500		380	a, e
2-Methyl-1-butene	1120		84600		2690	a, e
2-Methyl-2-butene	2270		126000		6360	a, e
4-Methyl-1-pentene					300	a, e

Identification notes: (a) authentic quantitative standard. (b) authentic quantitative standard for similar compound in series. (c) secondary standard. (d) detected as a methyl ester.

Sample collection notes: (e) collected in SUMA canister. (f) collected on denuder/filter/PUF sampling train. (g) collected on DNPH impregnated C<sub>18</sub> cartridges. (\*) not measured. See text for details.

Additional Notes: <sup>†</sup> Compound is too volatile for complete collection by denuder at sampling conditions; mass of this compound reported in the gas-phase includes mass collected on PUF cartridge.

Table 5.3. (continued - page 3)

Compound	Catalyst-Equipped Gasoline-Powered Motor Vehicle Tailpipe Emissions ( $\mu\text{g km}^{-1}$ )		Noncatalyst-Equipped Gasoline-Powered Motor Vehicle Tailpipe Emissions ( $\mu\text{g km}^{-1}$ )		Gasoline Composition ( $\mu\text{g gm}^{-1}$ )	Notes
	Gas Phase	Particle Phase	Gas Phase	Particle Phase		
Branched alkenes						
2-Methyl-1-pentene	230		26600		1250	a, e
2-Methyl-2-pentene	480		50400		2700	a, e
Diolefins						
1,3-Butadiene	770		15600		10	a, e
Alkynes						
Ethyne	12800		865000			a, e
Saturated cycloalkanes						
Cyclopentane	780		85400		4110	a, e
Methylcyclopentane	4320		604000		26200	a, e
Cyclohexane	1440		238000		8900	a, e
Methylcyclohexane	1860		274000		7870	a, e
Ethylcyclohexane					930	a, e
Nonylcyclohexane			17		7.8	b, f
Decylcyclohexane	1.2		14		12.9	b, f
Undecylcyclohexane	0.84		16.7			b, f
Dodecylcyclohexane	1.4		15.9			b, f
Tridecylcyclohexane	0.91		22.4	21.5		b, f
Tetradecylcyclohexane	0.67		21.3	66.1		b, f
Pentadecylcyclohexane	1.3		20.4	162		a, f
Hexadecylcyclohexane				206		b, f
Heptadecylcyclohexane				362		a, f
Octadecylcyclohexane				265		b, f
Nonadecylcyclohexane				241		b, f
Eicosylcyclohexane				144		b, f
Heneicosylcyclohexane				75		b, f
Unsaturated cycloalkenes						
Cyclopentene	480		31700		1120	a, e
Aromatic hydrocarbons						
Benzene	11900		473000		7530	a, e
Toluene	21300		2360000		59500	a, e
Ethylbenzene	4180		434000		12800	a, e
m & p-Xylene	14300		1720000		50500	a, e
o-Xylene	5410		562000		19700	a, e
i-Propylbenzene					830	a, e
n-Propylbenzene	830		97900		3500	a, e
p-Ethyltoluene	4040		385000		6080	a, e
m-Ethyltoluene	1750		175000		14200	a, e

Identification notes: (a) authentic quantitative standard. (b) authentic quantitative standard for similar compound in series. (c) secondary standard. (d) detected as a methyl ester.

Sample collection notes: (e) collected in SUMA canister. (f) collected on denuder/filter/PUF sampling train. (g) collected on DNPH impregnated  $\text{C}_{18}$  cartridges. (\*) not measured. See text for details.

Additional Notes: † Compound is too volatile for complete collection by denuder at sampling conditions; mass of this compound reported in the gas-phase includes mass collected on PUF cartridge.

Table 5.3. (continued - page 4)

Compound	Catalyst-Equipped Gasoline-Powered Motor Vehicle Tailpipe Emissions		Noncatalyst-Equipped Gasoline-Powered Motor Vehicle Tailpipe Emissions		Gasoline Composition ( $\mu\text{g gm}^{-1}$ )	Notes
	( $\mu\text{g km}^{-1}$ )		( $\mu\text{g km}^{-1}$ )			
	Gas Phase	Particle Phase	Gas Phase	Particle Phase		
Aromatic hydrocarbons						
1,3,5-Trimethylbenzene	1980		210000		7450	a, e
o-Ethyltoluene	1610		142000		4800	a, e
1,2,4-Trimethylbenzene	5720		602000		24600	a, e
Naphthalene <sup>†</sup>	≈ 1000		≈ 50000		1040	a, f
2-Methylnaphthalene <sup>†</sup>	≈ 1000		≈ 50000		1330	a, f
1-Methylnaphthalene <sup>†</sup>	≈ 500		≈ 30000		800	a, f
C <sub>2</sub> -Naphthalenes <sup>†</sup>	183		28500		624	a, f
C <sub>3</sub> -Naphthalenes <sup>†</sup>	62.5		5860		135	b, f
C <sub>4</sub> -Naphthalenes <sup>†</sup>	25.3		950		55.7	b, f
Acenaphthylene <sup>†</sup>	37.0		2180			a, f
Acenaphthene <sup>†</sup>	6.55		177			a, f
Fluorene	9.72		358	20.1	4.35	a, f
C <sub>1</sub> -Fluorene	6.34		398	388	10.0	b, f
C <sub>2</sub> -Fluorene	10.5		490	384	17.1	b, f
Phenanthrene	21.7		622	434	9.24	a, f
Anthracene	3.69		148	106	4.35	a, f
3-Methylphenanthrene	2.92		236	181	6.01	b, f
2-Methylphenanthrene	3.35		291	195	9.64	b, f
2-Methylanthracene	1.14		94.1	66.7	5.54	a, f
9-Methylphenanthrene	2.47		131	107	4.49	b, f
1-Methylphenanthrene	1.63		122	65.1	3.91	a, f
C <sub>2</sub> -MW 178 PAH	8.07		464	575	24.93	a, f
C <sub>3</sub> -MW 178 PAH	1.51		176	216	10.76	b, f
Fluoranthene	4.25	0.069	160	152	1.15	a, f
Acephenanthrylene	0.58	0.012	50.8	57.8	0.04	b, f
Pyrene	4.28	0.077	160	217	3.38	a, f
C <sub>1</sub> -MW 202 PAH	2.06		96.5	233	5.27	b, f
Benzo[ghi]fluoranthene	0.276	0.063	10.7	46.8		b, f
Cyclopenta[cd]pyrene		0.031	5.00	55.6		a, f
Benz[a]anthracene	0.181	0.097	4.80	51.9		a, f
Chrysene & Triphenylene	0.451	0.206	5.07	52.1		a, f
C <sub>1</sub> -MW 226 PAH		0.116				b, f
C <sub>1</sub> -MW 228 PAH		0.242	4.13	103		b, f
Benzo[k]fluoranthene		0.083		32.7	0.28	a, f
Benzo[b]fluoranthene				37.3		a, f
Benzo[j]fluoranthene		0.009		1.52		b, f
Benzo[e]pyrene		0.150		38.2	6.79	a, f

Identification notes: (a) authentic quantitative standard. (b) authentic quantitative standard for similar compound in series. (c) secondary standard. (d) detected as a methyl ester.

Sample collection notes: (e) collected in SUMA canister. (f) collected on denuder/filter/PUF sampling train. (g) collected on DNPH impregnated C<sub>18</sub> cartridges. (\*) not measured. See text for details.

Additional Notes: <sup>†</sup> Compound is too volatile for complete collection by denuder at sampling conditions; mass of this compound reported in the gas-phase includes mass collected on PUF cartridge.

Table 5.3. (continued - page 5)

Compound	Catalyst-Equipped Gasoline-Powered Motor Vehicle Tailpipe Emissions ( $\mu\text{g km}^{-1}$ )		Nocatalyst-Equipped Gasoline-Powered Motor Vehicle Tailpipe Emissions ( $\mu\text{g km}^{-1}$ )		Gasoline Composition ( $\mu\text{g gm}^{-1}$ )	Notes
	Gas Phase	Particle Phase	Gas Phase	Particle Phase		
	Aromatic hydrocarbons					
Benzo[a]pyrene		0.021		41.0		a, f
Perylene		0.031			2.79	a, f
Indeno[1,2,3-cd]fluoranthene		0.050		28.5		a, f
Indeno[1,2,3-cd]pyrene		0.436		92.0		a, f
Coronene				101		a, f
Tricyclic terpanes						
8 $\beta$ ,13 $\alpha$ -Dimethyl-14 $\beta$ - n-butylpodocarpene	1.13	0.20	46.9	119		c, f
8 $\beta$ ,13 $\alpha$ -Dimethyl-14 $\beta$ - [3'-methylbutyl]podocarpene	0.46	0.14	20.2	76.0		c, f
Diasteranes						
20S-13 $\beta$ (H),17 $\alpha$ (H)-Diacholestane				73.6		c, f
20R-13 $\beta$ (H),17 $\alpha$ (H)-Diacholestane				45.2		c, f
Hopanes						
18 $\alpha$ (H)-22,29,30-Trisnorhopane		0.038		125		c, f
17 $\alpha$ (H)-22,29,30-Trisnorhopane				69.0		c, f
17 $\alpha$ (H)-21 $\beta$ (H)-29-Norhopane		0.019		282		c, f
18 $\alpha$ (H)-29-Norhopane				75.6		c, f
17 $\alpha$ (H),21 $\beta$ (H)-Hopane		0.033		321		c, f
22R&S,17 $\alpha$ (H),21 $\beta$ (H)-30-Homohopane				259		c, f
22R&S,17 $\alpha$ (H),21 $\beta$ (H)-30-Bishomohopane				196		c, f
Steranes						
20R-5 $\alpha$ (H),14 $\beta$ (H),17 $\beta$ (H)-Cholestane				109		c, f
20R-5 $\alpha$ (H),14 $\alpha$ (H),17 $\alpha$ (H)-Cholestane				119		c, f
20R&S-5 $\alpha$ (H),14 $\beta$ (H),17 $\beta$ (H)-Ergostane				139		c, f
20R&S-5 $\alpha$ (H),14 $\beta$ (H),17 $\beta$ (H)-Sitostane				136		c, f
Ethers						
MTBE	5700		1620000		109000	a, e
ETBE	200		34600			a, e
TAME	*		*		550	a, e
Aliphatic aldehydes						
Formaldehyde	8690		884000		*	a, g
Acetaldehyde	3940		301000		*	a, g
Propanal	640		60000		*	a, g
Butanal & Isobutanal	310		31000		*	a, g
Pentanal	250		22000		*	a, g

Identification notes: (a) authentic quantitative standard. (b) authentic quantitative standard for similar compound in series. (c) secondary standard. (d) detected as a methyl ester.

Sample collection notes: (e) collected in SUMA canister. (f) collected on denuder/filter/PUF sampling train. (g) collected on DNPH impregnated C<sub>18</sub> cartridges. (\*) not measured. See text for details.

Additional Notes: † Compound is too volatile for complete collection by denuder at sampling conditions; mass of this compound reported in the gas-phase includes mass collected on PUF cartridge.

Table 5.3. (continued - page 6)

Compound	Catalyst-Equipped Gasoline-Powered Motor Vehicle Tailpipe Emissions ( $\mu\text{g km}^{-1}$ )		Nocatalyst-Equipped Gasoline-Powered Motor Vehicle Tailpipe Emissions ( $\mu\text{g km}^{-1}$ )		Gasoline Composition ( $\mu\text{g gm}^{-1}$ )	Notes
	Gas Phase	Particle Phase	Gas Phase	Particle Phase		
Aliphatic aldehydes						
Isopentanal			31000		*	a, g
Hexanal	490		27000		*	a, g
Heptanal	300		19000		*	a, g
Octanal	120		7300		*	a, g
Nonanal	190		2600		*	a, g
Decanal	30		2300		*	a, g
Undecanal	50		2200		*	a, g
Dodecanal	40		2500		*	a, g
Tridecanal			870		*	a, g
Tetradecanal			5800		*	a, g
Olefinic aldehydes						
Crotonaldehyde	1760		114000		*	a, g
Acrolein	60		3800		*	a, g
Methacrolein	300		23000		*	a, g
Aliphatic ketones						
Acetone	1190		42000		*	a, g
Butanone / Methylacrolein	470		32000		*	a, g
Aromatic aldehydes						
Benzaldehyde	1270		159000		*	a, g
o-Tolualdehyde	390		45000		*	a, g
m&p-Tolualdehyde	1340		145000		*	a, g
2,5-Dimethylbenzaldehyde	240		35000		*	a, g
Naphthalenecarboxaldehydes	5.3					b, f
Aromatic ketones						
Indanone <sup>†</sup>	30.6		908		*	a, f
Fluorenone	15.7				*	a, f
Xanthone	2.00		30.8		*	a, f
9,10-Anthracenedione	0.849		25.4		*	a, f
Dicarbonyls						
Glyoxal	170		28000		*	a, g
Methylglyoxal	50		10000		*	a, g
Biacetyl	40		1800		*	a, g
Other carbonyls						
2-Furaldehyde			1700		*	a, g

Identification notes: (a) authentic quantitative standard. (b) authentic quantitative standard for similar compound in series. (c) secondary standard. (d) detected as a methyl ester.

Sample collection notes: (e) collected in SUMA canister. (f) collected on denuder/filter/PUF sampling train. (g) collected on DNPH impregnated C<sub>18</sub> cartridges. (\*) not measured. See text for details.

Additional Notes: <sup>†</sup> Compound is too volatile for complete collection by denuder at sampling conditions; mass of this compound reported in the gas-phase includes mass collected on PUF cartridge.

Table 5.3. (continued - page 7)

Compound	Catalyst-Equipped Gasoline-Powered Motor Vehicle Tailpipe Emissions		Nocatalyst-Equipped Gasoline-Powered Motor Vehicle Tailpipe Emissions		Gasoline Composition ( $\mu\text{g gm}^{-1}$ )	Notes
	( $\mu\text{g km}^{-1}$ )		( $\mu\text{g km}^{-1}$ )			
	Gas Phase	Particle Phase	Gas Phase	Particle Phase		
n-Alkanoic acids						
Octanoic acid	12.2		86.0			a, f, d
Nonanoic acid	27.9		80.6			b, f, d
Decanoic acid	9.3		54.7			a, f, d
Undecanoic acid			75.6			b, f, d
Heptadecanoic acid		0.26		90.6		b, f, d
Octadecanoic acid		4.32		147		a, f, d
Nonadecanoic acid				9.3		b, f, d
Eicosanoic acid		0.16		14.0		a, f, d
Alkanedioic acids						
Octadecanedioic acid		4.1		42.4		a, f, d
Nonadecanedioic acid		21.5		177		a, f, d
Aromatic acids						
Benzoic acid	124					b, f, d
Methylbenzoic acids		0.74		55.4		a, f, d
Other compounds						
Benzofuran			200	29.2		a, f
Dibenzofuran	5.6	3.43	42.2	4.0		a, f
Dibenzothiophene	0.32		25.6			a, f
Dibenzothiazole	12.3	0.40				a, f

Identification notes: (a) authentic quantitative standard. (b) authentic quantitative standard for similar compound in series. (c) secondary standard. (d) detected as a methyl ester.

Sample collection notes: (e) collected in SUMA canister. (f) collected on denuder/filter/PUF sampling train. (g) collected on DNPH impregnated C<sub>18</sub> cartridges. (\*) not measured. See text for details.

Additional Notes: † Compound is too volatile for complete collection by denuder at sampling conditions; mass of this compound reported in the gas-phase includes mass collected on PUF cartridge.



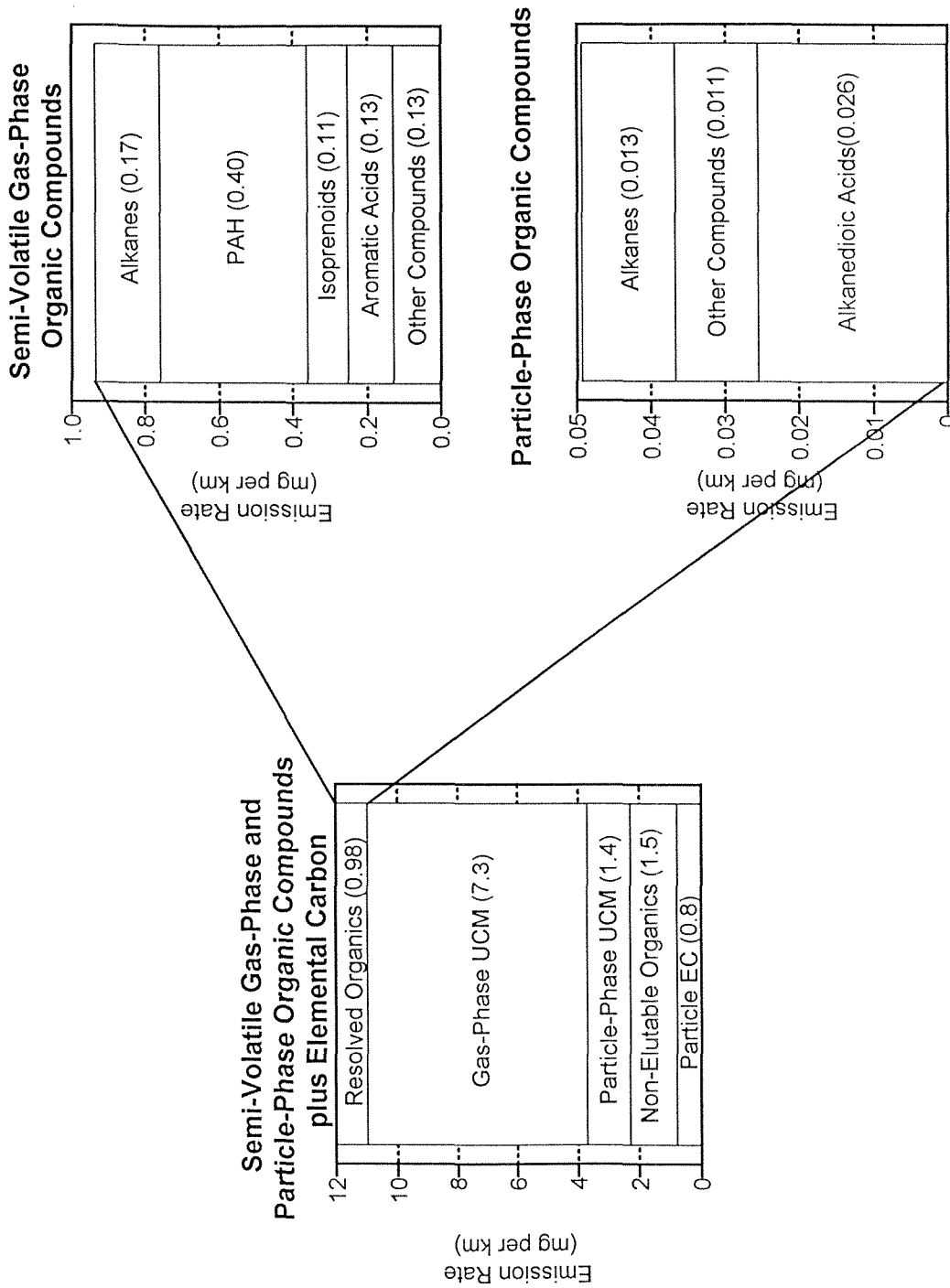


Figure 5.4. Mass balance on the semi-volatile and particle-phase organic compounds and elemental carbon emitted from catalyst-equipped gasoline-powered light-duty motor vehicles.

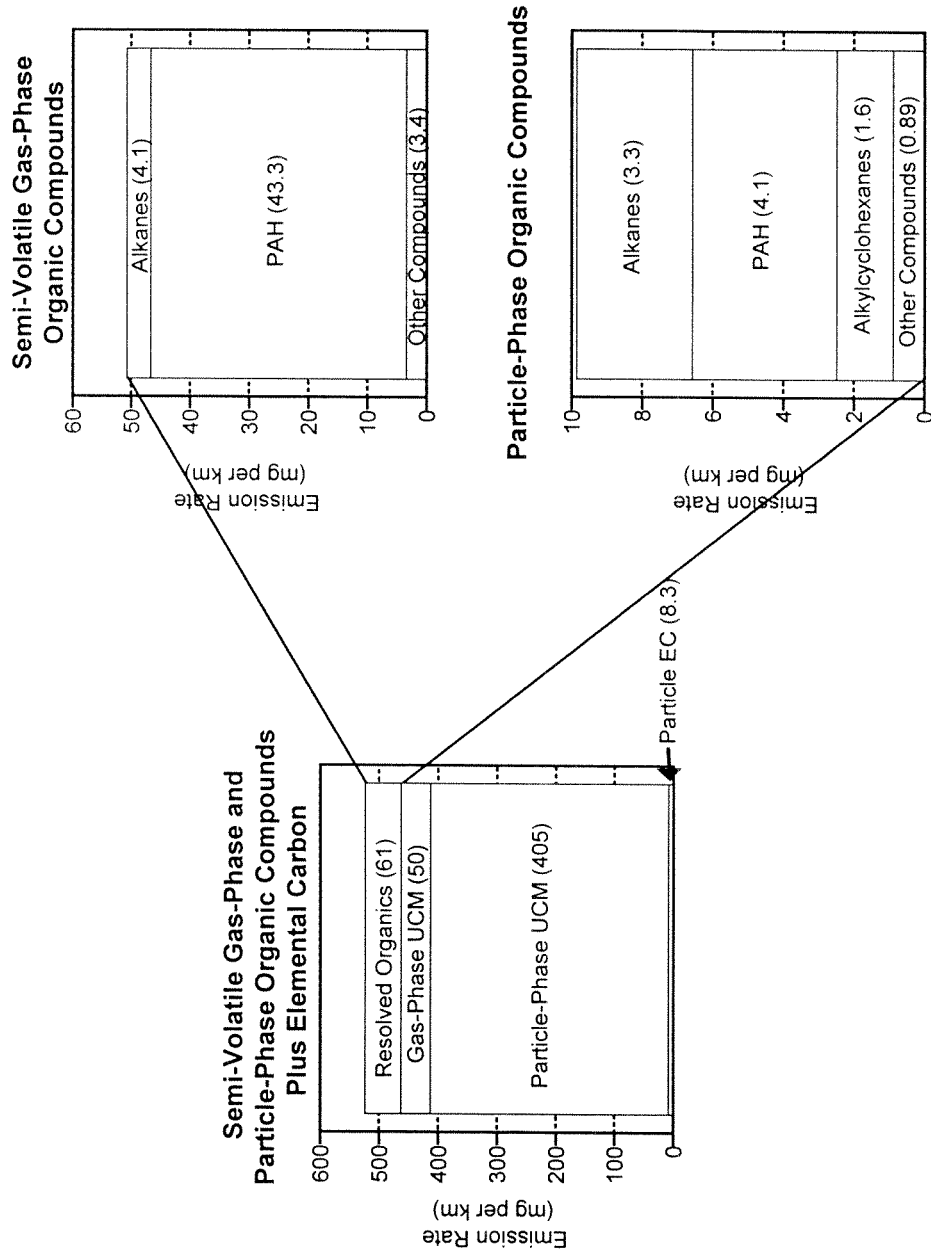


Figure 5.5. Mass balance on the semi-volatile and particle-phase organic compounds and elemental carbon emitted from noncatalyst-equipped gasoline-powered light-duty motor vehicles.

a GC trace makes up more than 7.3 mg per kilometer of the 12.0 mg of semi-volatile and particle-phase organic compounds plus elemental carbon emissions. The particle-phase UCM and particle-phase elemental carbon are emitted at 1.4 and 0.8 mg km<sup>-1</sup>, respectively. Of the resolved organic compounds, alkanes and PAH make up most of the gas-phase semi-volatile species, and alkanes and alkanedioic acids make up most of the particle-phase species.

Figure 5.5 shows the emissions of the semi-volatile and particle-phase organic compounds plus elemental carbon emissions from the noncatalyst equipped cars tested as measured by the denuder/filter/PUF sampling train. For the noncatalyst equipped motor vehicle emissions, 77% of the semi-volatile and particle-phase emissions shown are present in the particle-phase UCM. For these noncatalyst gasoline-powered vehicles, essentially all of the particulate organic carbon mass is extractable from the filter sample and will elute from the GC column after derivatization. The organic carbon measured by thermal evolution and combustion balances with the mass of organic carbon quantified by GC/MS. Of the resolved organic compounds, PAH make up 85% of the gas-phase semi-volatile species, while alkanes and PAH make up most of the particle-phase organic compounds.

The n-alkanes and isoprenoids (see Chapter 4 for isoprenoid chemical structures) with more than 11 carbon atoms emitted from the catalyst-equipped gasoline-powered vehicles show a distribution according to carbon number and

branching that is similar to that seen in the gasoline used to power the vehicles (Figure 5.6). The emissions from the noncatalyst equipped vehicles, however, show an increase in n-alkane emissions in the range of eicosane through heptacosane and significant flattening of the distribution of the isoprenoid emissions when compared to the composition of the gasoline burned. Since these heavier n-alkanes are not found in the engine motor oil in noticeable quantities (they are deliberately removed in the refining process) (18), it appears that these compounds are being formed in the engine during use by combustion or breakdown/recombination of the fuel components.

Figure 5.7 shows the distribution of PAH and alkyl-PAH ranging from fluorene through coronene in the gasoline fuel and in the vehicle emissions. Significant enrichment in the ratio of fluorene to methylfluorenes and dimethylfluorenes is observed in the catalyst-equipped vehicle exhaust when compared to the gasoline burned. The same trend is observed for the PAH with a molecular weight of 178 (phenanthrene plus anthracene). The increased dealkylation of the PAH in the catalyst equipped gasoline powered engine exhaust is likely due to increased thermal and catalytic processing in the engine and exhaust systems. It is also interesting to note that the distribution of the heavier PAH is significantly different in the fuel versus the tailpipe emissions. The parent fuel has increased relative concentrations of chrysene/triphenylene,

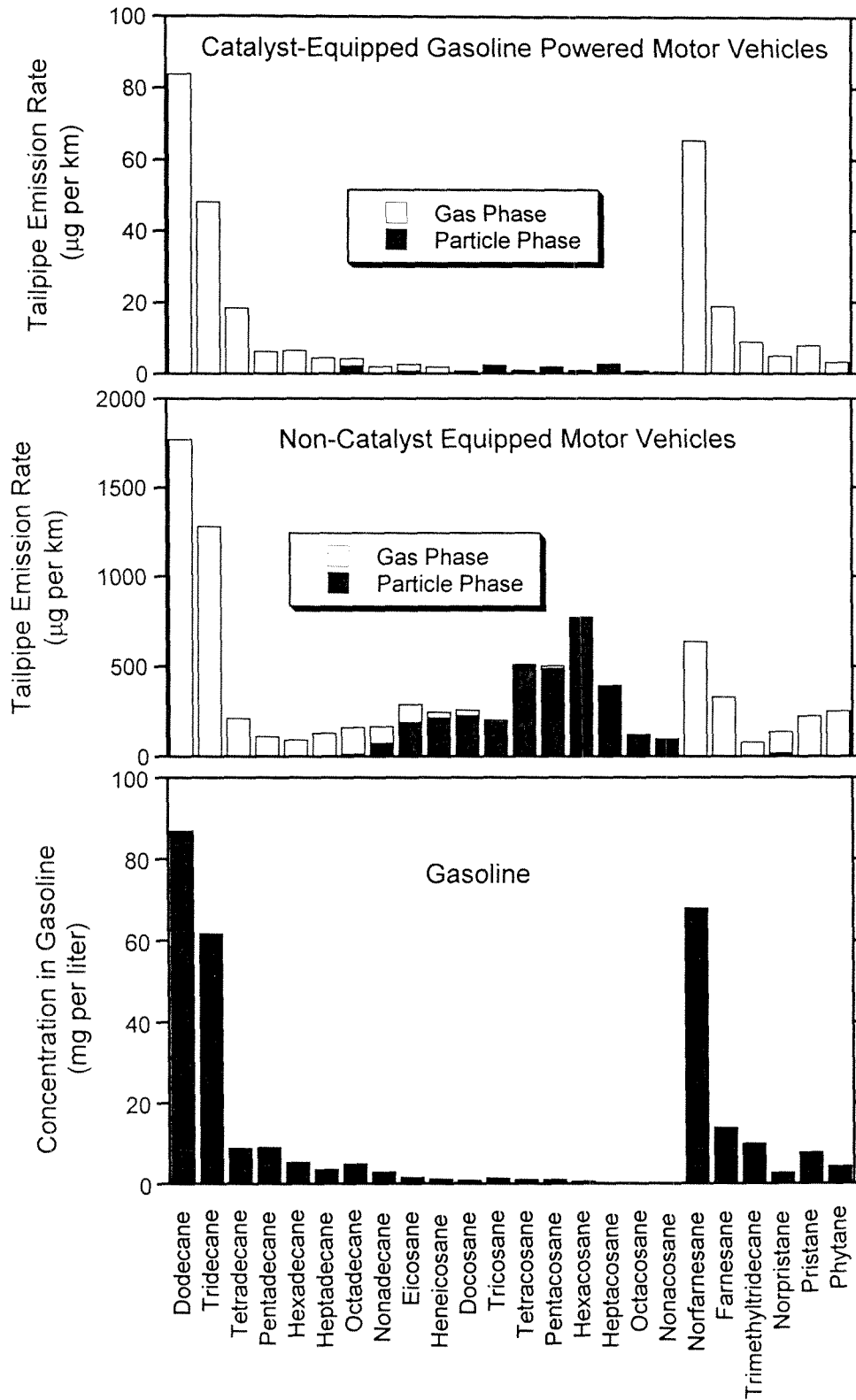


Figure 5.6. Emissions of n-alkanes and isoprenoids from gasoline-powered light-duty motor vehicles and the concentration of these compounds in gasoline.

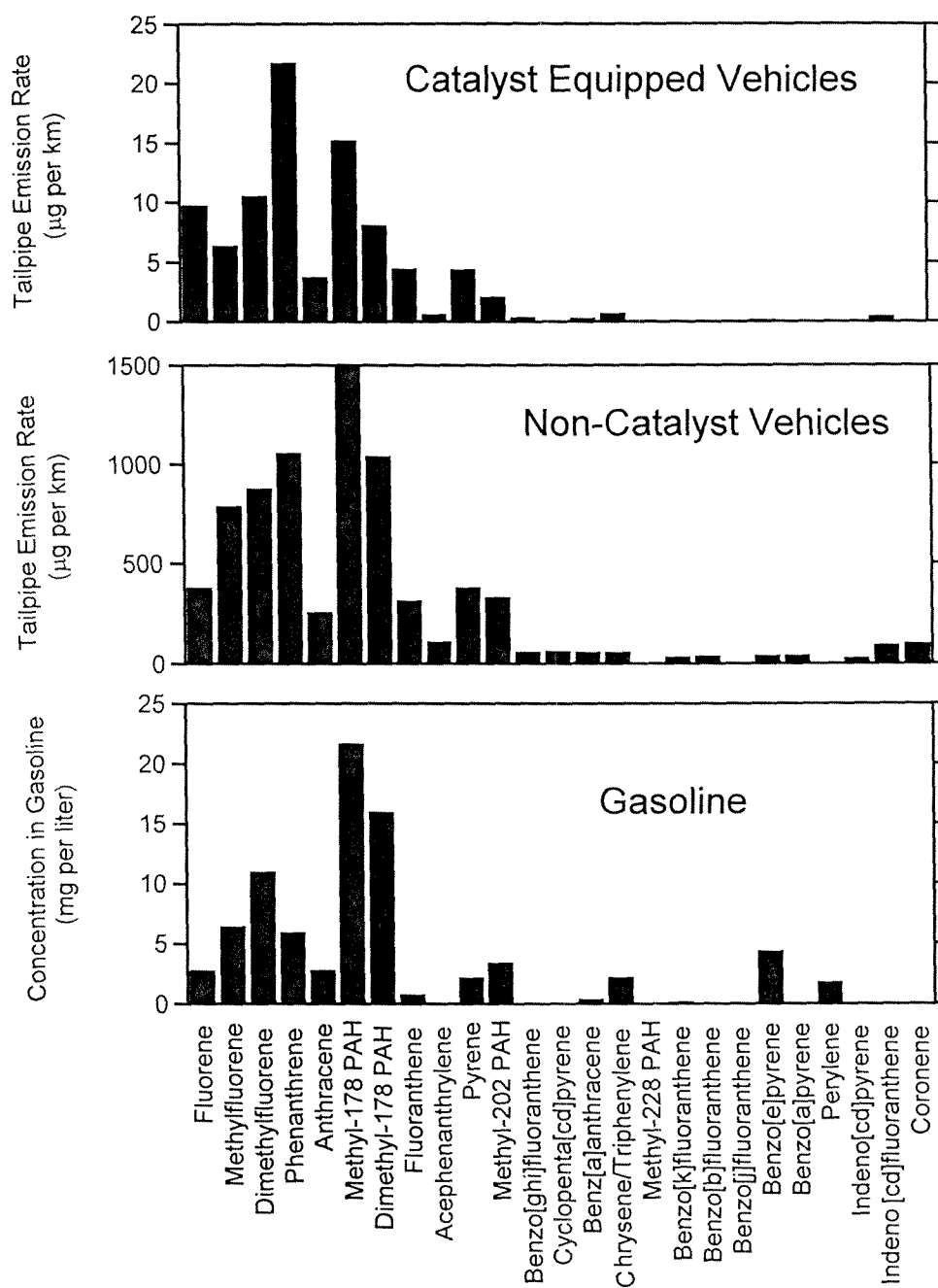


Figure 5.7. Emissions of PAH and alkyl-PAH from gasoline powered-motor light-duty vehicles and the concentration of these compounds in gasoline.

benzo[e]pyrene, and perylene while neither type of vehicle emissions shows this pattern.

As previously indicated the average fine particle emission rates from the catalyst-equipped gasoline-powered motor vehicles tested in the present study are about 58% lower than from a mid-1980's catalyst-equipped motor vehicle fleet made up of on-road vehicles in Southern California at that time. It is interesting to note that the emissions of fine particle organic carbon and elemental carbon are reduced even more than the reduction of fine particles between these tests. Fine particle organic carbon and elemental carbon average emission rate reductions are 73% and 81%, respectively. These reductions are likely due to improved combustion in the engines and improved organic compound destruction in the catalytic converters. The composition of the fine organic compound mass emitted from the catalyst-equipped cars has also changed. The ratio of hopanes plus steranes to organic carbon in the fine particle mass has dropped from 4.7 to 0.04 indicating either significant destruction of these compounds in either the engine or catalytic exhaust system. This reduction is not believed to be due to changes in the engine lubricant oil formulations as the same ratio in the noncatalyst equipped motor vehicles has increased over this time period from 2.4 to 5.3. The increase observed in the noncatalyst vehicles is likely due to the increased contribution of motor oil to the fine particle emissions resulting from engine wear. The relative destruction of

the hopanes and steranes observed in the current catalyst-equipped motor vehicle emissions tests parallels the destruction of these compounds observed in the thermal and catalytic processing that occurs in the petroleum refinery (19). Likewise, the increased contribution of n-alkanoic acids and alkanedioic acids in the fine particle mass emitted from the current catalyst-equipped motor vehicle fleet suggests a more complete oxidation of the organic compounds in the vehicle exhaust.

#### **5.3.4 Organic Compound Tracers for Gasoline-Powered Motor Vehicle Exhaust**

Rogge et al. (12) and Schauer et al. (11) have shown that the hopanes and steranes emitted in vehicle exhaust can be used as molecular tracers for the fine particulate matter emitted from motor vehicles. Although acetylene and carbon monoxide have been proposed by others as tracers for the gas-phase emissions from vehicles, these compounds also are present in the emissions from other combustion sources such as wood burning (see Chapter 6). For this reason, there is a need to identify additional potential tracers for gas-phase and semi-volatile organic compounds present in motor vehicle exhaust that are not emitted when burning wood. The isoprenoids and tricyclic terpanes measured in the current study are distinctive compounds characteristic of petroleum that cannot be confused with wood combustion exhaust. Although these compounds have also been identified in the exhaust from diesel powered vehicles (see



Chapter 4), the ratio of the emissions of these compounds to other lighter gas-phase hydrocarbon emissions, such as n-hexane and iso-hexane, is very much lower for gasoline powered motor vehicles than for diesel powered motor vehicles. While the isoprenoids and tricyclic terpanes are present in gasoline as well as vehicle exhaust, again the entire compound assemblage found in vehicle exhaust differs from the gasoline alone as explained earlier. These differences are expected to be useful in receptor modeling applications (20, 21).

## 5.4 References

1. Pierson, W. R.; Gertler, A. W.; Robinson, N. F.; Sagebiel, J. C.; Zielinska, B.; Bishop, G. A.; Stedman, D. H.; Zweidinger, R. B.; Ray, W. D. *Atmos. Environ.* **1996**, 30, 2232-2256.
2. Rapp, L. A.; Benson, J. D.; Burns, V. R.; Gorse Jr., R. A.; Hochhauser, J. C.; Knepper, J. C.; Koehl, W. J.; Leppard, W. R.; Painter, L. J.; Reuter, R. M.; Rutherford, J. A. *SAE Tech. Pap. Ser.* **1993**, No. 932726.
3. Stump, F.; Tejada, S.; Ray, W.; Dropkin, D.; Black, F.; Crews, W.; Snow, R.; Siudak, P.; Davis, C. O.; Baker, L.; Perry, N. *Atmos. Environ.* **1989**, 23, 307-320.
4. Stump, F.; Tejada, S.; Ray, W.; Dropkin, D.; Black, F.; Snow, R.; Crews, W.; Siudak, P.; Davis, C. O.; Carter, P. *Atmos. Environ.* **1990**, 24A, 2105-2112.
5. Sigsby, J. E.; Tejada, S.; Ray, W.; Lang, J. M.; Duncan, J. W. *Environ. Sci. Technol.* **1987**, 21, 466-475.
6. Harley, R. A.; Cass, G. R. *Atmos. Environ.* **1995**, 29, 905-922.
7. Dunker, A. M.; Morris, R. E.; Pollack, A. K.; Schleyer, C. H.; Yarwood, G. *Environ. Sci. Technol.* **1996**, 30, 787-801.

8. Schleyer, C. H.; Hoehl, W. J.; Leppard, W. R.; Dunker, A. M.; Yarwood, J. P.; Cohen, J. P.; Pollack, A. K. *SAE Tech. Pap. Ser.* **1994**, No. 940579.
9. National Research Council. *Rethinking the Ozone Problem in Urban and Regional Air Pollution*; National Academy Press: Washington, D. C. 1991.
10. Rogge, W. R.; Hildemann, L. M.; Mazurek, M. A.; Cass, G. R.; Simoneit, B. R. T. *Environ. Sci. Technol.* **1993**, 27, 636-651.
11. Schauer, J. J.; Rogge, W. R.; Hildemann, L. M.; Mazurek, M. A.; Cass, G. R.; Simoneit, B. R. T. *Atmos. Environ.* **1996**, 30, 3837-3855.
12. Rogge, W. R.; Hildemann, L. M.; Mazurek, M. A.; Cass, G. R.; Simoneit, B. R. T. *J. Geophys. Res.* **1996**, 101, 19379-19394.
13. *Auto/Oil Air Quality Improvement Research Program*; SAE Pub. **1992**, No. SP-920.
14. *Auto/Oil Air Quality Improvement Research Program - Volume II*; SAE Pub. **1993**, No. SP-1000.
15. Hildemann, L. M.; Markowski, G. R.; Cass, G. R. *Environ. Sci. Technol.* **1991**, 25, 744-759.
16. Hildemann, L. M.; Cass, G. R.; Markowski, G. R. *Aerosol Sci. Technol.* **1989**, 10, 193-204.

17. Horie, Y.; Thiele, M.; *On Road Motor Vehicle Activity Data, Volume II*, California Air Resources Board Report: Contract No. A132-182, **1994**.
18. Gary, J. H.; Handwerk, G. E. *Petroleum Refining - Technology and Economics*, 2<sup>nd</sup> Ed.; Marcel Dekker, Inc.: New York, 1984.
19. Peters, K. E.; Scheuerman, G. L.; Lee, C. Y.; Moldowan, J. M.; Reynolds, R. N.; Pena, M. M. *Energy & Fuels* **1992**, 6, 560-577.
20. Fujita, E. M.; Watson, J. G.; Chow, J. C.; Magliano, K. L. *Atmos. Environ.* **1995**, 29, 3019-3035.
21. Harley, R. A.; Hannigan, M. P.; Cass, G. R. *Environ. Sci. Technol.* **1992**, 26, 2395-2408.

## Chapter 6

# Organic Compounds from Fireplace Combustion of Wood

## 6.1 Introduction

Emissions from fireplace combustion of wood have been shown to be major contributors to air pollution during winter months in urban locations such as Portland, Oregon (1), Denver, Colorado (2), and Albuquerque, New Mexico (3). The relationships between direct primary emissions of wood smoke and ambient concentrations of particulate matter have been assessed in the past based on a variety of techniques. Non-mineral potassium is widely used as a tracer for wood smoke (3-5) but non-mineral potassium is contributed by several other major air pollution sources such as meat cooking exhaust (6, Chapter 2) and refuse incinerators (3). In addition, as is shown in the present study the emission rate of potassium from wood combustion varies widely among wood types. Khalil et al. (1) used the ratio of gas-phase methylchloride to particulate mass in the emissions from wood combustion to assess wood smoke concentrations in the Oregon atmosphere. Retene is the fully aromatized PAH resulting from thermal alteration of resin acids in conifer wood smoke. Ramdahl (7) proposed the use of retene as an organic tracer for wood smoke particles in

the atmosphere. Others have used the ratios of polycyclic aromatic hydrocarbons (PAH) and substituted PAH in wood smoke and in other source emissions to determine the contribution of wood smoke to atmospheric particle concentrations (8, 9). These methods have limited application since methylchloride is a widely used industrial chemical and many of the PAH used as tracers react fairly rapidly in the atmosphere.

Locker (10) used levoglucosan (1,6-anhydro- $\beta$ -D-glucose) to determine the contribution of wood burning to ambient total suspended particulate mass (TSP) concentrations. Hawthorne et al. (11) measured the relative concentrations of guaiacol (2-methoxyphenol), syringol (2,6-dimethoxyphenol), and derivatives of these compounds in the plumes downwind of residential wood stoves and fireplaces. Hawthorne et al. (12) showed that guaiacol and its derivatives (but not the syringol family) could be used to estimate the contribution of wood smoke to PM-10 concentrations in the wintertime urban atmosphere at several locations. The studies by Locker (11) and Hawthorne et al. (12) have helped to elucidate the effect of wood combustion on atmospheric particulate mass concentrations. Standley and Simoneit (13) and Simoneit et al. (14) have shown that the distribution of resin acids, resin acid thermal alteration products, phytosterols, lignans, and phenolic compounds from lignins can be used to separately identify the smoke from the combustion of coniferous trees, deciduous trees, and grasses. Rogge et al. (15) quantified the distribution of

organic compounds in the fine particles emitted from fireplace combustion of pine, oak, and synthetic logs. The data of Rogge et al. (15) were used by Schauer et al. (16) to show how to separately quantify the amount of wood smoke particles in the Southern California atmosphere in the presence of the effluent from eight other major source types.

The organic chemical tracer model of Schauer et al. (16) that originally addressed only particle-phase air pollutants currently is being extended to track volatile organic gases, gas-phase semi-volatile organic compounds as well as particle-phase organic compounds. In addition, advanced photochemical airshed models are being developed that can for the first time track gas-phase, semi-volatile and particle-phase organic compounds simultaneously, and compute their effect on photochemical smog formation and secondary aerosol formation. Air quality models of both of these types require emissions data for individual organic compounds that span the range from methane to heavy particle-phase organic compounds. The current research reports the C<sub>1</sub> through C<sub>29</sub> gas- and particle-phase organic compound emissions from wood combustion.

## 6.2 Experimental Methods

### 6.2.1 Comprehensive Source Sampling

The source sampler used for the wood combustion source tests is configured in the same manner as was used in the meat charbroiling source tests discussed in Chapter 2. Details of the sampler are presented in Chapter 2. Briefly, hot exhaust from the fireplace chimney was drawn isokinetically through a cyclone separator to remove particles with aerodynamic diameters greater than 10  $\mu\text{m}$ . The particles with aerodynamic diameters less than 10  $\mu\text{m}$  along with the gaseous pollutants passed through a heated stainless steel tube and through a venturi meter after which they were turbulently mixed with HEPA-filtered and activated carbon-filtered dilution air within a portable dilution tunnel to bring the mixture to ambient temperature and pressure. Most of the diluted and cooled exhaust was passed through a pre-baked quartz fiber filter (10 inch X 12 inch, Pallflex Tissuequartz 2500 QAO) located at the downstream end of the dilution tunnel. The remaining portion of the diluted exhaust was sent to a residence time chamber where the semi-volatile compounds were allowed time to partition between the gas and particle phases. From the residence time chamber, diluted exhaust was drawn through four AIHL cyclone separators (17) operated in parallel at a flow rate of 30 lpm each to remove particles with aerodynamic diameters greater than 1.8  $\mu\text{m}$ . Gases and fine particles with



diameters less than 1.8  $\mu\text{m}$  passed through the cyclones and were then directed to a series of sampling trains operated in parallel.

Semi-volatile and fine particle-phase organic compounds were collected continuously throughout the burn cycle by filter/PUF sampling trains operated downstream of the AIHL cyclone separators. A single filter/PUF unit consisted of a quartz fiber filter (47 mm diameter, Pallflex Tissuequartz 2500 QAO) followed by two polyurethane foam (PUF) cartridges (Atlas Foam; density =  $0.022 \text{ g cm}^{-3}$ , ILD = 30, 5.7 cm diameter by 7.6 cm long) operated in series. Particle-phase organic compounds were collected on the quartz fiber filter and gas-phase organic compounds were collected on the PUF cartridges located downstream of the quartz fiber filter. Compounds too volatile to be collected completely by the first PUF cartridge were then collected by the back-up PUF cartridge. If the mass of an individual organic compound on the second PUF cartridge was found to be more than 25% of the mass collected on the front PUF cartridge, then this compound was deemed to be too volatile to be measured by the filter/PUF sampling train under the given sampling conditions. Three filter/PUF units, each operating at a flowrate of 10 lpm, were connected to the outlet of each of two AIHL cyclone separator. These two complete AIHL cyclone filter/PUF assemblies were operated in parallel during each test.

In addition to the filter/PUF sampling trains, an organic compound denuder-based sampling train was employed to measure gas-phase, semi-volatile, and particle-phase organic compound emission rates during segments of the burn cycle. The capacity of the organic vapor denuders under the conditions of the present study limited denuder sampling times to a maximum of approximately 25 minutes, such that continuous sampling using the XAD-coated annular denuder was not practical. The organic vapor denuder-based sampling train operated at a flow rate of 30 lpm downstream of one AIHL fine particle cyclone separator and consisted of an XAD-coated annular denuder (URG, 400 mm, 4 channel) followed by three quartz fiber filters (47 mm diameter, Pallflex Tissuequartz 2500 QAO) operated in parallel which were in turn followed by two polyurethane foam (PUF) cartridges (Atlas Foam; density =  $0.022 \text{ g cm}^{-3}$ , ILD = 30, 5.7 cm diameter by 7.6 cm long) operated in series. The gas-phase semi-volatile organic compounds were collected by the annular denuder while particles and particle phase-associated organic compounds passed through the denuder and were collected on the filters downstream of the denuder. The PUF cartridge downstream of the filters collected any particle-phase semi-volatile compounds that blew off of the filters. The preparation of the XAD-coated denuders and additional details concerning denuder/filter/PUF sampling train operations and collection efficiency are discussed in Chapter 2. Denuder/filter/PUF sampling trains were operated for each of the wood

combustion source tests but were only analyzed for the pine wood combustion source test.

A third type of cyclone-based sampling unit also was used during the wood combustion source tests. An AIHL cyclone separator was followed by sampling substrates configured to measure the emissions of fine particulate matter, carbonyls, vapor-phase organic acids, and gas-phase hydrocarbons. Three stacked filter units each operating at 10 lpm and one carbonyl sampling line operated at a flow rate of 0.3 lpm were connected in parallel at the outlet of this AIHL cyclone separator. The first stacked filter unit consisted of two quartz fiber filters (47 mm diameter, Pallflex Tissuequartz 2500 QAO) in series which were used for elemental carbon and organic carbon (EC/OC) determination by thermal evolution and combustion analysis as described by Birch and Cary (18). The second filter stack contained three filters, a Teflon membrane filter (47 mm diameter, Gelman Teflo, 2  $\mu\text{m}$  pore size) followed by two KOH-impregnated quartz fiber filters in series. This Teflon membrane filter was used for gravimetric determination of the fine particle mass emissions rate and was analyzed by X-ray fluorescence for 35 trace elements (19). The tandem KOH-impregnated quartz fiber filters were used to collect vapor-phase organic acids which will be analyzed in association with other research activities and will not be reported here. The third filter holder assembly contained one Teflon membrane filter which was used for a duplicate fine particle mass emissions

measurement and for inorganic ion measurements by ion chromatography (20), atomic absorption spectroscopy and colorimetry (21). Downstream of that single Teflon filter the sample flow was divided, and a small portion of the flow was used to fill a 6 liter polished stainless steel SUMA canister for the collection of non-methane volatile hydrocarbons ranging from  $C_1$  to  $C_{10}$ . The 6 liter SUMA canister was filled continuously at a constant flowrate set to fill the canister over the entire wood burning cycle. Carbonyls were collected at the outlet of the AIHL cyclone separator by two  $C_{18}$  cartridges impregnated with dinitrophenylhydrazine (DNPH) that were operated in series (22). Non-methane volatile hydrocarbon samples were collected only during the pine wood combustion test. All other samples were collected and analyzed for all three wood burning tests.

Electronic particle sizing instruments and a pair of MOUDI impactors also were connected to the residence time chamber during the wood combustion source tests to obtain particle size distributions and particle chemical composition as a function of size. The size distributions and the results obtained from the MOUDI impactors will be reported elsewhere.

### **6.2.2 Source Testing Procedure**

The firewood burned in the wood combustion source tests was obtained from a large firewood distributor in the residential suburbs of Los Angeles in

Southern California. The three woods tested (pine, oak, and eucalyptus) represented the largest volumes of wood sold by this distributor. Kindling to start each fire was obtained by chopping up a log of the particular wood being tested and only a small number of sheets of newspaper (approximately five sheets per test) were burned to ignite the kindling. No other materials were used to start the fires or were burned with the wood. The mass of wood burned (logs plus kindling) was measured prior to each test, and the remaining mass of ashes was collected and weighed after each test. The difference between the mass of wood ignited and the mass of ashes remaining was defined as the mass of wood burned. In all tests, the mass of ash amounted to only a few percent of the original wood mass.

The firewood combustion source tests were conducted in a residential fireplace located in a two-story house. Emissions were withdrawn from a port installed in the chimney on the second floor level of the house approximately five meters above the fireplace grate. The total exhaust gas flow from the fireplace was measured at the chimney outlet and was monitored periodically throughout the wood burning cycle. In the pine wood test, 17.2 kilograms of wood were burned over a period of 189 minutes. In the oak wood combustion test, 15.4 kilograms of wood were burned over a period of 165 minutes, and in the eucalyptus wood combustion source test, 18.9 kilograms of wood were burned over a period of 218 minutes.

Denuder/filter/PUF samples were drawn for approximately 15 minutes directly after the fire was lit, and a second denuder-based sample was taken using a new set of substrates for another 15 minutes approximately midway through the burn cycle. All other sampling systems operated continuously through the entire length of each test.

### 6.2.3 Organic Chemical Analysis

The analytical procedures used in the present study for the identification and quantification of semi-volatile and particle-phase organic compounds in air pollution source emissions are presented in Chapter 2. Briefly, all of the quartz fiber filters, PUF cartridges, and XAD-coated denuders were spiked with a mixture of eight deuterated internal recovery standards: n-decane-d<sub>12</sub>, n-pentadecane-d<sub>32</sub>, n-tetracosane-d<sub>50</sub>, n-hexanoic acid-d<sub>11</sub>, n-decanoic acid-d<sub>19</sub>, phenol-d<sub>5</sub>, benzoic acid-d<sub>5</sub>, and benzaldehyde-d<sub>6</sub> prior to extraction. The quartz fiber filters were extracted under mild sonication twice with hexane (Fisher Optima Grade), followed by three successive benzene/isopropanol (2:1 mixture) extractions (benzene: E & M Scientific; isopropanol: Burdick & Jackson). The extracts were filtered, combined, reduced in volume to approximately 250 ml, and then split into two separate fractions. One fraction was then derivatized with diazomethane to convert organic acids to their methyl ester analogs which are amenable to GC/MS identification and quantification. Although substituted phenols, guaiacols, and syringols will convert to their

methoxy analogs when reacted with diazomethane, these compounds were identified and quantified in the underivatized fraction to assure correct identification of the hydroxy and methoxy substitution patterns.

The denuders were extracted four times successively using at each step 40 ml of a solvent mixture of dichloromethane/acetone/hexane (2:3:5) (Fisher Optima Grade) by pouring each aliquot into the denuder and shaking the Teflon capped denuder lightly for approximately 30 seconds per aliquot. The four aliquots from each of the two denuder samples were composited, reduced to a volume of approximately 250  $\mu$ l and then split into two separate fractions. One fraction was derivatized with diazomethane as above.

The PUF cartridges were extracted by four successive aliquots of the dichloromethane/acetone/hexane (2:3:5) (Fisher Optima Grade) solvent mixture. The foam plugs were repetitively compressed during the extraction. The extracts were filtered, combined, reduced in volume to approximately 250  $\mu$ l and then split into two separate fractions. One fraction was derivatized with diazomethane.

Filter, PUF, and denuder field blanks were analyzed with each set of source samples. The field blanks were prepared, stored and handled by exactly the same procedures as used for the source samples.

Both the derivatized and underivatized sample fractions were analyzed by GC/MS on a Hewlett-Packard GC/MSD system (GC Model 5890, MSD Model 5972) using a 30 meter long X 0.25 mm diameter HP-1701 capillary column (Hewlett-Packard). 1-Phenyl dodecane was used as a co-injection standard for all sample extracts and standard runs. The deuterated n-alkanes in the internal standard were used to determine extraction recovery for the compounds quantified in the underivatized samples. The deuterated acids were used to verify that the diazomethane reactions were driven to completion. In addition, the deuterated n-alkanoic acid recoveries were used in conjunction with the recovery of deuterated tetracosane to determine the recovery of the compounds quantified in the derivatized fraction.

Hundreds of authentic standards have been prepared for the positive identification and quantification of the organic compounds found in the wood combustion emissions. For a group of compounds with similar structure, such as the n-alkanes, standards were only prepared for some of the compounds within the series. Compounds within a homologous series for which standards were not available were identified by comparing their spectra to the standards for similar compounds within the series and by comparison to the NIST and Wiley mass spectral libraries. For these compounds, quantification was based on the response factors for the authentic standards of closely related compounds within the series. Compounds for which standards of similar compounds were not



available were tentatively identified by comparison of their spectra to the mass spectral libraries and by fundamental interpretation of the mass spectra. The emission rates of such compounds were not quantified.

Total non-methane organic gases (NMOG, EPA method TO12) and individual organic vapor-phase hydrocarbons ranging from C<sub>1</sub> to C<sub>10</sub> were analyzed from the SUMA canisters by gas chromatography/flame ionization detection (GC/FID) as described by Fraser et al. (23). Carbonyls collected by the C<sub>18</sub> impregnated cartridges were analyzed by liquid chromatography/UV detection as described by Grosjean et al. (24).

## **6.3 Results**

### **6.3.1 Fine Particle Emission Rates and Elemental Compositions**

Table 6.1 shows the elemental composition of the fine particle mass emitted from the fireplace combustion of the three wood types. Those species with emission rates greater than twice the standard error of each determination are shown in boldface type. Fine particle mass emissions from the fireplace combustion of pine wood were measured to be  $9.5 \pm 1.0$  grams per kilogram of wood burned. The fine particle mass emitted was found to be  $56.0 \pm 2.8$  percent organic carbon and  $1.4 \pm 0.1$  percent elemental carbon. Potassium and chloride were the next largest components comprising 0.28% and 0.18% of the

Table 6.1. Average Fine Particle Emission Rate and Fine Particle Chemical Composition of Emissions from Fireplace Combustion of Wood (Values shown in boldface are greater than zero by at least two standard errors).

	Fireplace Combustion of Pine Wood	Fireplace Combustion of Oak Wood	Fireplace Combustion of Eucalyptus Wood
Fine Particle Emissions Rate (AVG $\pm$ STD)	<b>9.5 <math>\pm</math> 1.0 grams kg<sup>-1</sup> of wood burned</b>	<b>5.1 <math>\pm</math> 0.5 grams kg<sup>-1</sup> of wood burned</b>	<b>8.5 <math>\pm</math> 0.8 grams kg<sup>-1</sup> of wood burned</b>
Elemental and Organic Carbon (Wt % of Fine Particle Mass)			
Organic Carbon	<b>56.0 <math>\pm</math> 2.8<sup>a</sup></b>	<b>59.1 <math>\pm</math> 3.0<sup>a</sup></b>	<b>43.7 <math>\pm</math> 2.2<sup>a</sup></b>
Elemental Carbon	<b>1.4 <math>\pm</math> 0.1</b>	<b>3.2 <math>\pm</math> 0.2</b>	<b>2.6 <math>\pm</math> 0.2</b>
Ionic Species (Wt % of Fine Particle Mass)			
Chloride	<b>0.29 <math>\pm</math> 0.04</b>	<b>0.20 <math>\pm</math> 0.01</b>	<b>1.70 <math>\pm</math> 0.05</b>
Nitrate	<b>0.19 <math>\pm</math> 0.01</b>	<b>0.44 <math>\pm</math> 0.01</b>	<b>0.45 <math>\pm</math> 0.01</b>
Sulfate	<b>0.12 <math>\pm</math> 0.01</b>	<b>0.41 <math>\pm</math> 0.01</b>	<b>0.24 <math>\pm</math> 0.01</b>
Ammonium	<b>0.09 <math>\pm</math> 0.01</b>	<b>0.10 <math>\pm</math> 0.01</b>	<b>0.45 <math>\pm</math> 0.01</b>
Sodium	<b>0.09 <math>\pm</math> 0.01</b>	<b>0.10 <math>\pm</math> 0.01</b>	<b>0.18 <math>\pm</math> 0.01</b>
X-ray Fluorescence (Wt % of Fine Particle Mass)			
Aluminum	0.004 $\pm$ 0.003	0.000 $\pm$ 0.010	0.006 $\pm$ 0.003
Silicon	<b>0.008 <math>\pm</math> 0.001</b>	<b>0.016 <math>\pm</math> 0.005</b>	<b>0.011 <math>\pm</math> 0.002</b>
Phosphorus	<b>0.004 <math>\pm</math> 0.001</b>	<b>0.007 <math>\pm</math> 0.002</b>	<b>0.012 <math>\pm</math> 0.002</b>
Sulfur	<b>0.059 <math>\pm</math> 0.002</b>	<b>0.148 <math>\pm</math> 0.004</b>	<b>0.056 <math>\pm</math> 0.003</b>
Chlorine	<b>0.181 <math>\pm</math> 0.003</b>	<b>0.127 <math>\pm</math> 0.006</b>	<b>1.290 <math>\pm</math> 0.008</b>
Potassium	<b>0.277 <math>\pm</math> 0.003</b>	<b>0.647 <math>\pm</math> 0.007</b>	<b>0.809 <math>\pm</math> 0.005</b>
Calcium	0.004 $\pm$ 0.005	0.008 $\pm$ 0.011	0.007 $\pm$ 0.013
Titanium	0.000 $\pm$ 0.010	0.000 $\pm$ 0.017	0.000 $\pm$ 0.009
Vanadium	0.000 $\pm$ 0.006	0.000 $\pm$ 0.007	0.000 $\pm$ 0.003
Chromium	0.000 $\pm$ 0.002	0.000 $\pm$ 0.002	0.000 $\pm$ 0.001
Manganese	0.000 $\pm$ 0.001	0.000 $\pm$ 0.001	0.000 $\pm$ 0.001
Iron	0.001 $\pm$ 0.001	0.000 $\pm$ 0.001	0.000 $\pm$ 0.001
Cobalt	0.000 $\pm$ 0.000	0.000 $\pm$ 0.001	0.000 $\pm$ 0.001
Nickel	0.000 $\pm$ 0.000	0.000 $\pm$ 0.001	0.000 $\pm$ 0.001
Copper	0.000 $\pm$ 0.001	0.000 $\pm$ 0.001	0.001 $\pm$ 0.001
Zinc	<b>0.006 <math>\pm</math> 0.001</b>	<b>0.005 <math>\pm</math> 0.001</b>	<b>0.005 <math>\pm</math> 0.001</b>
Gallium	0.000 $\pm$ 0.001	0.000 $\pm$ 0.002	0.000 $\pm$ 0.001
Arsenic	0.000 $\pm$ 0.001	0.000 $\pm$ 0.002	0.000 $\pm$ 0.001
Selenium	0.000 $\pm$ 0.001	0.000 $\pm$ 0.001	0.000 $\pm$ 0.001
Bromine	0.000 $\pm$ 0.000	0.000 $\pm$ 0.001	<b>0.013 <math>\pm</math> 0.001</b>
Rubidium	0.000 $\pm$ 0.001	0.000 $\pm$ 0.001	0.000 $\pm$ 0.001
Strontium	0.000 $\pm$ 0.001	0.000 $\pm$ 0.001	0.000 $\pm$ 0.000
Yttrium	0.000 $\pm$ 0.001	0.000 $\pm$ 0.001	0.000 $\pm$ 0.001
Zirconium	0.000 $\pm$ 0.001	0.000 $\pm$ 0.001	0.000 $\pm$ 0.001
Molybdenum	0.000 $\pm$ 0.001	0.000 $\pm$ 0.002	0.000 $\pm$ 0.001
Palladium	0.000 $\pm$ 0.003	0.000 $\pm$ 0.006	0.000 $\pm$ 0.003
Silver	0.000 $\pm$ 0.003	0.000 $\pm$ 0.007	0.001 $\pm$ 0.003
Cadmium	0.000 $\pm$ 0.004	0.000 $\pm$ 0.007	0.002 $\pm$ 0.004
Indium	0.000 $\pm$ 0.004	0.000 $\pm$ 0.008	0.000 $\pm$ 0.004
Tin	0.001 $\pm$ 0.006	0.001 $\pm$ 0.011	0.000 $\pm$ 0.005
Antimony	0.004 $\pm$ 0.007	0.000 $\pm$ 0.013	0.000 $\pm$ 0.006
Barium	0.000 $\pm$ 0.025	0.000 $\pm$ 0.048	0.002 $\pm$ 0.024
Lanthanum	0.001 $\pm$ 0.033	0.000 $\pm$ 0.065	0.000 $\pm$ 0.031
Mercury	0.000 $\pm$ 0.001	0.000 $\pm$ 0.002	0.000 $\pm$ 0.001
Lead	0.000 $\pm$ 0.002	0.000 $\pm$ 0.003	0.000 $\pm$ 0.002

Notes: (a) measured on a undenuded filter.

fine particle emissions, respectively.

The fine particle emissions from the combustion oak firewood and eucalyptus firewood were  $5.1 \pm 0.5$  and  $8.5 \pm 0.8$  grams per kilogram of wood burned, respectively. The fine particles emitted from oak wood combustion were found to be comprised of  $59.1 \pm 3.0$  percent organic carbon and  $3.2 \pm 0.2$  percent elemental carbon, while the fine particle mass emitted from eucalyptus wood combustion was found to be  $43.7 \pm 2.2$  percent organic carbon and  $2.6 \pm 0.2$  percent elemental carbon. The potassium content of the fine particle mass emitted from burning eucalyptus and oak was much greater than the content of this element in the pine smoke. The potassium content of the eucalyptus smoke and oak smoke were determined to be  $0.809 \pm 0.005$  percent and  $0.647 \pm 0.007$  percent, respectively, while the concentration of potassium in pine smoke was  $0.277 \pm 0.003$  percent. In addition, the chloride content of the fine particle mass emitted from eucalyptus was much higher than that found in the pine smoke or the oak smoke. Chloride comprised  $1.29 \pm 0.008$  to  $1.7 \pm 0.05$  percent of the fine particle mass emitted from eucalyptus combustion, while chloride only made up  $0.127 \pm 0.006$  to  $0.20 \pm 0.01$  percent of the fine particle mass emitted from oak wood combustion (comparison of two independent measurement methods). It is interesting to note that the sodium content of the fine particle emissions from eucalyptus wood combustion is  $0.18 \pm 0.01$  percent which is only 80% higher than the sodium content in oak smoke, while the chloride content of the

eucalyptus smoke is about ten times greater than that of oak smoke. These differences may be important if potassium and other inorganic elements are used as combined tracers for conifer and hardwood smoke particles.

### 6.3.2 Mass Balance on Organic Compound Emissions

Figure 6.1 shows a mass balance on the non-methane organic compound emissions from pine wood combustion. Gas-phase emissions make up most of the 23.8 grams of total non-methane organic compounds emitted from each kilogram of pine wood burned. The largest contributors to gas-phase organic compound emissions are aliphatic aldehydes which make up 4.1 grams  $\text{kg}^{-1}$  of the 14.9 grams  $\text{kg}^{-1}$  of identified organic compounds emitted. Gas-phase alkenes and alkynes, principally ethene and acetylene, also make up a significant fraction of the gas-phase emissions. Phenols and substituted phenols, as well as guaiacol (2-methoxyphenol) and substituted guaiacols with substituents at position 4, make up 1.46 and 1.33 grams per kilogram of the gas-phase emissions, respectively. Alkanes, aliphatic ketones, and dicarbonyls also make up noticeable portions of the gas-phase emissions.

Approximately half of the fine particulate organic compound mass emitted from the fireplace combustion of pine wood can be extracted and characterized by GC/MS. The largest single component of the extractable particle-phase

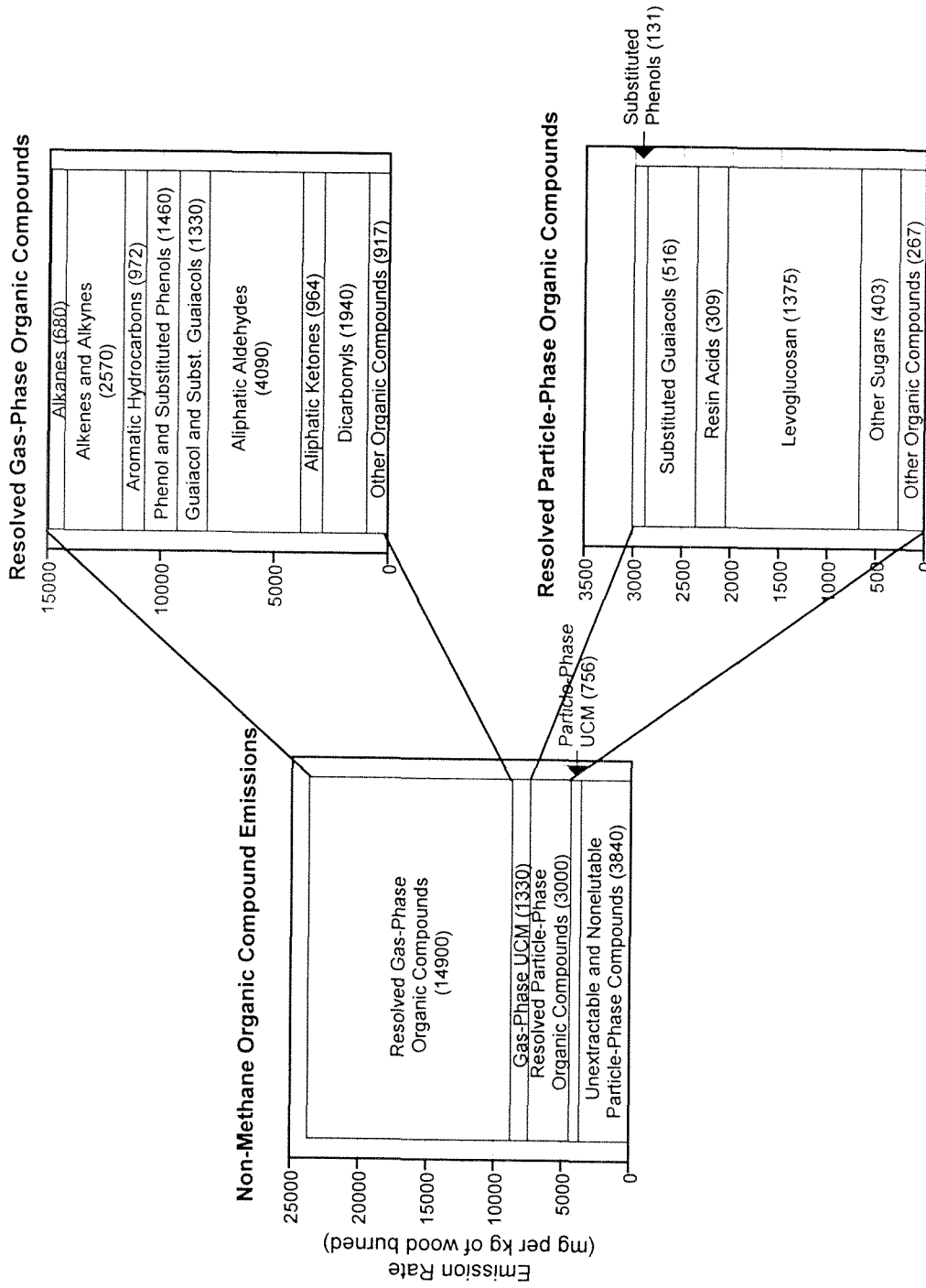


Figure 6.1. Mass balance on the non-methane organic compounds emitted from the fireplace combustion of pine wood.

organics mixture is levoglucosan (1,6-anhydro- $\beta$ -D-glucose), which comprises 18% of the total fine particle organic compound mass emitted. The next largest component of the fine particle organics mass is contributed by the unresolved complex mixture (UCM) which consists of highly branched and cyclic organic compounds that appear as a wide hump on a GC/MS trace and that is not resolved by gas chromatographic techniques. Although the UCM cannot be characterized on a single compound level, the fine particle UCM is a well defined portion of the pine combustion emissions. Substituted phenols, substituted guaiacols, and resin acids also make up significant fractions of the fine particle mass emitted from fireplace combustion of pine wood. In addition to levoglucosan, other sugar derivatives were found in the pine wood smoke and are quantified as a group in Figure 6.1. Although the sugar derivatives have not yet been identified, they have mass spectra and GC retention times very similar to levoglucosan and have been quantified assuming the same response factor as for levoglucosan. These additional sugar-like compounds also make up a noticeable fraction of the fine particle mass emitted.

Since the  $C_2$  through  $C_{10}$  gas-phase hydrocarbon emissions from the combustion of pine wood are dominated by the  $C_2$  hydrocarbons, ethene, ethylene and acetylene which are not very source specific, gas canister samples were not taken for the oak and eucalyptus wood combustion source tests. Mass balances on the carbonyls, semi-volatile gas-phase and particle-phase organic

compound emissions are shown in Figures 6.2 and 6.3 for the oak and eucalyptus wood combustion source tests, respectively. Gas-phase syringol (2,6-dimethoxyphenol) and the substituted syringols are emitted from the combustion of both oak and eucalyptus in significant quantities, 0.84 grams and 0.56 grams per kilogram of wood combusted, respectively. Syringol and substituted syringols differentiate the gas phase emissions from hardwood combustion in which they are present, from the gas-phase emissions from conifer (pine) wood combustion in which these compounds are virtually absent. Gas-phase guaiacol and substituted guaiacols are emitted from the combustion of these hardwoods at approximately half of the rate that is seen in the emissions from pine wood combustion. Phenol and substituted phenols also are emitted from the combustion of hardwoods at approximately 50% of the rate measured during the softwood combustion experiment.

Turning to the fine particle-phase emissions from hardwood combustion in Figures 6.2 and 6.3, we see that the extractable portion of the fine particles which elutes from the GC column under the present analytical conditions accounts for approximately half of the fine particle organic mass emitted, as was the case for pine wood smoke. Levoglucosan, however, makes up a much larger fraction of the fine particle mass emitted from eucalyptus wood combustion (72% of the resolved fine particle organic compound mass and 31% of the total fine particle organics mass) than is the case for pine and oak

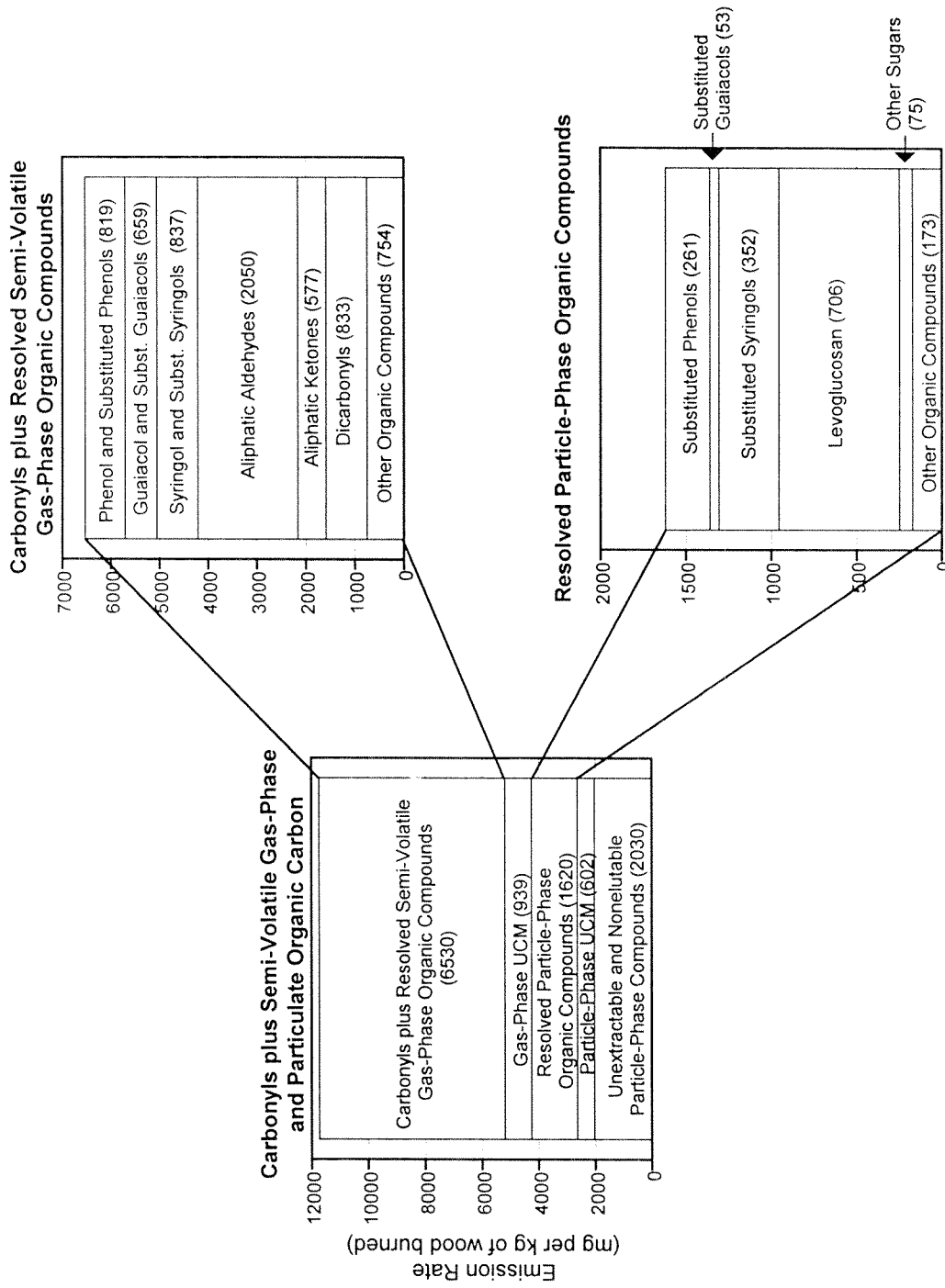


Figure 6.2. Mass balance on the carbonyl, semi-volatile, and particulate organic compounds emitted from the fireplace combustion of oak wood.



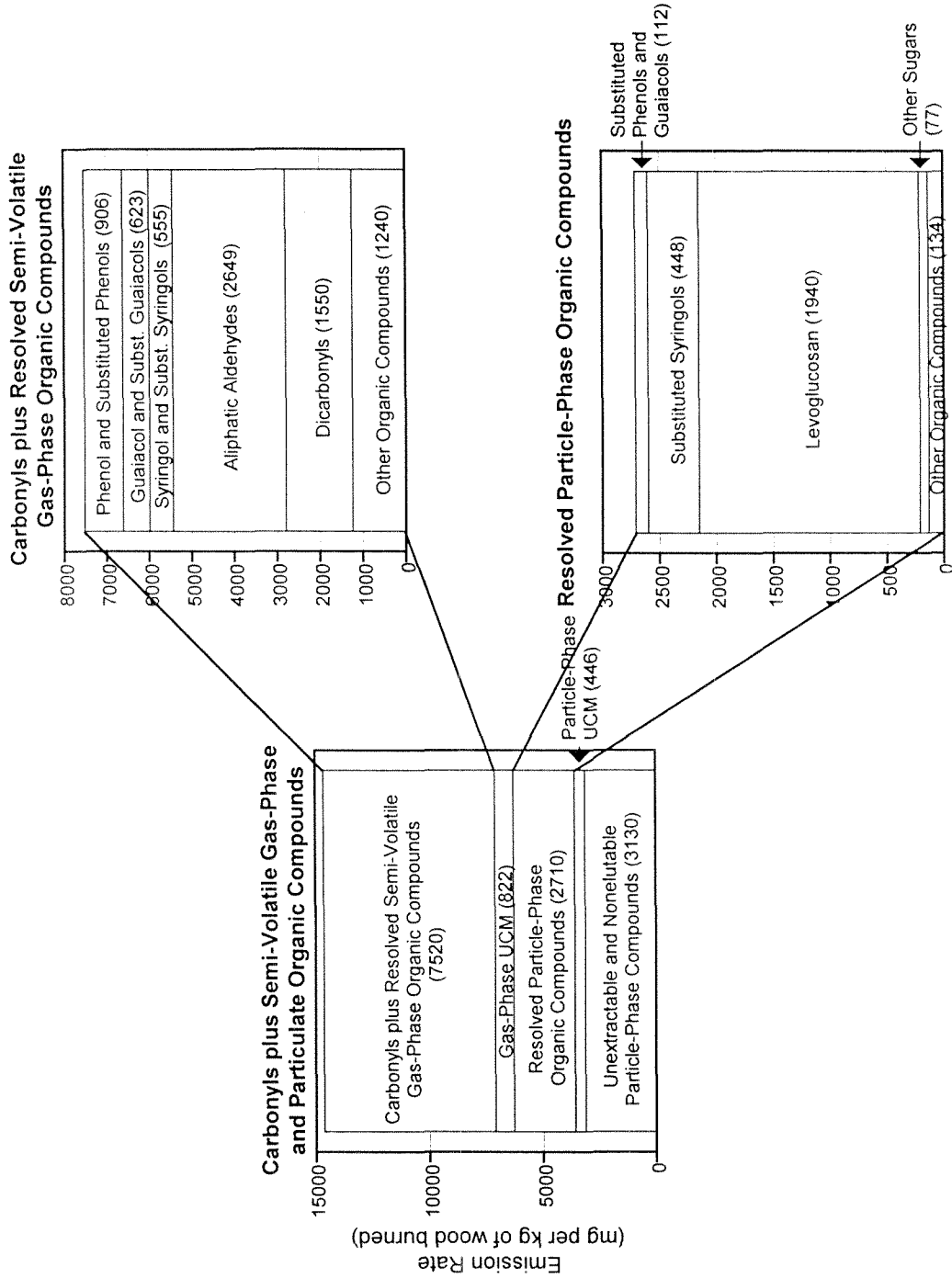


Figure 6.3. Mass balance on the carbonyl, semi-volatile, and particulate organic compounds emitted from the fireplace combustion of eucalyptus wood.

combustion. It is important to note that while the combined fine particle-phase emissions of substituted guaiacols and substituted syringols are very similar for all three woods burned in the present study at circa 400-560 mg kg<sup>-1</sup> of wood burned, the pine wood smoke emissions are clearly distinguishable by their high resin acids and substituted guaiacol emission rates when compared to the hardwood smokes which contain substantial quantities of substituted syringol compounds. These differences in resin acids and guaiacols versus substituted syringol emission rates are due to fundamental differences in the chemical composition of conifers and deciduous trees as explained by Simoneit et al. (14), and can be used to distinguish hardwood smoke from softwood smoke in the atmosphere.

### **6.3.3 Emission Rates of Individual Organic Compounds**

The emission rates of individual organic compounds are listed in Table 6.2 from the combustion of all three types of wood tested in the present study. Gas-phase alkanes are dominated by the emissions of methane, ethane, and propane with emission rates of 4120, 428, and 169 mg per kilogram of pine wood burned. n-Butane and n-heptane emissions are smaller but still significantly larger than the emissions of any of the remaining alkanes. Alkene emissions are dominated by ethene and propene, which are emitted at rates approximately 3 times greater than their alkane analogs, at 1120 and 429 mg kg<sup>-1</sup> of wood burned. Acetylene and 1,3-butadiene also are emitted at 702

Table 6.2. Organic Compound Emission Rates from Fireplace Combustion of Wood

Compound	Pine Wood (mg kg <sup>-1</sup> of Wood Burned )		Oak Wood (mg kg <sup>-1</sup> of Wood Burned )		Eucalyptus Wood (mg kg <sup>-1</sup> of Wood Burned )		Notes
	Gas	Particle	Gas	Particle	Gas	Particle	
	Phase	Phase	Phase	Phase	Phase	Phase	
n-Alkanes							
Methane	4120		*		*		a, e
Ethane	428		*		*		a, e
Propane	169		*		*		a, e
n-Butane	25.9		*		*		a, e
n-Pentane	4.7		*		*		a, e
n-Heptane	28.9		*		*		a, e
n-Octane	1.7		*		*		a, e
n-Nonane	3.9		*		*		a, e
n-Octadecane	0.356						a, f
n-Nonadecane	0.347		0.513		0.195		b, f
n-Eicosane	0.175	0.272	0.574		0.258		a, f
n-Heneicosane	0.111	0.473	0.264		0.179		b, f
n-Docosane	0.085	0.762	0.191		0.136		b, f
n-Tricosane	0.096	0.847			0.154		b, f
n-Tetracosane	0.086	0.727			0.088		a, f
n-Pentacosane		0.382					b, f
n-Hexacosane		0.423		0.330		0.259	b, f
n-Heptacosane		0.276		0.203		0.209	b, f
n-Octacosane				0.068			a, f
n-Nonacosane				0.231			b, f
Branched alkanes							
i-Pentane	5.6		*		*		a, e
2-Methylpentane	8.6		*		*		a, e
2-Methylhexane	2.6		*		*		a, e
n-Alkenes							
Ethene	1120		*		*		a, e
Propene	429		*		*		a, e
1-Butene	90.7		*		*		a, e
<i>trans</i> -2-Butene	66.5		*		*		a, e
<i>cis</i> -2-Butene	35.4		*		*		a, e
1-Pentene	8.6		*		*		a, e
<i>trans</i> -2-Pentene	16.0		*		*		a, e
<i>cis</i> -2-Pentene	10.4		*		*		a, e
<i>trans</i> -2-Hexene	8.6		*		*		a, e
Branched alkenes							
i-Butene	40.1		*		*		a, e
3-Methyl-1-butene	6.9		*		*		a, e
2-Methyl-1-butene	13.8		*		*		a, e
2-Methyl-2-butene	13.4		*		*		a, e
2-Methyl-2-Pentene	6.9		*		*		a, e

Identification notes: a) authentic quantitative standard. b) authentic quantitative standard for similar compound in series. c) identified by mass spectra. d) detected as a methyl ester.

Sample collection notes: e) collected in SUMA canister. f) collected on filter/PUF sampling train.

g) collected on DNPH impregnated C<sub>18</sub> cartridges. \*) not measured. +) detected but not quantified. See text for details.

Table 6.2. (continued - page 2)

Compound	Pine Wood (mg kg <sup>-1</sup> of Wood Burned )		Oak Wood (mg kg <sup>-1</sup> of Wood Burned )		Eucalyptus Wood (mg kg <sup>-1</sup> of Wood Burned )		Notes
	Gas	Particle	Gas	Particle	Gas	Particle	
	Phase	Phase	Phase	Phase	Phase	Phase	
Alkynes							
Ethyne (Acetylene)	702		*		*		a, c
Diolefins							
1,3-Butadiene	117		*		*		a, e
Isoprene	41.0		*		*		a, e
Cycloalkanes							
Methylcyclohexane	8.6		*		*		a, e
Cycloalkenes							
Cyclopentene	7.8		*		*		a, e
Aromatic hydrocarbons							
Benzene	383		*		*		a, e
Toluene	158		*		*		a, e
Ethylbenzene	22.9		*		*		a, e
m-Xylene + p-Xylene	60.0		*		*		a, e
o-Xylene	18.1		*		*		a, e
Naphthalene	227		*		*		a, f
2-Methylnaphthalene	15.0		9.61		5.69		a, f
1-Methylnaphthalene	10.6		6.39		4.31		a, f
Dimethylnaphthalene	13.8		11.5		7.24		a, f
Acenaphthylene	18.6		10.8		9.99		a, f
Acenaphthene	2.02		1.15		0.893		a, f
Fluorene	4.44		3.83		2.61		a, f
Phenanthrene	15.7	0.673	9.19	0.0695	8.14	0.0683	a, f
Anthracene	3.44	0.228	2.13	0.0230	1.76	0.0061	a, f
3-Methylphenanthrene	1.21	0.289	0.983	0.054	0.802		b, f
2-Methylphenanthrene	1.86	0.412	1.31	0.088	1.00		b, f
2-Methylanthracene	1.06	0.298	0.680	0.035	0.517		b, f
9-Methylphenanthrene	1.50	0.466	1.22	0.065	0.881		b, f
1-Methylphenanthrene	2.22	0.579	1.04	0.050	0.720		a, f
C <sub>2</sub> -178 MW PAH	3.58		1.57	0.326	1.05		a, f
Retene	1.38	8.52	1.21	1.12	0.151		a, f
Fluoranthene	3.05	3.95	3.61	1.20	3.75	0.509	a, f
Acephenanthrylene	0.961	1.88	1.16	0.575	1.35	0.292	a, f
Pyrene	1.87	3.78	2.40	1.23	2.70	0.585	a, f
C <sub>1</sub> -202 MW PAH	0.749	5.56	1.22	2.43	1.59	1.60	a, f
Benzo[ghi]fluoranthene	0.082	0.838	0.048	0.419	0.007	0.354	a, f
Cyclopenta[cd]pyrene		0.974		0.430	0.025	0.324	a, f
C <sub>1</sub> -226 MW PAH		1.37		0.201		0.357	b, f
Benz[a]anthracene		1.22		0.630	0.032	0.533	a, f
Chrysene/Triphenylene		1.14		0.755	0.027	0.593	a, f
C <sub>1</sub> -228 MW PAH		1.76		0.437		0.489	b, f

Identification notes: a) authentic quantitative standard. b) authentic quantitative standard for similar compound in series. c) identified by mass spectra. d) detected as a methyl ester.

Sample collection notes: e) collected in SUMA canister. f) collected on filter/PUF sampling train.

g) collected on DNPH impregnated C<sub>18</sub> cartridges. \*) not measured. +) detected but not quantified. See text for details.

Table 6.2. (continued - page 3)

Compound	Pine Wood (mg kg <sup>-1</sup> of Wood Burned )		Oak Wood (mg kg <sup>-1</sup> of Wood Burned )		Eucalyptus Wood (mg kg <sup>-1</sup> of Wood Burned )		Notes
	Gas	Particle	Gas	Particle	Gas	Particle	
	Phase	Phase	Phase	Phase	Phase	Phase	
Aromatic hydrocarbons							
Benzo[k]fluoranthene		0.671		0.303		0.286	a, f
Benzo[b]fluoranthene		0.790		0.400		0.327	a, f
Benzo[j]fluoranthene		0.466		0.073		0.121	b, f
Benzo[e]pyrene		0.459		0.231		0.212	a, f
Benzo[a]pyrene		0.712		0.245		0.301	a, f
Perylene		0.111		0.019		0.020	a, f
Indeno[1,2,3-cd]fluoranthene		0.224		0.018		0.010	b, f
Indeno[1,2,3-cd]pyrene		0.518				0.168	a, f
Benzo[ghi]perylene		0.437				0.173	a, f
Anthanthrene		0.052				0.008	b, f
Phenol and substituted phenols							
Phenol	525		300		434		a, f
o-Cresol	89.6		47.7	0.018	37.8	0.006	a, f
m&p-Cresol	380	0.500	179	0.210	110	0.055	a, f
Dimethylphenols	110	0.451	50.7		30.2	0.029	a, f
o-Benzenediol	312		142		215		b, f
p-Benzenediol	17.2	20.9	14.1	13.1	18.3	15.1	a, f
m-Benzenediol	2.81	47.0	4.47	26.0	10.0	13.0	a, f
Methylbenzenediols	10.4	54.5	56.0	28.9	38.4	18.1	b, f
Hydroxybenzaldehydes	12.1	7.91	14.1	0.529	11.4	0.316	b, f
4-(2-Hydroxyethyl)phenol			11.1	192	1.38	14.7	b, f
Guaiacol and substituted guaiacols							
Guaiacol	279	0.359	172	0.149	183	0.094	a, f
4-Methylguaiacol	339	0.854	101	0.113	81.3	0.110	b, f
4-Ethylguaiacol	203	0.939	100	0.054	56.7	0.058	b, f
4-Propylguaiacol	69.6	0.593	31.6		11.9		b, f
Eugenol	57.2	0.381	20.7		10.8		a, f
cis-Isoeugenol	41.2	0.702	13.1		9.25		b, f
trans-Isoeugenol	118	6.68	23.6	0.276	45.9	0.217	b, f
Vanillin	105	138	50.7	2.40	51.9	0.851	a, f
Acetovanillone	31.2	19.6	23.2	1.11	29.4	1.44	a, f
Guaiacyl acetone	88.6	118	123	33.7	143	29.0	b, f
Coniferyl aldehyde		230		15.1		19.3	a, f
Syringol and substituted syringols							
Syringol			397	1.99	287	2.22	a, f
4-Methylsyringol	0.301		174	5.06	130	2.74	b, f
4-Ethylsyringol	0.226		184	11.6	93.8	3.09	b, f
4-Propylsyringol			65.5	15.4	22.1	1.28	b, f
Allylsyringol			1.32	4.95	2.89	0.534	b, f
4-Propenylsyringol			1.27	36.2	5.70	5.60	a, f

Identification notes: a) authentic quantitative standard. b) authentic quantitative standard for similar compound in series. c) identified by mass spectra. d) detected as a methyl ester.

Sample collection notes: e) collected in SUMA canister. f) collected on filter/PUF sampling train. g) collected on DNPH impregnated C<sub>18</sub> cartridges. \*) not measured. +) detected but not quantified. See text for details.

Table 6.2. (continued - page 4)

Compound	Pine Wood (mg kg <sup>-1</sup> of Wood Burned )		Oak Wood (mg kg <sup>-1</sup> of Wood Burned )		Eucalyptus Wood (mg kg <sup>-1</sup> of Wood Burned )		Notes
	Gas	Particle	Gas	Particle	Gas	Particle	
	Phase	Phase	Phase	Phase	Phase	Phase	
Syringol and substituted syringols							
Syringaldehyde			7.77	25.3	9.32	50.5	b, f
Acetosyringone			1.02	28.1	1.19	55.3	b, f
Syringyl acetone	0.259		5.33	196	2.62	239	b, f
Propionylsyringol				8.79		16.0	b, f
Butyrylsyringol				0.353		14.2	b, f
Sinapyl aldehyde				18.4		57.4	b, f
Aliphatic aldehydes							
Formaldehyde	1165		759		599		a, g
Acetaldehyde	1704		823		1021		a, g
Propanal	255		153		155		a, g
Butanal	96		62		31		a, g
Pentanal	32		88		28		a, g
Hexanal	418		90		189		a, g
Heptanal	419		77		626		a, g
Aliphatic ketones							
Acetone	749		462		79		a, g
Butanone	215		115		77		a, g
Olefinic aldehydes							
Acrolein	63		44		56		a, g
Crotonaldehyde	276		177		198		a, g
Methacrolein	23		9.1		44		a, g
Aromatic carbonyls							
Benzaldehyde	49		16		21		a, g
m&p-Tolualdehyde	12				27		a, g
Acetophenone	3.9		5.3		14		a, g
2,5-Dimethylbenzaldehyde	12		20		50		a, g
Dicarbonyls							
Glyoxal	670		439		616		
Methylglyoxal	943		321		520		a, g
Biacetyl	89		73		73		a, g
2-Oxobutanal	241				337		a, g
n-Alkanoic acids							
n-Tetradecanoic acid	0.357	0.764		1.36		1.12	a, f, d
n-Hexadecanoic acid	2.00	19.9		16.9		15.4	a, f, d
n-Heptadecanoic acid	0.082	2.86		0.903			b, f, d
n-Octadecanoic acid		4.32		2.77		1.95	a, f, d
n-Nonadecanoic acid		0.645		0.347			b, f, d
n-Eicosanoic acid		7.25		0.958		0.992	a, f, d
n-Heneicosanoic acid		0.565		0.674		0.512	b, f, d
n-Docosanoic acid		20.8		7.61		5.09	a, f, d

Identification notes: a) authentic quantitative standard. b) authentic quantitative standard for similar compound in series. c) identified by mass spectra. d) detected as a methyl ester.

Sample collection notes: e) collected in SUMA canister. f) collected on filter/PUF sampling train.

g) collected on DNPH impregnated C<sub>18</sub> cartridges. \*) not measured. +) detected but not quantified. See text for details.

Table 6.2. (continued - page 5)

Compound	Pine Wood (mg kg <sup>-1</sup> of Wood Burned )		Oak Wood (mg kg <sup>-1</sup> of Wood Burned )		Eucalyptus Wood (mg kg <sup>-1</sup> of Wood Burned )		Notes
	Gas	Particle	Gas	Particle	Gas	Particle	
	Phase	Phase	Phase	Phase	Phase	Phase	
n-Alkanoic acids							
n-Tricosanoic acid		0.479		1.26		0.780	b, f, d
n-Tetracosanoic acid		10.2		17.6		11.2	b, f, d
n-Pentacosanoic acid		0.161		0.266		0.504	b, f, d
n-Hexacosanoic acid		0.573		2.23		11.8	b, f, d
n-Alkenoic acids							
n-9-Octadecenoic acid		59.0		11.7		13.9	a, f, d
n-9,12-Octadecadienoic acid		18.9		11.7		21.4	a, f, d
Resin acids							
Pimaric acid		5.09		0.212			b, f, d
Sandaracopimaric acid		3.40		0.242			b, f, d
Isopimaric acid		42.9		3.55			b, f, d
8,15-Pimaradien-18-oic acid		0.132					b, f, d
Dehydroabietic acid		43.6		2.07		0.424	a, f, d
Abietic acid		187		1.20			b, f, d
7-Oxodehydroabietic acid		2.34					b, f, d
Abieta-6,8,11,13,15-pentaen-18-oic acid		20.1					b, f, d
Abieta-8,11,13,15-tetraen-18-oic acid		4.46		0.055			b, f, d
Sugars							
Levoglucosan		1375		706		1940	a, f
Other sugars		403		75		77	b, f
PAH Ketones							
Indan-1-one	17.5	0.135	13.8		7.66		b, f
9H-Fluoren-9-one	6.68	1.95	6.00		3.92		b, f
1H-Phenalen-1-one	0.285	4.45		1.35	0.689	1.52	a, f
7H-Benz[de]anthracen-7-one		0.694		0.187		0.289	a, f
Other compounds							
Veratraldehyde	1.24	0.299					a, f
3,4-Dimethoxytoluene	12.7		38.2		3.25		a, f
Veratric acid		8.10	2.04	4.12	0.910	8.41	a, f
Hydroxymethylfurfural	142	62.3	145	64.5	439	30.8	a, f
2-Furaldehyde	111		200		161		a, g
2-Methylfuraldehyde	10		5.3		1.9		a, g
Divanillyl		+		+		+	c, f
Divanillyl methane		+		+		+	c, f
Vanillylmethylguaiacol		+		+		+	c, f

Identification notes: a) authentic quantitative standard. b) authentic quantitative standard for similar compound in series. c) identified by mass spectra. d) detected as a methyl ester.

Sample collection notes: e) collected in SUMA canister. f) collected on filter/PUF sampling train.

g) collected on DNPH impregnated C<sub>18</sub> cartridges. \*) not measured. +) detected but not quantified. See text for details.

and 117 mg per kilogram of pine wood burned. Although the emissions of acetylene and ethene, which are often used as motor vehicle exhaust tracers, will likely be dominated by motor vehicle emissions in urban locations like Los Angeles in the summer when wood is not generally burned for home heating, the ambient concentrations of these compounds will be significantly affected by wood combustion at times and places where greater wood burning occurs, as will be demonstrated later in the present work.

Benzene makes up 60% of the mono-aromatic hydrocarbon emissions from the combustion of pine wood with an emission rate of 383 mg per kilogram of wood burned. Benzene from wood combustion also will be a significant contributor to ambient benzene concentrations in high wood burning areas, as will be shown shortly.

As previously indicated, aliphatic aldehydes are major contributors to the gas-phase emissions from wood combustion. Acetaldehyde was emitted at the highest rate of all of the carbonyls, with an emission rate averaged over all three tests of 1180 mg per kilogram of wood burned. Formaldehyde, methylglyoxal and glyoxal were emitted at the next highest rates with average emissions of 841, 595, and 575 mg per kilogram of wood burned, respectively. Emissions of crotonaldehyde were also relatively high from all three types of wood burned, averaging 217 mg per kilogram of wood burned over all three tests.



Polycyclic aromatic hydrocarbons (PAH) are also emitted from wood combustion. Emissions of phenanthrene and anthracene average 11.2 and 2.5 mg per kilogram of wood burned, respectively. The methyl and dimethyl substituted homologs of these PAH are also emitted in significant quantities with emission rates of 7.6 and 2.2 mg per kilogram of wood burned averaged over all three tests. Retene (1-methyl-7-isopropylphenanthrene) is the fully aromatized thermal alteration product of resin acids present in conifer wood and is typically associated with the emissions from conifer wood combustion. In the current tests, the emission rate of gas- plus particle-phase retene from pine wood combustion was 9.9 mg per kilogram of wood burned, which is greater than the emissions of any of the other substituted phenanthrenes. Retene was also found in small amounts in the emissions from the fireplace combustion of the oak wood and in much lower quantities in the emissions from the combustion of eucalyptus wood. Volatilization of retene previously deposited on the chimney walls in earlier wood burning operations in the same fireplace might explain the presence of retene at low-levels in the emissions during the hardwood combustion experiments.

The patterns formed by the emissions of benzenediols, guaiacols, syringols, and resin acids are shown in Figure 6.4. The chemical structures of guaiacol, syringol, and their derivatives are shown in Figure 6.5 and the chemical structures of the resin acids have been previously described (14). As

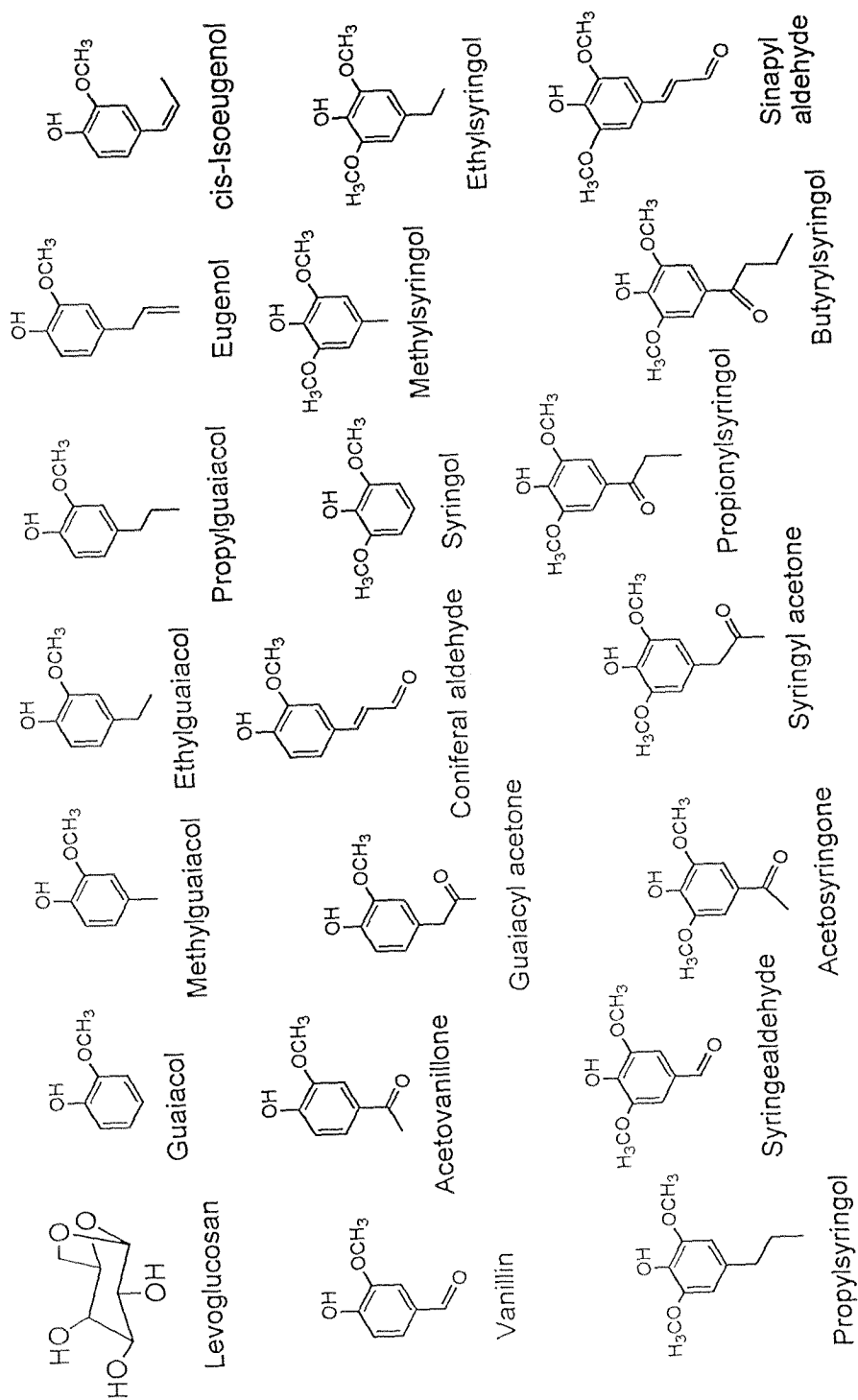


Figure 6.4. Chemical structure of levoglucosan, guaiacol, substituted guaiacols, syringol, and substituted syringols emitted from the fireplace combustion of wood.

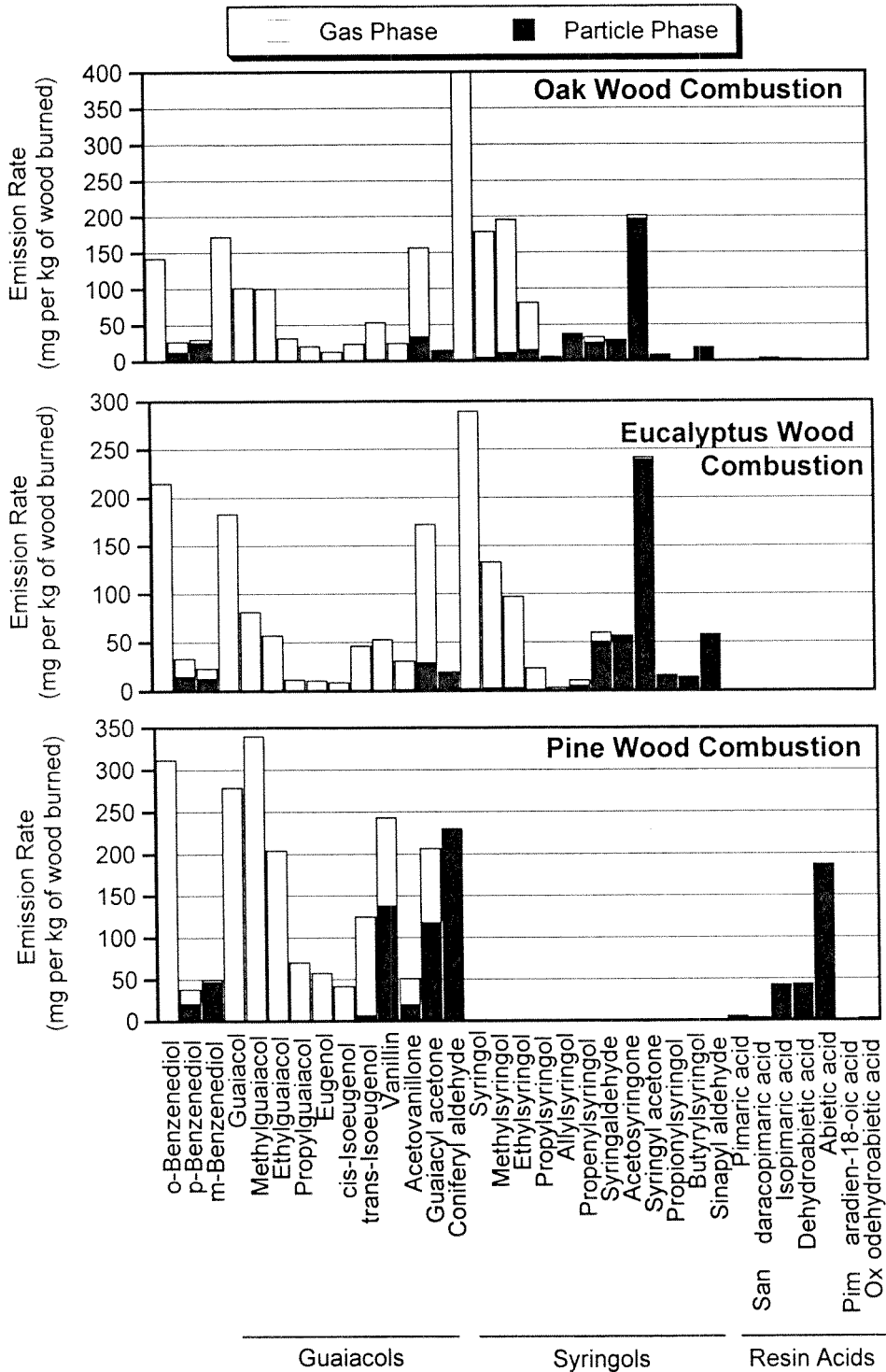


Figure 6.5. Emission rates of organic compounds from wood combustion and their gas/particle phase distributions in the diluted exhaust from a residential fireplace.

can be seen from Figure 6.4, significant differences exist in the emission profiles that distinguish pine wood combustion effluent from the emissions generated when the two hardwoods are burned. The emissions of resin acids from the combustion of pine wood can only be detected at trace levels in the emissions from the combustion of oak and eucalyptus firewood. The syringol and syringol derivatives which are present in the emissions from hardwood combustion are not detected at significant quantities in the softwood combustion emissions. Although trace concentrations of the pine smoke markers are found in the hardwood emissions possibly due to volatilization of deposits off of the chimney walls, only minute quantities of a few of the hardwood markers are found in the softwood emissions due to the fact that no hardwood was burned in the chimney used for the current source tests for at least three years prior to the pine wood combustion tests.

Guaiacols and the derivatives of guaiacol are emitted by the combustion of both the softwood and the hardwoods, but the emission rates of individual guaiacol derivatives are very different for the two types of wood. Coniferyl aldehyde and vanillin are emitted at significantly higher rates from pine wood combustion than from combustion of the hardwoods tested in the present study. The alkyl-substituted guaiacols and guaiacol are emitted at moderately higher rates from the pine wood combustion process but the relative distribution of

these compounds in the emissions from pine wood combustion is not significantly different from that in the hardwood combustion emissions.

The relative distribution of total benzenediol isomer emissions shown in Figure 6.4 is not very different for the combustion of the three types of wood tested, but the distribution of these compounds between the gas and particle phases in the diluted emissions varies significantly for the different isomers. The ortho-substituted benzenediol is completely in the gas phase while the para-substituted species is split evenly between the gas and particle phases. The meta-substituted species is found mostly in the particle phase for the pine and oak smoke but is evenly split between the two phases in the eucalyptus smoke.

#### 6.3.4 Gas/Particle Partitioning: Experiment Versus Theory

Gas/particle partitioning theory (25, 26) holds that the phase distribution of a semi-volatile organic compound is determined by its absorption into the particle phase matrix, and that this phase distribution can be described by a partitioning coefficient,  $K_{p, opm}$ , defined as:

$$K_{p, opm} = \frac{F_i OPM}{A} \quad (1)$$

where  $K_{p, opm}$  is the gas/particle partitioning coefficient based on organic particulate matter as the receiving particle phase substrate in units of  $\text{m}^3 \mu\text{g}^{-1}$ .  $F_i$  is the particle-associated mass concentration of the semi-volatile organic

compound of interest ( $\mu\text{g m}^{-3}$ ), OPM is the total organic particulate matter concentration into which the compound can partition ( $\mu\text{g m}^{-3}$ ), and A is the gas-phase mass concentration of the compound of interest ( $\mu\text{g m}^{-3}$ ). It is expected that the gas/particle partitioning coefficient,  $K_{p,opm}$ , will depend on the vapor pressure of the various organic compounds (27):

$$\text{Log}(K_{p,opm}) = m_{r,opm}\text{Log}(p_L^0) + b_{r,opm} \quad (2)$$

where  $p_L^0$  is the vapor pressure over a liquid pool of the semi-volatile organic compound of interest in torr, and  $m_{r,opm}$  and  $b_{r,opm}$  are coefficients that can be estimated by regressing a series of experimentally measured values of  $K_{p,opm}$  on the corresponding liquid vapor pressure values,  $p_L^0$ , for the members of a given organic compound class. If the compounds have similar activity coefficients when present in the particulate organic matrix and the partitioning process has reached equilibrium, then  $-m_{r,opm}$  should be close to unity. Under this condition,  $b_{r,opm}$  is a constant characteristic of the partitioning for that class of compounds with the specific particle matrix.

As previously indicated the phase distribution of the emitted PAH was measured throughout the complete wood burning cycle by filter/PUF sampling trains during each source test, and 15-minute samples were analyzed that represent two different times during the pine wood combustion source test using the denuder/filter/PUF sampling technology. A plot of  $K_{p,opm}$  as a function of  $p_L^0$

is presented in Figure 6.6 for all of the available PAH data. Values of  $m_{r,opm}$  and  $b_{r,opm}$  for PAH as measured by the filter/PUF sampling train in the diluted exhaust from hardwood combustion are  $-1.4 \pm 0.05$  and  $-10.4 \pm 0.22$ , respectively. For measurements made by the filter/PUF method in the diluted exhaust from the pine wood combustion,  $-m_{r,opm}$  is  $-1.3 \pm 0.07$  and  $b_{r,opm}$  is  $-9.4 \pm 0.31$ . In both of these cases,  $m_{r,opm}$  is significantly different from unity indicating that the partitioning of the PAH as determined by the filter/PUF sampling trains does not appear to be at equilibrium. However, also shown in Figure 6.6 are the  $K_{p,opm}$  values determined by the denuder/filter/PUF measurement technique in the diluted exhaust from pine wood combustion. For the denuder/filter/PUF measurements,  $m_{r,opm}$  is  $-0.93 \pm 0.03$  and  $b_{r,opm}$  is  $-7.6 \pm 0.16$ , which is in much better agreement with the partitioning theory described above. Measurements of the partitioning behavior of PAH by Liang and Pankow (27) using a filter/PUF sampler were found to have  $b_{r,opm}$  values of  $-7.0$  for tobacco smoke and  $-6.9$  for urban particulate matter.

### **6.3.5 Determination of the Contribution of Wood Smoke to Ambient VOC Concentrations**

Demonstration that the distribution of fine particle-phase organic compounds in wood smoke can be used to trace wood smoke contributions to atmospheric fine particle concentrations is provided by Schauer et al. (16) and will not be repeated here. The characterization of the gas-phase emissions from

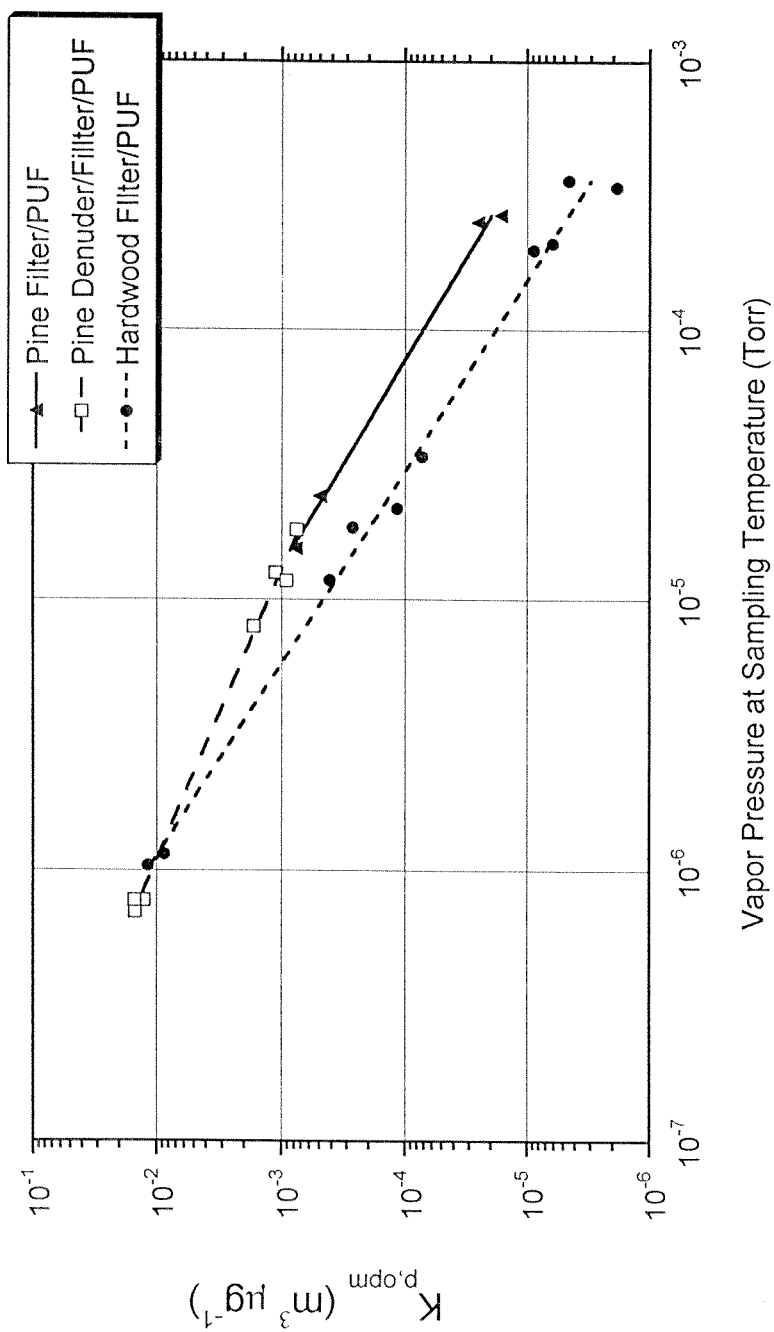


Figure 6.6. Gas/particle partitioning of PAH in the diluted exhaust from wood burned in a residential fireplace as a function of the vapor pressure of the pure compound.



wood combustion provided in the present study when combined with particle-phase wood smoke tracers now makes it possible to assess the contribution of wood combustion to ambient VOC concentrations. The concentrations of fine particulate organic compounds and gas-phase volatile hydrocarbons were measured in Fresno, California, in the winter of 1995-1996 as part of the San Joaquin Valley IMS95 air quality study. Ambient concentrations of benzene, ethene, acetylene, and levoglucosan for two episodes of 48 hours duration during the IMS95 study are listed in Table 6.3. Also included in this table are the emission rates of these compounds collected in the present study for pine wood combustion. Emissions and ambient concentrations that are normalized according to levoglucosan also are presented in Table 6.3. Given that the average emission rate of levoglucosan from hardwood combustion is close to that of the pine wood sample and given the fair similarity of the emissions rates of the lightest gas-phase compounds measured in all tests (e.g., the carbonyls) it is assumed that the levoglucosan and gas-phase emissions from pine wood combustion can be used to estimate the concentration of wood smoke-derived VOCs in the Fresno atmosphere. If levoglucosan is used as a tracer for woodsmoke, then the contributions of wood burning to the ambient concentrations of benzene, ethene, and acetylene can be estimated for these episodes. As shown in Table 6.3, the contributions from wood burning to the ambient benzene, ethene, and acetylene concentrations during the December 26-28, 1995, episode are 14%, 24% and 18%, respectively. This result is

Table 6.3. Estimate of the contribution from wood smoke to the ambient concentrations of benzene, ethene, and ethyne in Fresno, California, during two winter episodes using levoglucosan as a tracer for wood smoke

	Emission Rate from Firewood Combustion (mg per kilogram of wood burned)	Ambient Concentration ( $\mu\text{g m}^{-3}$ )	
		Fresno, California Dec. 26-28, 1995	Fresno, California Jan. 4-6, 1996
Benzene	383	15.1	12.0
Ethene	1120	25.8	16.7
Acetylene	702	21.7	16.5
Levoglucosan	1375	7.59	2.13
	Ratio of Emission to Levoglucosan	Contribution from Wood Combustion ( $\mu\text{g m}^{-3}$ )	
Benzene	0.279	2.1 (14.0%)	0.6 (5.0%)
Ethene	0.815	6.2 (24.0%)	1.7 (10.4%)
Acetylene	0.510	3.9 (17.8%)	1.1 (6.6%)

significant because benzene, acetylene, and ethene are often used as motor vehicle exhaust tracers within VOC receptor models in which they are used to distinguish the differences between whole gasoline vapors and gasoline-powered motor vehicle exhaust within atmospheric samples. The omission of the contributions from wood smoke VOCs within receptor modeling calculations could lead incorrectly to an overestimate of the contribution of tailpipe exhaust and an underestimate of the contribution of whole gasoline vapors to ambient VOC concentrations in communities where a significant amount of wood burning occurs.

## 6.4 References

1. Khalil, M. A. K.; Edgerton, S. A.; Rasmussen, R. A. *Environ. Sci. Technol.* **1983**, 17, 555-559.
2. Wolff, G. T.; Countess, R. J.; Groblicki, P. J.; Ferman, M. A.; Cadle, S. H.; Muhlbaier, J. L. *Atmos. Environ.* **1981**, 15, 2485-2502.
3. Sheffield, A. E.; Gordon, G. E.; Currie, L. A.; Riederer, G. E. *Atmos. Environ.* **1994**, 28, 1371-1384.
4. Sexton, K.; Liu, K. S.; Hayward, S. B.; Spengler, J. D. *Atmos. Environ.* **1985**, 19, 1225-1236.
5. Malm, W. C.; Gebhart, K. A. *J. Air Waste Man. Assoc.* **1997**, 47, 250-268.
6. Hildemann, L. M.; Markowski, G. R.; Cass, G. R. *Environ. Sci. Technol.* **1991**, 25, 744-759.
7. Ramdahl, T. *Nature* **1983**, 306, 580-582.
8. Benner, B. A. Jr.; Wise, S. A.; Currie, L. A.; Klouda, G. A.; Klinedinst, D. B.; Zweidinger, R. B.; Stevens, R. K.; Lewis, C. W. *Environ. Sci. Technol.* **1995**, 29, 2382-2389.

9. Daisey, J. M.; Chesney, J. L.; Lioy, P. J. *J. Air Pollut. Control. Assoc.* **1986**, 36, 17-33.
10. Locker, H. B. Ph.D. Thesis, Dartmouth College, Hanover, New Hampshire, 1988.
11. Hawthorne, S. B.; Krieger, M. S.; Miller, D. J.; Mathiason, M. B. *Environ. Sci. Technol.* **1989**, 23, 470-475.
12. Hawthorne, S. B.; Miller, D. J.; Langenfeld, J. J.; Krieger, M. S. *Environ. Sci. Technol.* **1992**, 26, 2251-2262.
13. Standley, L. J.; Simoneit, B. R. T. *Atmos. Environ.* **1990**, 24B, 67-73.
14. Simoneit, B. R. T.; Rogge, W. F.; Mazurek, M. A.; Standley, L. J.; Hildemann, L. M.; Cass, G. R. *Environ. Sci. Technol.* **1993**, 27, 2533-2541.
15. Rogge W. F.; Hildemann, L. M.; Mazurek, M. A.; Cass, G. R.; Simoneit, B. R. T. *Environ. Sci. Technol.* **1998**, 32, 13-27.
16. Schauer, J. J.; Rogge, W. R.; Hildemann, L. M.; Mazurek, M. A.; Cass, G. R.; Simoneit, B. R. T. *Atmos. Environ.* **1996**, 30, 3837-3855.
17. John, W.; Reischl, G. *JAPCA* **1980**, 30, 872-876.
18. Birch, M. E.; Cary, R. A. *Aerosol Sci. Technol.* **1996**, 25, 221-241.

19. Dzubay, T. G. *X-ray Analysis of Environmental Samples*, **1977**, Ann Arbor Science, Ann Arbor, MI.
20. Mueller, P. K.; Mendoza, B. V.; Collins, J. C.; Wilgus, E. A. "Application of Ion Chromatography to the Analysis of Anions Extracted from Airborne Particulate Matter," In *Ion Chromatographic Analysis of Environmental Pollutants*, **1978**, Sawicki, E.; Mulik, J. D.; Wittgenstein, E. Eds.; Ann Arbor Science, Ann Arbor, MI, pp. 77-86.
21. Solorzano, L. *Limnol. Oceanogr.* 1969, 14, pp. 799-801.
22. Grosjean, E.; Grosjean, D. *Int. J. Envir. Anal. Chem.* **1995**, 61, 343-360.
23. Fraser, M. P.; Cass G. R.; Simoneit B. R. T.; Rasmussen R. A. *Environ. Sci. Technol.* **1997**, 31, 2356-2367.
24. Grosjean, E.; Grosjean, D.; Fraser M. P.; Cass G. R. *Environ. Sci. Technol.* **1996**, 30, 2687-2703.
25. Pankow, J. F.; Bidleman, T. F. *Atmos. Environ.* **1992**, 26A, 1071-1080.
26. Pankow, J. F. *Atmos. Environ.* **1994**, 28, 185-188.
27. Liang, C.; Pankow, J. F. *Environ. Sci. Technol.* **1996**, 30, 2800-2805.

## Chapter 7

# Organic Compounds in Cigarette Smoke

## 7.1 Introduction

Organic compounds present in the emissions from air pollution sources and in ambient air can be used to determine the contribution of cigarette smoking to outdoor ambient fine particle concentrations. Calculations by Schauer et al. (1) show that cigarette smoke particles contributed approximately 0.7% of the fine particle mass in the Los Angeles area atmosphere in the early 1980's. The approach used in that analysis involved a chemical mass balance model in which high molecular weight iso- and anteiso-alkanes effectively acted as markers for cigarette smoke in ambient air while other chemical substances were used to simultaneously trace the presence of eight other fine particle source types. Although this technique has not yet been employed in indoor environments, the same approach can be used to determine the contributions to indoor fine particle concentrations from cigarette smoke, food cooking emissions, wood combustion, as well as other important air pollution sources.

The study by Schauer et al. (1) employed low volatility particle-phase organic compounds as environmental tracers, while others have pursued the use of more abundant semi-volatile organic compounds such as nicotine (2) as tracers for particulate matter emitted from cigarette smoke. Semi-volatile organic compounds exist simultaneously in both the gas and particle phases. If such compounds are to be followed in the environment it is valuable to assemble a source emissions data base that simultaneously quantifies both the gas-phase and particle-phase emissions.

Gas- and particle-phase organic compound emissions from air pollution sources including wood smoke, food cooking operations, and motor vehicle exhaust are presented in Chapters 2 through 6. Chemical profiles from these source tests can be used within a chemical mass balance source apportionment model to simultaneously determine the contributions of air pollution sources to ambient concentrations of organic gases and fine particulate matter. If a similar emissions profile is generated for cigarette smoke, then this approach can also be applied to indoor environments to apportion source contributions to gas- and particle phase-pollutants, as well as to identify the sources of individual organic compounds. To this end the current study has been undertaken to measure gas- and particle-phase organic compounds as well as the distribution of compounds between the gas and particle phases in the emissions from cigarette smoke.



## 7.2 Experimental Methods

### 7.2.1 Comprehensive Source Sampling

The source sampling system used for the present study consists of a dilution source sampler with a chamber that houses a human smoker built into the center of the apparatus. A cigarette customer steps inside the smoking chamber which is fabricated from a large sheet metal laboratory storage cabinet with the shelves removed. Commercially purchased high purity dilution air is purged to this chamber through two air inlet ports located near the top of the smoking chamber. A 152 cm diameter transfer line connects the side of the smoking chamber to the residence time chamber of the dilution source sampler described in Chapter 2. An ashtray was placed at the inlet of the transfer line such that virtually all of the sidestream smoke from a cigarette at those times when it was smoldering in the ashtray was drawn through the transfer line into the residence time chamber from which aged diluted cigarette smoke samples were taken. The smoker held the cigarette at the inlet to the transfer line when inhaling and exhausted the exhaled mainstream smoke directly into the transfer line. This procedure exhausted virtually all of the cigarette smoke through the transfer line without allowing the smoke to build up in the smoking chamber. The flow of high purity dilution air was set at 300 lpm while the flowrate through the transfer line was set at 240 lpm, thereby creating a slight over pressure

within the cabinet. Additional air at a flowrate of 30 lpm were withdrawn from the lower section of the smoking chamber to a background air sampling train to quantify any back-mixing of emissions into the smoking chamber and to quantify whether or not any contaminants were present in the dilution air. The excess air going into the smoking chamber prevented intrusion of ambient air into the smoking chamber. All of the seals in the downstream transfer line and the residence time chamber of the sampler were air-tight.

The mainstream and sidestream cigarette emissions plus the dilution air passed through the transfer line into the residence time chamber, where the semi-volatile species in the diluted emissions were allowed to equilibrate between the gas and particle phases. From the residence chamber, the diluted exhaust was pulled through eight AIHL-design cyclone separators operated in parallel at a flowrate of 30 lpm each (3) that removed particles with aerodynamic diameters greater than 1.8  $\mu\text{m}$ . Gases and particles with diameters less than 1.8  $\mu\text{m}$  passed through the cyclones and were sampled by a series of sampling trains operated in parallel.

Semi-volatile and fine particle-phase organic compounds were collected continuously throughout the cigarette smoking cycle by the denuder/filter/PUF sampling train and the filter/PUF sampling train. Details of these sampling trains are provided in Chapter 2. One denuder-based sampling train was operated

during each composite test in which two cigarettes were smoked. Four filter/PUF sampling trains were operated in parallel with the denuder-based sampling train during the cigarette smoking source tests.

The sixth cyclone-based sampling unit used during the cigarette smoking source tests was configured with sampling substrates to measure the emissions of fine particulate matter mass, carbonyls, organic acids, and gas-phase hydrocarbons. This sampling unit is described in Chapter 2 and is shown in Figure 2.1 of Chapter 2.

The background sampler, which was used to sample the air in the smoking chamber, consisted of three filter packs connected at the outlet of an AIHL cyclone separator. The first stacked filter unit consisted of two quartz fiber filters (47 mm diameter, Pallflex Tissuequartz 2500 QAO) in series which were used for elemental carbon and organic carbon (EC/OC) determination by thermal evolution and combustion analysis as described by Birch and Cary (4). The second filter pack contained a Teflon membrane filter (47 mm diameter, Gelman Teflo, 2  $\mu\text{m}$  pore size) which was used for gravimetric determination of the fine particle mass emitted and also was analyzed by X-ray fluorescence for 35 trace elements (5). The third filter holder assembly contained one Teflon membrane filter which was used for a duplicate fine particle mass emissions measurement and for inorganic ion measurements by ion chromatography (6), atomic absorption spectroscopy and colorimetry (7). Downstream of the second

Teflon filter the sample flow was divided, and a small portion of the flow was used to fill a 6 liter polished stainless steel SUMA canister for the collection of non-methane volatile hydrocarbons ranging from  $C_1$  to  $C_{10}$ . The 6 liter SUMA canister was filled continuously at the same flowrate as the SUMA canister used to collect the cigarette smoke samples.

Electronic particle sizing instruments and a pair of MOUDI impactors also were connected to the residence time chamber during the cigarette smoke tests to obtain particle size distributions and particle chemical composition as a function of size. The MOUDI impactors were connected to the 7<sup>th</sup> and 8<sup>th</sup> AIHL-design cyclone separator. The size distributions and the results obtained from the MOUDI impactors will be reported elsewhere.

### **7.2.2 Source Testing Procedure**

Two cigarettes were smoked during each cigarette smoking source test. At the beginning of each source test the smoking chamber was purged with purified dilution air for 5 minutes and then the cigarette customer entered the smoking chamber. The chamber was then purged for an additional 3 minutes. All of the sampling train flowrates were established 30 seconds prior to lighting the first cigarette. The smoker inhaled and exhaled the cigarette smoke according to their customary smoking habits. The cigarette was left in the ashtray between inhalations. When the cigarette was completely smoked, the

cigarette was extinguished in the ashtray and the sampling flows were continued for an additional 60 seconds. Typical cigarette smoking times were 5 minutes per cigarette, diluting the mainstream plus sidestream smoke from one cigarette to 1.2 m<sup>3</sup> of the flowing dilution air.

After the test of the first cigarette was complete, one Teflon filter and the quartz fiber filters designated for EC/OC analysis were replaced with new filters, permitting us to determine the mass emission rates and organic carbon emission rates for each cigarette. All other sampling collection devices were left in place for the second cigarette smoking test. At the beginning of the second cigarette smoking test, the smoking chamber was repurged with purified dilution air as was done for the first cigarette. Air flows through the sampling trains were reestablished 30 seconds before the second cigarette was lit, and the cigarette was smoked under the same conditions as described above. After the second cigarette was extinguished, the sampler flows were continued for 60 seconds and then all flows were stopped. All substrates were then unloaded for analysis except the SUMA canisters which continued to be filled over all six cigarettes smoked.

The cigarettes smoked in the present study are listed in Table 7.1. These six cigarettes were chosen to represent a market share average of the cigarettes smoked in the United States in the mid-1990's. The six cigarettes represent four

Table 7.1. Cigarettes Smoked in Present Study

<u>Brand</u>	<u>Manufacturer</u>	<u>Length (mm)*</u>	<u>Filter</u>	<u>Regular or Light</u>	<u>Menthol</u>
Camel	R. J. Reynolds	69	No	Regular	No
Kent Kings	Lorillard	63	Yes	Regular	No
Kool Filters	Brown & Williamson	63	Yes	Regular	Yes
Marlboro Light	Philip Morris	57	Yes	Light	No
Marlboro Regular	Philip Morris	60	Yes	Regular	No
Winston Filters	R. J. Reynolds	62	Yes	Regular	No

\* Length of cigarette tobacco bed

of the major cigarette manufacturers, with one cigarette without a filter, one menthol flavored cigarette, one light cigarette, and three regular filter-tip cigarettes.

### 7.2.3 Organic Chemical Analysis

The analytical procedures used in the present study for the identification and quantification of semi-volatile and particle-phase organic compounds in air pollution source emissions are discussed in Chapter 2.

Filter, PUF, and denuder field blanks were analyzed with each set of source samples. The field blanks were prepared, stored and handled by exactly the same procedures as used for the source samples.

Hundreds of authentic standards have been prepared for the positive identification and quantification of the organic compounds found in the current source test program. When quantitative standards could not be obtained for a given compound or compound class, significant effort was made to obtain a non-quantitative secondary standard that could be used for unique identification of the organic compounds. An example of such a secondary standard is the use of petroleum wax as a source of high molecular weight *iso*-alkanes and *anteiso*-alkanes that were used to help identify these compounds in the cigarette smoke. Quantification of compounds identified using secondary standards has been

estimated from the response factors for compounds having similar retention times and chemical structures.

Total non-methane organic gases (NMOG, EPA method TO12) and individual vapor-phase hydrocarbons ranging from C<sub>1</sub> to C<sub>10</sub> were analyzed from the SUMA canisters by gas chromatography/flame ionization detection (GC/FID) as described by Fraser et al. (8). Carbonyls collected by the C<sub>18</sub>-impregnated cartridges were analyzed by liquid chromatography/UV detection as described by Grosjean et al. (9).

## 7.3 Results

### 7.3.1 Fine Particle Emissions Rates and Compositions

Fine particle mass emission rates for the six cigarettes averaged  $27.0 \pm 1.3$  mg per cigarette smoked. The fine particle mass collected in this fashion consisted of 62.5% organic carbon and 0.45% elemental carbon. Table 7.2 shows the elemental composition of the fine particle mass collected from cigarette smoking. Although nitrogen was not directly measured, the nitrogen associated with the specific organic compounds that were quantified in Table 7.3 accounts for 1.4% of the fine particle mass emitted. Potassium and chlorine were measured to be the next largest components of the fine particle mass comprising  $0.64 \pm 0.11$  to  $0.49 \pm 0.07$  percent and  $0.44 \pm 0.09$  to  $0.34 \pm 0.06$  percent of the fine particle mass, respectively (range of the two independent



Table 7.2. Average Fine Particle Emission Rate and Fine Particle Chemical Composition for Cigarette Smoking (Values shown in boldface are greater than zero by at least two standard errors).

Fine Particle Mass Emissions Rate (AVG ± STD)		<b>27.0 ± 1.3 mg per cigarette</b>	
Elemental and Organic Carbon (Wt % of Fine Particle Mass)			
Organic Carbon	<b>46.0 ± 1.8<sup>a</sup></b>	Elemental Carbon	<b>0.45 ± 0.10</b>
Ionic Species (Wt % of Fine Particle Mass)			
Chloride	<b>0.44 ± 0.09</b>	Ammonium	<b>0.03 ± 0.01</b>
Nitrate	<b>0.06 ± 0.03</b>	Sodium	<b>0.03 ± 0.01</b>
Sulfate	<b>0.07 ± 0.02</b>	Potassium	<b>0.49 ± 0.07</b>
X-ray Fluorescence (Wt % of Fine Particle Mass)			
Aluminum	0.00 ± 0.03	Selenium	0.00 ± 0.00
Silicon	0.00 ± 0.02	Bromine	0.00 ± 0.00
Phosphorus	0.00 ± 0.01	Rubidium	0.00 ± 0.01
Sulfur	<b>0.13 ± 0.03</b>	Strontium	0.00 ± 0.00
Chlorine	<b>0.34 ± 0.06</b>	Yttrium	0.00 ± 0.00
Potassium	<b>0.64 ± 0.11</b>	Zirconium	0.00 ± 0.00
Calcium	0.00 ± 0.02	Molybdenum	0.00 ± 0.01
Titanium	0.00 ± 0.01	Palladium	0.00 ± 0.01
Vanadium	0.00 ± 0.01	Silver	0.00 ± 0.01
Chromium	0.00 ± 0.01	Cadmium	0.02 ± 0.02
Manganese	0.00 ± 0.01	Indium	0.00 ± 0.01
Iron	<b>0.03 ± 0.01</b>	Tin	0.01 ± 0.02
Nickel	0.01 ± 0.01	Antimony	0.00 ± 0.02
Copper	0.02 ± 0.01	Barium	0.00 ± 0.10
Zinc	0.01 ± 0.01	Lanthanum	0.00 ± 0.13
Gallium	0.00 ± 0.00	Mercury	0.00 ± 0.00
Germanium	0.00 ± 0.00	Lead	0.00 ± 0.00
Arsenic	0.00 ± 0.00		

Notes: (a) measured downstream of organics denuder. Organic carbon collected on undenuded filter is 62.5 percent of the fine particle mass.

Table 7.3. Organic Compounds Measured in Cigarette Smoke

Compound	Cigarette Smoking Emissions		Notes
	(µg per cigarette)		
	Gas Phase	Particle Phase	
n-Alkanes			
Methane	4440		a, e
Ethane	1330		a, e
Propane	602		a, e
n-Butane	178		a, e
n-Pentane	52		a, e
n-Hexane	51		a, e
n-Heptane	31		a, e
n-Octane	16		a, e
n-Nonane	9		a, e
n-Decane	6		a, e
n-Pentacosane		4.52	b, f
n-Heptacosane		32.7	b, f
n-Octacosane		2.8	a, f
n-Nonacosane		35.4	b, f
n-Triacontane		11.2	b, f
n-Hentriacontane		148.2	b, f
n-Dotriacontane		17.9	a, f
n-Tritriacontane		49.9	b, f
Branched alkanes			
iso-Butane	277		a, e
iso-Pentane	46		a, e
2,2-Dimethylbutane	50		a, e
2-Methylpentane	22		a, e
2,4-Dimethylpentane	45		a, e
iso-Nonacosane		7.40	b, f
anteiso-Triacontane		25.8	b, f
iso-Hentriacontane		57.0	b, f
anteiso-Dotriacontane		52.0	b, f
iso-Tritriacontane		15.9	b, f
n-Alkenes			
Ethene	1590		a, e
Propene	1260		a, e
1-Butene	138		a, e
<i>trans</i> -2-Butene	159		a, e
<i>cis</i> -2-Butene	97		a, e
1-Pentene	91		a, e
<i>trans</i> -2-Pentene	54		a, e
<i>cis</i> -2-Pentene	39		a, e
1-Hexene	130		a, e
<i>cis</i> -2-Hexene	100		a, e

Identification notes: (a) authentic quantitative standard. (b) authentic quantitative standard for similar compound in series. (c) secondary standard. (d) detected as a methyl ester.

Sample collection notes: (e) collected in SUMA canister. (f) collected on denuder/filter/PUF sampling train. (g) collected on DNPH impregnated C<sub>18</sub> cartridges. \*) not measured. See text for details.

Additional Notes: † Compound is too volatile for accurate determination of phase distribution by denuder/filter/PUF sampling train; reported emissions are from filter/PUF sampling train.

Table 7.3. (continued - page 2)

Compound	Cigarette Smoking Emissions ( $\mu\text{g}$ per cigarette)		Notes
	Gas Phase	Particle Phase	
Branched alkenes			
Isobutene	521		a, e
3-Methyl-1-butene	80		a, e
2-Methyl-1-butene	124		a, e
2-Methyl-2-pentene	87		a, e
Neophytadiene	59.8	31.2	b, f
Diolefins			
1,3-Butadiene	88		a, e
Isoprene	3000		a, e
Alkynes			
Ethyne	340		a, e
Saturated cycloalkanes			
Methylcyclopentane	36		a, e
Cyclohexane	12		a, e
Methylcyclohexane	21		a, e
Aromatic hydrocarbons			
Benzene	481		a, e
Toluene	829		a, e
Ethylbenzene	94		a, e
m & p-Xylene	469		a, e
o-Xylene	74		a, e
Styrene	132		a, e
iso-Propylbenzene	8		a, e
n-Propylbenzene	17		a, e
p-Ethyltoluene	58		a, e
m-Ethyltoluene	23		a, e
o-Ethyltoluene	27		a, e
1,3,5-Trimethylbenzene	14		a, e
1,3,4-Trimethylbenzene	111		a, e
Naphthalene <sup>†</sup>	41.0	0.39	a, f
2-Methylnaphthalene <sup>†</sup>	14.8		a, f
1-Methylnaphthalene <sup>†</sup>	17.3		a, f
C <sub>2</sub> -Naphthalenes <sup>†</sup>	34.8	0.11	a, f
C <sub>3</sub> -Naphthalenes <sup>†</sup>	13.9	0.08	b, f
Acenaphthylene <sup>†</sup>	6.23		a, f
Acenaphthene <sup>†</sup>	3.62		a, f
Fluorene	2.38	0.35	a, f
Phenanthrene	3.28	0.94	a, f
Anthracene	0.81		a, f
C <sub>1</sub> MW 178 PAH	2.48	4.12	a, f

Identification notes: (a) authentic quantitative standard. (b) authentic quantitative standard for similar compound in series. (c) secondary standard. (d) detected as a methyl ester.

Sample collection notes: (e) collected in SUMA canister. (f) collected on denuder/filter/PUF sampling train. (g) collected on DNPH impregnated C<sub>18</sub> cartridges. \*) not measured. See text for details.

Additional Notes: <sup>†</sup> Compound is too volatile for accurate determination of phase distribution by denuder/filter/PUF sampling train; reported emissions are from filter/PUF sampling train.

Table 7.3. (continued - page 3)

Compound	Cigarette Smoking Emissions		Notes
	(µg per cigarette)		
	Gas Phase	Particle Phase	
Aromatic hydrocarbons			
Fluoranthene	0.12	1.00	a, f
Acephenanthrylene	0.02	0.50	b, f
Pyrene	0.10	0.81	a, f
Benz[a]anthracene		0.40	a, f
Chrysene & Triphenylene		0.69	a, f
Aliphatic aldehydes			
Formaldehyde	165		a, g
Acetaldehyde	2120		a, g
Propanal	165		a, g
Butanal	114		a, g
Hexanal	82		a, g
Octanal	60		a, g
Nonanal	17		a, g
Decanal	10		a, g
Aliphatic ketones			
Acetone	736		a, g
Butanone	156		a, g
2-Pentanone	140		a, g
Olefinic aldehydes			
Crotonaldehyde	116		a, g
Acrolein	171		a, g
Olefinic ketones			
Solanone	14.0	3.2	b, f
Geranyl acetone	11.9		b, f
Aromatic aldehydes			
Benzaldehyde	59		a, g
Dicarbonyls			
Glyoxal	353		a, g
Methylglyoxal	575		a, g
Biacetyl	101		a, g
2-Oxobutanal	391		a, g
Furaldehydes			
2-Furaldehyde	81		a, g
5-Hydroxymethylfuraldehyde	45		a, g
Phenols			
Phenol <sup>†</sup>	409	6.12	a, f
o-Cresol <sup>†</sup>	24.9	0.435	a, f
m&p-Cresol <sup>†</sup>	73.1	1.50	a, f

Identification notes: (a) authentic quantitative standard. (b) authentic quantitative standard for similar compound in series. (c) secondary standard. (d) detected as a methyl ester.

Sample collection notes: (e) collected in SUMA canister. (f) collected on denuder/filter/PUF sampling train. (g) collected on DNPH impregnated C<sub>18</sub> cartridges. \*) not measured. See text for details.

Additional Notes: <sup>†</sup> Compound is too volatile for accurate determination of phase distribution by denuder/filter/PUF sampling train; reported emissions are from filter/PUF sampling train.

Table 7.3. (continued - page 4)

Compound	Cigarette Smoking Emissions ( $\mu\text{g}$ per cigarette)		Notes
	Gas	Particle	
	Phase	Phase	
Phenols			
Ethylphenols <sup>†</sup>	19.6	1.40	a, f
Dimethylphenols <sup>†</sup>	44.2	1.61	a, f
Ethylphenol	15.2	7.41	b, f
p-Benzenediol		147	a, f
m-Benzenediol		9.03	a, f
Methylbenzenediols		9.48	b, f
Ethylbenzenediols		27.64	b, f
n-Alkanoic acids			
Tetradecanoic acid	0.50	17.0	a, d, f
Hexadecanoic acid	1.68	237	a, d, f
Octadecanoic acid		57.1	a, d, f
Eicosanoic acid		13.4	a, d, f
Heicosanoic acid		2.98	b, d, f
Docosanoic acid		10.0	a, d, f
Tricosanoic acid		4.44	b, d, f
Tetracosanoic acid		5.01	a, d, f
Alkenoic acids			
9-Octadecenoic acid		64.4	a, d, f
9,12-Octadecadienoic acid		119	a, d, f
9,12,15-Octadecatrienoic acid		169	a, d, f
Carbonyl acids			
Glyoxylic acid		19	a, g
Pyruvic acid		11	a, g
N-Containing compounds			
1-Methyl-1H-pyrido[2,3-b]pyridine <sup>†</sup>	60.7		b, f
Quinoline <sup>†</sup>	16.6		a, f
Isoquinoline <sup>†</sup>	8.35		a, f
Phenylpyridine	6.08		b, f
Myosmine	81.2	53.1	b, f
Indole <sup>†</sup>	79.4	6.08	b, f
Methylindoles	30.2	8.81	b, f
$\beta$ -Nicotyrine	47.3	36.4	b, f
Nicotine	2040	2000	a, f
Bipyridyl	14.7	14.9	b, f
N-Methylsuccinimide	3.52	9.54	b, f
Carbazole	0.18	3.46	b, f
Cotinine	1.53	18.6	b, f
N-Oxynicotine		20.5	b, f

Identification notes: (a) authentic quantitative standard. (b) authentic quantitative standard for similar compound in series. (c) secondary standard. (d) detected as a methyl ester.

Sample collection notes: (e) collected in SUMA canister. (f) collected on denuder/filter/PUF sampling train. (g) collected on DNPH impregnated C<sub>18</sub> cartridges. \*) not measured. See text for details.

Additional Notes: <sup>†</sup> Compound is too volatile for accurate determination of phase distribution by denuder/filter/PUF sampling train; reported emissions are from filter/PUF sampling train.

Table 7.3. (continued - page 5)

<u>Compound</u>	<u>Cigarette Smoking Emissions</u> ( <u>µg per cigarette</u> )		<u>Notes</u>
	<u>Gas</u>	<u>Particle</u>	
	<u>Phase</u>	<u>Phase</u>	
N-Containing compounds			
Nicotinic acid		12.7	b, f
Hydroxypyridine		41.5	b, f
Other compounds			
Furancarboxylic acid		19.4	b, f
Menthol <sup>†</sup>	179	31.1	a, f
Triacetin (glyceryl triacetate)	415	66.2	a, f
Levoglucozan		119	a, f
Vitamin E		11.1	a, f
6,7-Dimethoxy-coumarin		12.6	b, f
Phenylacetic acid		13.6	b, f

Identification notes: (a) authentic quantitative standard. (b) authentic quantitative standard for similar compound in series. (c) secondary standard. (d) detected as a methyl ester.

Sample collection notes: (e) collected in SUMA canister. (f) collected on denuder/filter/PUF sampling train. (g) collected on DNPH impregnated C<sub>18</sub> cartridges. \*) not measured. See text for details.

Additional Notes: <sup>†</sup> Compound is too volatile for accurate determination of phase distribution by denuder/filter/PUF sampling train; reported emissions are from filter/PUF sampling train.

determinations). Sulfur, sodium ion, and ammonium ion comprised smaller but measurable portions of the fine particle mass emitted from cigarette smoking.

### **7.3.2 Emissions of CO and CO<sub>2</sub>**

An overall carbon balance on the emissions from human smoking of cigarettes cannot be accurately closed since the CO<sub>2</sub> introduced from human respiration is larger than the production of CO<sub>2</sub> from a cigarette under normal smoking conditions. For this reason the CO<sub>2</sub> emission rate from smoking cannot be accurately measured by the techniques employed in this study. CO emissions, however, can be accurately measured from human smoking of cigarettes. CO emissions amounted to 98,000 μg per cigarette smoked, which is in good agreement with previously reported CO emissions for cigarettes (10, 11).

### **7.3.3 Mass Balance on Organic Compound Emissions**

The sum of gas-phase plus particle-phase non-methane organic compounds emitted from the average cigarette smoked in the present experiment is 45.4 mg per cigarette, as shown in Figure 7.1. This accounts for approximately 6.2% of the mass of the tobacco found in the cigarettes smoked in the present study. Gas-phase species accounted for approximately 66% of the overall organic compound emissions. The largest fraction of the gas-phase emissions consisted of olefins and carbonyls, which made up 26% and 19% of

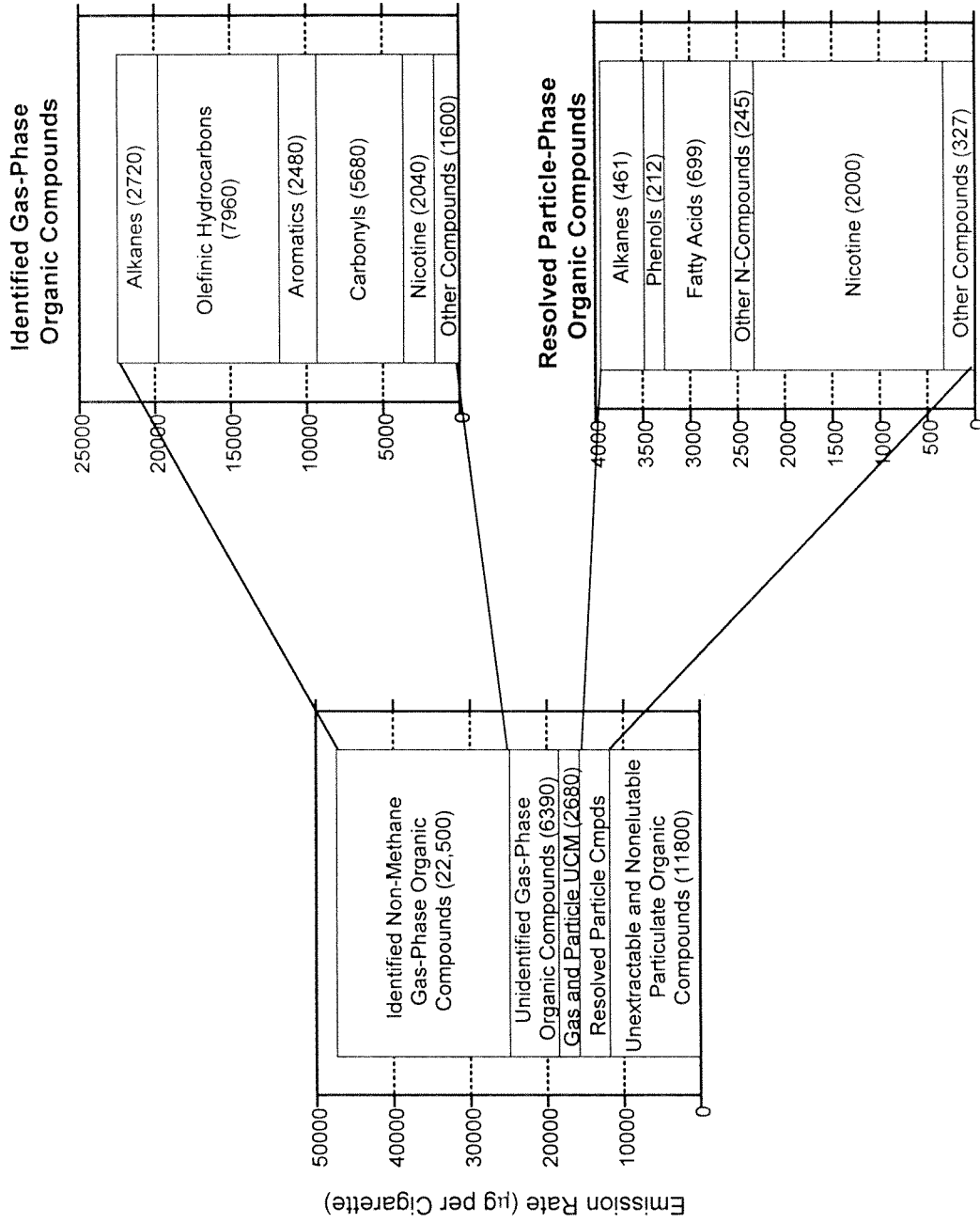


Figure 7.1. Mass balance on the non-methane organic mass emitted from the cigarette smoking.



the non-methane organic gas emissions, respectively. Alkanes and aromatic hydrocarbons each made up slightly less than 10% of the gas-phase emissions. Approximately 21% of the light gas-phase organic carbon mass was not identified at the single compound level and is believed to be comprised of low molecular weight alcohols, alkanolic acids, and nitrogen-containing species which are not detected by the analytical methods employed in the present study.

The unresolved complex mixture (UCM) appears as a wide hump that underlies the resolved compounds on a GC trace and consists of highly branched and cyclic organics that cannot be separated from each other by the present methods. The semi-volatile gas-phase UCM makes up a small portion of the gas-phase emissions, contributing only 3.6% of the gas-phase organic compound emissions. Likewise, the particle-phase UCM emissions are relatively small making up only 10% of the 15.4 mg of fine particulate organic mass emitted per cigarette. In contrast, the non-extractable and non-elutable fraction of the fine organic particulate matter mass emitted from cigarette smoking is relatively large, making up 77% of the fine particle organic mass.

The absolute mass emission rate of nicotine is split evenly between the gas and particle phases at the dilution rate used in the present study. Nicotine makes up over half of the organic compounds which can be extracted, eluted,

and separated by the GC/MS techniques used here. Fatty acids (n-alkanoic acids and n-alkenoic acids) make up the next largest fraction of the organic compounds identified in the particle phase followed by the alkanes.

### **7.3.4 Emission Rates of Individual Organic Compounds**

The gas- and particle-phase emission rates of 137 organic compounds quantified in the cigarette smoke are shown in Table 7.3. All of the semi-volatile and particle-phase organic compounds shown in Table 7.3 were quantified using the denuder/filter/PUF sampling train except for the 17 most volatile species which were quantified by the filter/PUF sampling train and are noted in Table 7.3 with a dagger. Nicotine is emitted at a rate of 4000  $\mu\text{g}$  per cigarette smoked, the highest rate of any of the compounds identified, and is consistent with previously reported measurements (10). The compounds with the next highest emissions rates are isoprene and acetaldehyde which are emitted at rates of 3000 and 2120  $\mu\text{g}$  per cigarette smoked, respectively.

Figure 7.2 shows the emission rates of the volatile hydrocarbons containing between 2 and 8 carbon atoms in the effluent from cigarette combustion, meat charbroiling, and wood combustion. As previously indicated the emissions rate of isoprene from cigarette smoking is very large compared to the emissions of other light hydrocarbons, almost twice the emissions rate of ethene and more than twice the emissions rate of propene. This is very different

than the emissions of these compounds from meat charbroiling and fireplace combustion of wood where isoprene emissions are only a small fraction of the ethene and propene emissions. In addition the ratio of the emissions of ethene to propene in cigarette smoke is 1.3, compared to 5.1 and 2.6 for meat charbroiling and wood combustion, respectively. Although isoprene and propene are very reactive under many atmospheric conditions, the differences in these ratios could be useful in less reactive environments (i.e., nighttime, cold winter days, and some indoor environments) for the determination of the origin of gaseous pollutants. Isoprene has been used in the past to qualitatively distinguish cigarette smoke from the emissions of motor vehicles (12) and from the emissions of food cooking operations (13).

As can be seen in Figure 7.2, the abundance of the low molecular weight n-alkanes emitted from cigarette smoking decreases with increasing carbon number from ethane to n-pentane, a pattern which is also seen in the emissions from meat charbroiling and wood combustion. In contrast, however, the monoaromatic hydrocarbons in cigarette smoke show toluene emissions that exceed both benzene and xylene isomer emissions, while the emissions of the monoaromatic hydrocarbons from meat charbroiling and wood combustion both decrease with increasing carbon number from benzene to toluene to the xylenes.

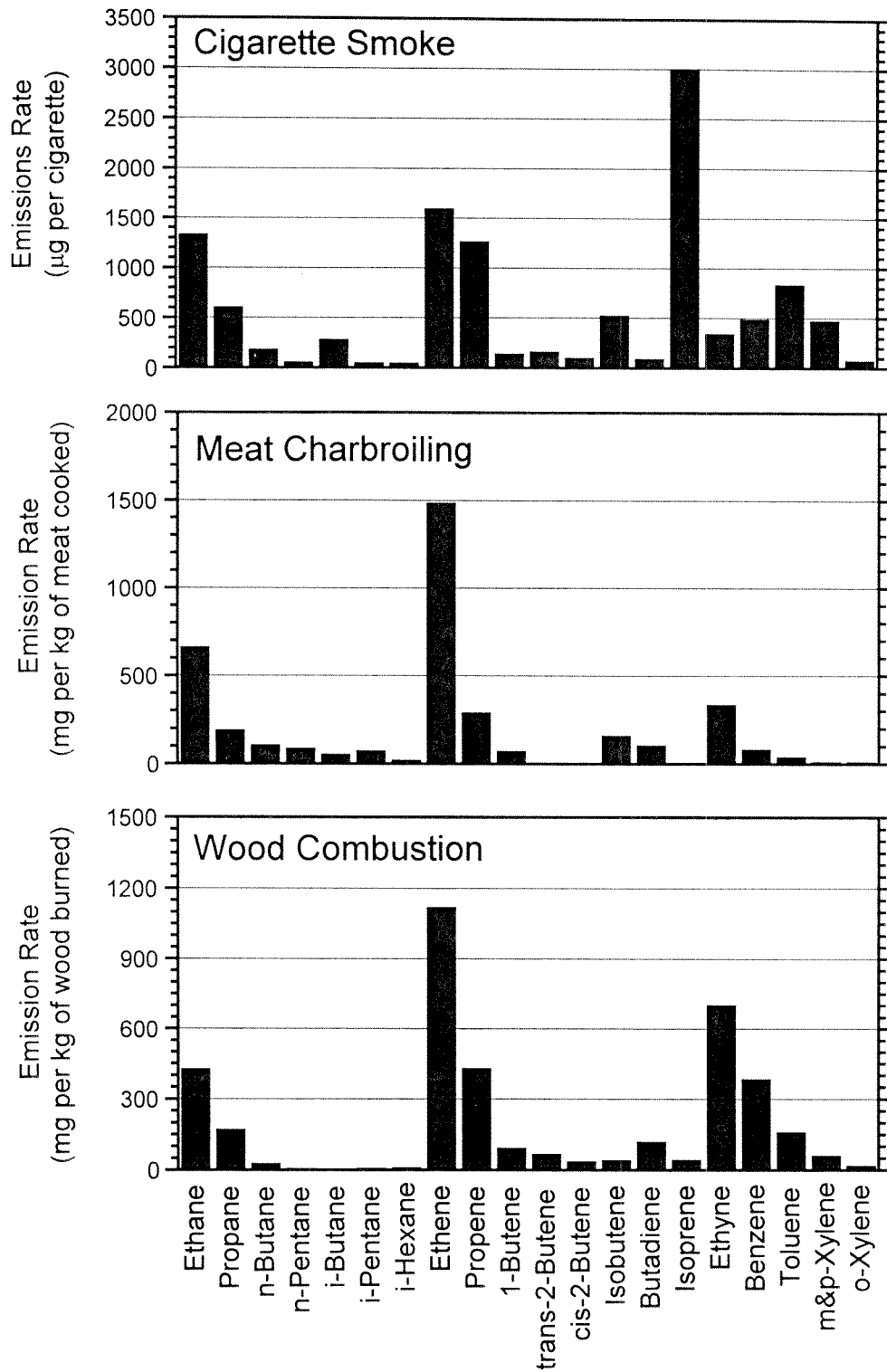


Figure 7.2. Mass emission rates of C<sub>2</sub> through C<sub>8</sub> hydrocarbons emitted from cigarette smoking, meat charbroiling, and fireplace combustion of wood.

The distributions of the light gas-phase carbonyls emitted from cigarette smoking, meat charbroiling, and wood combustion are shown in Figure 7.3. The ratio of the emissions of formaldehyde to acetaldehyde in cigarette smoke differs from that in wood combustion and meat charbroiling effluent. For cigarette smoke this ratio is 12.8 and for meat charbroiling and wood combustion this ratio is close to unity.

Several unusual semi-volatile and particle phase organic compounds have been identified and quantified in the emissions from cigarette smoking. The structures of these compounds are shown in Figure 7.4 and the gas- and particle-phase emission rates observed at the dilution rates of the present study are shown in Figure 7.5. As seen in Figure 7.5, nicotine emissions are more than 8 times greater than the emissions of any of the other semi-volatile organic compounds studied. Two other semi-volatile organics which are emitted at relatively high emission rates are triacetin and menthol. Both of these compounds are believed to be added to the cigarettes during manufacturing as triacetin is reported to be used as a flavor enhancer (14) and menthol is likely emitted from the menthol flavored cigarette. In contrast, neophytadiene, solanone, and geranyl acetone are derived from the tobacco content of the cigarettes smoked. They are not expected to be emitted from a large number of other sources. These three compounds are likely to suffer from high chemical reactivity under some atmospheric conditions due to the olefinic bonds and

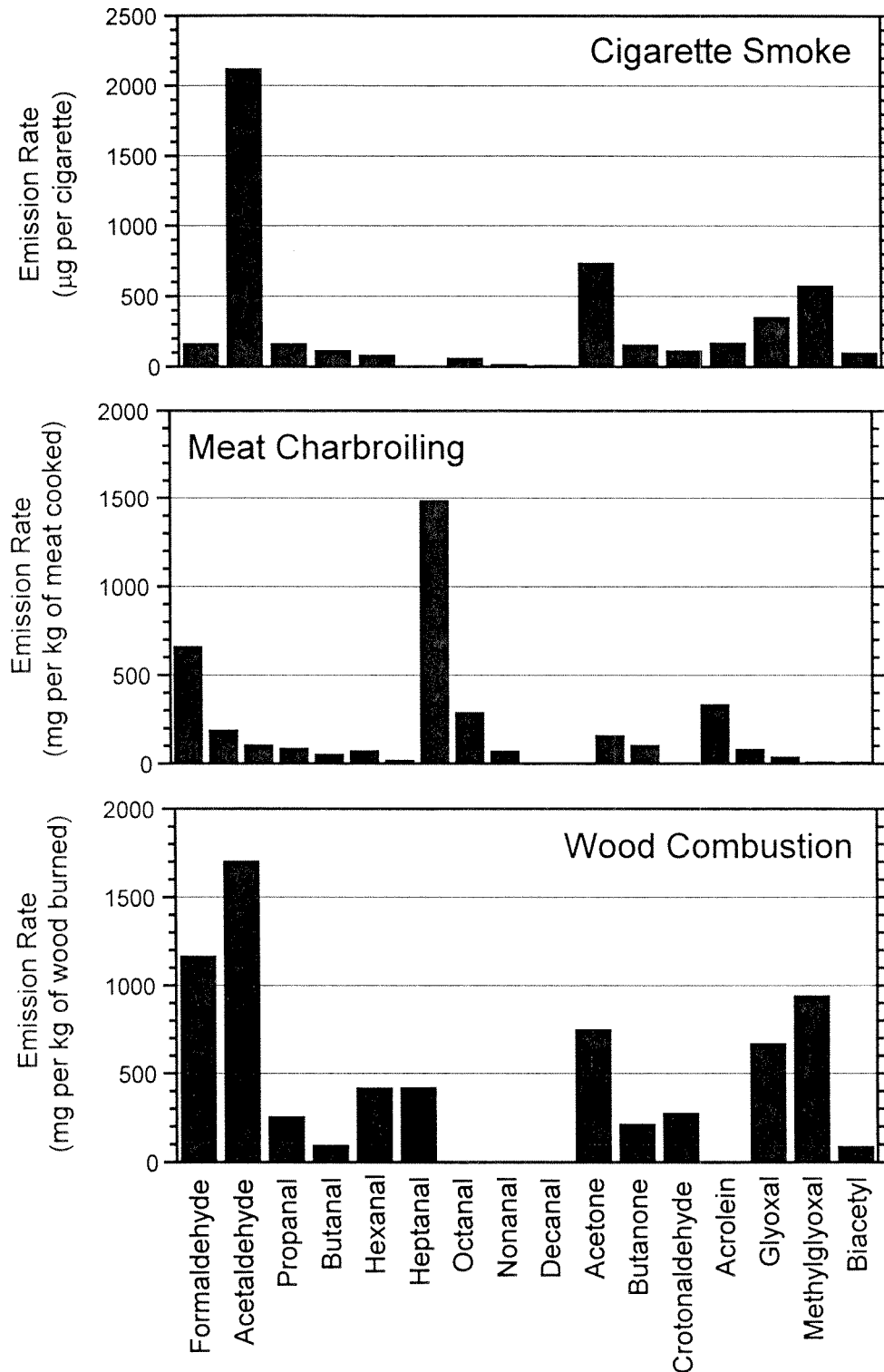


Figure 7.3. Mass emission rates of light gas-phase carbonyls emitted from cigarette smoking, meat charbroiling, and fireplace combustion of wood.

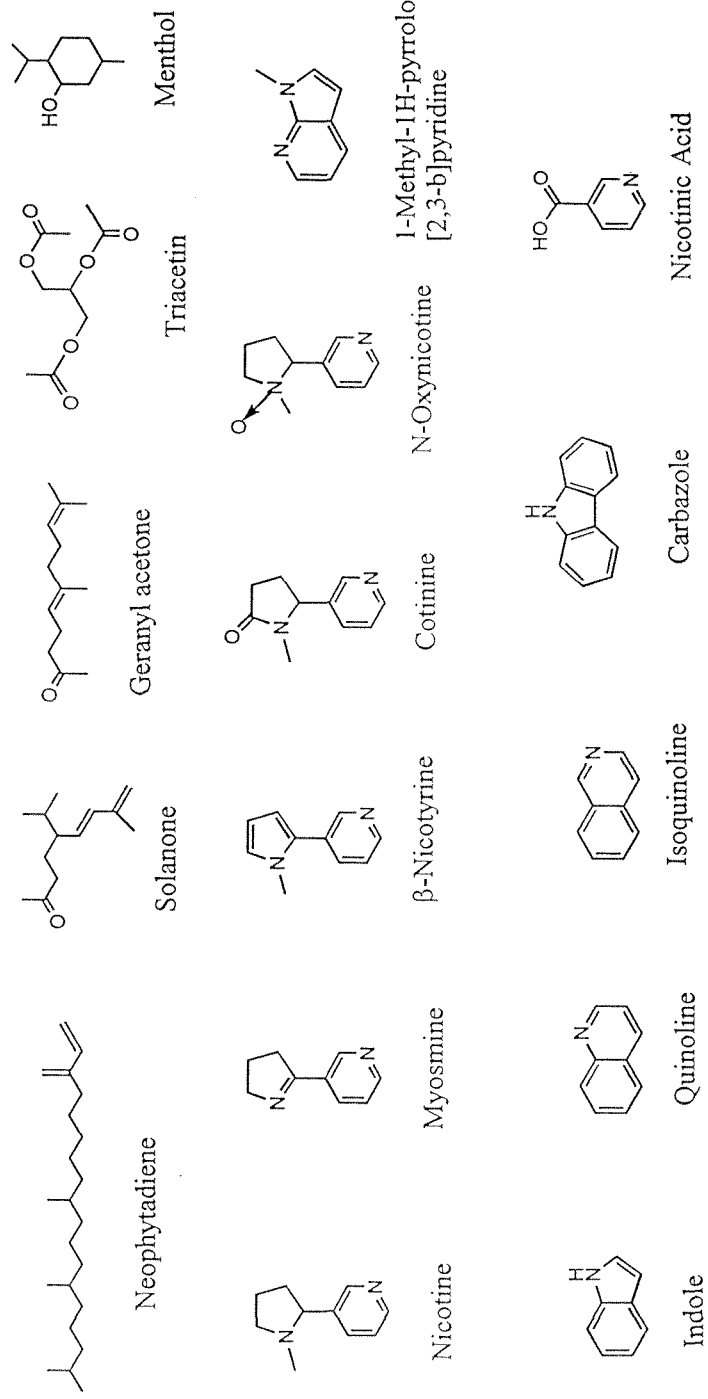


Figure 7.4. Chemical structures of selected semi-volatile organic compounds emitted from cigarette smoke.

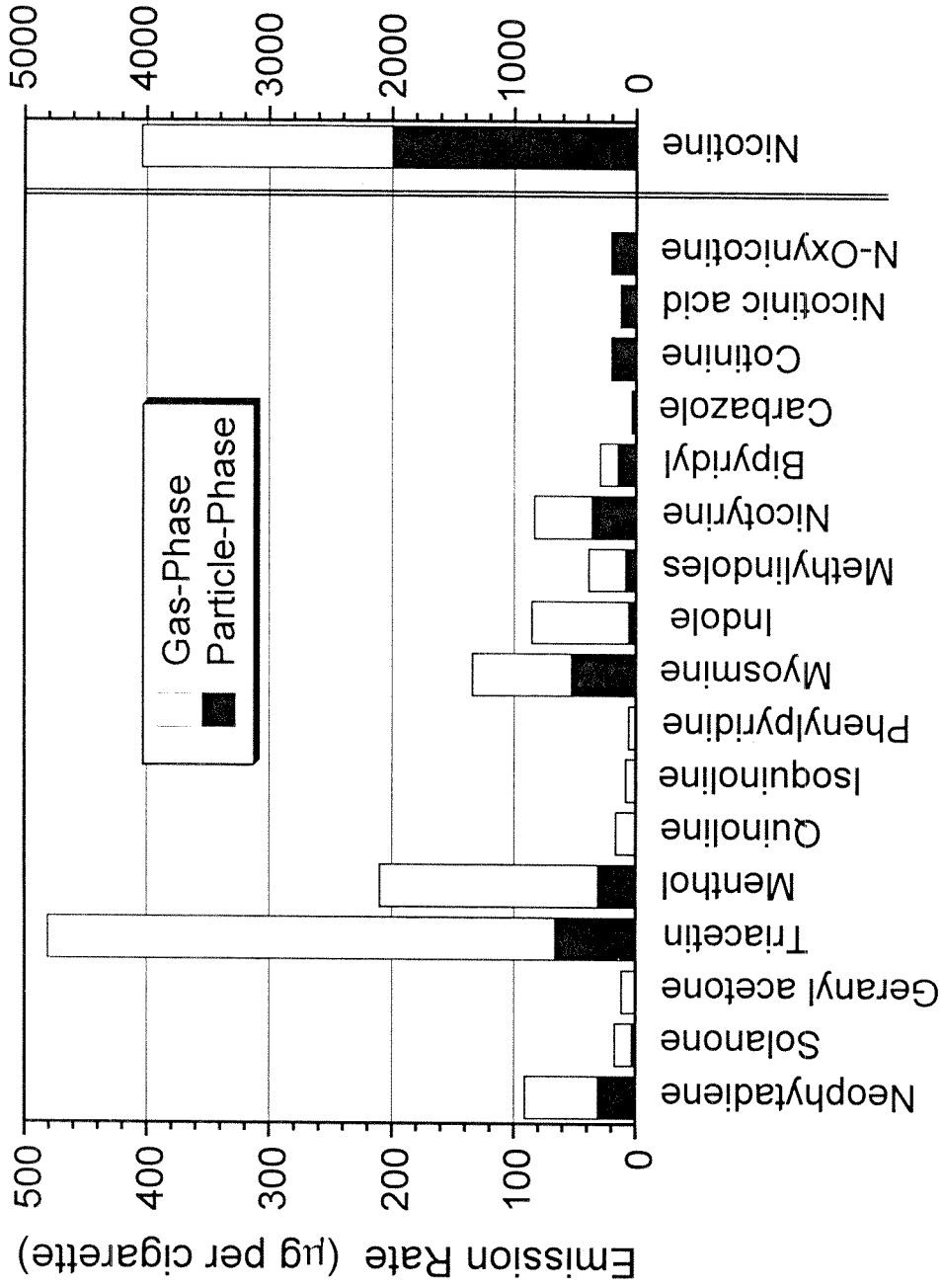


Figure 7.5. Gas and particle phase emission rate of semi-volatile organic compounds emitted from cigarette smoking.



carbonyl groups in these molecules. For this reason, these compounds should not be used routinely as tracers for cigarette smoke unless information is available that shows that these compounds will be adequately conserved in the air parcels of interest.

The remaining compounds shown in Figure 7.5 are organic compounds which contain nitrogen and tend to be characteristic of cigarette smoke. The most volatile of these, quinoline, isoquinoline, and phenylpyridine, are virtually entirely present in the gas-phase, whereas indole and the methyl-substituted indoles are found in noticeable quantities in the particle-phase but are still predominately in the gas phase. Myosmine, nicotyrine, and bipyridyl partition between the gas and particle phases to an extent similar to nicotine, with about half in the gas-phase and half in the particle-phase under the present experimental conditions. Carbazole, cotinine, nicotinic acid and N-oxynicotine are virtually completely in the particle phase and may supplement the use of the iso and anteiso-alkanes as atmospheric tracers for the particulate matter from cigarette smoke.

## 7.4 References

1. Schauer, J. J.; Rogge, W. R.; Hildemann, L. M.; Mazurek, M. A.; Cass, G. R.; Simoneit, B. R. T. *Atmos. Environ.* **1996**, 30, 3837-3855.
2. Leaderer, B. P.; Hammond, S. K. *Environ. Sci. Technol.* **1991**, 25, 770-777.
3. John, W.; Reischl, G. *JAPCA* **1980**, 30, 872-876.
4. Birch, M. E.; Cary, R. A. *Aerosol Sci. Technol.* **1996**, 25, 221-241.
5. Dzubay, T. G. *X-ray Analysis of Environmental Samples* **1977**, Ann Arbor Science, Ann Arbor, MI.
6. Mueller, P. K.; Mendoza, B. V.; Collins, J. C.; Wilgus, E. A. "Application of Ion Chromatography to the Analysis of Anions Extracted from Airborne Particulate Matter," In *Ion Chromatographic Analysis of Environmental Pollutants* **1978**, Sawicki, E.; Mulik, J. D.; Wittgenstein, E. Eds.; Ann Arbor Science, Ann Arbor, MI, pp. 77-86.
7. Solorzano, L. *Limnol. Oceanogr.* **1969**, 14, pp. 799-801.
8. Fraser, M. P.; Cass G. R.; Simoneit B. R. T.; Rasmussen R. A. *Environ. Sci. Technol.* **1997**, 31, 2356-2367.

9. Grosjean, E.; Grosjean, D.; Fraser M. P.; Cass G. R. *Environ. Sci. Technol.* **1996**, 30, 2687-2703.
10. "Environmental tobacco smoke: Measuring exposure and assessing health effects," National Research Council Committee on Passive Smoking, **1986**, National Academy Press, Washington, D. C., pp. 30-31.
11. "Indoor air pollutants," National Research Council Committee on Indoor Pollutants, **1981**, National Academy Press, Washington, D. C., pp.157-158.
12. Barresfors, G.; Petersson, G. *J. Chromat.* **1993**, 643, 71-76.
13. Lofroth, G.; Stensman, C.; Brandhorstsatzkorn, M. *Mutation Research* **1991**, 21-28.
14. *Merck index: an encyclopedia of chemicals, drugs, and biologicals*, 12<sup>th</sup> edition, Susan Budavari editor, **1996**, Merck, Whitehouse Station, N. J.

## Chapter 8

# Organic Compounds from Industrial Spray Painting Operations

## 8.1 Introduction

Volatile organic compounds emitted from surface coating operations can be studied to determine their effect on urban air pollutant concentrations through the use of receptor-based air quality models that use organic compounds as tracers (1-4). Typically the source emissions profiles that describe the organic chemical composition of paint product vapors in these studies are based on the stated composition of the original product as reflected, for example, in the Material Safety Data Sheets (MSDS) that accompany the paint.

Certain aspects of the emissions from actual paint application simply cannot be reproduced from the manufacturer's ingredient list alone. In particular, selective segregation of some paint ingredients into the finished painted object, accompanied by removal of other ingredients by the emissions control system used on paint spray booths, argues that the direct measurement of the emissions from paint spray operations would be desirable. Further, when reported paint composition data are compared against atmospheric organic compound data often the only comparisons that can be made across both data

sets are for the lowest molecular weight components of the paint vapors. Use of only the lowest molecular weight volatile organic compounds to trace the presence of the effluent from painting operations encounters difficulties because many of the most easily measured and most volatile components of paint mixtures are organic chemicals that are emitted from a wide variety of sources. Meanwhile, many of the more unusual compounds found in some paints (e.g., glycol-type compounds) are semi-volatile organics that are both difficult to collect and to analyze chemically in the atmospheric samples against which source samples must be compared. Data are needed on those unusual compounds found in paint formulations which are relatively easily assayed in an atmospheric sample. Finally, bulk analysis of the raw paint materials does not allow for measurements of the distribution of the emissions from paint spray coating operations between the gas and particle phases. For these reasons, the current study has been undertaken to directly measure the gas and particle phase emissions from paint spray coating operations using air pollutant sampling techniques that can be readily applied to characterize both air pollution source emissions and ambient atmospheric pollutant concentrations.

## 8.2 Experimental Methods

### 8.2.1 Source Sampling

Gas-phase and particle-phase emissions from paint spray coating operations were sampled at the outlet of the exhaust vent of a licensed paint spray booth located in the Los Angeles area. Sampling took place downstream of the particle filters in the paint booth exhaust system, which was operated at an air flowrate of 180,000 lpm. Solvent vapors and paint particle overspray from the spraying operation that exited the booth's emissions control system were accompanied by ambient air which was pulled into the paint booth by the ventilation system exhaust fan. Since the ambient air used for dilution contained atmospheric pollutants, the air entering the paint booth was sampled by the same sampling techniques as used for the exhaust emissions during these source tests. Emission rates were determined after background subtraction of the pollutant concentrations entering the paint booth.

Samples were withdrawn isokinetically from the outlet of the exhaust system into AIHL-design cyclone separators (5) that removed particles with aerodynamic diameters greater than 1.8  $\mu\text{m}$ . Gases and particles with diameters less than 1.8  $\mu\text{m}$  passed through the cyclones and were sampled by a series of sampling trains operated in parallel. Semi-volatile and fine particle-phase

organic compounds were collected continuously downstream of these cyclone separators by the denuder/filter/PUF sampling train and a filter/PUF sampling train. Details of both sampling configurations are discussed in Chapter 2. One denuder based sampling train and one filter/PUF sampling train were operated during the paint spray booth source tests.

A third cyclone-based sampling train also was used to measure the emissions of fine particulate matter, carbonyls, organic acids, and low molecular weight gas-phase hydrocarbons. This sampling train is also discussed in Chapter 2.

The dilution air sampling units were located at the inlet of the paint booth ventilation system. Pollutant concentrations in the inlet air were measured using one cyclone/filter/PUF sampling unit and one cyclone/filter pack/SUMA canister/carbonyls sampling unit, as was used for measuring the paint booth exhaust emissions. As shown in Chapter 2, the total mass collected by the cyclone/denuder/filter/PUF sampling train and by the cyclone/filter/PUF sampling train show excellent agreement, such that minimal problems arise when air pollutant concentrations in the dilution air obtained by the filter/PUF sampling train are subtracted from the source samples collected with the denuder/filter/PUF sampling train.

### **8.2.2 Source Testing Procedure**

The oil-based paint used in the present study was an oil-based primer (Z-Prime, Zehrunge Corp., Portland, OR). The primer was cut with lacquer thinner (3:1 primer: lacquer thinner) and was sprayed with a high-volume low-pressure air gun which was operated at a paint gun cup pressure of 7 psig. A total of 1.9 liters of cut primer was sprayed by a professional painter over a period of 40 minutes. Sample collection commenced 1 minute prior to the start of spray painting and ended 1 minute after painting was finished.

Suprema Latex low gloss enamel (Dunn-Edwards Corp., Los Angeles, CA) was used as the water-based paint in the present study. The water-based paint was cut with water (3:2 paint: water) and was sprayed with the same air gun as used for the oil-based paint. Over a period of 40 minutes 2.4 liters of cut paint was sprayed. The same sampling protocol was used for both source tests.

### **8.2.3 Organic Chemical Analysis**

The analytical procedures used in the present study for the identification and quantification of semi-volatile and particle-phase organic compounds in air pollutant source emissions are the same as was used for the other source tests described in Chapters 2 through 7. Details are provided in Chapter 2.



Filter, PUF, and denuder field blanks were analyzed with each set of source samples. The field blanks were prepared, stored and handled by exactly the same procedures as used for the source samples.

Hundreds of authentic standards have been prepared for the positive identification and quantification of the organic compounds found in the current source test program. When quantitative standards could not be obtained for a given compound or compound class, significant effort was made to obtain a non-quantitative secondary standard that could be used for unique identification of the organic compounds. An example of such a secondary standard is the use of the small amounts of 2,2,4-trimethyl-1,3-pentanediol diisobutyrate present in the Texanol standard as a secondary standard. Quantification of compounds identified using secondary standards has been estimated from the response factors for compounds having similar retention times and chemical structures.

Total non-methane organic gases (NMOG, EPA method TO12) and individual organic vapor-phase hydrocarbons ranging from  $C_1$  to  $C_{10}$  were analyzed from the SUMA canisters by gas chromatography/flame ionization detection (GC/FID) (see Chapter 2). Carbonyls collected by the  $C_{18}$  impregnated cartridges were analyzed by liquid chromatography/UV detection (see Chapter 2).

## 8.3 Results

### 8.3.1 Fine Particle Emission Rates and Composition

Fine particle emission rates from the oil-based and the water-based spray coating operations were  $104 \pm 40$  and  $74.8 \pm 29.0$  mg per liter of cut-paint sprayed, respectively. Clearly, the fine particle mass emissions from these operations were reduced significantly by the filtration system present in the paint booth exhaust system. Due to the fact that the exhaust filters were located at the inlet to the exhaust system, samples of the unfiltered emissions could not be obtained from the exhaust duct. The elemental composition of the fine particle mass collected downstream of the exhaust filters are shown in Table 8.1.

Organic carbon and titanium are the largest contributors to the fine particle emissions from the water-based paint spraying operations. Assuming that the titanium is in the form of titanium dioxide and that the ratio of fine particle organic compound mass to organic carbon is 1.4, then the emissions of titanium dioxide plus particulate organic compound mass is not significantly different from the gravimetrically measured fine particle mass emission rate, indicating that indeed these species account for the entirety of the emissions from the water-based paint spraying test. The ratio of fine particulate organic compound mass to fine particle titanium dioxide is 2.4 in the water-based paint fine particle emissions.

Table 8.1. Average Fine Particle Emission Rate and Fine Particle Chemical Composition from Architectural Spray Coating Operations (Values shown in boldface are greater than zero by at least two standard errors).

	Oil Based Paint	Water Based Paint
Fine Particle Emissions Rate (AVG $\pm$ STD)	<b>104 <math>\pm</math> 40 mg per liter sprayed</b>	<b>74.8 <math>\pm</math> 29.0 mg per liter sprayed</b>
Elemental and Organic Carbon (Wt % of Fine Particle Mass)		
Organic Carbon	<b>22.4 <math>\pm</math> 3.6<sup>a</sup></b>	<b>35.3 <math>\pm</math> 4.2<sup>a</sup></b>
Elemental Carbon	1.0 $\pm$ 2.0	0.4 $\pm$ 2.3
X-ray Fluorescence (Wt % of Fine Particle Mass)		
Aluminum	<b>6.26 <math>\pm</math> 0.88</b>	1.13 $\pm$ 1.84
Silicon	<b>7.57 <math>\pm</math> 0.60</b>	0.05 $\pm$ 0.51
Phosphorus	0.00 $\pm$ 0.71	0.00 $\pm$ 0.72
Sulfur	0.00 $\pm$ 0.31	0.00 $\pm$ 0.35
Chlorine	0.49 $\pm$ 0.29	0.00 $\pm$ 0.79
Potassium	0.59 $\pm$ 0.74	0.00 $\pm$ 0.75
Calcium	<b>6.60 <math>\pm</math> 0.49</b>	0.98 $\pm$ 0.50
Titanium	<b>38.5 <math>\pm</math> 3.5</b>	<b>12.5 <math>\pm</math> 3.9</b>
Vanadium	0.00 $\pm$ 2.60	0.00 $\pm$ 1.59
Chromium	0.00 $\pm$ 0.72	0.00 $\pm$ 0.36
Manganese	0.00 $\pm$ 0.33	0.00 $\pm$ 0.27
Iron	0.00 $\pm$ 0.10	0.10 $\pm$ 0.10
Cobalt	0.00 $\pm$ 0.18	0.02 $\pm$ 0.19
Nickel	0.00 $\pm$ 0.18	0.00 $\pm$ 0.18
Copper	0.00 $\pm$ 0.19	0.00 $\pm$ 0.19
Zinc	0.00 $\pm$ 0.20	0.00 $\pm$ 0.21
Gallium	0.00 $\pm$ 0.27	0.00 $\pm$ 0.31
Arsenic	0.00 $\pm$ 0.32	0.00 $\pm$ 0.35
Selenium	0.00 $\pm$ 0.17	0.00 $\pm$ 0.18
Bromine	0.00 $\pm$ 0.15	0.03 $\pm$ 0.17
Rubidium	0.02 $\pm$ 0.14	0.00 $\pm$ 0.16
Strontium	0.00 $\pm$ 0.16	0.01 $\pm$ 0.18
Yttrium	0.00 $\pm$ 0.20	0.00 $\pm$ 0.22
Zirconium	0.13 $\pm$ 0.24	0.00 $\pm$ 0.26
Molybdenum	0.00 $\pm$ 0.43	0.01 $\pm$ 0.48
Palladium	0.00 $\pm$ 1.17	0.00 $\pm$ 1.26
Silver	0.00 $\pm$ 1.40	0.00 $\pm$ 1.51
Cadmium	0.14 $\pm$ 1.50	0.00 $\pm$ 1.54
Indium	0.00 $\pm$ 1.71	0.00 $\pm$ 1.88
Tin	0.00 $\pm$ 2.14	0.00 $\pm$ 2.34
Antimony	0.00 $\pm$ 2.53	1.42 $\pm$ 2.85
Barium	0.00 $\pm$ 9.30	3.78 $\pm$ 10.3
Lanthanum	2.23 $\pm$ 12.3	3.41 $\pm$ 13.8
Mercury	0.00 $\pm$ 0.38	0.00 $\pm$ 0.42
Lead	0.00 $\pm$ 0.47	0.09 $\pm$ 0.53

Notes: (a) measured on undenuded filter

Fine particle emissions from oil-based spray coating operations also are influenced largely by organic carbon and titanium which comprise 22.4% and 38.5% of the fine particle mass emissions, respectively. If the titanium once again is expressed as titanium dioxide and fine particulate organic carbon emissions are converted to an estimate of organic compound mass by multiplying by a factor of 1.4, then the ratio of organic compound mass to titanium dioxide mass is 0.5 for the fine particles emitted from spray coating with oil-based paint, much lower than in the fine particle emissions from the water-based paint spraying operations. In addition to organic compounds and titanium dioxide, the fine particle mass emitted from the oil-based paint spraying contains about 6 to 8 percent each of aluminum, silicon, and calcium.

The concentrations of water-soluble sulfate ion, ammonium ion, chloride ion, nitrate ion, and sodium ion in the exhaust emissions from the paint spray booth were not significantly different from the concentrations of these species in the dilution air input to the paint spray booth, such that the emissions of these species from the spray coating operations are lower than can be detected in this study.

### **8.3.2 Mass Balance on Organic Compound Emissions**

Figure 8.1 shows a mass balance on the organic compounds measured during the spray coating source tests in the current study. It should be noted

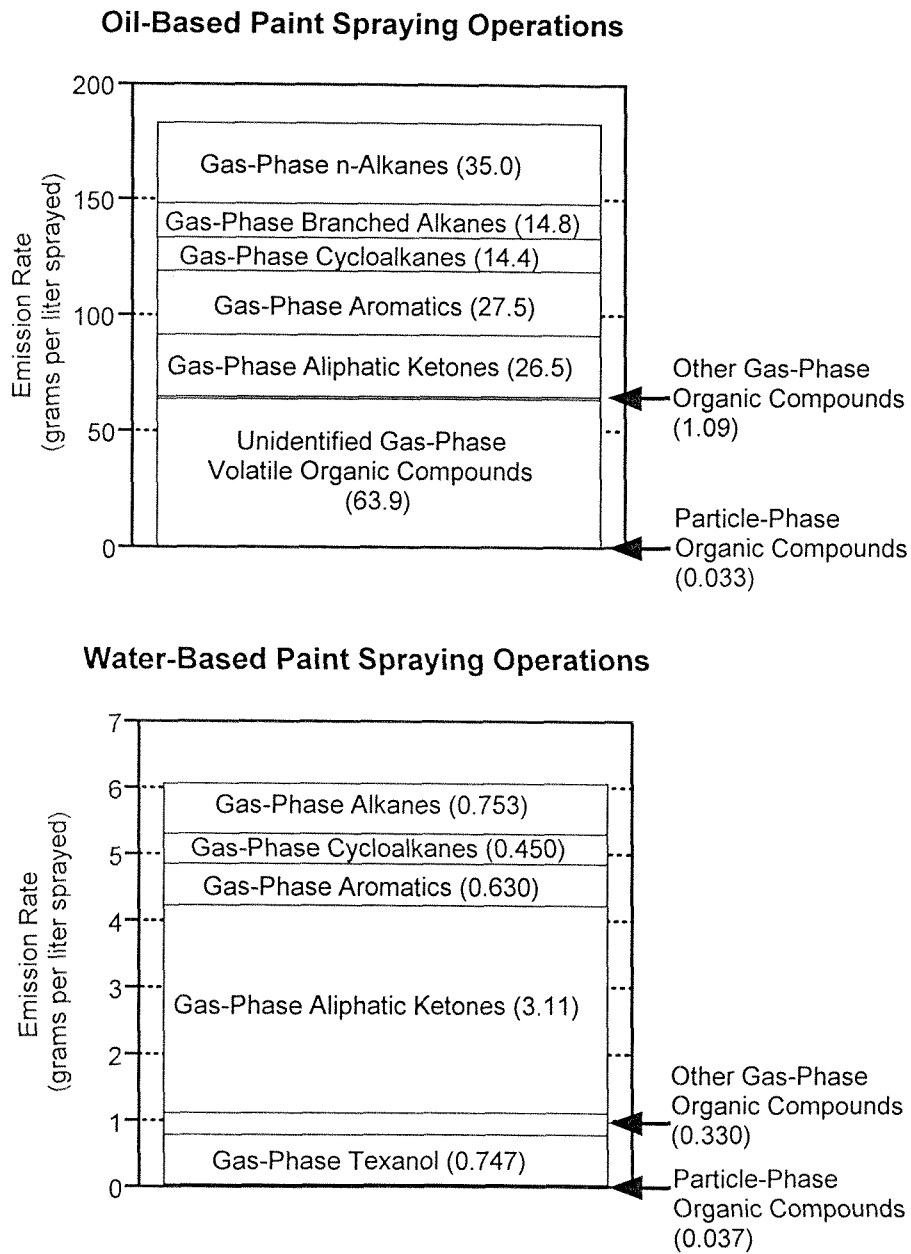


Figure 8.1. Mass balance on the non-methane organic compounds measured in the emissions from oil-based paint spray coating and water-based paint spray coating operations conducted in an industrial-scale paint spray booth.

that some highly polar volatile organic compounds such as ethylene glycol are not detected by the non-methane organic gas analysis (TNMOG, EPA Method TO-12) and therefore do not appear in the emissions from this study. Although the TO-12 method does not respond to formaldehyde and has only a reduced response for other carbonyls, the carbonyls can be properly accounted for since these compounds are measured by the DNPH-impregnated cartridges. While the absence of data on compounds like ethylene glycol appears to present a problem, it is important to note that the analytical methods used here are exactly the same as the methods commonly used to monitor ambient air quality, so these species are consistently absent from the ambient data sets as well. In the case of particle-phase carbon, the thermal evolution technique used here responds to all carbonaceous material and thus the entire mass emissions rate of fine particulate organic carbon is measured.

As seen in Figure 8.1, gas-phase emissions dominate the organic compounds released from both types of spray coating operations. The total organic compound emissions from the oil-based paint spraying source test amount to 183 grams per liter of solvent-cut paint sprayed, while particulate carbon emissions account for only 0.033 grams per liter of solvent-cut paint sprayed. Gas-phase emissions show significant contributions from n-alkanes, branched alkanes, cycloalkanes, aromatics, and ketones. The gas-phase organic compound emissions from the water-based paint spraying operations

are significantly lower at 6.0 grams per liter of water-cut paint sprayed. These gas-phase emissions are about half from aliphatic ketones, accompanied by smaller but significant contributions from alkanes, cycloalkanes, aromatics, and Texanol. Particle phase organic carbon emissions from the water-based paint spraying operations are similar to the oil-based paint spraying at 0.037 grams of fine particulate matter per liter of water-cut paint sprayed.

### **8.3.3 Emission Rates of Individual Organic Compounds**

The organic compounds quantified in the emissions from the spray coating operations studied here are listed in Table 8.2. The major components of the emissions for both water-based and solvent-based spray coating operations are shown in Figure 8.2. Emissions from the water-based spray coating operation are dominated by acetone, butanone, and Texanol. Acetone and butanone are both emitted at rates of approximately 1400 mg per liter of solvent-cut paint sprayed and Texanol is emitted at 763 mg per liter sprayed. The emissions of acetone and butanone from spray coating with the oil-based primer (11400 and 15100 mg per liter sprayed, respectively) are approximately ten times the emissions from water-based paint spraying (1410 and 1510 mg per liter sprayed, respectively). However, Texanol emissions are about ten times less from the oil-based paint spraying than from the water-based paint spraying. The oil-based paint spraying also results in significant emissions of C<sub>7</sub> through C<sub>10</sub> n-alkanes, branched alkanes, aromatics and methylcyclohexane. Much of

Table 8.2. Organic Compounds Present in the Emissions from an Industrial-Scale Paint Spray Coating Booth.

Compound	Oil Based Paint (mg per liter of solvent cut paint sprayed)		Water Based Paint (mg per liter of solvent cut paint sprayed)		Notes
	Gas Phase	Particle Phase	Gas Phase	Particle Phase	
n-Alkanes					
Propane	10				a, c
n-Butane	110		10		a, c
n-Pentane	10				a, c
n-Hexane	10				a, c
n-Heptane	6480		200		a, c
n-Octane	12000		20		a, c
n-Nonane	4660		20		a, c
n-Decane	9980		40		a, c
n-Undecane	1460		60		a, d
n-Dodecane	200		30		a, d
n-Tridecane	3		2		b, d
n-Tetradecane	1				a, d
Branched alkanes					
i-Butane	10				a, c
i-Pentane	10		10		a, c
2,4-Dimethylpentane	10				a, c
2-Methylhexane	460		40		a, c
2,3-Dimethylpentane	190		20		a, c
3-Methylhexane	1010		70		a, c
2,2,4-Trimethylpentane	1080		40		a, c
2,5-Dimethylhexane	1120		30		a, c
2,4-Dimethylhexane	840		30		a, c
2,3,4-Trimethylpentane	160				a, c
2,3-Dimethylhexane	590		10		a, c
2-Methylheptane	5440		40		a, c
3-Ethylhexane	3830		30		a, c
Saturated cycloalkanes					
Cyclohexane	30				a, c
Methylcyclohexane	14400		450		a, c
Aromatic hydrocarbons					
Toluene	9620		260		a, c
Ethylbenzene	2860		50		a, c
m & p-Xylene	8830		210		a, c
o-Xylene	4630		80		a, c
1,2,4-Trimethylbenzene	1590		30		a, c
Aliphatic aldehydes					
Formaldehyde	120		30		a, e
Acetaldehyde	200		210		a, e

Identification notes: (a) authentic quantitative standard. (b) authentic quantitative standard for similar compound in series.

Sample collection notes: (c) collected in SUMA canister. (d) collected on denuder/filter/PUF sampling train. (e) collected on DNPH impregnated C<sub>18</sub> cartridges. See text for details.

Additional Notes: † Compound is too volatile for complete collection by denuder at sampling conditions; mass of this compound reported in the gas-phase includes mass collected on PUF cartridge.



Table 8.2. (continued - page 2)

Compound	Oil Based Paint (mg per liter of solvent cut paint sprayed)		Water Based Paint (mg per liter of solvent cut paint sprayed)		Notes
	Gas Phase	Particle Phase	Gas Phase	Particle Phase	
Aliphatic aldehydes					
Propanal	70		30		a, e
Hexanal	30		20		a, e
Aliphatic ketones					
Acetone	11400		1510		a, e
Butanone	15100		1410		a, e
4-Methyl-2-pentanone	420		190		a, e
Dicarbonyls					
Glyoxal	40		40		a, e
Methylglyoxal	10				a, e
Other compounds					
2,2,4-Trimethyl-1,3-pentanediol monoisobutyrate (Texanol)	76.6	4.6	747	18.1	a, d
2,2,4-Trimethyl-1,3-pentanediol diisobutyrate	5.8	0.5	5.6		b, d
2-Butoxyethanol <sup>†</sup>	530		102		b, d
2-(2-Butoxyethoxy)ethanol	40.5		12.7		b, d

Identification notes: (a) authentic quantitative standard. (b) authentic quantitative standard for similar compound in series.

Sample collection notes: (c) collected in SUMA canister. (d) collected on denuder/filter/PUF sampling train. (e) collected on DNPH impregnated C<sub>18</sub> cartridges. See text for details.

Additional Notes: <sup>†</sup> Compound is too volatile for complete collection by denuder at sampling conditions; mass of this compound reported in the gas-phase includes mass collected on PUF cartridge.

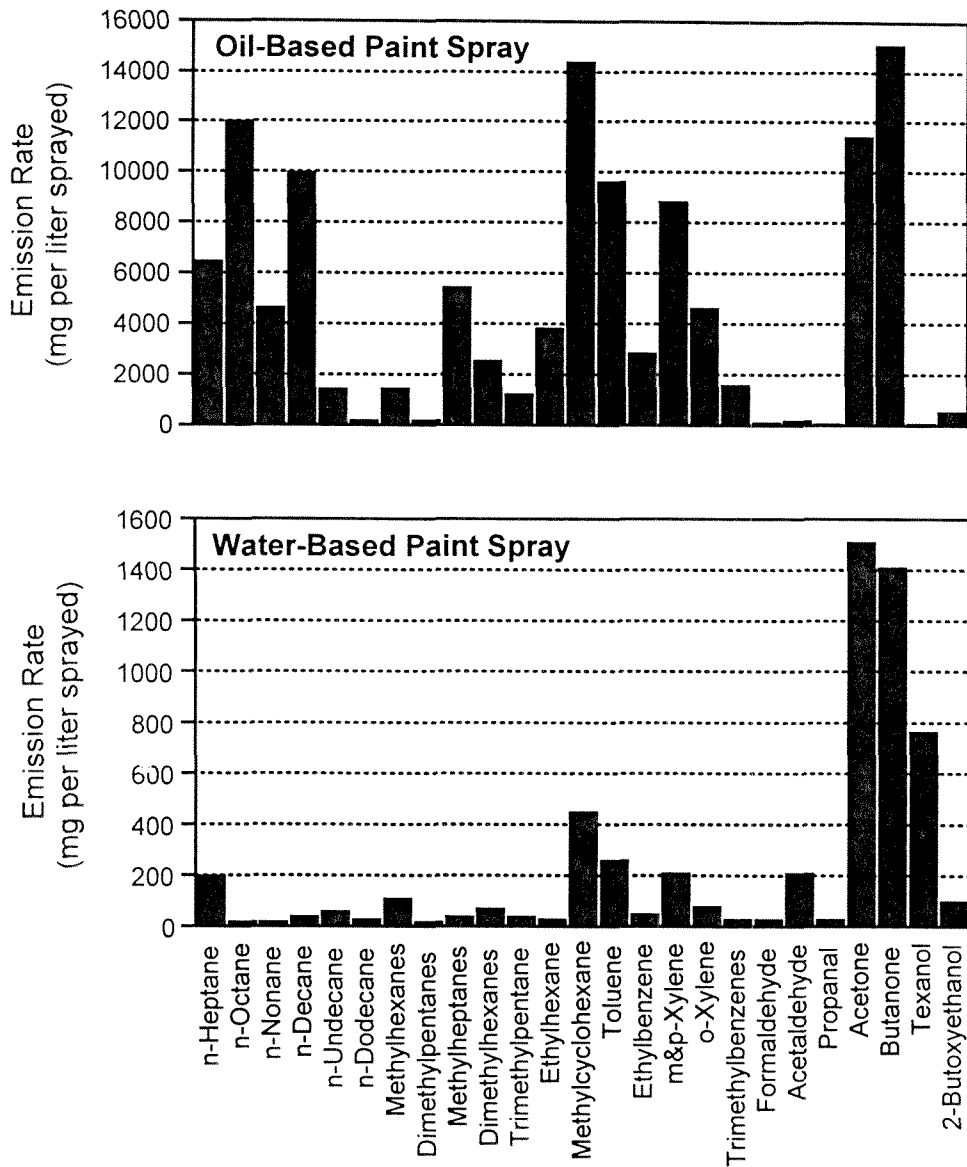


Figure 8.2. Mass emission rates for selected individual organic compounds emitted from oil-based paint spray coating and water-based paint spray coating operations.

these emissions are due to the cutting solvent needed to properly spray the paint with a spray gun.

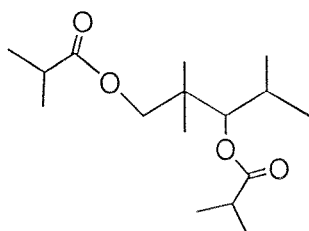
The only organic compounds identified in the particle phase were Texanol and the diisobutyrate analog of Texanol, 2,2,4-trimethyl-1,3-pentanediol diisobutyrate. The remainder of the organic mass in the particle-phase is unextractable and non-elutable under the conditions of this experiment.

#### **8.3.4 Texanol as a Tracer for Water-Based Spray Coating Operations**

Texanol is produced by Eastman Kodak and is added to water-based paint to enhance the coating properties of the paint (6). Texanol has two isomers both of which are found in technical grade Texanol. The chemical structures of these two isomers are shown in Figure 8.3. In addition, the diisobutyrate analog of Texanol was found in smaller but noticeable quantities in a sample of technical grade Texanol purchased from ChemService Inc. (West Chester, PA). The structure of the diisobutyrate form also is shown in Figure 8.3. Analysis of the water-based paint used in this study showed that the relative concentration of the two monoisobutyrate and the diisobutyrate species in the paint was similar to the relative abundance of these compounds found in the technical grade Texanol sample that was analyzed. It is therefore expected that all three forms will be present in the urban atmosphere. As previously noted, Texanol has not been reported in the ambient atmosphere, largely due to



2,2,4-Trimethyl-1,3-pentanediol monoisobutyrate



2,2,4-Trimethyl-1,3-pentanediol diisobutyrate

Figure 8.3. Chemical structures of the organic compounds present in technical grade Texanol.

the fact that sampling techniques for semi-volatile organic compounds must be employed to properly collect this semi-volatile species. Smaller concentrations of Texanol were measured in the solvent-cut paint used for the oil-based spray painting source tests and in the emissions from this test. It is unclear if Texanol was used as an ingredient in the primer manufacturing process or if contamination of the primer occurred in the paint shop.

## 8.4 References

1. Harley, R. A.; Hanningan, M. P.; Cass, G. R. *Environ. Sci. Technol.* **1992**, 26, 2395-2408.
2. Sweet, C. W.; Vermette, S. J. *Environ. Sci. Technol.* **1992**, 26, 165-173.
3. Scheff, P. A.; Wadden, R. A. *Environ. Sci. Technol.* **1993**, 27, 617-625.
4. Fujita, E. M.; Watson, J. G.; Chow, J. C.; Lu. *Environ. Sci. Technol.* **1994**, 28, 1633-1649.
5. John, W.; Reischl, G. *JAPCA* **1980**, 30, 872-876.
6. Eastman Chemical Company Web Site  
(<http://www.eastman.com/cirbo/estalc.shtml>), 1997.

## Chapter 9

# Source Apportionment of Airborne Particulate Matter Using Organic Compounds as Tracers

### 9.1 Introduction

Suspected adverse health effects of even low levels of airborne particulate matter have led to increased concern over how fine particulate concentrations might best be controlled (Dockery et al., 1993). The development of effective control strategies for fine particulate air pollution abatement in turn requires a knowledge of the relative importance of the various sources that contribute to the particulate matter concentrations at ambient air monitoring sites (Atkinson and Lewis, 1974; Harley et al., 1989).

Two approaches can be employed to evaluate source contributions from source emissions data and ambient monitoring data: source-oriented models and receptor-oriented models. Source-oriented models use emissions data and fluid mechanically explicit transport calculations to predict pollutant concentrations at specific receptor air monitoring locations. This type of model is validated by comparison of the predicted spatial and temporal distribution of pollutant concentrations against measured concentrations (Bencala and

Seinfeld, 1979; Liu and Seinfeld, 1975). Receptor-oriented models infer source contributions by determining the best-fit linear combination of emission source chemical composition profiles needed to reconstruct the measured chemical composition of ambient samples (Watson, 1984).

Determination of source contributions from ambient monitoring data by receptor modeling techniques relies on the ability to characterize and distinguish differences in the chemical composition of different source types. The elemental composition of source emissions has been used on many occasions to separately identify different sources of airborne particles (Miller et al., 1972; Hopke et al., 1976; Gordon, 1980; Cooper and Watson, 1980; Cass and McRae, 1983). Unfortunately, a large number of sources that emit fine particulate matter do not produce emissions that have unique elemental compositions; instead many sources emit principally organic compounds and elemental carbon. Examples of such sources include diesel engine exhaust, combustion of unleaded gasoline, the effluent from meat cooking operations, and cigarette smoke (Hildemann et al., 1991). When such important sources of primary particle emissions cannot be identified in ambient samples, then much of the true nature of a particulate air pollution problem remains obscured.

Recent advances in source testing techniques make it possible to measure the concentrations of hundreds of specific organic compounds in the fine aerosol emitted from air pollution sources (Rogge et al., 1991, 1993b,



1993c, 1993d, 1993e, 1994; Rogge, 1993). By analogous methods, the organic compounds present in the fine aerosol collected at ambient sampling sites also can be determined (Rogge et al., 1993a; Rogge, 1993). The relative distribution of single organic compounds in source emissions provides a means to fingerprint sources that cannot be uniquely identified by elemental composition alone. These advances in measurement methods therefore create the practical possibility of devising receptor models for aerosol source apportionment that rely on organic compound concentration data and that potentially can identify separately the contributions of many more source types than has been possible based on elemental data alone.

In the present paper, receptor modeling methods will be developed that use organic compound distributions in both source samples and in ambient samples to determine source contributions to airborne particulate matter samples. Two critical aspects of this work are (1) selection of the sources to be included in such a model and (2) identification of the organic compounds for which material balances can be written. Methods developed will be tested by application to data taken in Southern California.

## 9.2 Experimental Section

### 9.2.1 Ambient Samples

Throughout 1982, airborne fine particulate matter ( $d_p < 2 \mu\text{m}$ ) samples were collected for 24 hours every sixth day at ten Los Angeles-area air quality monitoring sites and one upwind remote off-shore island (Gray et al., 1986). The present study uses samples from four of these sampling sites: West Los Angeles, Downtown Los Angeles, Pasadena, and Rubidoux (see Figure 9.1).

The ambient aerosol samples used in this study were collected downstream of an AIHL cyclone separator operated at 25.9 lpm that removed particles with aerodynamic diameters larger than  $2 \mu\text{m}$  (John and Reischl, 1980). Air leaving the cyclone was divided between four parallel 47 mm diameter filter assemblies: two containing quartz fiber filters (Pallflex Tissuequartz 2500 QAO), one containing a Teflon membrane filter (Membrana  $0.5 \mu\text{m}$  pore size), and one containing a Nuclepore filter ( $0.4 \mu\text{m}$  pore size). Each of the quartz fiber filters was operated at an air flowrate of 10 lpm, while the Teflon filters and the Nuclepore filters were operated at 4.9 lpm and 1.0 lpm, respectively. The quartz fiber filters were baked at  $600 \text{ }^\circ\text{C}$  for a minimum of two hours prior to sample collection to lower residual carbon levels associated with untreated filters.

One quartz fiber filter from each day at each sampling site was analyzed for elemental carbon (EC) and organic carbon (OC) by the method of Huntzicker

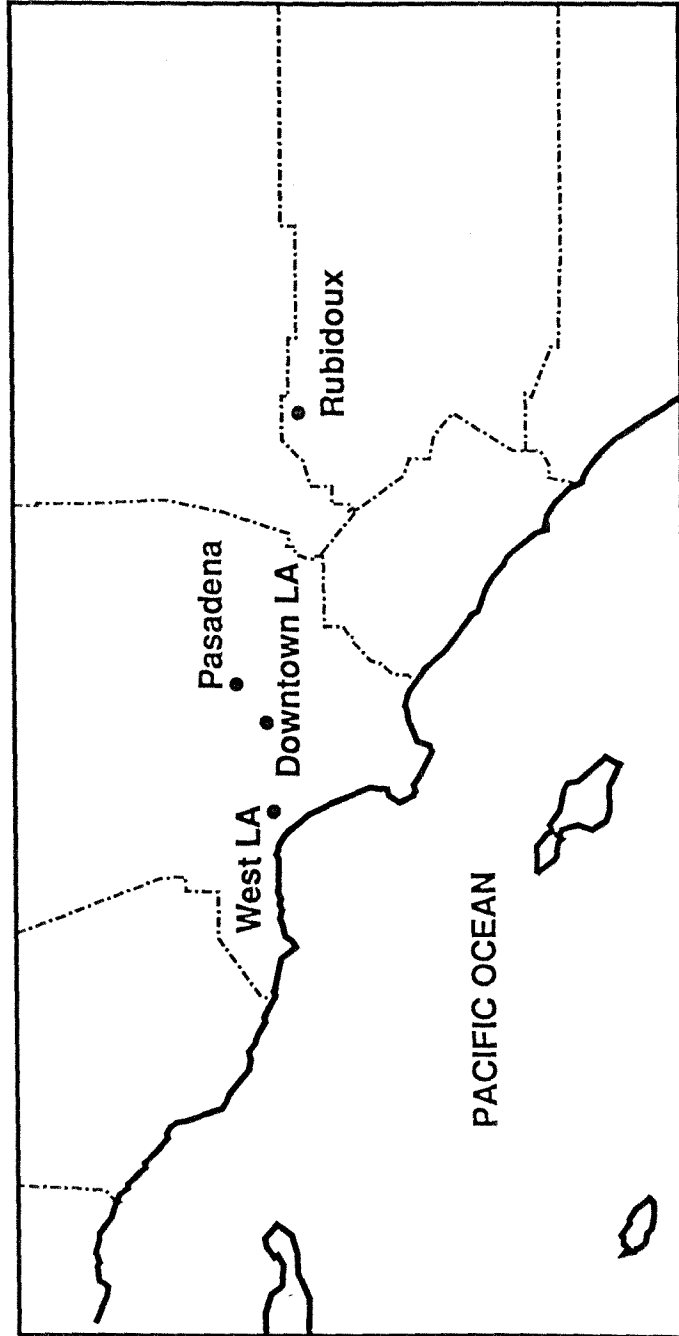


Figure 9.1. Air quality monitoring sites in Southern California used in the present study.

et al. (1982) and Johnson et al. (1981). Monthly composites formed by utilizing the second quartz fiber filter from each site on each day were reserved for the identification and quantification of the individual organic compounds present by high resolution gas chromatography (HRGC) and gas chromatography/mass spectrometry (GC/MS) (Rogge et al., 1993a; Rogge, 1993).

The particulate matter collected on the Teflon filters was used to determine total fine particulate mass concentrations by gravimetric analysis. The Teflon filters were also analyzed by X-ray fluorescence to quantify the concentrations of 34 trace elements including aluminum and silicon, which will be used in the present study. Samples collected on the Nuclepore filters were analyzed for sulfate and nitrate by ion chromatography (Mueller et al., 1978), and for ammonium ion by the phenol-hypochlorite method (Solorzano, 1967).

### **9.2.2 Source Samples**

A source sampling program was undertaken in order to determine the mass emission rate and chemical composition of the fine particulate matter released from the most prominent sources of carbonaceous aerosol emissions in Southern California. As shown in Table 9.1, 15 source types were tested that accounted for approximately 80% of the fine carbonaceous aerosol emissions in the Los Angeles basin during the 1982 period for which ambient samples are available (Gray, 1986; Hildemann et al., 1991). Detailed descriptions of

**Table 9.1. Estimate of Fine Aerosol Organic Carbon (OC) Emissions within an 80 x 80 km square Study Area Centered Over Los Angeles for 1982 (Gray, 1986; Hildemann et al., 1991).**

Source Type	OC emitted kg/day	Profile no. of source tested in this study	Source profile used to represent source for inventory purposes <sup>a</sup>
(1) Meat-cooking operations			
Charbroiling	4938	1 <sup>b</sup>	1
Frying	1393	2	2
(2) Paved road dust	4728	3	3
(3) Fireplaces			
Pine wood	3332	4	4
Oak wood	840	5	5
Synthetic logs	n.k.		
(4) Noncatalyst gasoline vehicles			
Automobiles	2088	6	6
Other vehicles <sup>c</sup>	1372		6
(5) Diesel vehicles			
Heavy-duty trucks	1242	7	7
Other vehicles <sup>d</sup>	617		7
(6) Surface coating	1433		
(7) Forest fires	877		
(8) Cigarettes	802	8	8
(9) Catalyst-equipped gasoline vehicles			
Automobiles	780	10	9
Other vehicles <sup>c</sup>	79		9
(10) Organic chemical processes	692		
(11) Brake lining wear debris	690	10	10
(12) Roofing tar pots	556	11	11
(13) Tire wear debris	414	12	12
(14) Misc industrial point sources	393		
(15) Natural gas combustion			
Residential/commercial	30	13	13
Other sources <sup>f</sup>	262		13
(16) Misc petroleum industry processes	278		
(17) Primary metallurgical processes	228		
(18) Railroad (diesel oil)	211		7
(19) Residual oil stationary sources <sup>g</sup>	206		14
(20) Refinery gas combustion	195		13
(21) Secondary metallurgical processes	167		
(22) Mineral industrial processes	158		
(23) Other organic solvent use	106		
(24) Jet aircraft	92		
(25) Asphalt roofing manufacturing	81		11
(26) Coal burning	76		
(27) Wood processing	74		

Table 9.1. (Continued - page 2)

Source Type	OC emitted kg/day	Profile no. of source tested in this study	Source profile used to represent source for inventory purposes <sup>a</sup>
(28) Residual oil-fired ships	66		
(29) Structural fires <sup>b</sup>	63		4
(30) Distillate oil stationary sources			
Industrial <sup>i</sup>	13	14	14
Other <sup>j</sup>	23		14
(31) Vegetative detritus			
Green leaf abrasion products <sup>k</sup>	1000	15	15
Dead leaf abrasion products	n.k.		
(32) Other sources <sup>l</sup>	226		6,7
Total	30822		

n.k. = not known

<sup>a</sup> source profiles of sources tested also are used to characterize emissions from similar source types.

<sup>b</sup> charbroiling regular hamburger meat with a fat content of 21%.

<sup>c</sup> noncatalyst light trucks, medium trucks, heavy-duty trucks, off-road gasoline vehicles, and motorcycles (for more details see Gray, 1986).

<sup>d</sup> diesel autos, diesel light trucks, and off-road diesel vehicles (for more details see Gray, 1986).

<sup>e</sup> catalyst-equipped light and medium trucks (for more details see Gray, 1986).

<sup>f</sup> electric utility boilers NG, electric utility turbines NG, refineries NG, industrial boilers NG; NG = natural gas used (for more details see Gray, 1986).

<sup>g</sup> electric utility boilers burning residual oil, refineries burning residual oil, industrial boilers burning residual oil, residential/commercial combustion of residual oil (for more details see Gray, 1986).

<sup>h</sup> structural fires are assumed to show a similar organic compound profile as found for pine wood combustion in residential fireplaces.

<sup>i</sup> test no. 2 is used (see Rogge, 1993).

<sup>j</sup> residential/commercial distillate oil combustion (for more details see Gray, 1986).

<sup>k</sup> the emissions of vegetative detritus within the inventory area are estimated from a small chemical mass balance receptor modeling calculation based on silica, alumina, and alkanes from vegetation, road dust and cigarette smoke, with vegetation emissions then scaled from the known cigarette smoke emission rate in proportion to their relative ambient concentrations.

<sup>l</sup> other sources included in emission inventory: diesel powered ships (42.1 kg/day), industrial rubber and plastics operations (35.7 kg/day), petroleum refining FCC units (24.5 kg/day), fugitive emissions from livestock feedlots (20.4 kg/day), industrial waste burning (20.2 kg/day), industrial internal combustion engines using gasoline (19.0 kg/day), industrial internal combustion engines using digester gas (18.6 kg/day), industrial printing operations (12.9 kg/day), aviation gas mobile sources (9.6 kg/day), residential and high priority commercial LPG combustion (7.8 kg/day), industrial degreasing operations (5.1 kg/day), industrial food and agricultural operations (5.0 kg/day), agricultural burning operations (2.5 kg/day), industrial textile manufacturing (1.8 kg/day), non-refinery industrial/ low priority commercial LPG combustion (1.3). Of these, the diesel ships have been assigned to profile 7, the gasoline engines have been assigned to profile 6, and the remaining sources are not used in the model.

the procedures used for fine particulate source sampling from each source have been presented previously (Hildemann et al., 1991). Briefly, combustion source emissions were collected utilizing a dilution stack sampling system (Hildemann et al., 1989). Dilution air, which was passed through a HEPA filter and an activated carbon bed, was mixed with source emissions to simulate the condensation process that occurs due to dilution and cooling as a plume enters the atmosphere. After sufficient residence time in the sampler, several streams of diluted emissions were drawn through AIHL cyclones at conditions designed to remove particles with aerodynamic diameters greater than 2  $\mu\text{m}$ , followed by fine particle collection on appropriate filter substrates. Quartz fiber filters (Pallflex Tissuequartz 2500 QAO) were used in the same manner as described for ambient sampling for both EC/OC analysis and for identification and quantification of organic compounds by HRGC and GC/MS. Samples collected on Teflon filters (Gelman Teflo, 2  $\mu\text{m}$  pore size) were used for gravimetric determination, X-ray fluorescence analysis, and for ion chromatography. The emissions from catalyst-equipped autos, non-catalyst autos, diesel trucks, oil fired boilers, natural gas home appliances, meat charbroiling and frying, and fireplace combustion of wood were measured in this manner.

The diesel trucks tested by Hildemann et al. (1991) represented vehicles newer than the fleet of diesel trucks in operation in the Los Angeles basin in 1982, when the ambient samples used in this study were collected. Comparison

of Hildemann et al.'s source test data for newer trucks to source test data on older diesel trucks summarized by Gray (1986) shows that the organic compound emission rates from both the newer and older trucks are similar, while the elemental carbon emissions from the older trucks are much higher than for the newer trucks. For this reason, the elemental carbon emissions rate used in the present study to represent diesel powered vehicles in 1982 is taken from Gray et al. (1986), while the emissions rate and distribution of the organic compounds is taken from Hildemann et al. (1991).

Cigarette smoke and roofing tar pot emissions were sampled with a modified dilution sampler (Hildemann et al., 1991) that employed the same cyclone and filter collection equipment that was used for the hot ducted combustion sources. Vehicular brake dust, paved road dust, and vegetative detritus were collected following particle resuspension in clean Teflon bags. The resuspended particulate matter was passed through AIHL cyclones to remove particles with aerodynamic diameters greater than 2  $\mu\text{m}$ , followed by collection on quartz fiber and Teflon filters as described above for the hot source samples. Due to the electrostatic nature of tire dust, resuspension within the Teflon bags is not possible. For this reason, the chemical composition of the tire dust samples was analyzed from total particulate matter samples, which included coarse particles (Hildemann et al., 1991). This should not pose a problem for



the relative chemical composition data needed here since tire tread is a well-mixed industrial material.

### 9.2.3 Organic Compound Identification and Quantification

Both ambient samples and source samples collected on quartz fiber filters were subjected to identical filter handling and analytical protocols to identify and quantify the organic compounds present. The methods used were developed for trace level quantification of organics in airborne particulate matter by HRGC and GC/MS techniques and have been discussed extensively elsewhere (Mazurek et al., 1987, 1989, 1991; Rogge et al., 1991). Briefly, the composited filters were spiked with an internal recovery standard, perdeuterated tetracosane ( $n\text{-C}_{24}\text{D}_{50}$ ). The samples were extracted twice with hexane, followed by three successive benzene/2-propanol (2:1) extractions. Extracts were combined and each final extract mixture was reduced to 200-500  $\mu\text{l}$  total volume. An aliquot of the concentrated extract was derivatized with diazomethane to convert organic acids to their methyl ester analogues (Mazurek et al., 1987). Then the concentrations of the 100 individual organic compounds, listed in Table 9.2, were quantified in the ambient fine particulate samples by GC/MS techniques (Rogge et al., 1993a; Rogge, 1993). The same compounds plus other readily-identified organics were sought in the source samples. Tracer compound mass concentrations in both source and ambient samples were corrected for recovery efficiency during extraction (see Mazurek et al., 1987 for example) such that the total tracer

Table 9.2. List of Compounds Available for Possible Use in the Receptor Model-1982, Los Angeles

Compound name	Range of annual average ambient fine particulate concentration (ng m <sup>-3</sup> )	Used in receptor model	Reason not used *
<u>n-ALKANES</u>			
n-Tricosane	3.2 - 6.7	Yes	
n-Tetracosane	3.9 - 5.0	Yes	
n-Pentacosane	6.7 - 11.2	Yes	
n-Hexacosane	4.3 - 8.2	Yes	
n-Heptacosane	5.2 - 6.7	Yes	
n-Octacosane	2.1 - 3.1	Yes	
n-Nonacosane	4.7 - 7.1	Yes	
n-Triacontane	2.4 - 2.7	Yes	
n-Hentriacontane	9.3 - 12.6	Yes	
n-Dotriacontane	1.0 - 1.5	Yes	
n-Tritriacontane	1.5 - 2.3	Yes	
n-Tetratriacontane	0.36 - 0.68	Yes	
<u>iso- and anteiso- ALKANES</u>			
anteiso-Triacontane	<0.03 - 0.23	Yes	
iso-Hentriacontane	0.73 - 1.50	Yes	
anteiso-Hentriacontane	<0.03 - 0.12	Yes	
iso-Dotriacontane	<0.03 - 0.13	Yes	
anteiso-Dotriacontane	0.89 - 1.31	Yes	
iso-Tritriacontane	0.30 - 0.33	Yes	
<u>HOPANES AND STERANES</u>			
20S&R-5 $\alpha$ (H),14 $\beta$ (H),17 $\beta$ (H)-Cholestanes	0.34 - 1.18	Yes	
20R-5 $\alpha$ (H),14 $\alpha$ (H),17 $\alpha$ (H)-Cholestane	0.34 - 1.23	Yes	
20S&R-5 $\alpha$ (H),14 $\beta$ (H),17 $\beta$ (H)-Ergostanes	0.51 - 1.75	Yes	
20S&R-5 $\alpha$ (H),14 $\beta$ (H),17 $\beta$ (H)-Sitostanes	0.52 - 1.67	Yes	
22,29,30-Trisnorneohopane	0.32 - 0.93	Yes	
17 $\alpha$ (H),21 $\beta$ (H)-29-Norhopane	0.66 - 2.42	Yes	
17 $\alpha$ (H),21 $\beta$ (H)-Hopane	1.32 - 4.02	Yes	
22S-17 $\alpha$ (H),21 $\beta$ (H)-30-Homohopane	0.52 - 1.42	Yes	
22R-17 $\alpha$ (H),21 $\beta$ (H)-30-Homohopane	0.36 - 1.06	Yes	
22S-17 $\alpha$ (H),21 $\beta$ (H)-30-Bishomohopane	0.33 - 0.84	Yes	
22R-17 $\alpha$ (H),21 $\beta$ (H)-30-Bishomohopane	0.20 - 0.58	Yes	
<u>n-ALKENOIC ACIDS</u>			
cis-9-n-Octadecenoic acid	17.3 - 26.0	Yes	
<u>ALDEHYDES</u>			
Nonanal	5.7 - 9.5	Yes	

\* a: Significant source not in model

b: Species fails check for apparent conservation in the atmosphere (it behaves as if it is formed or depleted)

c: Some monitoring sites have missing data

Table 9.2. (continued - page 2)

Compound name	Range of annual average ambient fine particulate concentration (ng m <sup>-3</sup> )	Used in receptor model	Reason not used *
<u>n-ALKANOIC ACIDS</u>			
n-Nonanoic acid	3.3 - 9.9	No	a
n-Decanoic acid	1.3 - 3.1	No	a
n-Undecanoic acid	2.8 - 6.0	No	a
n-Dodecanoic acid	3.7 - 7.0	No	a
n-Tridecanoic acid	3.3 - 4.9	No	a
n-Tetradecanoic acid	14.4 - 22.8	No	a
n-Pentadecanoic acid	4.3 - 6.1	No	a
n-Hexadecanoic acid	118 - 141	No	a
n-Heptadecanoic acid	3.4 - 5.2	No	a
n-Octadecanoic acid	41.1 - 59.2	No	a
n-Nonadecanoic acid	0.79 - 1.1	No	a
n-Eicosanoic acid	3.1 - 6.1	No	a
n-Heneicosanoic acid	1.4 - 2.3	No	a
n-Docosanoic acid	5.7 - 9.9	No	a
n-Tricosanoic acid	1.5 - 2.5	No	a
n-Tetracosanoic acid	9.2 - 6.5	No	a
n-Pentacosanoic acid	1.1 - 1.6	No	a
n-Hexacosanoic acid	5.3 - 9.3	No	a
n-Heptacosanoic acid	0.47 - 0.81	No	a
n-Octacosanoic acid	2.7 - 4.9	No	a
n-Nonacosanoic acid	0.33 - 0.57	No	a
n-Triacontanoic acid	1.0 - 2.2	No	a
<u>DICARBOXYLIC ACIDS</u>			
Propanedioic acid	28.0 - 51.0	No	b
2-Butenedioic acid	0.58 - 1.3	No	b
Butanedioic acid	51.2 - 84.1	No	b
Methylbutanedioic acid	11.6 - 20.3	No	b
Pentanedioic acid	28.3 - 38.7	No	b
Methylpentanedioic acid	15.5 - 23.7	No	b
Hydroxybutanedioic acid	7.8 - 22.1	No	b
Hexanedioic acid	14.1 - 24.3	No	b
Octanedioic acid	2.5 - 4.1	No	b
Nonanedioic acid	22.8 - 44.7	No	b
<u>AROMATIC CARBOXYLIC ACIDS</u>			
1,2-Benzenedicarboxylic acid	53.5 - 60.6	No	b
1,3-Benzenedicarboxylic acid	2.1 - 3.4	No	b
1,4-Benzenedicarboxylic acid	0.88 - 2.8	No	b
4-Methyl-1,2-benzenedicarboxylic acid	15.2 - 28.8	No	b
1,2,4-Benzenetricarboxylic acid	0.45 - 0.84	No	b
1,3,5-Benzenetricarboxylic acid	11.3 - 22.6	No	b
1,2,4,5-Benzenetetracarboxylic acid	0.40 - 0.80	No	b

\* a: Significant source not in model

b: Species fails check for apparent conservation in the atmosphere (it behaves as if it is formed or depleted)

c: Some monitoring sites have missing data

Table 9.2. (continued - page 3)

Compound name	Range of annual average ambient fine particulate concentration (ng m <sup>-3</sup> )	Used in receptor model	Reason not used *
<u>WOOD SMOKE MARKERS</u>			
Dehydroabietic acid	10.2 - 23.6	No	b
13-Isopropyl-5 $\alpha$ -podocarpa-6,8,11,13-tetraen-16-oic acid	0.30 - 1.2	No	b
8,15-Pimaradien-18-oic acid	0.07 - 1.1	Yes	
Pimaric acid	0.94 - 4.8	Yes	
Isopimaric acid	0.71 - 2.3	Yes	
7-Oxodehydroabietic acid	1.9 - 4.1	No	b
Sandaracopimaric acid	0.60 - 2.2	No	b
Retene	0.01 - 0.10	Yes	
<u>POLYCYCLIC AROMATIC HYDROCARBONS</u>			
Fluoranthene	0.07 - 0.15	No	b
Pyrene	0.12 - 0.26	No	b
Benz[a]anthracene	0.09 - 0.29	No	b
Cyclopenta[cd]pyrene	0.04 - 0.41	No	b
Benzo[ghi]fluoranthene	0.11 - 0.39	No	b
Chrysene/triphenylene	0.23 - 0.61	No	b
Benzo[k]fluoranthene	0.33 - 1.20	Yes	
Benzo[b]fluoranthene	0.68 - 1.23	Yes	
Benzo[e]pyrene	0.38 - 0.97	Yes	
Benzo[a]pyrene	0.18 - 0.44	No	b
Indeno[1,2,3-cd]pyrene	0.07 - 0.43	Yes	
Indeno[1,2,3-cd]fluoranthene	0.26 - 1.09	Yes	
Benzo[ghi]perylene	1.12 - 4.47	Yes	
Coronene	2.41 <sup>c</sup>	Yes	
<u>PAH KETONES AND QUINONES</u>			
7H-Benz[de]anthracen-7-one	0.25 - 0.84	Yes	
Benz[a]anthracene-7,12-dione	0.12 - 0.25	Yes	
Benzo[cd]pyren-6-one	0.02 - 1.24	Yes	
<u>STEROIDS</u>			
Cholesterol	1.9 - 2.7	No	c
<u>N-CONTAINING COMPOUNDS</u>			
3-Methoxypyridine	0.46 - 1.4	No	b
Isoquinoline	0.61 - 1.1	No	b
1-Methylisoquinoline	0.24 - 1.1	No	b
1,2-Dimethoxy-4-nitrobenzene	0.22 - 3.9	No	b
<u>INORGANIC ELEMENTS</u>			
Elemental carbon	3030 - 4870	Yes	
Particulate aluminum	249 - 330	Yes	
Particulate silicon	336 - 600	Yes	

\* a: Significant source not in model

b: Species fails check for apparent conservation in the atmosphere (it behaves as if it is formed or depleted)

c: Some monitoring sites have missing data

content of each sample was measured. Single compound mass emission rates from each of the 15 source types studied are reported by Rogge et al. (1991; 1993b; 1993c; 1993d; 1993e; 1994) and by Rogge (1993). These references by Rogge et al. when combined with gravimetric mass concentration data and total carbon data reported by Gray et al. (1986) and Hildemann et al. (1991) yield source profiles and ambient aerosol composition data that show the fine particle mass, overall organic carbon and elemental carbon content, extractable organics content, individual organic compound content and trace element content of each sample.

Confidence intervals for the organic compound quantification procedures used in this study were estimated from analysis of the variance of the historical ambient data along with more recent experiments conducted in our laboratory. The annual average ambient organic compound concentrations represent the mean of 12 monthly composites of daily samples taken at six day intervals. The uncertainties in the annual means of these atmospheric samples ( $\pm 1 \sigma$ ) typically are approximately  $\pm 20\%$ , and arise mainly from the fact that not all days of the year were sampled. The quantifiable uncertainties in the source samples are principally analytical uncertainties and also average approximately  $\pm 20\%$  ( $\pm 1 \sigma$ ).

## 9.3 Source/Receptor Reconciliation

### 9.3.1 Chemical Mass Balance Approach

The chemical composition of the emissions from individual sources can be used to estimate source contributions to atmospheric samples taken at receptor air monitoring sites (Hidy et al., 1974; Miller et al., 1972; Friedlander, 1973; Cass and McRae, 1983). One useful method for assigning ambient particulate matter concentration increments to the sources from which they originate is the chemical mass balance (CMB) technique. In the CMB method, a mass balance is constructed in which the concentration of specific chemical constituents in a given ambient sample is described as arising from a linear combination of the relative chemical compositions of the contributing sources. The concentration of chemical constituent  $i$  at receptor site  $k$ ,  $c_{ik}$ , can be expressed as:

$$c_{ik} = \sum_{j=1}^m f_{ijk} a_{ij} s_{jk} \quad (1)$$

where  $s_{jk}$  is the increment to total particulate mass concentration at receptor site  $k$  originating from source  $j$ ,  $a_{ij}$  is the relative concentration of chemical constituent  $i$  in the emissions from source  $j$ , and  $f_{ijk}$  is the coefficient of fractionation that represents the modification of  $a_{ij}$  during transport from source  $j$

to receptor  $k$ . The fractionation coefficient accounts for selective loss of constituent  $i$  due to processes such as gravitational settling, chemical transformation, or evaporation; it can also be used to account for selective gains in constituent  $i$  due to chemical formation or condensation. In the present study, chemical constituents which do not have fractionation coefficients near unity will not be used in mass balance calculations. With the chemical composition of both the source samples ( $a_{ij}$ ) and the ambient samples ( $c_{ik}$ ) known from experimental measurements and with  $f_{ijk}$  near unity for each chosen chemical substance, the system of equations (1) can be solved for the unknown source contributions,  $s_{jk}$ , to the ambient pollutant concentrations.

If the number of chemical constituents included in the mass balance calculations exceeds the number of sources then the system of equations (1) is overdetermined, and exact agreement between the ambient concentrations and a unique linear combination of the source profiles is not expected due to the presence of small measurement errors. In this usual case, an ordinary least squares solution to the system of equations (1) can be employed. Alternatively, an effective variance weighted least squares solution, which takes advantage of known uncertainties in ambient measurements and emissions data, can be used to solve the linear system of equations (Watson et al., 1984). In the present study, the system of equations (1) will be solved using the CMB7 source-

receptor modeling computer program (Watson et al., 1990) that employs this effective variance weighted least squares technique.

### **9.3.2 Selection of Sources and Organic Compounds: An Emissions Inventory Assisted Approach**

For the use of a chemical mass balance receptor model to be successful, several criteria must be met. First, if the coefficient of fractionation,  $f_{ijk}$ , in equation (1) is to be set to unity, then the chemical species for which material balance equations are written must be sufficiently stable that they are conserved during transport from their sources to the receptor air monitoring sites. The species must not be significantly depleted from the fine particulate fraction by volatilization or chemical reaction, and the species concentration must not be significantly increased by atmospheric chemical formation processes. Second, all major sources of each chemical species used in the mass balance must be included in the model, and the relative chemical compositions of the emissions from different source types that are included in the model must be different from each other in a statistical sense such that the problems of source profile collinearity are avoided. Little prior experience exists to show how a chemical mass balance receptor model based on organic tracer compounds should be constructed in order to exclude compounds that are insufficiently stable chemically, to assure that all major source types are included, and to detect and deal with source profiles from sources that are so similar to each other that



collinearity problems would arise. In the following sections of the present paper, these issues are addressed within the context of example calculations in the Los Angeles area. In general, the methods used are similar to the emissions inventory-assisted chemical mass balance modeling procedures developed previously for data sets involving trace metals by Cass and McRae (1983).

#### *9.3.2.1 A Test for Apparent Chemical Stability*

One hundred organic compounds, listed in Table 9.2, were quantified both in source emissions and in fine aerosol samples collected at the four urban air monitoring sites used in this study (Rogge et al., 1993a; Rogge, 1993). An individual organic compound listed in Table 9.2 can be used successfully in the present CMB model only if it is conserved during transport from source to receptor ( $f_{ijk} \approx 1$ ). Since the atmospheric stability of many of these organic compounds has not been examined in this light previously, the first step in our analysis is to perform an initial screening to identify and exclude compounds that do appear to be significantly modified during transport from source to receptor. The approach taken is to examine the ratio of the average atmospheric concentration to the area-wide emission rate for each organic compound studied. Fine elemental carbon particles have been employed previously as a nearly conserved tracer because they are not depleted by chemical reaction and because, by virtue of their small size (Ouimette and Flagan, 1982; Venkataraman and Friedlander, 1994), they are not depleted rapidly by dry

deposition (Sehmel, 1980). Those organic compounds in fine particles that likewise are conserved in the atmosphere ought to show a ratio of ambient concentration to source emission rate that is fairly similar to that for elemental carbon particles. Those compounds that are formed by atmospheric reactions will have a much higher than average ratio of atmospheric concentration to mass emissions, while those compounds that are depleted rapidly by evaporation or chemical reaction will show lower average ratios of their ambient concentrations to emissions than is the case for a conserved species like elemental carbon.

The first step in this procedure for screening the compounds to be used is to construct a comparison of area-wide emissions and ambient concentrations for each chemical substance. Table 9.1 provides an emissions inventory for fine organic aerosol mass within an 80 x 80 km area centered over the city of Los Angeles for 1982 (Hildemann et al., 1991). The sources sampled by Hildemann et al. (1991) and analyzed by Rogge et al. (1991; 1993a; 1993b; 1993c; 1993d; 1994; Rogge, 1993) are indicated in Table 9.1. Several sources which were not tested by Hildemann et al. (1991) can be approximated, for purposes of an emissions inventory, by sources for which detailed emissions data are available (see Table 9.1). Including untested sources which can be represented by a tested source, the speciated emissions inventory data account for approximately 84% of the fine organic aerosol emissions within the 80 x 80 km inventory area. Using the atmospheric organic compound concentration data of Rogge et al.

(1993a), along with chemical composition profiles generated by Hildemann et al. (1991) and Rogge et al. (1991; 1993b; 1993c; 1993d; 1993e; 1994; Rogge, 1993), a quantitative comparison of emissions and ambient concentrations for each compound can be constructed. Figures 9.2a and 9.2b show the ratio of average airborne organic aerosol compound concentrations to the area-wide emissions rate within the 80 x 80 km inventory area for each of the 100 fine aerosol organic compounds in Table 9.2, plus fine particle silicon, fine particle aluminum, and fine particle elemental carbon. For our inert indicator species, fine elemental carbon, fine silicon, and fine aluminum, there exists reasonable consistency between estimated area-wide emission rates and the average ambient concentration at the three central basin air monitoring sites that are within the emission inventory area: West Los Angeles, Downtown Los Angeles and Pasadena. Organic compounds having a ratio of ambient concentration to primary emission rate in the same range as seen for fine elemental carbon, silicon, and aluminum will pass our initial screening check that  $f_{ijk} \approx 1$  over the relatively short distance from source to receptor that exists in the western and central portions of the Los Angeles basin. To formalize that concept, an organic compound having an atmospheric concentration to emission rate ratio falling within a specific interval will be considered to be sufficiently stable that it can be used for mass balance calculations. That interval is defined by the mean of the ambient concentration to emissions ratio seen for the inert reference species elemental carbon, fine aluminum and fine silicon, plus and minus two standard

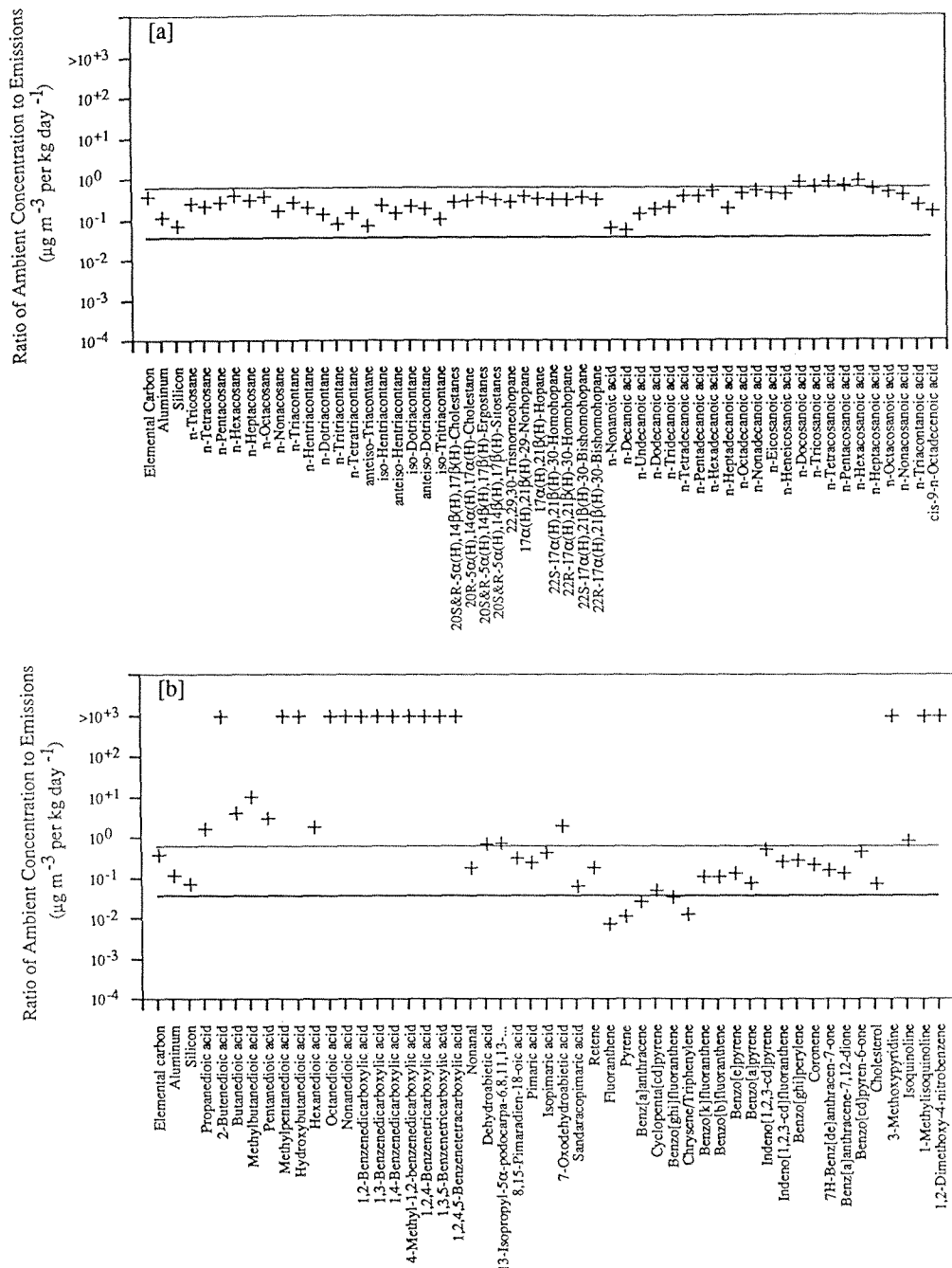


Figure 9.2. Central basin 1982 annual average ambient compound concentrations divided by compound emissions within the 80X80 km emissions inventory area centered over Downtown Los Angeles (Hildemann et al., 1991). Solid lines represent the average  $\pm$  two standard deviations of the ratio of concentration to emission rate observed for the conserved reference materials: elemental carbon, fine particle aluminum, and fine particle silicon. Central basin average ambient concentrations include all data from within the emissions inventory area: Pasadena, West Los Angeles, and Downtown Los Angeles. Values shown at  $10^3$  are greater than or equal to  $10^3$ .

deviations of that population of three reference species ratios. This range is shown between the horizontal solid lines in Figures 9.2a and 9.2b. Emissions inventories for elemental carbon, fine aluminum and fine silicon are taken from Gray (1986).

Figure 9.2 shows that on a yearly average the normal alkanes are not removed from fine aerosols any more rapidly than inert substances such as elemental carbon, fine aluminum, or fine silicon over the time scale of transport between sources and receptors in the western and central Los Angeles basin. Similarly, regular steranes, pentacyclic triterpanes, iso-alkanes, and anteiso-alkanes show the same basic relationship between emission rates and ambient concentrations and therefore do not appear to have major selective losses or gains from the fine aerosol fraction. This empirical result is consistent with the expected decay rates of these species. All of the above-noted conserved organic compounds are considered to react relatively slowly. On a yearly average their fractionation coefficient can be taken to be close to one. Therefore, these compounds will be included in the base case CMB model.

In contrast, the polycarboxylic aromatic acids, the dicarboxylic acids, 3-methoxypyridine, 1-methylisoquinoline, and 1,3-dimethoxy-4-nitrobenzene show very high values of the ratio of their ambient concentration to their emissions rate within the area-wide primary particle emissions inventory. The concentrations of these compounds are thought to be dominated by secondary

formation due to atmospheric chemical reactions. Aliphatic dicarboxylic acids are known to be formed from gas phase precursors under photochemical smog conditions (Appel et al., 1980; Cronn et al., 1977; Grosjean, 1977; Grosjean and Friedlander, 1980; Satsumabayashi and Kurita, 1989). Emissions of aromatic polycarboxylic acids are below detection limits in all of the sources tested here, and cluster analysis applied to atmospheric concentration data shows that the concentrations of these compounds follow the behavior of the aliphatic dicarboxylic acids (Rogge et al., 1993a). Thus aromatic polycarboxylic acids are also believed to be formed by atmospheric chemical reactions. These compounds that appear to be formed by atmospheric chemical reactions will not be used within the model.

The selective loss of many of the lower molecular weight primary particle-phase polycyclic aromatic hydrocarbons (PAH) is suggested by Figure 9.2ab. All of the PAH with molecular weights less than benzo[k]fluoranthene, with the possible exception of cyclopenta[cd]pyrene, have normalized ambient concentrations that are much lower than is exhibited by the conserved species. The lighter of these compounds, fluoranthene, pyrene, and benz[a]anthracene, would be expected to be lost from the fine particle phase due to volatilization. The losses of some of these PAH also are believed to result from heterogeneous reactions in the particle phase (Kamens et al., 1988), although little data exist to quantify the rate of these reactions under ambient conditions. Kamens et al.

(1988) measured the reactivity of several PAH on wood soot particles in a smog chamber and found a semi-empirical correlation for reactivity that depends on temperature, total solar radiation intensity, and humidity. Cyclopenta[cd]pyrene, benz[a]anthracene, and benzo[a]pyrene were found to have the fastest reaction rates under the conditions tested by Kamens et al. (1988) on wood soot particles. For that reason, these three compounds will be excluded as fitting species in the base case CMB model, even though the average particle composition and the atmospheric conditions of Kamens et al.'s tests may be very different than the annual average particle composition and atmospheric conditions experienced in the Los Angeles basin. For these reasons, all of the PAH with molecular weights less than 252 (i.e., those having lower molecular weights than benzo[k]fluoranthene) are also not used as mass balance species in the CMB model.

For the PAH with molecular weights of 252 or greater (except for benzo[a]pyrene), there is insufficient data to allow a sharp dividing line to be drawn between individual compounds that should be included or excluded from our analysis. For this reason, two cases have been investigated. In the base case, all of the PAH with molecular weights greater than or equal to 252 (i.e., PAH having molecular weights at least as great as that of benzo[k]fluoranthene), except benzo[a]pyrene, are included as if they were stable compounds in the mass balance calculations. In an alternative case, only the four highest

molecular weight PAH are included: indeno[1,2,3-cd]pyrene, indeno[1,2,3-cd]fluoranthene, benzo[ghi]perylene, and coronene. While Figure 9.2 suggests that the longer list of PAH can be used as if they were conserved species over the short distance transport within the central Los Angeles basin, a similar analysis shows that benzo[k]fluoranthene, benzo[b]fluoranthene, and benzo[e]pyrene can be depleted over the longer transport distance to downwind Rubidoux.

Kamens et al. (1988; 1989) also have examined the stability of several polycyclic aromatic ketones and quinones (oxy-PAH) and a wood smoke marker, retene, in smog chamber experiments. Retene was found to react at a rate comparable to benzo[a]pyrene on wood smoke particles under conditions of high solar irradiance, humidity, and temperature, but showed much lower relative reactivity at lower solar irradiance, humidity, and temperature. Since retene appears from Figure 9.2 to be conserved based on the relationship of its emissions and ambient concentration, retene is used as a mass balance species in our model. Of the remaining wood smoke components, only 8,15-pimaradien-18-oic acid, pimaric acid, isopimaric acid, and sandaracopimaric acid pass the initial screening test. As seen in Figure 9.2, sandaracopimaric acid does not cluster with the three other wood smoke components just mentioned above and therefore will not be included in the base case model application. Dehydroabietic acid, 13-isopropyl-5 $\alpha$ -podocarpa-6,8,11,13-tetraen-16-oic acid,



and 7-oxodehydroabietic acid, all have ratios of ambient concentrations to emission rates that fail the initial screening test.

The several oxy-PAH tested by Kamens et al. (1989) were found to be stable both in the absence of sunlight and in the absence of appreciable ozone on wood smoke particles. The three oxy-PAH shown in Figure 9.2, 7H-benz[de]anthracen-7-one, benz[a]anthracene-7,12-dione, and benzo[cd]pyren-6-one, appear to be conserved over short transport distances within the central Los Angeles basin, but a further analysis shows that they are not very well conserved over longer downwind transport to Rubidoux. These three oxy-PAH are emitted predominantly by natural gas home appliances and non-catalyst gasoline-powered vehicles in Los Angeles, while Kamens et al.'s results apply to oxy-PAH adsorbed onto wood smoke particles. Our analysis in Figure 9.2 plus the work of Kamens et al. (1989) suggest that these compounds are reasonably well conserved over short distance transport. For this reason, these compounds are included as mass balance compounds in the base case air quality model.

Oleic acid appears from Figure 9.2 to be present in about the expected quantity in airborne fine particles even though oleic acid is an olefinic compound susceptible to ozone attack. This compound is a key tracer for aerosols from food cooking and therefore should not be excluded from the present model unless it is absolutely clear that it must be excluded. Thus oleic acid is used as

a mass balance species in this study. The sensitivity of the CMB model results to this assumption will be discussed later.

Although cholesterol is thought to be an excellent marker for the aerosol released from meat cooking (Rogge et al., 1991), quantification of trace cholesterol concentrations in ambient samples was not possible for some samples. Cholesterol is therefore not included in the base case model as a mass balance component. Alternative case models, which include cholesterol as a mass balance compound, will be presented later for the apportionment of sources contributing to the two air monitoring sites for which cholesterol data are available, West Los Angeles and Pasadena. Coronene elutes very late from the chromatographic column used here and was only quantified in the West Los Angeles samples. Coronene is only included in the model for that site. Similarly, the anteiso-C<sub>30</sub> and C<sub>31</sub> alkanes and the iso-C<sub>32</sub> alkane were not identified in the Downtown Los Angeles and Rubidoux ambient samples and thus are also not included in the base case model at those sites. Table 9.2 summarizes those compounds that are included in the base case model.

#### *9.3.2.2 Elimination of Collinearity between Source Profiles*

Use of the chemical mass balance model requires that the source profiles be sufficiently different from each other. Therefore, several steps were taken to remove collinearities. Elemental carbon plus silicon and aluminum

measurements from the source sampling program (Hildemann et al., 1991) and the ambient sampling program (Gray et al., 1986) were added to the database. The aluminum and silicon data when combined with the organics yield a distinguishing fingerprint for paved road dust. The elemental carbon data when combined with the organic compound concentrations provides a unique fingerprint for diesel engine exhaust. There are three generic source types that each have two source profiles in our data base: gasoline-powered vehicles, fireplace combustion of wood, and meat cooking. Within pairs, these source profiles are sufficiently similar that each pair was combined to form a single emissions-weighted average source profile. Catalyst-equipped gasoline-powered vehicle emissions and non-catalyst gasoline-powered vehicle emissions were combined in proportions equivalent to their contributions to the fine organic aerosol emissions inventory to produce a single emissions-weighted overall source profile for gasoline-powered vehicles. Similarly, source profiles for fireplace combustion of hardwood and softwood were combined to form an emissions-weighted average wood smoke source profile. The source profiles for meat charbroiling and meat frying also were combined into a single emissions-weighted average meat cooking source profile. Following creation of these combined source profiles, a total of 12 separate source profiles remain for use in the CMB model.

### 9.3.2.3 Completeness of the Source Profile Library

More than 70 different carbon particle emissions source types can be identified in the Los Angeles area (Cass et al., 1982; Gray, 1986). As a practical matter, receptor models based on elemental composition data seldom can resolve as many as a half dozen separate source contributions within a real application. The species selected for use in a mass balance model that seeks to resolve less than the full set of sources actually present must be chosen carefully so that the sources included in the model in fact do complete a mass balance on the subset of chemical species entered into the model. As a starting point, such a check for the completeness of the set of sources used can be constructed based on emissions inventory data. Using the set of 15 source profiles available together with the knowledge that they represent more than 80% of the primary organic aerosol emissions within the Los Angeles airshed, emission inventories were constructed for each chemical compound listed in Table 9.2 that was found in the source emissions. The contributions of the individual sources to the emissions of each organic compound are shown in Figures 9.3abc. Before running the CMB7 computer code, these figures were used to perform consistency checks to assure that if a source profile must be deleted from the model (e.g., because it makes an insignificant contribution to the ambient aerosol), then at no time a species remained as a mass balance component when a significant known source of that compound was missing from

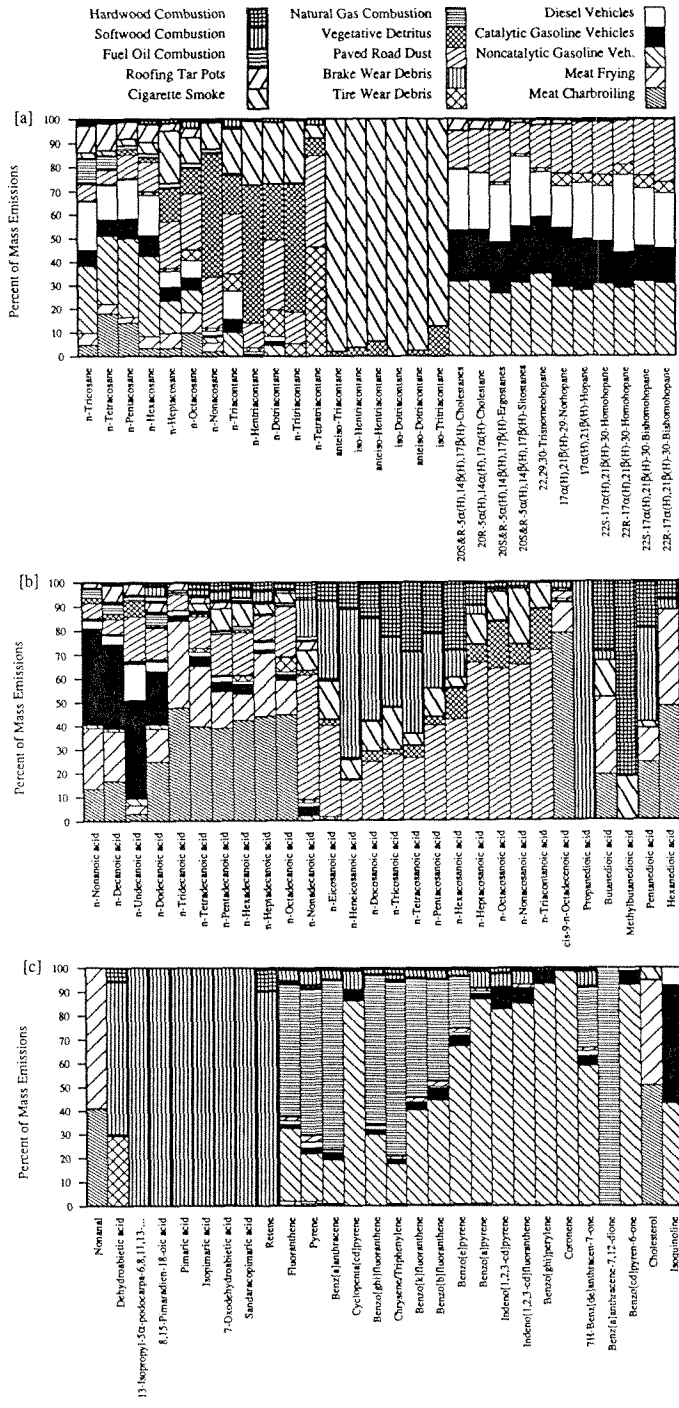


Figure 9.3. Distribution of particulate organic compound emissions by source type within the Los Angeles basin, 1982.

the model. No compounds had to be deleted from the list of mass balance species due to this screening step.

The alkanolic acids shown in Figure 9.2 appear to be stable enough chemically to be used in receptor modeling calculations. However, we suspect that cooking with seed oils is a significant source of n-alkanoic acids emissions to the urban atmosphere (Eckey, 1954), and the emission rate from such activities is not presently known. For that reason, we have not included the n-alkanoic acids in the base case model.

Following the application of the above consistency checks, 45 organic compounds plus data on silicon, aluminum, and elemental carbon concentrations remain for use in the model, and 12 separate source profiles remain.

## 9.4 Results

The chemical mass balance model constructed above was tested by application to the Southern California data base. Compounds included as mass balance species in the base case model are listed in Table 9.2. As previously indicated, coronene and three of the iso- and anteiso-alkanes were eliminated from the mass balance calculations on a site-by-site basis in those cases where ambient data were not available.

A comparison of the modeled and measured ambient concentrations of each of the mass balance species at Downtown Los Angeles is given in Figure 9.4. Generally excellent agreement is obtained between observations and model predictions across the 45 diverse organic compounds used, plus aluminum, silicon, and elemental carbon. For each group of chemically similar tracers, the mean of the ratio of measured to predicted concentrations as well as the standard error of that ratio for the population of tracers in each chemical class was computed as follows: n-alkanes ( $0.88 \pm 0.29$ ), iso- and anteiso-alkanes ( $1.03 \pm 0.42$ ), hopanes and steranes ( $0.85 \pm 0.14$ ), alkenoic acids (1.00), aldehydes (1.09), conifer resin acids and their thermal alteration products ( $1.01 \pm 0.26$ ), PAH ( $1.14 \pm 0.35$ ), and oxy-PAH ( $0.87 \pm 0.34$ ).

Source contributions to annual average particulate organics mass and overall fine particulate mass concentrations that are statistically different from zero with greater than 95% confidence can be determined at West Los Angeles, at Downtown Los Angeles and at Pasadena for nine separate source types: diesel engine exhaust, paved road dust, gasoline-powered vehicle exhaust, emissions from food cooking and wood smoke, natural gas combustion aerosol, cigarette smoke, plant fragments, and tire dust as shown in Table 9.3. At the Rubidoux site, contributions from the first eight of the above sources can be identified. The emissions from industrial boilers burning distillate fuel oil, vehicular brake lining wear, and roofing tar pot effluent could not be identified in

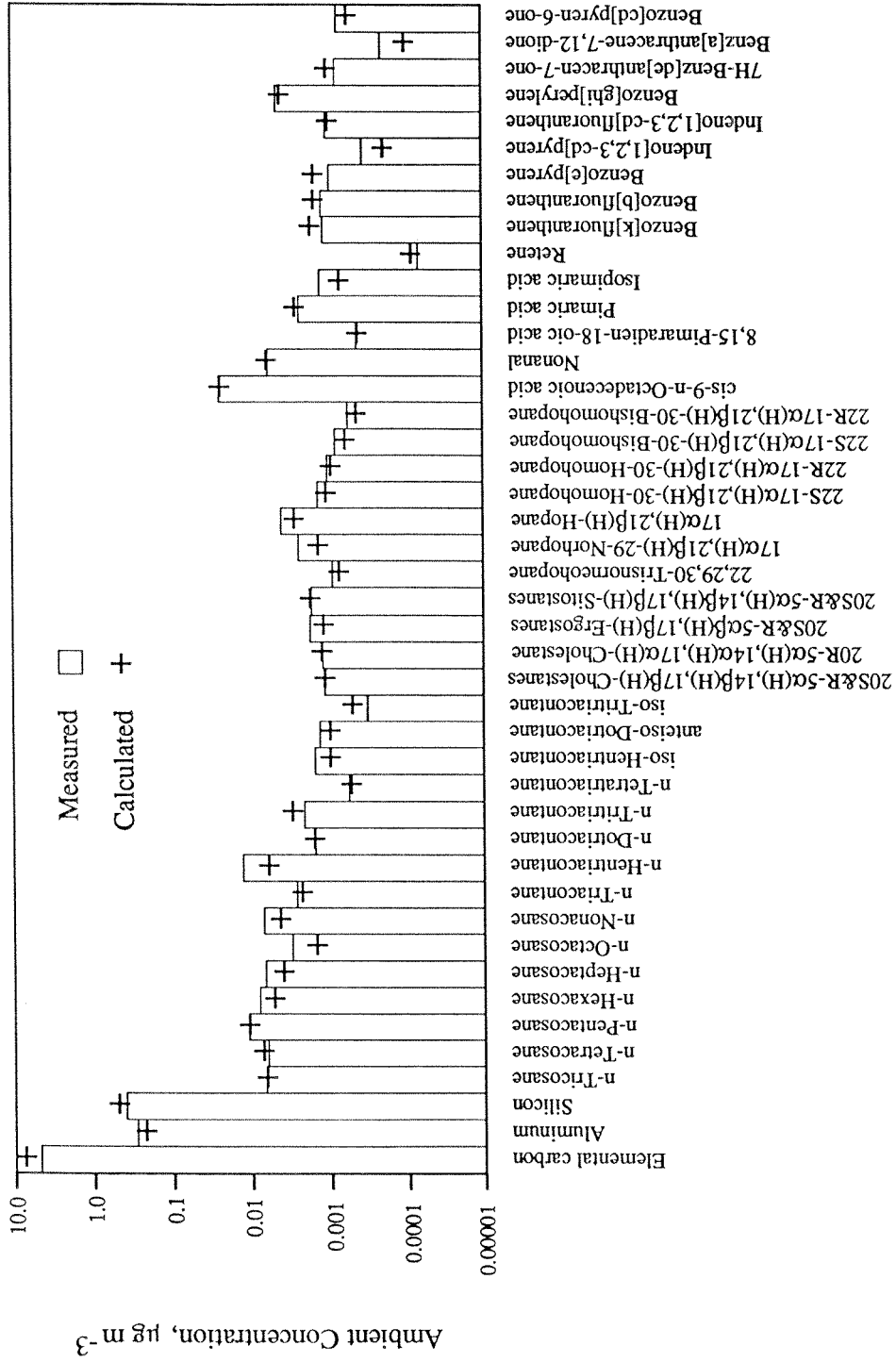


Figure 9.4. Comparison of model predictions to measured ambient concentrations for the mass balance compounds - Downtown Los Angeles, 1982 annual average.



the ambient samples. Each of these is a minor source according to the emissions inventory. The nine sources that remain in the model account for approximately 80% of the primary aerosol organic carbon emissions according to the emissions inventory. The standard errors of the source contribution estimates reported for each source type in Table 9.3 are smaller than the standard error of the combined source contributions estimated for any linear combination of these source profiles, as judged by the absence of any similarity/uncertainty clusters within the CMB7 program results (see Watson et al., 1990).

In an alternative model calculation, three PAH with questionable stability were removed from the base case list of compounds: benzo[k]fluoranthene, benzo[b]fluoranthene and benzo[e]pyrene. For all four monitoring sites, this alternative model calculation produced the same result as the base case within 95% confidence limits.

A second alternative case examined cholesterol as a marker for meat cooking operations. Cholesterol data are only available for two sites, West Los Angeles and Pasadena. Generally, cholesterol concentrations in the atmosphere are less than would be expected from the ambient concentrations of compounds largely derived from meat cooking operations, oleic acid, nonanal, and the C<sub>23</sub> through C<sub>27</sub> normal alkanes. If we add cholesterol data to the base case model compounds, we find that the quantity of ambient meat cooking

Table 9.3. Source Apportionment of Primary Fine Organic Aerosol: 1982 Annual Average Determined by Chemical Mass Balance

SOURCE	Pasadena	Downtown LA	West Los Angeles	Rubidoux
	Source Contribution avg $\pm$ std $\mu\text{g m}^{-3}$	Source Contribution avg $\pm$ std $\mu\text{g m}^{-3}$	Source Contribution avg $\pm$ std $\mu\text{g m}^{-3}$	Source Contribution avg $\pm$ std $\mu\text{g m}^{-3}$
Diesel Exhaust	1.24 $\pm$ 0.17	2.72 $\pm$ 0.28	1.02 $\pm$ 0.15	1.26 $\pm$ 0.12
Tire Wear Debris	0.13 $\pm$ 0.046	0.096 $\pm$ 0.040	0.11 $\pm$ 0.040	*
Paved Road Dust	0.56 $\pm$ 0.070	0.59 $\pm$ 0.075	0.49 $\pm$ 0.063	0.89 $\pm$ 0.099
Vegetative Detritus	0.13 $\pm$ 0.039	0.095 $\pm$ 0.046	0.15 $\pm$ 0.043	0.07 $\pm$ 0.033
Natural Gas Combustion Aerosol	0.048 $\pm$ 0.020	0.041 $\pm$ 0.019	0.034 $\pm$ 0.016	0.029 $\pm$ 0.008
Cigarette Smoke	0.13 $\pm$ 0.018	0.19 $\pm$ 0.033	0.14 $\pm$ 0.020	0.13 $\pm$ 0.023
Meat Charbroiling and Frying	1.69 $\pm$ 0.32	1.22 $\pm$ 0.240	1.42 $\pm$ 0.27	1.35 $\pm$ 0.25
Catalyst and Non-Catalyst Gasoline-Powered Vehicle Exhaust	1.20 $\pm$ 0.15	1.56 $\pm$ 0.170	1.06 $\pm$ 0.12	0.25 $\pm$ 0.04
Wood Smoke	1.57 $\pm$ 0.25	1.07 $\pm$ 0.18	1.54 $\pm$ 0.24	0.31 $\pm$ 0.060
SUM	6.68 $\pm$ 0.41	7.56 $\pm$ 0.38	5.97 $\pm$ 0.37	4.30 $\pm$ 0.27
Measured†	8.14 $\pm$ 0.52	8.72 $\pm$ 0.66	7.00 $\pm$ 0.61	6.24 $\pm$ 0.35

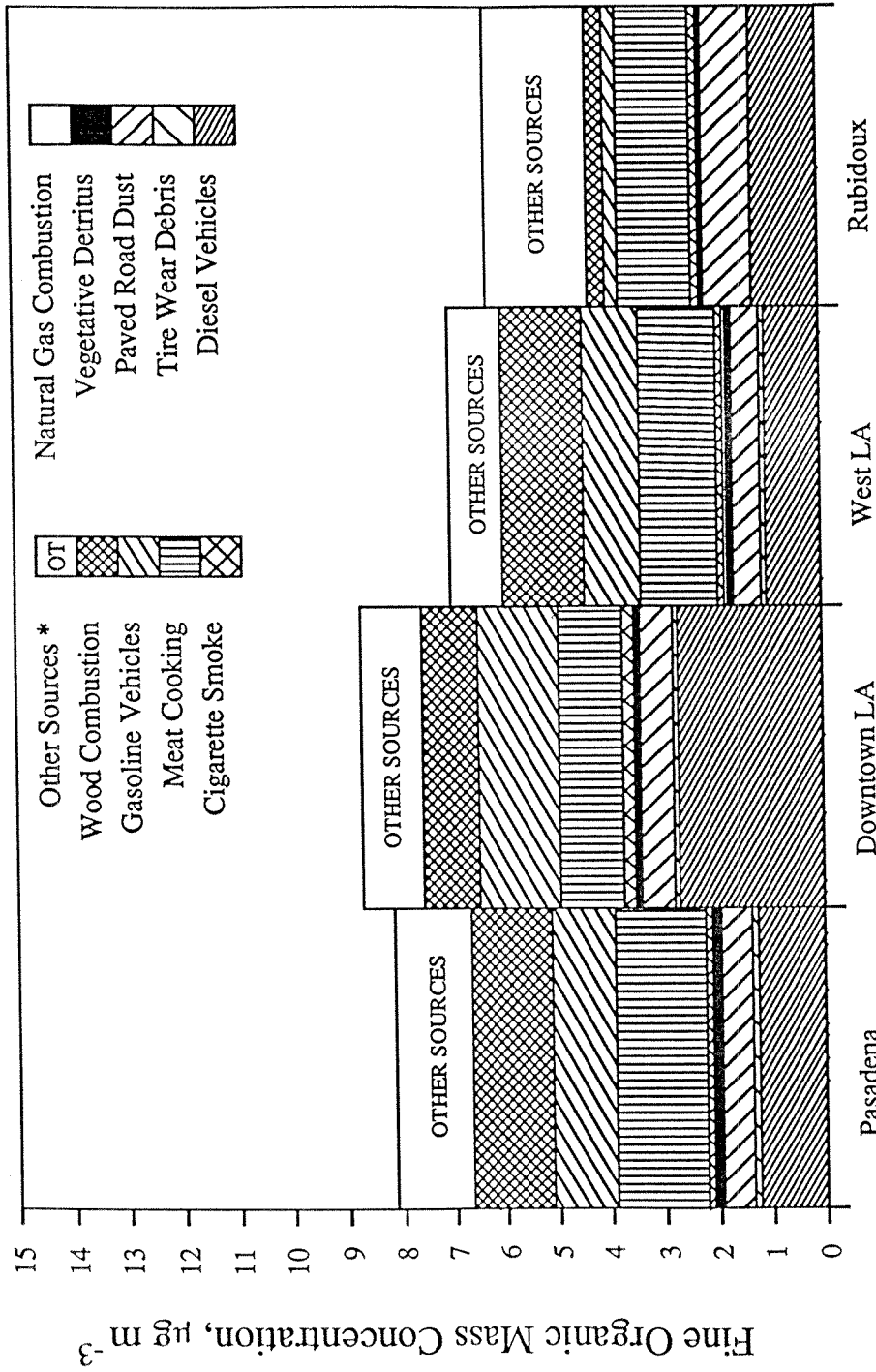
\* Not statistically different from zero with greater than 95% confidence.

† Includes secondary organic aerosol; receptor model results should be less than or equal to measured total fine particle organic concentration.

aerosol predicted by the model is decreased. For West Los Angeles, the results of this alternative case were not statistically different from the base case, while for Pasadena the ambient aerosol mass concentration increment assigned to meat cooking was decreased by  $0.78 \mu\text{g m}^{-3}$  and none of the other source contributions changed significantly from the base case model results.

Computed source contributions to the annual average fine organic aerosol at each monitoring site are shown in Figure 9.5. The contribution from "other sources," which includes secondary organic aerosol formation, is obtained by subtracting the concentration increments due to identified sources from the annual average fine organic compound concentration measurements reported by Gray et al. (1986) (organic compounds  $\approx 1.2 \times \text{OC}$ ).

The dominant sources of fine organic aerosol were found to be diesel exhaust, gasoline-powered vehicle exhaust, meat cooking operations, and wood combustion. Paved road dust is the next largest contributor followed by four smaller sources: tire wear, vegetative detritus, natural gas combustion, and cigarette smoke. The relative and absolute contributions are very similar for West Los Angeles and Pasadena, while the Downtown Los Angeles site is noticeably different from the other two sites in the western portion of the air basin. The diesel exhaust contribution to the Downtown Los Angeles site is approximately twice the value seen at the other two more residential sites in the western basin. This increase is believed to be a result of the higher density of



\* Other Sources include secondary formation

Figure 9.5. Source apportionment of ambient fine organic aerosol mass concentration - 1982 annual average.

commercial trucking and the presence of a major railroad yard near the Downtown Los Angeles sampling site. Auto exhaust aerosol is also significantly increased near the Downtown Los Angeles sampling site.

The quantity of organic aerosol that cannot be attributed to the nine primary sources resolved by the model places an upper limit on the annual average secondary organic aerosol concentration that could be present due to gas-to-particle conversion processes in the atmosphere. Both qualitative consideration of transport direction and air mass aging plus quantitative analysis of the ambient samples used here to determine the concentrations of likely secondary aerosol reaction products (e.g., dicarboxylic acids, see Rogge et al., 1993a) suggest that the secondary aerosol levels should be highest at the far downwind site at Rubidoux. The model results indeed show that 31% of the organic aerosol at Rubidoux cannot be attributed to the major primary sources. This places an upper limit of 31% on the contribution of secondary organic aerosol at that site. At West Los Angeles, Downtown Los Angeles, and Pasadena, the comparable upper limit on secondary organic aerosol concentrations in 1982 is in the range of 15-18 percent of the fine organic aerosol. These estimates can be compared to previous work. Based on the ratio of organic carbon to elemental carbon in ambient samples and in source emissions, Gray et al. (1986) estimated that 27-38 percent of the organic aerosol at Rubidoux in 1982 was secondary in origin. The photochemical trajectory

modeling study by Pandis et al. (1992) placed secondary organic aerosol concentrations as a fraction of total organic aerosol during a 1987 summer smog episode in the Los Angeles area at 5-8 percent at near-coastal sites and at about 15-22 percent at Claremont, California (located approximately half-way between Pasadena and Rubidoux). Based on differences observed between ambient organic aerosol concentrations versus primary source contributions to acidic organics calculated using a Lagrangian transport model, Hildemann et al. (1993) estimated as an upper limit that 18-27 percent of the organic aerosol was secondary in origin at the three western basin sites studied here. The upper limits on secondary organic aerosol concentrations established by the present study are consistent with these prior estimates.

The relative contribution of the various primary sources to the concentrations of individual particulate organic compounds also can be computed from the model. The percentage of the modeled individual organic compound concentrations predicted to be due to each of the primary sources studied is illustrated for Downtown Los Angeles in Figure 9.6.

#### **9.4.1 Total Fine Particulate Mass Apportionment**

The ratio of single organic compound concentrations to both the total organic aerosol mass concentration and to the overall fine particulate mass concentration is known for both the source emissions and ambient data sets

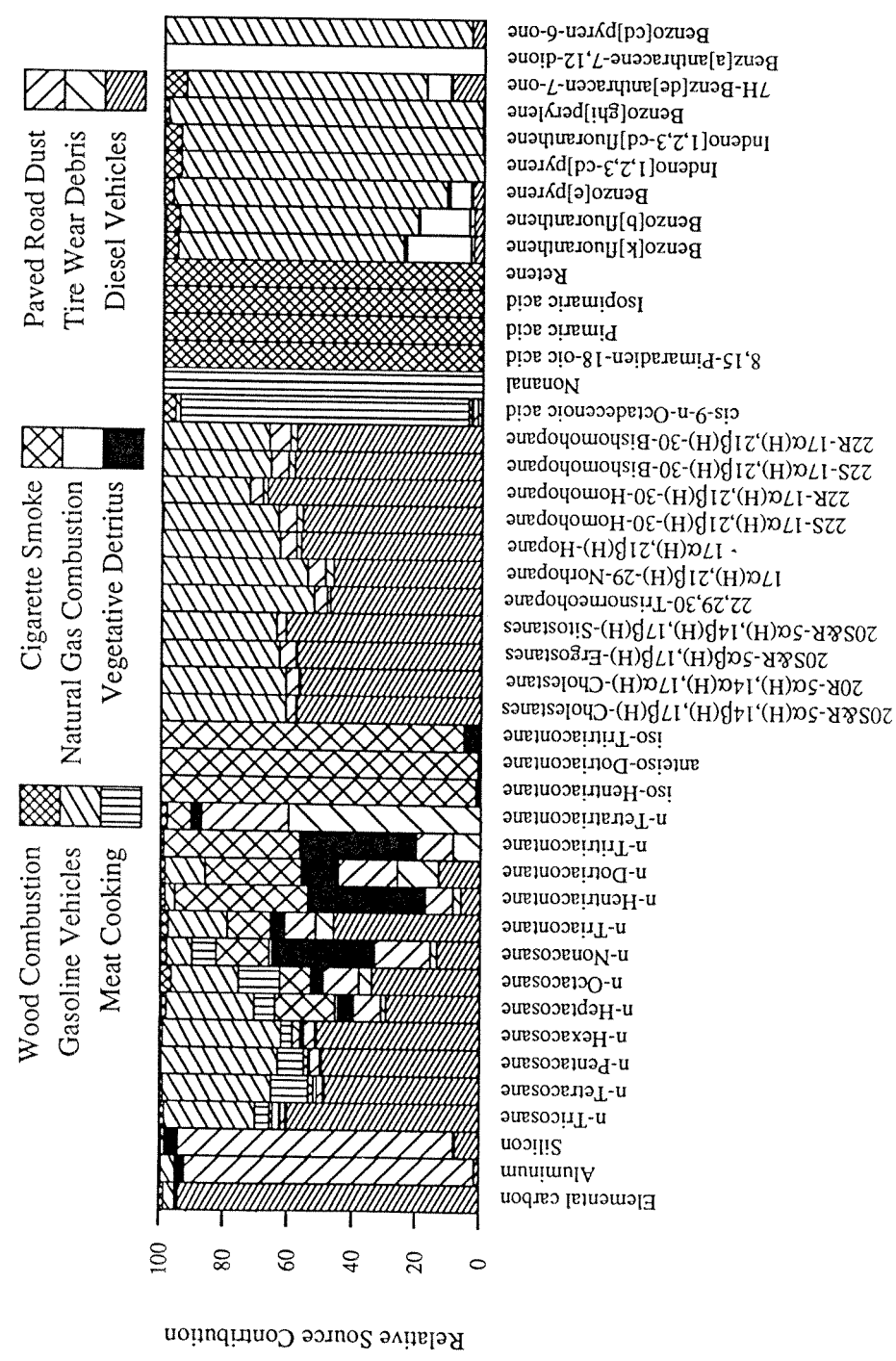


Figure 9.6. Relative source contribution to modeled ambient concentrations of organic compounds used in the mass balance at Downtown Los Angeles - 1982 annual average.

used here (Gray et al., 1986; Rogge et al., 1993a; Hildemann et al., 1991). Therefore, the receptor model can be used to apportion total fine particulate mass concentrations between contributing sources. The results of that calculation are shown in Figure 9.7 and Table 9.4. In that figure, the sulfate, nitrate and ammonium ion increments shown are obtained from the  $\text{SO}_4^-$ ,  $\text{NO}_3^-$ , and  $\text{NH}_4^+$  ion concentrations reported by Gray et al. (1986) after subtracting the primary sulfate, nitrate and ammonium ion concentrations that accompany the direct emissions from the primary sources studied here according to the source emission profiles of Hildemann et al. (1991). The sulfate, nitrate and ammonium ion increments shown in Figure 9.7 are largely due to local secondary aerosol formation, but also include contributions from background air transported from upwind plus possible small increments from primary  $\text{SO}_x$  sources that are not included in the model (e.g., refinery FCC Units; see Cass, 1981). The secondary organic aerosol is contained within the Other Organics category as discussed earlier. The total fine particulate mass concentrations assigned to the sources studied by the model plus secondary aerosol are not statistically different from the total fine particulate mass concentrations measured by Gray et al. (1986). Within  $\pm 1\text{-}2 \mu\text{g m}^{-3}$ , all major sources of airborne fine particulate mass are accounted for in the model at West Los Angeles, Downtown Los Angeles and Pasadena; results at Rubidoux are still within  $\pm 2\sigma$  of closing a material balance on the origin of the entire fine aerosol. As seen in Figure 9.7, the major primary fine particulate source contributions are attributed to diesel



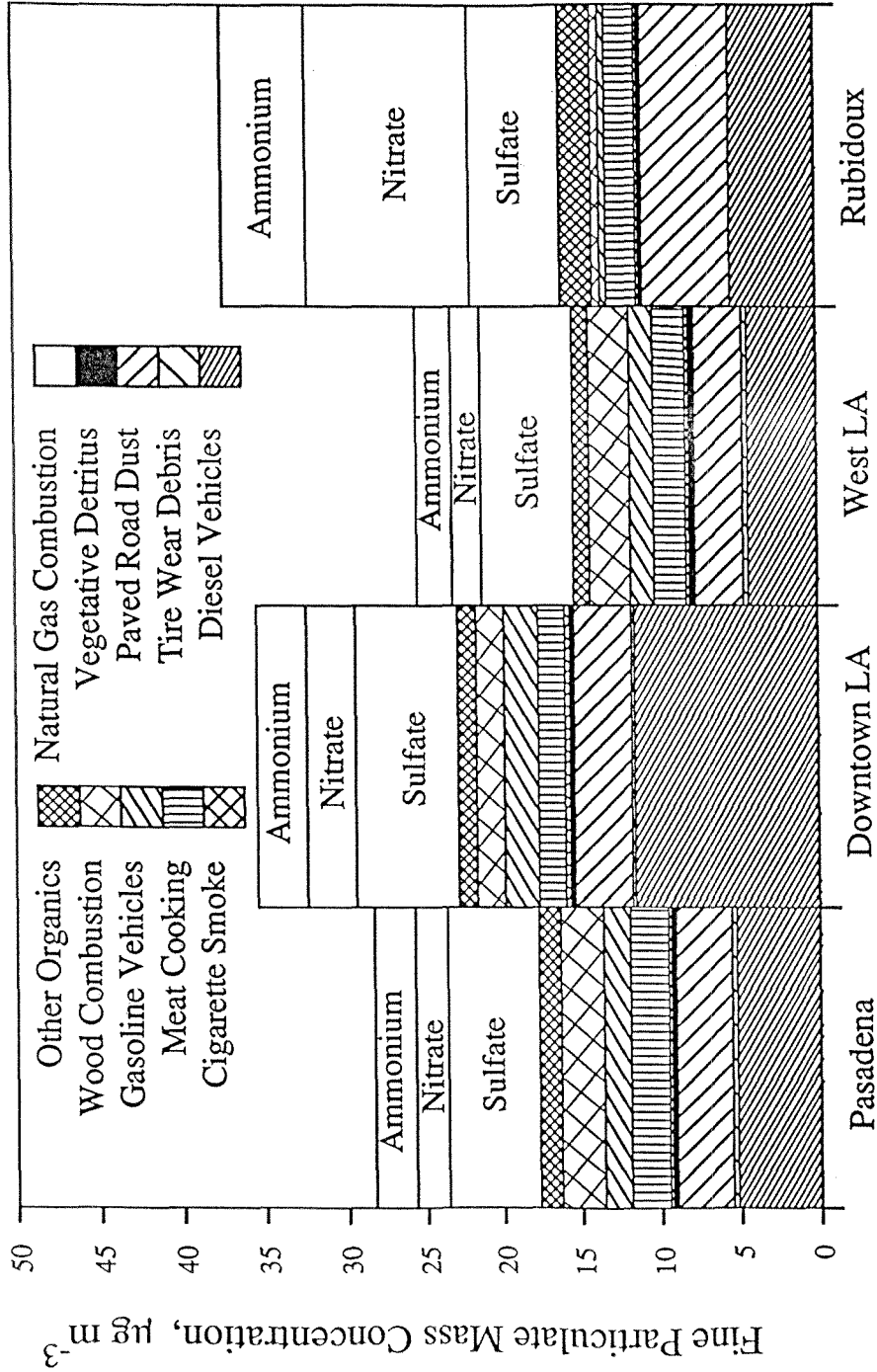


Figure 9.7. Source apportionment of fine particulate mass concentrations - 1982 annual average.

Table 9.4. Source Apportionment of Fine Particulate Mass Concentration: 1982 Annual Average Determined by Chemical Mass Balance

SOURCE	Pasadena	Downtown LA	West Los Angeles	Rubidoux
	Source Contribution avg $\pm$ std $\mu\text{g m}^{-3}$	Source Contribution avg $\pm$ std $\mu\text{g m}^{-3}$	Source Contribution avg $\pm$ std $\mu\text{g m}^{-3}$	Source Contribution avg $\pm$ std $\mu\text{g m}^{-3}$
Diesel Exhaust	5.27 $\pm$ 0.72	11.6 $\pm$ 1.19	4.36 $\pm$ 0.64	5.35 $\pm$ 0.51
Tire Wear Debris	0.29 $\pm$ 0.11	0.22 $\pm$ 0.09	0.25 $\pm$ 0.09	*
Paved Road Dust	3.46 $\pm$ 0.43	3.62 $\pm$ 0.46	3.00 $\pm$ 0.39	5.50 $\pm$ 0.61
Vegetative Detritus	0.33 $\pm$ 0.10	0.24 $\pm$ 0.12	0.38 $\pm$ 0.11	0.18 $\pm$ 0.08
Natural Gas Combustion Aerosol	0.047 $\pm$ 0.02	0.040 $\pm$ 0.019	0.034 $\pm$ 0.016	0.029 $\pm$ 0.008
Cigarette Smoke	0.18 $\pm$ 0.03	0.26 $\pm$ 0.045	0.20 $\pm$ 0.028	0.19 $\pm$ 0.032
Meat Charbroiling and Frying	2.41 $\pm$ 0.46	1.74 $\pm$ 0.34	2.03 $\pm$ 0.39	1.94 $\pm$ 0.35
Catalyst and Non-Catalyst Gasoline-Powered Vehicle Exhaust	1.63 $\pm$ 0.20	2.12 $\pm$ 0.23	1.44 $\pm$ 0.16	0.34 $\pm$ 0.05
Wood Smoke	2.70 $\pm$ 0.43	1.85 $\pm$ 0.31	2.65 $\pm$ 0.41	0.54 $\pm$ 0.07
Organics (Other + Secondary)	1.46 $\pm$ 0.66	1.16 $\pm$ 0.76 †	1.03 $\pm$ 0.71 †	1.94 $\pm$ 0.44
Sulfate ion (Secondary + Background)	5.9 $\pm$ 0.60	6.6 $\pm$ 0.65	5.9 $\pm$ 0.60	5.8 $\pm$ 0.51
Secondary nitrate ion	2.1 $\pm$ 0.27	3.0 $\pm$ 0.54	1.9 $\pm$ 0.29	10.4 $\pm$ 1.2
Secondary ammonium ion	2.6 $\pm$ 0.34	3.0 $\pm$ 0.37	2.3 $\pm$ 0.23	5.1 $\pm$ 0.59
SUM	28.3 $\pm$ 1.5	35.5 $\pm$ 1.9	25.3 $\pm$ 1.4	37.3 $\pm$ 1.8
Measured	28.2 $\pm$ 1.9	32.5 $\pm$ 2.8	24.5 $\pm$ 2.0	42.1 $\pm$ 3.3

\* Not statistically different from zero with greater than 95% confidence, and therefore removed from CMB Model.

† Not statistically different from zero with greater than 95% confidence.

soot, paved road dust, gasoline-powered motor vehicles exhaust, food cooking operations and wood smoke with small but quantifiable contributions from cigarette smoke, natural gas combustion aerosol, tire wear debris, and plant fragments. Secondary aerosol concentrations again are highest at the farthest downwind site at Rubidoux, as expected.

## 9.5 References

- Appel B. R., Wall S. M. and Knights R. L. (1980) Characterization of carbonaceous materials in atmospheric aerosols by high-resolution mass spectrometric thermal analysis. In *The Character and Origin of Smog Aerosols, Advances in Environmental Science and Technology* (edited by Pitts J. N. Jr. and Metcalf R. L.), Vol. 9, pp. 353-365, Wiley, New York.
- Atkinson S. E. and Lewis D. H. (1974) A cost-effective analysis of alternative air quality control strategies. *J. Environ. Econ. Manage.* **1**, 237-250.
- Bencala K. E. and Seinfeld J. H. (1979) An air quality model performance assessment package. *Atmos. Environ.* **13**, 1181-1185.
- Cass G. R. (1981) Sulfate air quality control strategy design. *Atmos. Environ.* **15**, 1227-1249.
- Cass G. R., Boone P. M. and Macias E. S. (1982) Emissions and air quality relationships for atmospheric carbon particles in Los Angeles. In *Particulate Carbon: Atmospheric Life Cycle* (edited by Wolff G. T. and Klimisch R. L.), pp. 207-243, Plenum Press, New York.
- Cass G. R. and McRae G. J. (1983) Source-receptor reconciliation of routine air monitoring data for trace metals: An emissions inventory assisted approach. *Environ. Sci. Technol.* **17**, 129-139.

- Cooper J. A. and Watson J. G. (1980) Receptor oriented methods of air particulate source apportionment. *JAPCA* **30**, 1116-1125.
- Cronn D. L., Charlson R. J. and Appel B. R. (1977) A study of the molecular nature of primary and secondary components of particles in urban air by high-resolution mass spectrometry. *Atmos. Environ.* **11**, 929-937.
- Dockery D. W., Pope C. A. III, Xu X., Spengler J. D., Ware J. H., Martha E. F., Ferris B. G. Jr. and Speizer F. E. (1993) An association between air pollution and mortality in six U.S. Cities. *N. Engl. J. Med.* **329**, 1753-1759.
- Eckey E. W. (1954) *Vegetable Fats and Oils*. p. 25, Reinhold, New York.
- Friedlander S. K. (1973) Chemical element balances and identification of air pollution sources. *Environ. Sci. Technol.* **7**, 235-240.
- Gordon, G. E. (1980) Receptor Models. *Environ. Sci. Technol.* **14**, 792-800.
- Gray H. A. (1986) Control of atmospheric fine primary carbon particle concentrations. Ph.D. Thesis, California Institute of Technology, Pasadena, CA.

- Gray H. A., Cass G. R., Huntzicker J. J., Heyerdahl E. K. and Rau J. A. (1986) Characterization of atmospheric organic and elemental carbon particle concentrations in Los Angeles. *Sci. Tot. Environ.* **20**, 580-589.
- Grosjean D. (1977) Aerosols, Chapter 3. In *Ozone and other photochemical oxidants* National Academy of Sciences, Washington, D. C.
- Grosjean D. and Friedlander S. K. (1980) Formation of organic aerosols from cyclic olefins and diolefins. In *The character and origin of smog aerosols, Advances in Environmental Science and Technology* (edited by Pitts J. N. Jr. and Metcalf, R. L.), Vol. 9, pp. 435-473, Wiley, New York.
- Harley R. A., Hunts S. E. and Cass G. R. (1989) Strategies for the control of particulate air quality: Least-cost solutions based on receptor oriented models. *Environ. Sci. Technol.* **23**, 1007-1014.
- Hildemann L. M., Markowski G. R. and Cass G. R. (1989) A dilution stack sampler for collection of organic aerosol emissions: design, characterization, and field tests. *Aerosol Sci. Technol.* **10**, 193-204.
- Hildemann L. M., Markowski G. R. and Cass G. R. (1991) Chemical composition of emissions from urban sources of fine organic aerosol. *Environ. Sci. Technol.* **25**, 744-759.

- Hildemann L. M., Cass G. R., Mazurek M. A. and Simoneit B. R. T. (1993) Mathematical modeling of urban organic aerosol: Properties measured by high-resolution gas chromatography. *Environ. Sci. Technol.* **27**, 2045-2055.
- Hopke P. K., Gladney E. S., Gordon G. E., Zoller W. H. and Jones A. G. (1976) The use of multivariate analysis to identify sources of selected elements in Boston aerosol. *Atmos. Environ.* **10**, 1015-1025.
- Huntzicker J.J., Johnson R. L., Shah J. J., and Cary R. A. (1982) Analysis of organic and elemental carbon in ambient samples by a thermal optical method. In *Particulate Carbon: Atmospheric Life Cycle* (edited by Wolff G. T. and Klimisch R. L.), pp. 79-85, Plenum Press, New York.
- John W. and Reischl G. (1980) A cyclone for size-selective sampling of ambient air. *JAPCA* **30**, 872-876.
- Johnson R. L., Shah J. J., Cary R. A. and Huntzicker J. J. (1981) An automated thermal-optical method for the analysis of carbonaceous aerosol. In *Atmospheric aerosols: source/air quality relationship* (edited by E. S. Macias and P. K. Hopke) American Chemical Society, Washington, D. C.
- Kamens R. M., Guo Z., Fulcher J. N. and Bell D. A. (1988) Influence of humidity, sunlight, and temperature on the daytime decay rate of polyaromatic

- hydrocarbons on atmospheric soot particles. *Environ. Sci. Technol.* **22**, 103-108.
- Kamens R. M., Karam H., Guo J., Perry J. M. and Stockburger L. (1989) Behavior of oxygenated polycyclic aromatic hydrocarbons on atmospheric soot particles. *Environ. Sci. Technol.* **23**, 801-806.
- Liu M. K. and Seinfeld J. H. (1975) On the validity of grid and trajectory models of urban air pollution. *Atmos. Environ.* **9**, 555-574.
- Mazurek M. A., Simoneit B. R. T., Cass G. R. and Gray H. A. (1987) Quantitative high-resolution gas chromatography and high-resolution gas chromatography/mass spectrometry analysis of carbonaceous fine aerosol particles. *Intern. J. Environ. Anal. Chem.* **29**, 119-139.
- Mazurek M. A., Simoneit B. R. T. and Cass G. R. (1989) Interpretation of high-resolution gas chromatography and high-resolution gas chromatography/mass spectrometry data acquired from atmospheric aerosol samples. *Aerosol Sci. Technol.* **10**, 408-419.
- Mazurek M. A., Cass G. R. and Simoneit B. R. T. (1991) Biological input to visibility-reducing particles in the remote arid southwestern United States. *Environ. Sci. Technol.* **25**, 684-694.



- Mazurek M. A., Hildemann L. M., Cass G. R., Simoneit B. R. T. and Rogge W. F. (1993) Methods of analysis for complex organic aerosol mixtures from urban emission sources of particle carbon. In *Measurement of Airborne Compounds: Sampling, Analysis, and Data Interpretation*. (edited by Winegar E. D. and Keith L. H.), pp. 177-190, American Chemical Society Symposium Series, CRC Press, Boca Raton, FL.
- Miller M.S., Friedlander S. K. and Hidy G. M. (1972) A chemical element balance for the Pasadena aerosol. *Colloid Interface Sci.* **39**, 165-176.
- Mueller P. K., Mendoza B. V., Collins, J. C. and Wilgus E. A. (1978) Application of ion chromatography to the analysis of anions extracted from airborne particulate matter. In *Ion Chromatographic Analysis of Environmental Pollutants* (edited by Sawicki E., Mulik J. D., and Wittgenstein E.), pp. 77-86, Ann Arbor Science, Ann Arbor, MI.
- Ouimette J. R. and Flagan R. C. (1982) The extinction coefficient of multicomponent aerosols. *Atmos. Environ.* **16**, 2405-2419.
- Pandis S. N., Harley R. A., Cass G. R. and Seinfeld J. H. (1992) Secondary organic aerosol formation and transport. *Atmos. Environ.* **26A**, 2269-2282.

- Rogge W. F., Hildemann L. M., Mazurek M. A., Cass G. R. and Simoneit B.R.T.  
(1991) Sources of fine organic aerosol. 1. Charbroilers and meat cooking operations. *Environ. Sci. Technol.* **25**, 1112-1125.
- Rogge W. F., Mazurek M. A., Hildemann L. M., Cass G. R. and Simoneit B.R.T.  
(1993a) Quantification of urban organic aerosols at a molecular level: Identification, abundance and seasonal variation. *Atmos. Environ.* **27**, 1309-1330
- Rogge W. F., Hildemann L. M., Mazurek M. A., Cass G. R. and Simoneit B.R.T.  
(1993b) Sources of fine organic aerosol. 2. Noncatalyst and catalyst-equipped automobiles and heavy duty diesel trucks. *Environ. Sci. Technol.* **27**, 636-651.
- Rogge W. F., Hildemann L. M., Mazurek M. A., Cass G. R. and Simoneit B.R.T.  
(1993c) Sources of fine organic aerosol. 3. Road dust, tire debris, and organometallic brake lining dust: Roads as sources and sinks. *Environ. Sci. Technol.* **27**, 1892-1904
- Rogge W. F., Hildemann L. M., Mazurek M. A., Cass G. R. and Simoneit B.R.T.  
(1993d) Sources of fine organic aerosol. 4. Particulate abrasion products from leaf surfaces of urban plants. *Environ. Sci. Technol.* **27**, 2700-2711.

- Rogge W. F., Hildemann L. M., Mazurek M. A., Cass G. R. and Simoneit B.R.T. (1993e) Sources of fine organic aerosol. 5. Natural gas home appliances. *Environ. Sci. Technol.* **27**, 2736-2744.
- Rogge W. F. (1993) Molecular tracers for sources of atmospheric carbon particles: Measurements and model predictions. Ph.D. Thesis. California Institute of Technology, Pasadena, CA
- Rogge W. F., Hildemann L. M., Mazurek M. A., Cass G. R. and Simoneit B.R.T., (1994) Sources of fine organic aerosol: 6. Cigarette smoke in the urban atmosphere. *Environ. Sci. Technol.* **28**, 1375-1388.
- Satsumabayashi H. and Kurita H. (1989) Photochemical formation of particulate dicarboxylic acids under long-range transport in central Japan. *Atmos. Environ.* **24A**, 1443-1450.
- Sehmel G. A. (1980) Particle and gas dry deposition: A review. *Atmos. Environ.* **14**, 983-1011.
- Solorzano L. (1969) Determination of ammonia in natural waters by the phenolhypochlorite method. *Limnol. Oceanogr.* **14**, 799-801.
- Venkataraman C. and Friedlander S. K. (1994) Size distribution of polycyclic aromatic hydrocarbons and elemental carbon. 2. Ambient measurements

and effects of atmospheric processes. *Environ. Sci. Technol.* **28**, 563-572.

Watson J. G. (1984) Overview of receptor model principles. *JAPCA* **34**, 619-623.

Watson J. G., Cooper J. A. and Huntzicker J. J. (1984) The effective variance weighting for least squares calculations applied to the mass balance receptor model. *Atmos. Environ.* **18**, 1347-1355.

Watson J. G., Robinson N. F., Chow J. C., Henry R. C., Kim B. M., Pace T. G., Meyer E. I. and Nguyen Q. (1990) The USEPA/DRI chemical mass balance receptor model, CMB 7.0. *Environ. Softw.* **5**, 38-49.

## Chapter 10

# Source Apportionment of Wintertime Gas-Phase and Particle-Phase Air Pollutants Using Organic Compounds as Tracers

### 10.1 Introduction

Chemical mass balance receptor modeling methods have been developed recently that employ fine particulate organic compounds as tracers for the sources that contribute to fine particle concentrations in the atmosphere (Schauer et al., 1996). To date it has been demonstrated that the annual average primary contributions of nine air pollution source types to fine particulate mass, fine particle organic compound mass, and individual fine particle organic compound concentrations can be separately identified in the Los Angeles atmosphere. This technique provides a powerful tool in understanding the long-term average contributions to atmospheric fine particle concentrations. However, in many cases the source contributions to episodic situations of a few days duration over which high atmospheric fine particle concentrations occur are sought. Such episodes occur in California's San Joaquin Valley in the winter months (Chow et. al., 1992; Chow et al, 1993).

The 1995 Integrated Monitoring Study (IMS95) was commissioned to address these high fine particle concentration episodes experienced in the San

Joaquin Valley during the winter months. Two of the objectives of the IMS95 project are (1) to determine the primary and secondary contributions to fine particle mass concentrations and the origin of the gas-phase pollutants in the San Joaquin Valley during high pollution episodes and (2) to determine whether the contributions to the atmospheric pollutant concentrations in the San Joaquin Valley during the high pollution episodes are uniform throughout the valley which would indicate a regional air pollution problem or alternatively to determine the extent to which the high pollutant concentrations experienced in the urban areas are dominated by local emission sources.

To address these questions, the organic chemical tracer-based receptor model developed by Schauer et al. (1996) is used in the present paper to apportion source contributions to fine particle mass concentrations at three sites in the San Joaquin Valley during two 48-hour high pollution episodes. In addition, a second source apportionment model is developed that can identify contributions to the wintertime concentrations of non-methane organic gases. In the past, chemical mass balance receptor models for vapor-phase organic compounds have relied heavily on the atmospheric concentrations of acetylene, ethylene, and benzene to distinguish the differences between the tailpipe emissions from gasoline-powered motor vehicles versus the vapors from whole gasoline spillage (Harley et al., 1992; Scheff and Wadden, 1993; Fujita et al., 1994). Since acetylene, ethylene, and benzene are emitted in relatively high

concentrations from wood combustion (Chapter 6) and other combustion sources, the concentrations of these compounds in the atmosphere during periods of high home heating fuel consumption (e.g., wood, natural gas, heating oil) likely will be influenced by emissions from sources other than the tailpipes of motor vehicles. Improper accounting for the emissions of acetylene, ethylene, and benzene from these home heating sources would lead to an incorrect attribution of a portion of the whole gasoline vapor emissions to motor vehicle tailpipe emissions. In the present study, a combined gas-phase and fine particle-phase organic compound tracer model is developed that can apportion source contributions to organic vapor concentrations without the use of acetylene, ethylene, and benzene as tracers for motor vehicle combustion products. This is accomplished by bringing to bear on the problem the particle-phase tracers for motor vehicle exhaust, wood combustion, etc., that have been previously used in the particulate matter source apportionment study of Schauer et al. (1996).

## **10.2 Experimental Methods**

### **10.2.1 Ambient Samples**

The fine particle ambient samples used in the present study were collected at the three core air monitoring sites used in the IMS95 wintertime sampling program in the San Joaquin Valley: Fresno, Bakersfield, and Kern

Wildlife Refuge. Maps and a description of these sampling locations have been provided by Chow and Egami (1997). The Fresno site is located between a residential neighborhood and farmland within a city in the central San Joaquin Valley, while the Bakersfield site is located within a major city between a residential and an industrial neighborhood in the southern region of the valley. The Kern Wildlife Refuge site is at a remote location in the south-central region of the valley slightly west of a straight line between Fresno and Bakersfield.

Fine particle samples were collected for organic carbon analysis, elemental carbon analysis, and organic compound speciation using high-volume dichotomous virtual impactors (Solomon et al., 1983). Starting at noon and ending at noon the following day, 24-hour samples were collected on quartz fiber filters (102 mm diameter, Pallflex Tissuequartz 2500 QAO). Samples were taken daily from December 9, 1995, to January 6, 1996; samples collected over December 26-28, 1995, and January 4-6, 1996, are selected for detailed analysis in the present paper. The quartz fiber filters were baked at 550 °C for 12 hours prior to sampling and were stored in baked aluminum foil pouches before use and were stored in cleaned glass jars with Teflon lid liners after sample collection. Sections cut from the fine particle filters from the high-volume dichotomous samplers were used for organic carbon and elemental carbon concentration determination as described by Birch and Cary (1996). Another section of each filter was used for individual organic compound



identification and quantification by gas chromatography/mass spectrometry (GC/MS) analysis, as will be described shortly.

The particulate organic carbon and organic compound data described above are accompanied by ambient measurements of fine particle mass concentrations, fine particle aluminum and silicon concentrations, and fine particle sulfate ion, nitrate ion, and ammonium ion concentrations made using medium-volume samplers that were co-located alongside the high-volume dichotomous samplers (Chow and Egami, 1997). Eight consecutive 3-hour medium-volume filter samples were collected by the staff of the Desert Research Institute over the duration of each 24-hour high volume dichotomous virtual impactor sample. Daily averaged fine particle mass concentrations and chemical compositions were computed from the 4-hour measurements taken by the co-located samplers. Fine particle mass and chemical composition measurements made on the medium-volume filter samples were conducted by Dr. Judy Chow and associates at the Desert Research Institute (DRI). Ambient volatile gas-phase hydrocarbons were collected in SUMA canisters over the same 24-hour cycle on which the high volume dichotomous sampler was operated. The ambient concentrations of gas-phase volatile hydrocarbons were measured by gas chromatography/flame ionization detection by Dr. Reinhard Rasmussen and associates. Gas-phase hydrocarbon uncertainties were

estimated to be 5% down to a threshold of  $0.1 \mu\text{g m}^{-3}$ , which is based on duplicate samples taken during the IMS95 project.

The glass jar that contained the high volume dichotomous virtual impactor sample from the Fresno site on January 4, 1996, was cracked during shipping. Although the sample shows no signs of significant contamination, we still wish to note this anomaly and have limited the particulate matter source apportionment results for the January 4-6, 1996, episode in Fresno accordingly.

### **10.2.2 Source Samples**

A series of air pollution source tests has been conducted to obtain comprehensive emissions source profiles that describe gas-phase, semi-volatile, and particle-phase organic compounds, including hydrocarbons, carbonyls, and organic acids, plus fine particle emission rates and fine particle elemental composition (Chapters 2 through 8). A dilution source sampler was employed to dilute hot exhaust emissions with HEPA-filtered and activated carbon-filtered dilution air to near ambient temperatures and pressures. The sampler is equipped with a residence time chamber that provides time for the cooled semi-volatile gases to equilibrate between the gas and particle phases. The diluted exhaust then was sampled from the residence time chamber by the same analytical techniques used for ambient air pollutant measurements. From these measurements the phase-distribution of the semi-volatile compounds can be

determined under the conditions that occur in the diluted plume immediately downwind of an air pollution source.

A detailed description of the dilution source sampler and associated sampling equipment has been presented previously (Hildemann et al., 1989; Hildemann et al., 1991; Chapter 2) and will not be repeated, but a brief description of the measurements is given here. Fine particle organic compound emissions were sampled by two simultaneous sampling trains, a denuder/filter/PUF system and a filter/PUF system. In both sampling trains, diluted exhaust was withdrawn from the residence time chamber of the source sampler through AIHL-design cyclone separators (John and Reischl, 1980) that removed coarse particles. In the present receptor modeling study, semi-volatile organic compounds are not used as tracers, such that the organic compounds of concern are those that are entirely collected on the quartz fiber filters (47 mm diameter, Pallflex Tissuequartz 2500 QAO) present in both the denuder/filter/PUF sampling train and the filter/PUF sampling trains.

In addition to the above sampling trains, a third type of cyclone-based sampling unit was operated during each source test to collect fine particulate matter and gas-phase hydrocarbons. In this sampling train, one AIHL fine particle cyclone separator is followed by three filter packs operated in parallel. The first filter pack is a stacked filter unit consisting of two quartz fiber filters (47 mm diameter, Pallflex Tissuequartz 2500 QAO) in series which are used for

elemental and organic carbon (EC/OC) determination by the same method as for the atmospheric particle samples. The second filter stack in this sampling train contains a Teflon membrane filter (47 mm diameter, Gelman Teflo, 2  $\mu\text{m}$  pore size) which was used for gravimetric determination of the fine particle mass emissions rate and for analysis of aluminum and silicon by the same X-ray fluorescence technique as used for the ambient samples. The third filter holder assembly contained one Teflon membrane filter which was used for a duplicate fine particle mass emissions measurement and for sulfate ion, nitrate ion, and ammonium ion determination by ion chromatography and colorimetry. Downstream of the Teflon filter the sample flow was divided, and a small portion of the flow was used to fill a 6 liter polished stainless steel SUMA canister for the collection of non-methane volatile hydrocarbons ranging from  $\text{C}_1$  to  $\text{C}_{10}$  and total non-methane organic gases (EPA method TO12). The 6 liter SUMA canister was filled continuously at a constant flowrate set to fill the canister over the entire source test cycle. Volatile hydrocarbons in the source emissions were analyzed by the same laboratory as used for the San Joaquin Valley ambient measurements according to the procedure described by Fraser et al. (1996). Uncertainties ( $\pm 1\sigma$ ) for the volatile hydrocarbon emissions measurements were determined to be  $\pm 10\%$ .

Emissions from gasoline-powered motor vehicle engines, diesel engines, fireplace combustion of hardwoods, fireplace combustion of softwood, and meat

cooking operations were measured by the sampling system described above. The diesel trucks described in Chapter 4 were 1995 model year medium-duty diesel trucks that emitted particulate matter with a lower fine particle elemental carbon content than the heavy-duty diesel trucks measured by Hildemann et al. (1991). Since heavy duty trucks dominate the emissions from the diesel fleet, the source profile for diesel trucks used in the present study combines the organic chemical composition of diesel exhaust measured as discussed in Chapter 4 with the higher fraction elemental carbon emission rate measured for heavy duty diesel trucks by Hildemann et al. (1991).

In addition, several other emissions profiles were required for the present receptor modeling study. A road dust emissions profile was generated by resuspending road dust collected in the San Joaquin Valley during the IMS95 study (Ashbaugh, 1996) and then introducing the road dust/air mixture into the residence time chamber of the dilution source sampler. Samples were drawn through AIHL-design cyclone separators to remove coarse particles and were collected on quartz fiber filters and Teflon filters as described above for the other sources tested. Gas-phase measurements were not made for the road dust sample as road dust is not thought to be a significant source of gas-phase pollutants. (Emissions profiles for the IMS95 road dust samples are included in Appendix A.) In addition, fine particle emissions profiles that describe the organic chemical composition of vegetative detritus and residential natural gas

combustion aerosol were taken from the work of Rogge et al. (1993a, 1993b). Individual gas-phase hydrocarbon and total non-methane organic gas emissions data for these sources were not available. Finally, a 1995 gasoline sample assembled as a market share weighted average of the product of the five largest gasoline retailers in Southern California was collected and analyzed to obtain a whole gasoline vapor emissions profile.

Two additional source profiles were needed for the present study, a gasoline headspace vapor profile that corresponds to the 1995 gasoline sample and a natural gas leakage profile. Conner et al. (1995) have shown that the composition of the headspace vapors above a liquid pool of gasoline can be accurately calculated from the liquid gasoline composition and the Raoult's law coefficients for the individual gasoline components in a gasoline mixture. The gasoline headspace vapor composition for this study was therefore calculated using Raoult's law coefficients from the data collected by Aulich et al. (1994). (The whole gasoline and gasoline headspace vapor emissions profiles are included in Appendix B.) The natural gas leakage profile was taken from Harley et al. (1992), and will capture the effect of unburned natural gas emitted from poorly operated natural gas combustors as well.

### 10.2.3 Organic Chemical Analysis

The filter handling and extraction procedures employed to quantify particle-phase organic compounds collected in atmospheric samples and in source emissions samples have been discussed in great detail elsewhere (Chapters 2 through 8, Rogge et al., 1993a; Rogge et al, 1993b). Briefly, before the quartz fiber filters were extracted, they were spiked with a mixture of seven deuterated internal recovery standards: n-decane-d<sub>12</sub>, n-pentadecane-d<sub>32</sub>, n-tetracosane-d<sub>50</sub>, n-hexanoic acid-d<sub>11</sub>, n-decanoic acid-d<sub>19</sub>, phenol-d<sub>5</sub>, benzoic acid-d<sub>5</sub>, and benzaldehyde-d<sub>6</sub>. The samples were extracted twice with hexane (Fisher Optima Grade), followed by three successive benzene/isopropanol (2:1) extractions (benzene: E&M Scientific high purity lots; isopropanol: Burdick & Jackson). Extracts were filtered, combined, and reduced in volume to approximately 250 µl, and were split into two separate fractions. One fraction was then derivatized with diazomethane to convert organic acids to their methyl ester analogues which are amenable to GC/MS identification and quantification.

Both the derivatized and underivatized sample fractions were analyzed by GC/MS on a Hewlett-Packard GC/MSD (GC Model 5890, MSD Model 5972) using a 30 m X 0.25 mm diameter HP-1701 capillary column (Hewlett-Packard). 1-Phenyldodecane was used as a co-injection standard for all sample extracts and standard runs. The deuterated n-alkanes in the internal standard were used to determine extraction recovery for the compounds quantified in the

underivatized samples. The deuterated acids were used to verify that the diazomethane reactions were driven to completion, and were used in conjunction with the recovery of deuterated tetracosane to determine the recovery of the compounds quantified in the derivatized fraction.

Hundreds of authentic standards have been prepared for the positive identification and quantification of the organic compounds found in the current source test program and ambient sampling program. When quantitative standards could not be obtained for a given compound or compound class, significant effort was made to obtain a non-quantitative secondary standard that could be used for unique identification of the organic compounds. An example of such a secondary standard is the use of motor oil as a source of hopanes and steranes that was used to help identify these compounds in the fine particle diesel exhaust and in the atmospheric samples. Quantification of compounds identified using secondary standards has been estimated from the response factors for compounds having similar retention times and chemical structure.

The uncertainties ( $\pm 1\sigma$ ) for the quantification of organic compounds in the particulate matter collected from source emissions and in atmospheric samples was determined to average  $\pm 20\%$ .



## 10.3 Source/Receptor Reconciliation

### 10.3.1 Chemical Mass Balance Approach

Organic compounds have been used in the past as tracer species in chemical mass balance models (Harley et al., 1992; Scheff and Wadden, 1993; Fujita et al., 1994; Schauer et al., 1996). In these models, the total ambient concentration of each of the organic compounds used in the mass balance model is reconstructed from the best linear combination of source emissions profiles that reproduce the composition of the ambient sample as a whole. The chemical mass balance model can be expressed by the following set of linear equations:

$$c_{ik} = \sum_{j=1}^m a_{ij} s_{jk} \quad (1)$$

where  $c_{ik}$ , the concentration of chemical species  $i$  in fine particles at receptor site  $k$ , equals the sum over  $m$  source types of the product of  $a_{ij}$ , the relative concentration of chemical constituent  $i$  in the fine particle emissions from source  $j$ , multiplied by  $s_{jk}$ , the increment to total fine particulate mass concentration at receptor site  $k$  originating from source  $j$ . The system of equations (1) states that the ambient concentration of each mass balance species must result only from the  $m$  sources included in the model and that no selective loss or gain of species  $i$  occurs in transport from the source to the receptor site. Therefore, the selection

of mass balance compounds must be limited to: (1) species for which all major sources are included in the model, (2) species that do not undergo selective removal by chemical reaction or other mechanisms over the time scale for transport between the source and the receptor site, and (3) species which are not significantly formed by chemical reactions in the atmosphere.

In the present study, the system of equations (1) is solved using the CMB7 receptor modeling computer program (Watson et al., 1990) which seeks an effective variance weighted least-squares solution to the overdetermined set of mass balance equations, and which takes into account the known uncertainties in the atmospheric measurements and the emissions data.

### **10.3.2 Selection of Sources and Organic Compounds**

The selection criteria for the particle-phase organic compounds which are used as tracers in the current study are based on the previous work by Schauer et al. (1996). We begin with the list of tracer compounds adopted by Schauer et al. (1996) and then extend the list based on the results of the new source tests discussed above. Of most significance is the recent quantification of levoglucosan in the emissions from both hardwood and softwood combustion (Chapter 6) and in the ambient air in the San Joaquin Valley. Levoglucosan is a major constituent of the fine particle emissions from wood combustion and is therefore added as an additional wood smoke tracer. Likewise,

propionylsyringol and butyrylsyringol in the emissions from hardwood combustion are identified as tracers that are unique to hardwood combustion; when used in conjunction with the resin acids emitted from pinewood combustion plus levoglucosan, a unique set of source fingerprints are provided that can be used to separate hardwood combustion emissions from softwood combustion emissions. With the advent of better tracers for wood smoke, retene (which is semi-volatile and thus subject to possible evaporation in the atmosphere) is removed as a tracer species for wood smoke.

9-Octadecenoic acid has been used in the past with particle-bound nonanal to help trace emissions from meat cooking operations. Recent source tests indicate that 9-octadecenoic acid also is emitted from cooking operations that use seed oils, but that 9-hexadecenoic acid is relatively unique to meat cooking emissions. For this reason 9-hexadecenoic acid is used to replace 9-octadecenoic acid as a tracer species in cases where emissions from cooking operations that use seed oils are not included in the model.

The particle-phase emissions from catalyst-equipped gasoline-powered motor vehicles and noncatalyst gasoline-powered motor vehicles are too similar to be differentiated from each other based on organic compounds alone. Therefore, the organic chemical profiles for all gasoline-powered motor vehicles were combined into one emissions profile generated by weighting the two profiles according to vehicle miles traveled (VMT) by vehicles of each type in the

three counties included in the IMS95 study area, Fresno County, Kings County, and Kern County, CA.

Selection of the gas-phase hydrocarbon tracers used in the combined gas and particle phase tracer model is based on the criteria outlined by Harley et al. (1992), except that acetylene, ethene, and benzene are deleted from mass balance calculations; their function is replaced by the more specific tracers for combustion source effluents that are obtained from the fine particle emissions data set. As previously indicated, acetylene, ethene, and benzene constitute a noticeable portion of the volatile hydrocarbon emissions from wood combustion (Chapter 6), from motor vehicle exhaust, and are believed to be emitted from other combustion sources such as natural gas combustion. Rogge et al. (1993b) showed that polycyclic aromatic hydrocarbons (PAH) make up a noticeable fraction of the fine particle emissions from some natural-gas fired household appliances. Since the formation of acetylene, ethene, and benzene is known to be associated with PAH formation during combustion, it is reasonable to assume that acetylene, ethene, and benzene will be enriched in the volatile hydrocarbon emissions from certain natural gas combustion sources. Although a gas-phase hydrocarbon emissions profile is available for wood combustion, such a profile is not currently available for natural-gas fired household appliances. For this reason, ethene, acetylene, and benzene are removed from the list of mass balance species. If such a profile were available and evidence indicated that

there were no other significant sources of acetylene, ethene, and benzene that are not included in the model then, these species could be included as mass balance compounds. The particle-phase organic compound selection criteria for the combined gas- and particle-phase tracer model is the same as used for the fine particle tracer model.

## 10.4 Results

### 10.4.1 Characterization of Fine Organic Compound Mass Present in Ambient Samples

More than 100 organic compounds were quantified in the atmospheric fine particulate matter collected during the IMS95 study including n-alkanes, n-alkanoic acids, n-alkenoic acids, resin acids, substituted guaiacols, substituted syringols, alkane dicarboxylic acids, aromatic dicarboxylic acids, and levoglucosan. Table 10.1 lists the atmospheric concentrations of the particle-phase organic compounds quantified in the atmosphere at Fresno, Bakersfield, and the Kern Wildlife Refuge during the IMS95 study episodes: December 26-28, 1995, and January 4-6, 1996. Figure 10.1 shows a mass balance on the fine organic compound mass measured at the Bakersfield site during the December 26-28, 1995, episode. As seen in Figure 10.1, 84% of the fine particle organic compound mass concentration of  $19.4 \mu\text{g m}^{-3}$  is either unextractable or will not elute from the GC column used under the present analytical conditions. The unextractable and nonelutable organic mass is believed to be comprised of

Table 10.1. Atmospheric Concentrations of Fine Particle-Phase Organic Compounds During the IMS95 Experiments

Compound	Fresno (ng m <sup>-3</sup> )		Bakersfield (ng m <sup>-3</sup> )		Kern Wildlife Refuge (ng m <sup>-3</sup> )		Notes
	Dec. 26-28 1995	Jan. 4-6 1996	Dec. 26-28 1995	Jan. 4-6 1996	Dec. 26-28 1995	Jan. 4-6 1996	
	n-Alkanes						
n-Tetracosane	42.3	14.2	12.7	16.5	2.52	2.04	a
n-Pentacosane	41.2	17.3	14.2	17.9	2.73	2.44	b
n-Hexacosane	29.9	12.6	10.7	13.8	1.49	1.81	b
n-Heptacosane	25.0	15.2	10.8	12.0	1.59	1.50	b
n-Octacosane	12.3	8.27	5.24	6.84	0.95	0.78	a
n-Nonacosane	33.8	40.4	23.6	23.4	3.22	8.75	b
n-Triacontane	7.39	5.31	4.27	4.96	0.37	0.28	b
n-Hentriacontane	16.1	10.8	9.66	9.83	0.68	0.88	b
n-Dotriacontane	2.61	1.98	3.50	3.71			a
n-Tritriacontane	5.02	4.42	3.31	3.56			b
Polycyclic aromatic hydrocarbons (PAH)							
Retene	6.02	0.716	0.563	0.740			a
Fluoranthene	2.52	0.379	0.553	1.01	0.055	0.071	a
Acephenanthrylene	0.834	0.141	0.302	0.291			a
Pyrene	3.28	0.471	0.564	0.938	0.057	0.053	a
C <sub>1</sub> -202 MW PAH	11.7	1.25	3.80	1.94			a
Benzo[ghi]fluoranthene	6.05	1.18	1.25	1.50	0.043		a
Cyclopenta[cd]pyrene	1.90	0.696	0.496	0.937			a
C <sub>1</sub> -226 MW PAH	10.1	2.29	1.48	2.34	0.019	0.080	b
Benzo[a]anthracene	13.8	3.92	2.49	3.35	0.176	0.189	a
Chrysene/Triphenylene	7.70	1.74	1.50	1.20			a
C <sub>1</sub> -228 MW PAH	17.6	4.99	5.35	4.19			b
Benzo[k]fluoranthene	8.69	3.49	2.13	3.14	0.036	0.177	a
Benzo[b]fluoranthene	10.7	4.47	2.48	3.30		0.096	a
Benzo[j]fluoranthene	3.62	0.909	0.499	0.670			b
Benzo[e]pyrene	7.20	3.06	1.98	2.72	0.127	0.130	a
Benzo[a]pyrene	8.23	2.86	1.77	2.38			a
Perylene	1.50	0.055	0.246	0.423			a
Indeno[1,2,3-cd]fluoranthene	1.36	1.07	0.764	1.04			b
Indeno[1,2,3-cd]pyrene	6.84	4.09	2.56	2.63			a
Benzo[ghi]perylene	9.75	5.63	3.49	4.82			a
Anthanthrene	0.180		0.131	0.101			b
Coronene		1.22		3.41			a
Substituted phenols							
p-Benzenediol	3.46						a
m-Benzenediol	7.59						a
Hydroxybenzaldehydes	2.64		0.604				b
Guaiacol and substituted guaiacols							
Guaiacol	0.889	0.246	0.832	0.700	0.087		a
4-Methylguaiacol	0.606	0.105	0.387	0.481			b
trans-Isoeugenol	1.45		1.04				b

Identification notes: a) authentic quantitative standard. b) authentic quantitative standard for similar compound in series. c) identified by mass spectra, but not quantified. d) detected as a methyl ester. See text for details.

Table 10.1. (continued - page 2)

Compound	Fresno (ng m <sup>-3</sup> )		Bakersfield (ng m <sup>-3</sup> )		Kern Wildlife Refuge (ng m <sup>-3</sup> )		Notes
	Dec. 26-28 1995	Jan. 4-6 1996	Dec. 26-28 1995	Jan. 4-6 1996	Dec. 26-28 1995	Jan. 4-6 1996	
	Guaiacol and substituted guaiacols						
Vanillin	26.8	3.48	6.05	4.47			a
Acetovanillone	3.23		0.705	0.363			a
Guaiacyl acetone	10.8	1.77	4.29	1.89			b
Coniferyl aldehyde	47.0						a
Syringol and substituted syringols							
Syringol	1.16	0.222	0.845	0.692			a
4-Methylsyringol	1.72	0.310	1.77	1.21			b
4-Ethylsyringol	2.28	0.470	2.39	1.65			b
4-Propylsyringol	0.871						b
4-Propenylsyringol	4.38	1.02	1.40	1.93			a
Syringaldehyde	135	10.8	44.5	27.2	0.335	0.422	b
Acetosyringone	171	14.0	55.7	38.6			b
Acetonylsyringol	406	22.4	68.1	35.8			b
Propionylsyringol	32.1	4.68	16.2	13.4			b
Butyrylsyringol	15.3	1.40	6.18	5.24			b
Sinapyl aldehyde	15.9						b
n-Alkanoic acids							
n-Decanoic acid	0.711	0.211	0.164	0.244	0.098	0.105	a, d
n-Dodecanoic acid	0.905	0.522	0.803	0.735	0.812	0.660	b, d
n-Tridecanoic acid	6.17	1.82	1.78	2.32	0.372	0.403	a, d
n-Tetradecanoic acid	9.42	3.71	4.01	4.03	2.17	2.72	a, d
n-Pentadecanoic acid	33.7	10.1	5.63	13.0	1.30	1.48	b, d
n-Hexadecanoic acid	166	56.8	54.4	84.1	9.58	10.4	a, d
n-Heptadecanoic acid	13.6	4.29	3.77	5.30	0.474	0.671	b, d
n-Octadecanoic acid	60.0	26.6	24.1	38.3	4.90	4.96	a, d
n-Nonadecanoic acid	10.7	2.82	2.58	2.75	0.238	0.342	b, d
n-Eicosanoic acid	41.2	12.8	10.4	12.3	1.28	1.23	a, d
n-Heneicosanoic acid	20.8	6.25	6.46	7.26	0.505	0.639	b, d
n-Docosanoic acid	160	48.1	43.1	53.6	4.10	4.30	a, d
n-Tricosanoic acid	32.1	10.6	9.71	10.9	0.787	0.728	b, d
n-Tetracosanoic acid	205	65.5	78.0	74.0	4.21	4.64	a, d
n-Pentacosanoic acid	15.4	5.48	6.59	5.35		0.48	b, d
n-Hexacosanoic acid	174	59.4	81.3	61.7	1.89	3.20	b, d
n-Heptacosanoic acid	2.56	1.54	2.38	0.903			b, d
n-Octacosanoic acid	21.3	8.60	9.65	5.25			b, d
n-Nonacosanoic acid	1.46	2.14	2.11				b, d
n-Triacontanoic acid	4.32	5.23	5.79	3.13			b, d
n-Alkenoic acids							
n-9-Hexadecenoic acid	18.8	1.55	3.96	4.92		0.457	a, d
n-9-Octadecenoic acid	27.1	2.11	3.96	29.0			a, d
n-9,12-Octadecanedienoic acid	13.6	1.06	1.83	14.2		1.41	a, d

Identification notes: a) authentic quantitative standard. b) authentic quantitative standard for similar compound in series. c) identified by mass spectra, but not quantified. d) detected as a methyl ester. See text for details.

Table 10.1. (continued - page 3)

Compound	Fresno (ng m <sup>-3</sup> )		Bakersfield (ng m <sup>-3</sup> )		Kern Wildlife Refuge (ng m <sup>-3</sup> )		Notes
	Dec. 26-28 1995	Jan. 4-6 1996	Dec. 26-28 1995	Jan. 4-6 1996	Dec. 26-28 1995	Jan. 4-6 1996	
	Alkane dicarboxylic acids						
Methylpropanedioic acid	2.13	4.10		3.66	3.14	3.81	a, d
Methylbutanedioic acid	24.0	12.5	8.80	12.7	3.45	4.18	a, d
Pentanedioic acid	21.3	12.5	10.5	17.8	5.32	7.35	a, d
Hexanedioic acid	3.39	3.17	3.07	3.15	1.71	2.21	a, d
Heptanedioic acid	2.22	0.904	1.03	1.29	1.93	1.54	a, d
Octanedioic acid	4.41	1.77	13.4	1.93	0.415	0.613	a, d
Nonanedioic acid	19.9	9.15	8.22	10.3	1.83	1.52	a, d
Aromatic carboxylic acids							
1,2-Benzenedicarboxylic acid	9.16	9.09	6.78	13.1	4.71	5.43	a, d
1,4-Benzenedicarboxylic acid	5.16	3.70	4.48	4.45	1.00	0.602	a, d
1,3-Benzenedicarboxylic acid	3.41	2.12	1.98	1.89	0.433	0.349	a, d
Benzenetricarboxylic acids	14.4	7.19	8.77	8.27	3.55	2.81	a, d
Resin acids							
Pimaric acid	9.97	1.86	0.735	1.70			b, d
Sandaracopimaric acid	8.91	0.999	0.525	1.32			b, d
Isopimaric acid	127	24.2	7.95	22.9			b, d
8,15-Pimaradien-18-oic acid	0.48	0.14	0.03	0.12			b, d
Dehydroabietic acid	98.5	17.8	8.01	16.1	0.249	0.268	a, d
Abietic acid	30.4	1.80	0.784	1.79			b, d
7-Oxodehydroabietic acid	6.68	2.95	1.43	1.40	0.075	0.075	b, d
Abieta-6,8,11,13,15-pentaen-18-oic acid	11.8	2.87	2.43	2.36			b, d
Abieta-8,11,13,15-tetraen-18-oic acid	2.62	0.341	0.251	0.441			b, d
Sugars							
Levoglucosan	7590	2130	1100	1370	25.3	22.5	a, d
Other sugars	1070	218	171	211			b, d
Other compounds							
1H-Phenalen-1-one	7.96	0.817	0.588	0.391			a, f
7H-Benz[de]anthracen-7-one	7.80	3.58	1.48	1.89			a, f
Veratric acid	2.49	0.483	0.406	0.533			a, f
Nonanal	19.4	7.29	3.01	8.07			a, f
Divanillyl	19.4	1.84	3.18	2.67			c, f
Divanillyl methane	2.39						c, f
Vanillylmethylguaiacol	3.24		0.568				c, f
Organic compound mass	55700	20500	18700	19400	6380	5870	
Unresolved complex mixture (UCM)	5180	1660	1840	1580	380	520	
Unextractable and nonelutable carbon	39100	15800	14800	15300	5910	5240	

Identification notes: a) authentic quantitative standard. b) authentic quantitative standard for similar compound in series. c) identified by mass spectra, but not quantified. d) detected as a methyl ester. See text for details.



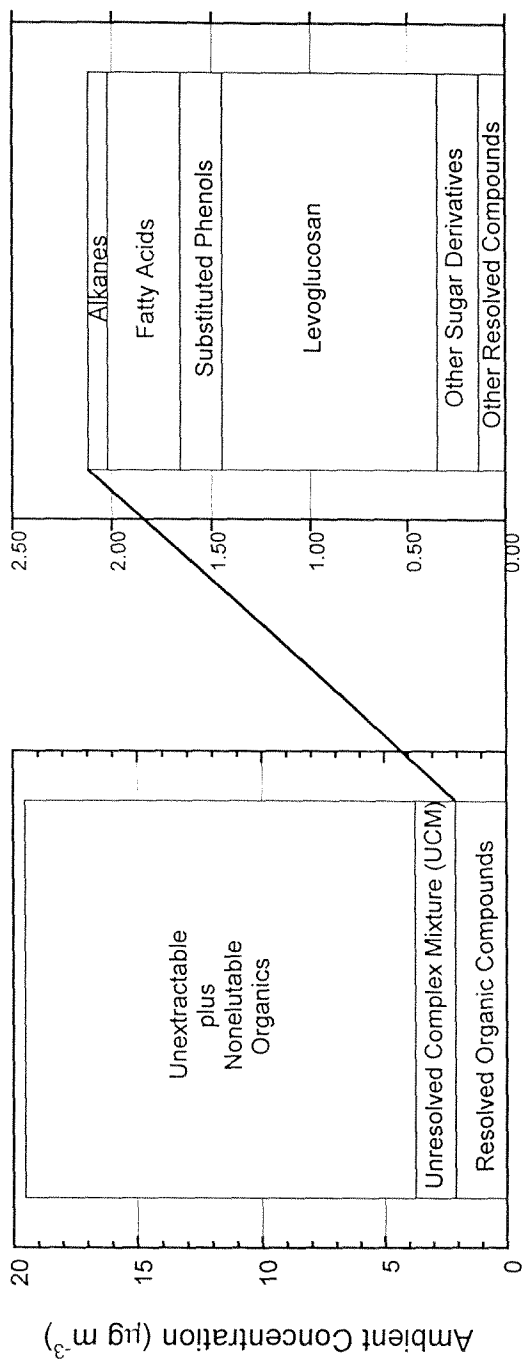


Figure 10.1. Mass balance on the fine particle organic compounds measured at Bakersfield, California, between December 26-28, 1995.

very high molecular weight compounds like lignans and cellulose, as well as highly polar organic compounds. Additionally, the fine particle organic compound mass contains  $1.6 \mu\text{g m}^{-3}$  of organic material within an unresolved complex mixture (UCM) which is composed of highly branched and cyclic compounds which cannot be resolved by gas chromatography. The remaining  $2.07 \mu\text{g m}^{-3}$  of organic compound mass is identified at the single compound level. Levoglucosan is present at by far the highest concentration of any of the organic compounds which are resolved at the single compound level, making up 5.7% of the entire organic compound mass in the fine particles in the Bakersfield atmosphere during this period. Significant contributions also are present from fatty acids (n-alkanoic acids and alkenoic acids), substituted phenols, and other sugar derivatives with structures similar to levoglucosan which have not yet been identified. The ambient concentrations of fine particle organic compound mass, unextractable and nonelutable organic compound mass as well as the magnitude of the UCM are listed at the end of Table 10.1 at each monitoring site for both episodes studied. It should be noted that the ambient fine organic compound mass concentration in Fresno from noon, December 26, through noon, December 28, averaged  $55.7 \mu\text{g m}^{-3}$ , of which the levoglucosan concentration alone averaged  $7.6 \mu\text{g m}^{-3}$ , indicating the significant influence of wood combustion at that time.

Organic and elemental carbon concentration data also were available

from the filter samples collected by the co-located medium-volume samplers which were deployed for fine particle mass measurements. The elemental and organic carbon concentrations on these three-hour filter samples were measured at DRI by a different carbon analysis method (Chow et al., 1993) than was used for the source samples of the present study. The two carbon analysis methods have been shown to give a different split between elemental carbon and organic carbon for ambient particulate matter samples that contain wood smoke, but the two methods have been shown to show good agreement for total carbon analysis in all cases tested (Chow et al., 1993). Figure 10.2 shows a comparison of the atmospheric fine particle total carbon concentrations obtained from the high volume dichotomous virtual impactor samples and from the medium volume three-hour filter samples along with their associated method of analysis. As seen in Figure 10.2, good agreement is observed except during the 2 days of very high concentrations of wood smoke in Fresno from December 26-28, 1995. In addition, a material balance on all chemical species (carbon, ions, metals) constructed from the three-hour average samples during these time periods shows good agreement with the gravimetric mass measurements for all periods except the two high wood smoke days experienced in Fresno. Based on the carbon concentration anomaly of Figure 10.2 and the inability to close a material balance on the elemental composition of these three-hour average samples, we do not expect to be able to use the three-hour average samples at Fresno between December 26-28, 1995, with as much confidence as at the other

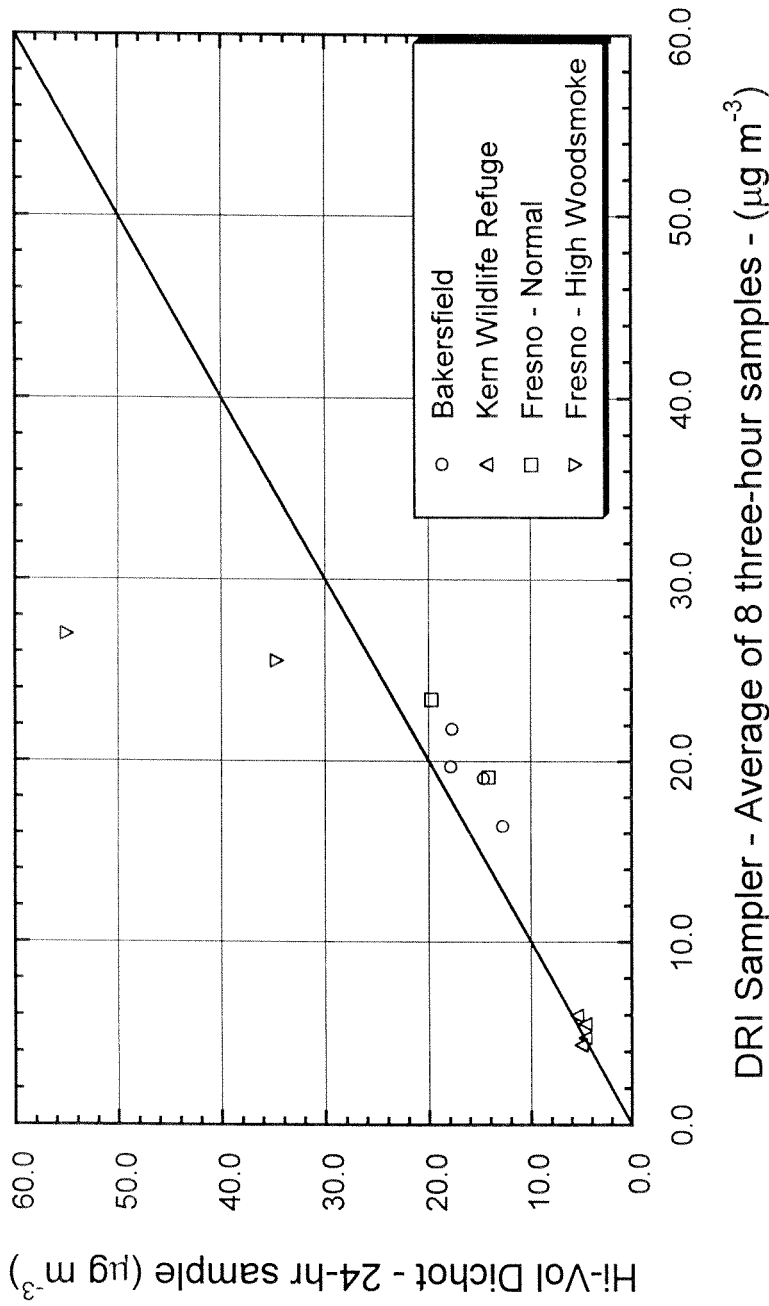


Figure 10.2. Comparison of fine particle total carbon collected by the high volume dichotomous sampler and analyzed by Sunset Labs according to the method of Birch and Cary (1996) and the total carbon collected by the co-located medium-volume 3-hour samplers and analyzed by DRI by the method of Chow et al. (1993) for the IMS95 winter study episodes.

sites and times studied.

#### **10.4.2 Fine Particle Organic Carbon and Fine Particle Mass Apportionment**

The fine particle organic chemical tracer model of equation (1) was applied to the source and ambient data sets at all three monitoring sites for both events studied. Figure 10.3 shows the agreement between the measured and the model-calculated mass balance compound concentrations at the Fresno site for the December 26-28, 1995, episode. Excellent agreement is observed between the measured concentrations and the calculated concentrations of individual organic compounds for this site as well as for the other sites. The calculated contributions to ambient fine particulate organic carbon concentrations made by the eight sources included in the model are shown in Figure 10.4 and are detailed in Table 10.2. The "other" organic carbon category accounts for the residual difference between the measured organic carbon concentrations and the sum of the apportioned contributions of the eight specific sources studied. As previously indicated, the glass jar that contained one of the two samples from the January 4-6 episode at the Fresno site was damaged in shipping. For this reason, a conservative approach has been employed during modeling and the contributions from hardwood and softwood combustion were lumped and were not separately apportioned for this site during this period only.

As can be seen in Figure 10.4, the unapportioned fraction of the organic

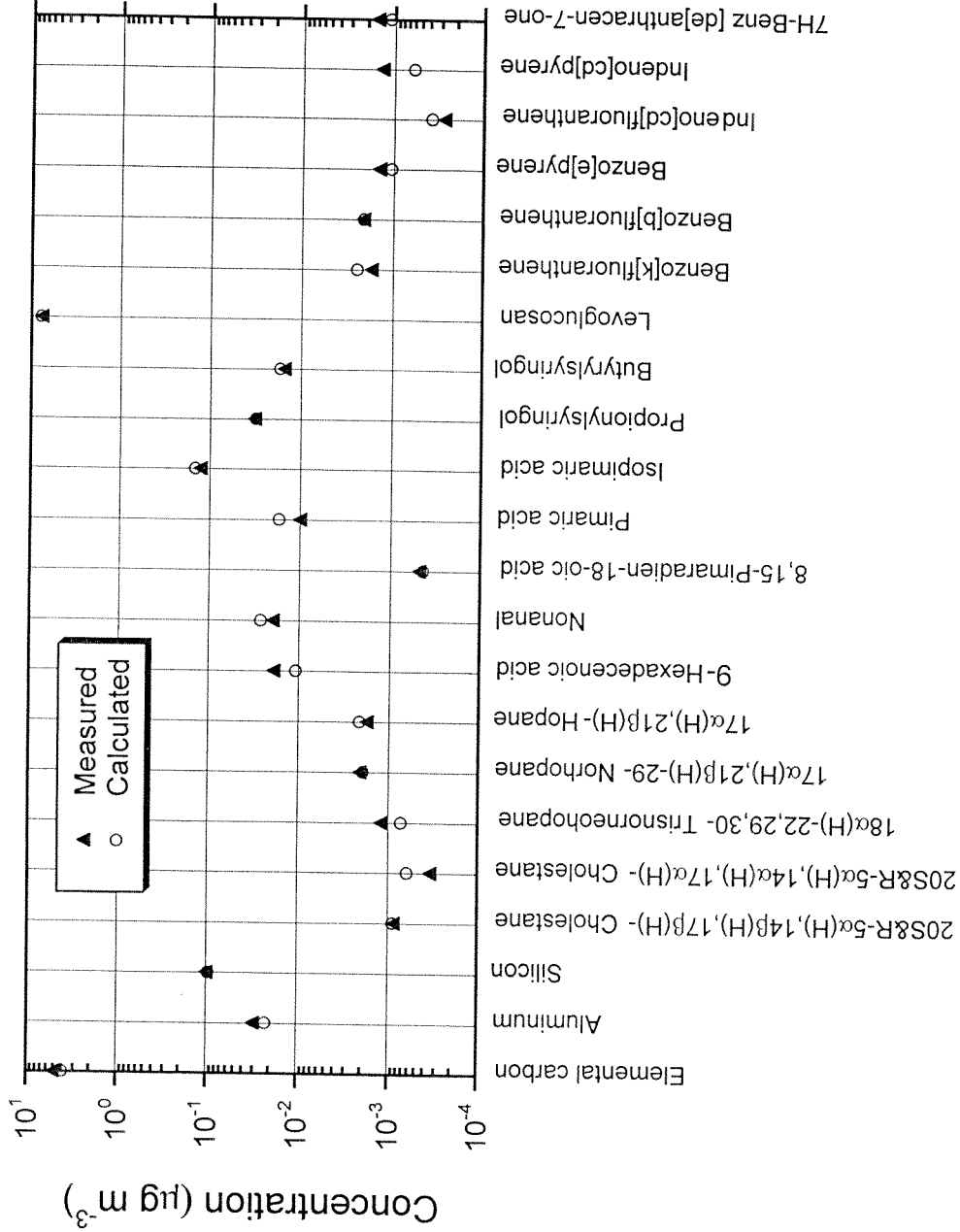


Figure 10.3. Comparison of the measured and calculated ambient concentrations of the mass balance species used in the fine particle CMB model at the Fresno, California, site for December 26-28, 1995.

Table 10.2. Source apportionment of fine primary organic carbon: determined by chemical mass balance

	Bakersfield (avg $\pm$ std in $\mu\text{g m}^{-3}$ )		Fresno (avg $\pm$ std in $\mu\text{g m}^{-3}$ )		Kern Wildlife Refuge (avg $\pm$ std in $\mu\text{g m}^{-3}$ )	
	Dec. 26-28, 95	Jan. 4-6, 96	Dec. 26-28, 95	Jan. 4-6, 96	Dec. 26-28, 95	Jan. 4-6, 96
Hardwood Combustion	3.42 $\pm$ 0.67	2.93 $\pm$ 0.58	8.70 $\pm$ 1.97		0.10 $\pm$ 0.028	0.087 $\pm$ 0.025
Softwood Combustion	0.75 $\pm$ 0.17	2.50 $\pm$ 0.47	17.5 $\pm$ 2.58		0.41 $\pm$ 0.069	0.54 $\pm$ 0.081
Combined Wood Combustion				8.24 $\pm$ 2.33		
Diesel Exhaust	1.21 $\pm$ 0.16	1.64 $\pm$ 0.20	2.98 $\pm$ 0.38	1.59 $\pm$ 0.19		
Gasoline Powered Vehicle Exhaust	1.33 $\pm$ 0.16	1.41 $\pm$ 0.18	2.36 $\pm$ 0.44	0.90 $\pm$ 0.19		
Meat Cooking	0.84 $\pm$ 0.19	1.98 $\pm$ 0.41	5.64 $\pm$ 1.19	0.85 $\pm$ 0.21		
Road Dust	0.14 $\pm$ 0.012	0.083 $\pm$ 0.013	0.89 $\pm$ 0.19	0.10 $\pm$ 0.017	0.075 $\pm$ 0.021	
Natural Gas Combustion	0.27 $\pm$ 0.048	0.37 $\pm$ 0.066				
Vegetative Detritus					0.26 $\pm$ 0.046	0.37 $\pm$ 0.063
Sum of Identified Sources	7.95 $\pm$ 0.76	10.9 $\pm$ 0.89	38.1 $\pm$ 3.51	11.7 $\pm$ 2.35	0.84 $\pm$ 0.090	1.00 $\pm$ 0.11
Measured <sup>†</sup>	13.4 $\pm$ 0.72	13.8 $\pm$ 0.75	39.8 $\pm$ 2.09	14.6 $\pm$ 0.79	4.56 $\pm$ 0.28	4.19 $\pm$ 0.26

\* Not statistically different from zero with 95 percent confidence, and therefore removed from CMB model

<sup>†</sup> Includes secondary organic aerosol: receptor model results should be less than or equal to the total fine particle organic carbon concentrations

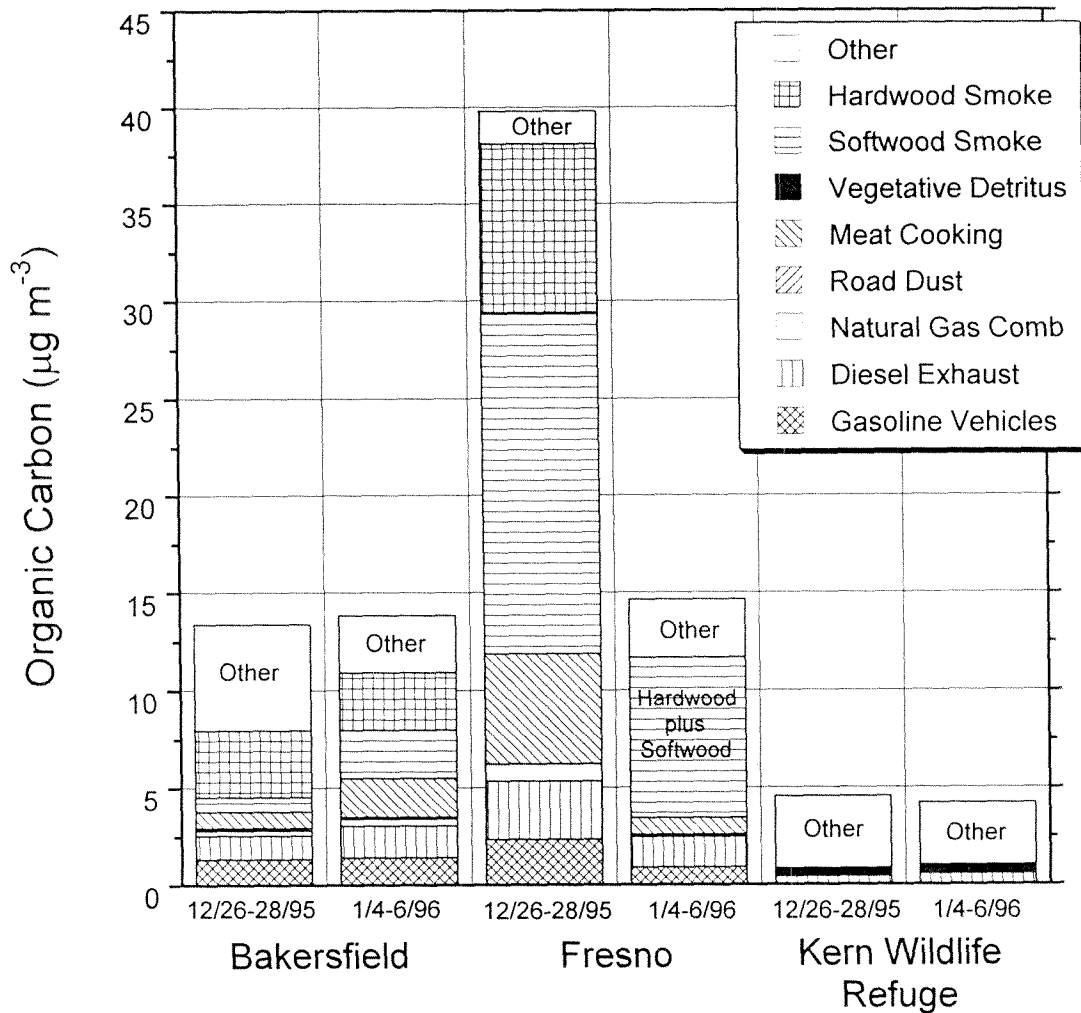


Figure 10.4. Source contributions to fine particle organic carbon concentrations.



carbon does not differ significantly between the three sites during the two episodes studied, averaging  $4.5 \mu\text{g m}^{-3}$ . Of particular significance is the low primary contribution from wood smoke, vehicle exhaust and meat cooking at the remote site, Kern Wildlife Refuge. These findings support the notion that a low regional background of aerosol, likely due to secondary aerosol formation, exists throughout the valley and that the higher concentrations of organic carbon in the urban locations are due to local emissions from the primary sources listed above. At the rural site, only vegetative detritus and diesel smoke are found to contribute to the primary fine organic aerosol. In contrast, at the two urban sites hardwood combustion and softwood combustion are the largest primary contributors to the fine organic aerosol followed by important contributions from diesel exhaust, gasoline-powered motor vehicle exhaust and meat cooking effluent. Smaller, but measurable, contributions from road dust and natural gas combustion aerosol also are quantified.

Since the ratio of the emissions of fine organic carbon to fine particle mass are known for each of the sources in the model, source contributions to fine particle mass concentrations also can be calculated. Figure 10.5 and Table 10.3 show the fine particle mass contributions from the primary sources plus the unapportioned material as well as secondary sulfate, nitrate, and ammonium ion concentrations. The "other" organic carbon that could not be assigned to a specific primary source was converted to an estimate of organic compound mass

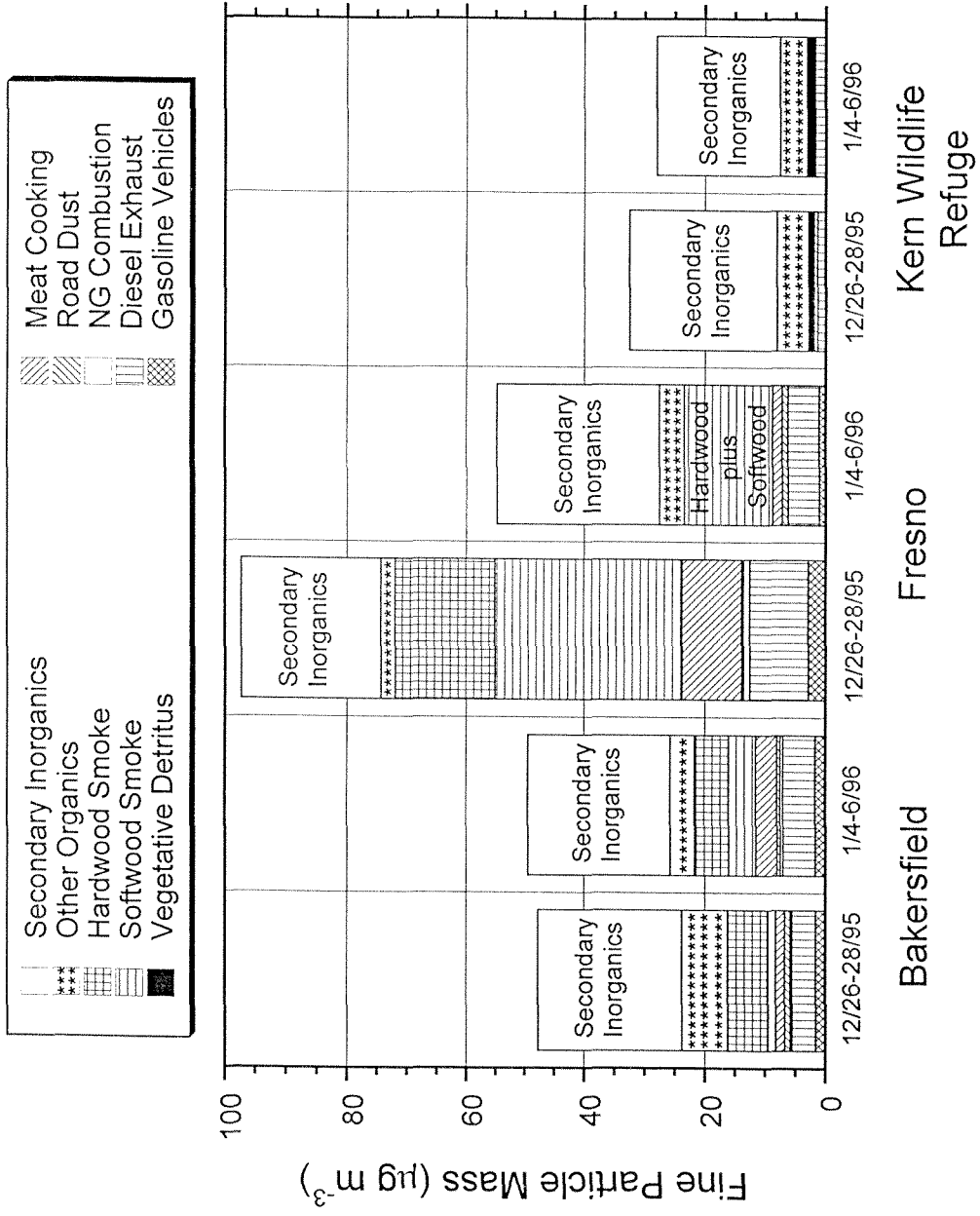


Figure 10.5. Source contributions to fine particle mass concentrations.

Table 10.3. Source apportionment of fine particulate mass concentrations: determined by chemical mass balance

	Bakersfield (avg $\pm$ std in $\mu\text{g m}^{-3}$ )		Fresno (avg $\pm$ std in $\mu\text{g m}^{-3}$ )		Kern Wildlife Refuge (avg $\pm$ std in $\mu\text{g m}^{-3}$ )	
	Dec. 26-28, 95	Jan. 4-6, 96	Dec. 26-28, 95	Jan. 4-6, 96	Dec. 26-28, 95	Jan. 4-6, 96
Hardwood Combustion	6.63 $\pm$ 1.30	5.68 $\pm$ 1.11	16.9 $\pm$ 3.81			
Softwood Combustion	1.34 $\pm$ 0.30	4.46 $\pm$ 0.84	31.3 $\pm$ 4.61			
Combined Wood Combustion				14.7 $\pm$ 4.16	0.18 $\pm$ 0.049	0.16 $\pm$ 0.044
Diesel Exhaust	3.92 $\pm$ 0.52	5.32 $\pm$ 0.65	9.68 $\pm$ 1.23	5.15 $\pm$ 0.62	1.32 $\pm$ 0.23	1.75 $\pm$ 0.26
Gasoline Powered Vehicle Exhaust	1.63 $\pm$ 0.20	1.73 $\pm$ 0.22	2.89 $\pm$ 0.54	1.10 $\pm$ 0.23	*	*
Meat Cooking	1.49 $\pm$ 0.34	3.50 $\pm$ 0.72	9.97 $\pm$ 1.19	1.51 $\pm$ 0.36	*	*
Paved Road Dust	0.91 $\pm$ 0.09	0.55 $\pm$ 0.089		1.00 $\pm$ 0.17	0.58 $\pm$ 0.16	*
Natural Gas Combustion	0.31 $\pm$ 0.057	0.43 $\pm$ 0.078	1.04 $\pm$ 0.23	*		
Vegetative Detritus					0.81 $\pm$ 0.14	1.13 $\pm$ 0.20
Organics (other + secondary)	7.60 $\pm$ 1.04	4.06 $\pm$ 1.17	2.35 $\pm$ 4.09 <sup>†</sup>	4.15 $\pm$ 2.48 <sup>†</sup>	5.21 $\pm$ 0.29	4.46 $\pm$ 0.28
Sulfate (secondary + background)	2.33 $\pm$ 0.44	2.99 $\pm$ 0.37	1.90 $\pm$ 0.33	2.80 $\pm$ 0.31	1.43 $\pm$ 0.20	2.07 $\pm$ 0.26
Secondary Nitrate	16.0 $\pm$ 1.12	15.4 $\pm$ 1.07	16.4 $\pm$ 1.19	18.9 $\pm$ 1.34	18.0 $\pm$ 1.26	14.2 $\pm$ 1.06
Secondary Ammonium Ion	5.51 $\pm$ 0.31	5.29 $\pm$ 0.33	4.64 $\pm$ 0.27	5.49 $\pm$ 0.31	5.02 $\pm$ 0.29	4.13 $\pm$ 0.25
Sum of Identified Sources	47.7 $\pm$ 2.20	49.4 $\pm$ 2.39	97.3 $\pm$ 7.78	54.8 $\pm$ 7.49	32.6 $\pm$ 1.38	28.0 $\pm$ 1.22
Measured	55.5 $\pm$ 2.99	52.1 $\pm$ 2.79	76.4 $\pm$ 4.77 <sup>Δ</sup>	55.3 $\pm$ 3.06	36.3 $\pm$ 1.95	33.5 $\pm$ 1.84

\* Not statistically different from zero with greater than 95 percent confidence, and therefore removed from CMB model

† Not statistically different from zero with greater than 95 percent confidence

Δ Ambient particle mass measurement does not show good agreement with ambient chemical species measurements

by multiplying the residual organic carbon by a factor of 1.4. As seen in Figure 10.5 the contributions from primary sources plus secondary aerosol formation account for between 84% and 99% of the measured fine particle mass except for the high wood smoke event in Fresno during the period of December 26-28, 1995, where the summed contributions from specific sources exceed the gravimetric measured fine particle mass concentration. As mentioned above, the fine particle atmospheric mass measurements made by the three-hour sampler during this period are questionable, and it is believed from the source apportionment results that the fine particle mass concentrations during this period were actually higher than previously reported. As seen in Figure 10.5, the summed contributions from secondary sulfate, nitrate, and ammonium ion are significant and do not vary much across sites and between the two episodes, accounting for  $23.8 \mu\text{g m}^{-3}$  averaged over both episodes and all three sites. During the highest wood smoke episode of December 26-28 in Fresno, primary emissions from wood smoke contributed 42% of the ambient fine particle mass concentration as determined by the source apportionment model. At all other times and locations, no one single primary particle source dominates the atmospheric fine particle mass concentrations.

Source contributions to the mass balance compounds are shown in Figure 10.6 for the high wood smoke episode in Fresno. As it can be seen in Figure 10.6, hardwood combustion contributes about 40% of the levoglucosan

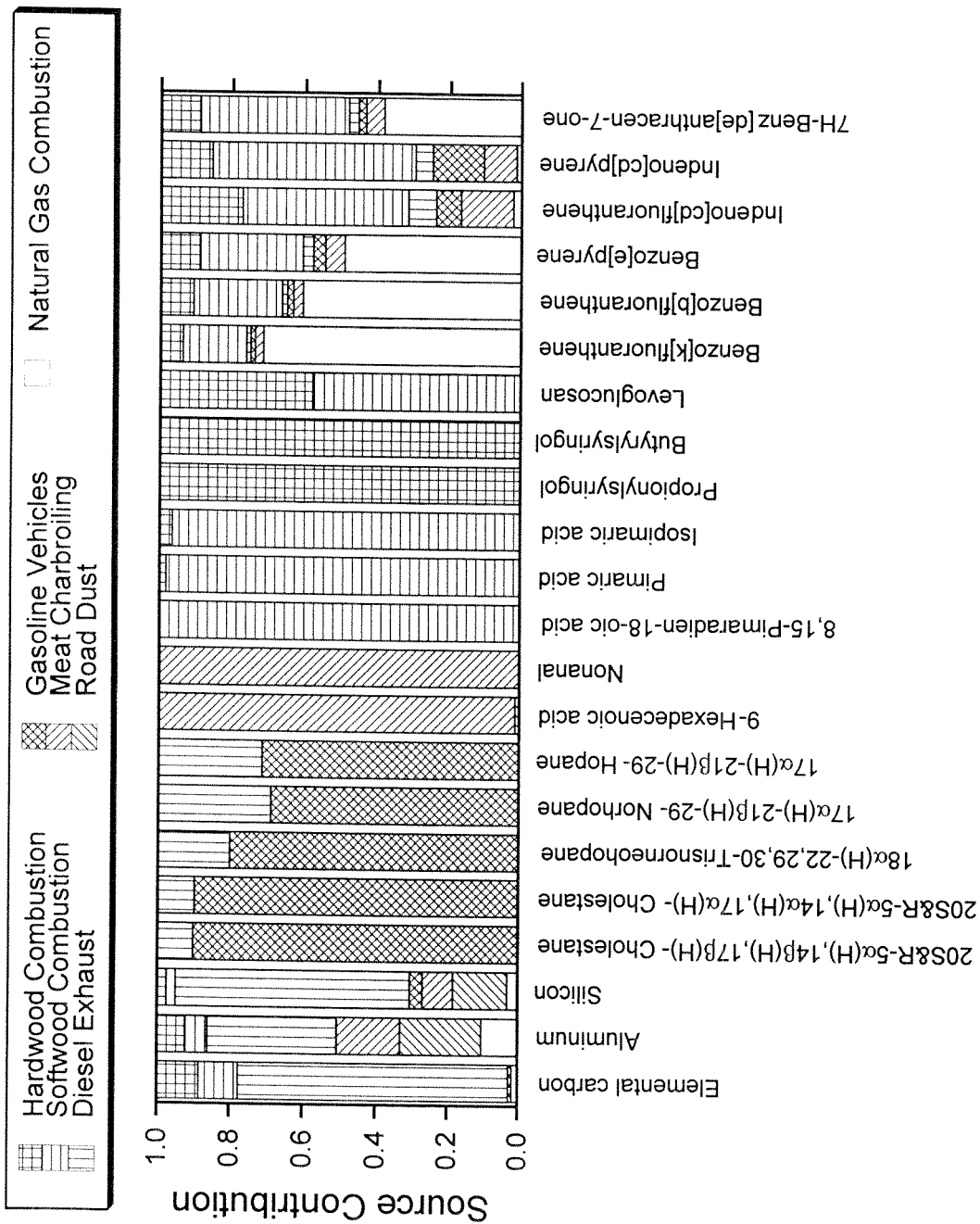


Figure 10.6. Source contributions to the atmospheric concentrations of the mass balance species used in the fine particle CMB model at Fresno, California, on December 26-28, 1995.

ambient concentrations and softwood combustion accounts for the remaining 60% of the ambient concentration. Likewise, hardwood and softwood combustion combined contribute a little over 20% of the ambient elemental carbon concentrations. In addition, benzo[k]fluoranthene, benzo[b]fluoranthene, and benzo[e]pyrene concentrations are dominated by natural gas combustion and wood combustion, whereas indeno[cd]fluoranthene and indeno[cd]pyrene concentrations are dominated by wood smoke emissions.

#### **10.4.3 Non-Methane Organic Gases Apportionment**

The measured and calculated concentrations of the mass balance species for the combined gas and particle phase organic chemical tracer model application are shown in Figure 10.7 for the high wood smoke event in Fresno. Excellent agreement between the calculated and measured concentrations exists for both periods modeled. Shown in Figure 10.8 and in Table 10.4 are the source contributions to non-methane organic gases concentrations calculated by the organic compound-based receptor model for both periods studied. As previously stated, gas-phase organic compound concentrations cannot be apportioned at the other sites since 24-hour gas-phase measurements were not made at these locations. Gasoline-powered motor vehicle exhaust and whole gasoline vapors are the largest contributors to the non-methane organic gases concentrations followed by natural gas leakage. Smaller but quantifiable contributions from gasoline headspace vapor emissions, meat cooking, diesel

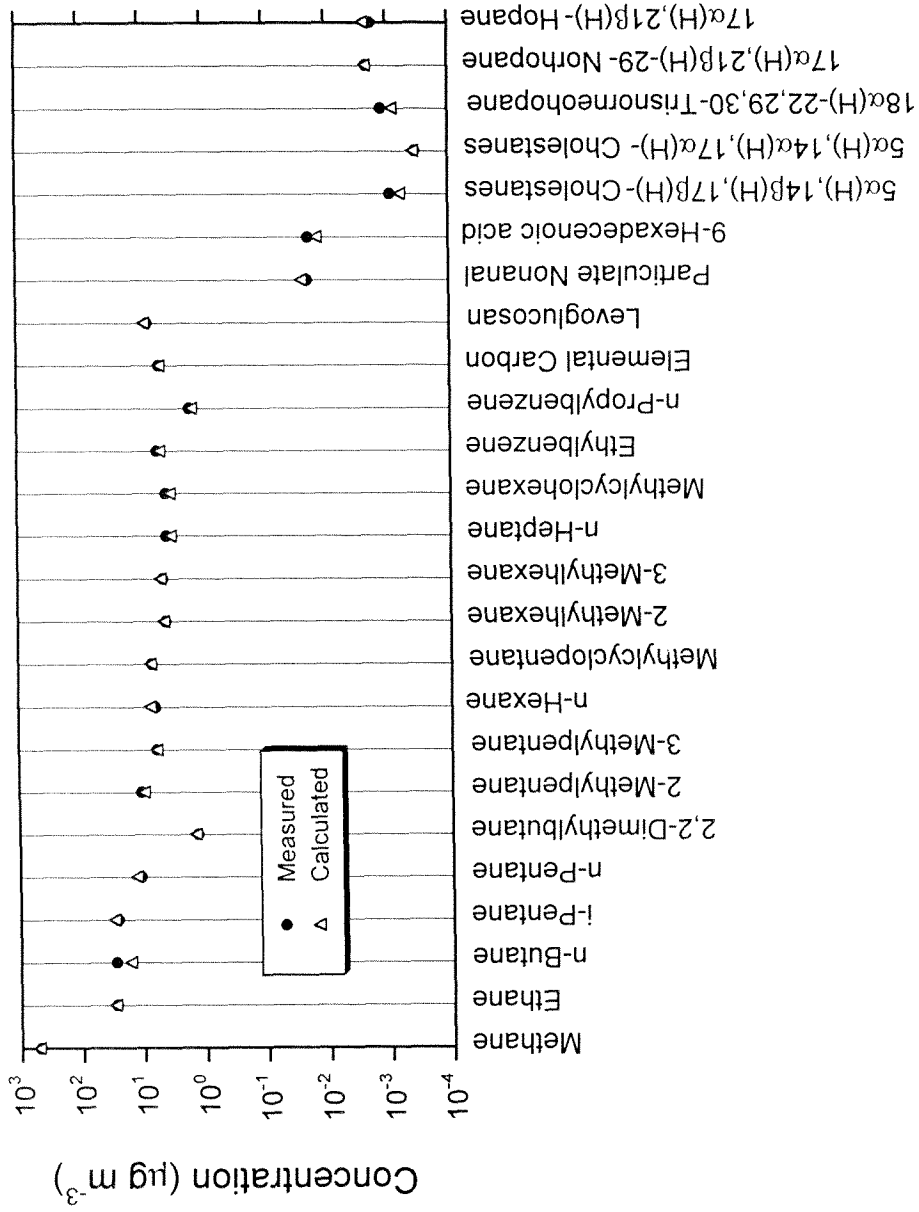


Figure 10.7. Comparison of the measured and calculated ambient concentrations of the mass balance species used in the combined gas- and particle-phase CMB model at Fresno, California, on December 26-28, 1995.

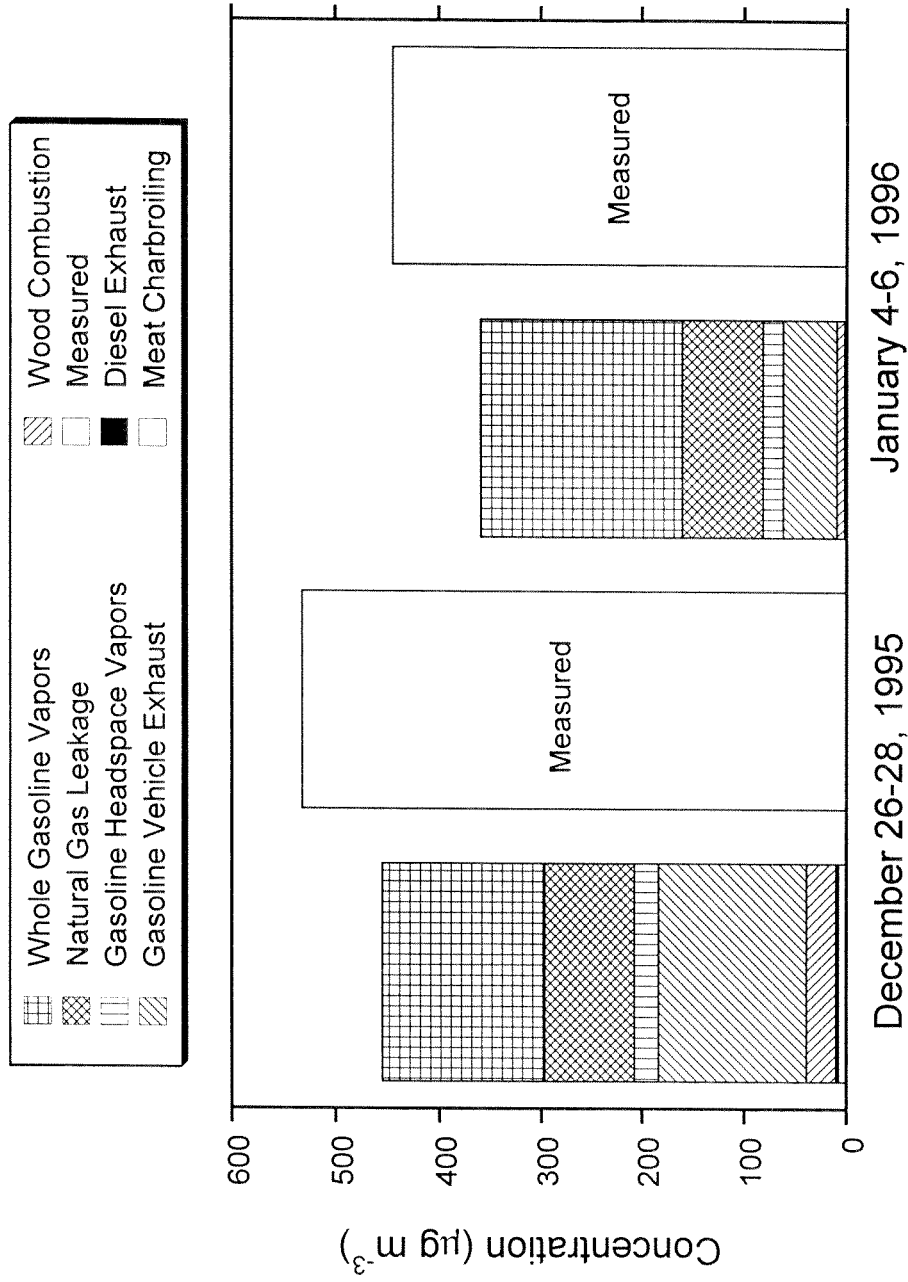


Figure 10.8. Source contributions to non-methane organic gases concentrations at Fresno, California, on December 26-28, 1995.



Table 10.4. Source apportionment of non-methane organic gases: determined by chemical mass balance

	<b>Fresno</b>	
	(avg $\pm$ std in $\mu\text{g m}^{-3}$ )	
	<u>Dec. 26-28, 95</u>	<u>Jan. 4-6, 96</u>
Gasoline Powered Vehicle Exhaust	145 $\pm$ 21.7	71.0 $\pm$ 11.1
Natural Gas Leakage	89.4 $\pm$ 6.2	78.9 $\pm$ 5.3
Whole Gasoline Vapors	159 $\pm$ 23.2	180 $\pm$ 14.6
Combined Wood Combustion	28.6 $\pm$ 7.5	7.4 $\pm$ 2.1
Gasoline Headspace Vapors	23.5 $\pm$ 10.7	18.2 $\pm$ 9.1
Diesel Exhaust	2.7 $\pm$ 0.3	1.2 $\pm$ 0.2
Meat Cooking	7.9 $\pm$ 1.6	1.2 $\pm$ 0.3
Sum	456 $\pm$ 35	358 $\pm$ 21
Measured	532 $\pm$ 26	445 $\pm$ 22

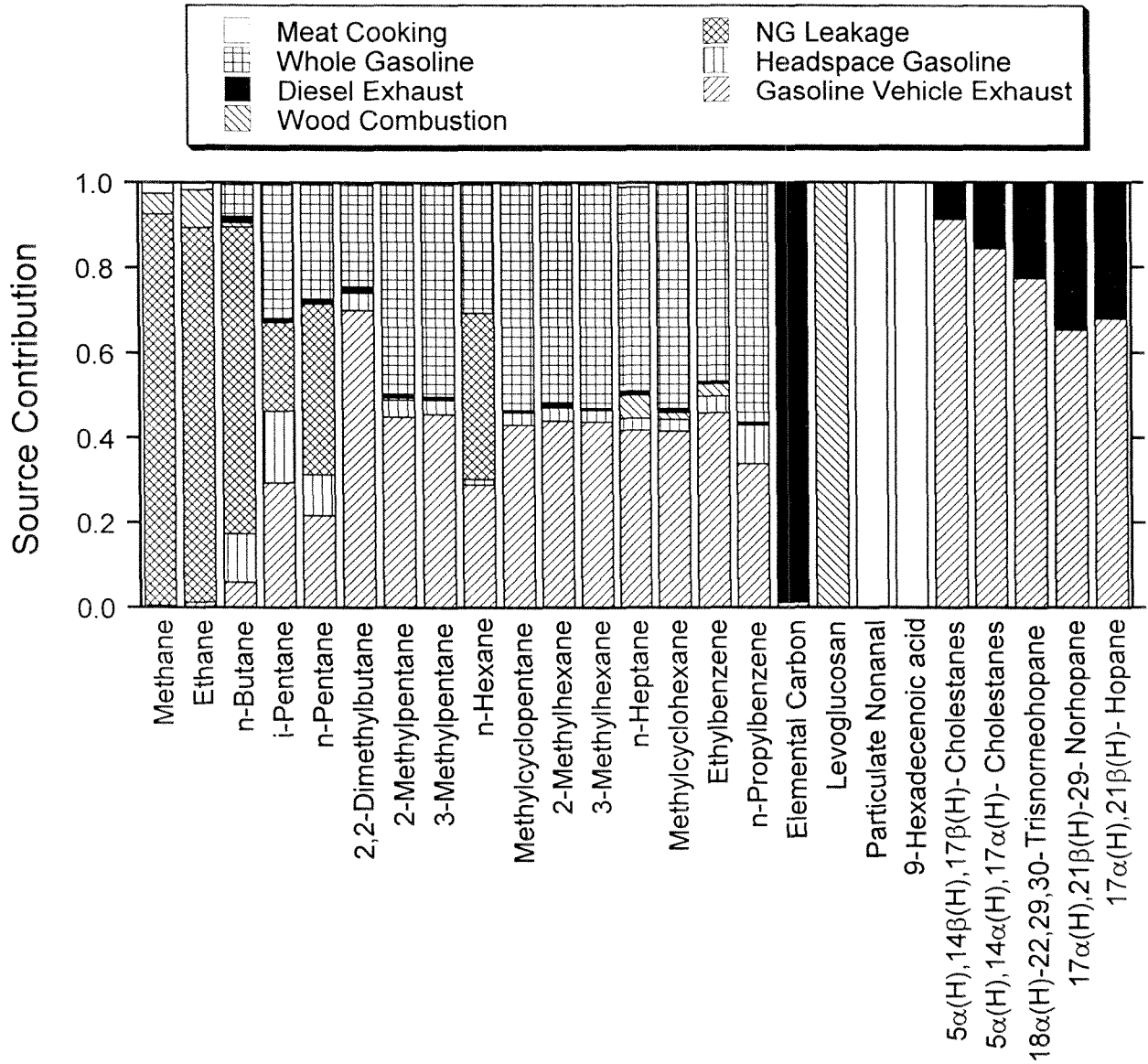


Figure 10.9. Source contributions to the atmospheric concentrations of the mass balance species used in the combined gas- and particle-phase CMB model at Fresno, California.

exhaust and wood combustion also exist. Figure 10.9 shows the source contributions to each of the mass balance species used in the combined gas- and particle-phase source apportionment model.

Two alternative cases were examined where acetylene, ethene, and benzene were included as mass balance species. In the first alternative case, all particle-phase tracers were excluded as mass balance species. In this case, the contribution from gasoline-powered motor vehicle exhaust exceeded the measured overall non-methane organic gas contributions, which of course is impossible. In the second alternative case, the particle-phase tracers were included along with acetylene, ethene, and benzene. In this case, the gasoline-powered motor vehicle exhaust concentration in the atmosphere is capped by the knowledge that the observed hopanes and steranes concentrations in the particle phase should not be exceeded and instead the wood smoke contributions are forced excessively high to balance the acetylene, ethene, and benzene such that the non-methane organic gases are once again overbalanced and the wood smoke particle contributions are also overbalanced. Clearly there are other as yet unidentified sources of acetylene, ethene, and benzene emissions that are not yet available to be inserted into the model (e.g., from natural gas combustion), and until those sources can be represented correctly, the particle-phase combustion tracers should be used in place of acetylene, ethene, and benzene.

## 10.5 References

- Ashbaugh, L. L. (1999) University of California at Davis. Personal correspondence.
- Aulich, T. R., He, X. M., Grisanti, A. A. and Knudson, C. L. (1994) Gasoline evaporation-ethanol and nonethanol blends. *J. Air & Waste Manage. Assoc.* **44**, 1004-1009.
- Birch, M. E. and Cary, R. A. (1996) Elemental carbon-based method for monitoring occupational exposures to particulate diesel exhaust. *Aerosol Sci. Technol.* **25**, 221-241.
- Conner, T. A., Lonneman, W. A. and Seila, R. L. (1995) Transportation-related volatile hydrocarbon source profiles measured in Atlanta. *J. Air & Waste Manage. Assoc.* **45**, 383-394.
- Chow J. C., Watson J. G., Lowenthal, D. H., Solomon, P. A., Magliano, K., Ziman, S. D. and Richards, L. W. (1992) PM<sub>10</sub> source apportionment in California's San Joaquin Valley. *Atmos. Environ.* **26A**, 3335-3354.
- Chow J. C., Watson J. G., Lowenthal, D. H., Solomon, P. A., Magliano, K., Ziman, S. D. and Richards, L. W. (1993a) PM<sub>10</sub> and PM<sub>2.5</sub> compositions in California's San Joaquin Valley. *Aerosol Sci. Technol.* **18**, 105-128.

- Chow, J. C., Watson, J. G., Pritchett, L. C., Pierson, W. R., Frazier, C. A. and Purcell, R. G. (1993b) The DRI thermal/optical reflectance carbon analysis system: description, evaluation, and application in U.S. air quality studies. *Atmos. Environ.* **27A**, 1185-1201.
- Chow, J. C. and Egami, R. T. (1997) San Joaquin Valley 1995 integrated monitoring study: documentation, evaluation, and descriptive data analysis of PM<sub>10</sub>, PM<sub>2.5</sub>, and precursor gas measurements. California regional particulate air quality study report. DRI document no. 5460.1F1, Desert Research Institute, Reno, NV.
- Fraser, M. P., Grosjean, D., Grosjean, E., Rasmussen, R. A. and Cass, G. R. (1996) Air quality model evaluation data for organics. 1. Bulk chemical composition and gas/particle distribution factors. *Environ. Sci. Technol.* **30**, 1731-1743.
- Fujita, E. M., Watson, J. G., Chow, J. C. and Magliano, K. L. (1995) Receptor model and emissions inventory source apportionments of nonmethane organic gases in California's San Joaquin Valley and San Francisco Bay area. *Atmos. Environ.* **29**, 3019-3035.
- Harley, R. A., Hannigan, M. P. and Cass, G. R. (1992) Respeciation of organic gas emissions and the detection of excess unburned gasoline in the atmosphere. *Environ. Sci. Technol.* **26**, 2395-2408.

- Hildemann L. M., Markowski G. R. and Cass G. R. (1989) A dilution stack sampler for collection of organic aerosol emissions: design, characterization, and field tests. *Aerosol Sci. Technol.* **10**, 193-204.
- Hildemann L. M., Markowski G. R. and Cass G. R. (1991) Chemical composition of emissions from urban sources of fine organic aerosol. *Environ. Sci. Technol.* **25**, 744-759.
- John W. and Reischl G. (1980) A cyclone for size-selective sampling of ambient air. *JAPCA* **30**, 872-876.
- Rogge W. F., Hildemann L. M., Mazurek M. A., Cass G. R. and Simoneit B.R.T. (1993a) Sources of fine organic aerosol. 4. Particulate abrasion products from leaf surfaces of urban plants. *Environ. Sci. Technol.* **27**, 2700-2711.
- Rogge W. F., Hildemann L. M., Mazurek M. A., Cass G. R. and Simoneit B.R.T. (1993b) Sources of fine organic aerosol. 5. Natural gas home appliances. *Environ. Sci. Technol.* **27**, 2736-2744.
- Schauer J. J., Rogge W. F., Hildemann L. M., Mazurek M. A., Cass G. R. and Simoneit (1996) Source apportionment of airborne particulate matter using organic compounds as tracers. *Atmos. Environ.* **30**, 3837-3855.

- Scheff, P. A. and Wadden, R. A. (1993) Receptor modeling of volatile organic compounds. 1. Emissions inventory and validation. *Environ. Sci. Technol.* **27**, 617-625.
- Solomon, P. A., Moyers, J. L. and Fletcher, R. A., (1984) High-volume dichotomous virtual impactor for the fractionation and collection of particles according to aerodynamic size. *Aerosol. Sci. Technol.* **4**, 455-464.
- Watson J. G., Robinson N. F., Chow J. C., Henry R. C., Kim B. M., Pace T. G., Meyer E. I. and Nguyen Q. (1990) The USEPA/DRI chemical mass balance receptor model, CMB 7.0. *Environ. Softw.* **5**, 38-49.

## Chapter 11

# Source Reconciliation of Atmospheric Gas-Phase and Particle-Phase Pollutants Using Organic Compounds as Tracers

### 11.1 Introduction

Most chemical mass balance (CMB) receptor models applied to air quality problems have been employed to calculate either the source origin of particle-phase pollutants (Miller et al., 1972; Friedlander, 1973; Cass and McRae, 1983) or the source origin of gas-phase pollutants (Harley et al., 1992; Scheff and Wadden, 1993; Fujita et al., 1994). In a few cases, particle-phase tracers have been incorporated into the gas-phase pollutant models to allow additional sources to be resolved by the receptor modeling calculations (Chapter 10). For the same reasons, gas-phase species occasionally have been incorporated into receptor models for particulate matter (Harrison et al., 1996; Hawthorne et al., 1992; Khalil et al., 1983), but these models have not been expanded to simultaneously determine the source contributions to entire suites of gas-phase and particle-phase pollutants.



The ability to simultaneously identify the origin of gas- and particle-phase pollutants is desirable since regulatory agencies are often faced with the task of developing combined emission control strategies that will both reduce gaseous and particulate pollutant concentrations. In addition, the comprehensive and simultaneous apportionment of atmospheric gaseous and particulate pollutants allows maximal source separation since the information contained in the emissions profiles included for the low molecular weight gas-phase species, the semi-volatile species, and the non-volatile particle-phase species all can be exploited. To this end, in the present study a comprehensive organic compound-based receptor model for gas-phase, semi-volatile and particulate air pollutants is developed and applied to atmospheric data collected during a severe photochemical smog episode in Southern California during the summer of 1993. The present study is the first application of an organic compound-based receptor model to determine the source contributions to fine particulate matter concentrations during a severe photochemical smog episode.

## **11.2 Experimental Methods**

### **11.2.1 Ambient Samples**

The ambient data used in the present study were collected during the summer of 1993 in the South Coast Air Basin of California that surrounds Los Angeles. The concentrations of hundreds of gas-phase, semi-volatile and particle-phase organic compounds were measured over a two-day smog episode

during which peak 1-hour ozone concentrations reached 0.29 ppm. Conditions during this study are described in detail elsewhere (Fraser et al., 1996; Fraser et al., 1997; Fraser, 1998) and are briefly summarized here. Data were collected during the period September 8-9, 1993, at four urban air monitoring sites: Long Beach, Central Los Angeles, Azusa, and Claremont, California. These sites are shown in Figure 1 of Fraser et al. (1996). Data were taken over eight 4-hour sampling periods centered within consecutive 6-hour time intervals during the 48-hour study. The ambient data used in the present model evaluation effort were averaged by site thereby providing time-averaged ambient concentration data for the 48-hour sampling study at each of the four monitoring sites. The data collected by Fraser et al. (1996) which were used in the present study consist of ambient measurements of total non-methane organic gases, gas-phase volatile hydrocarbons, gas-phase semi-volatile organic compounds, fine particle-phase organic compounds, and fine particle mass and elemental composition. Gas-phase hydrocarbons and non-methane organic gases were collected in polished stainless steel SUMA canisters and were analyzed by gas chromatography/flame ionization detection (GC/FID). Fine particulate mass concentrations and bulk chemical composition were determined from filter samples collected downstream of AIHL-design cyclone separators (John and Reischl, 1980). Teflon membrane filters (47 mm diameter Teflo, Gelman) were used for collecting fine particle samples for gravimetric mass determination and for measurement of trace metals by X-ray fluorescence analysis and inorganic ions by ion chromatography

and colorimetry. Fine particle samples collected on quartz fiber filters (47 mm diameter Tissuequartz 2500 QAO, Pallflex) were used for organic and elemental carbon analysis as described by Birch and Carey (1996). The concentrations of individual fine particle organic compounds and semi-volatile organic compounds were measured by gas chromatography/mass spectrometry (GC/MS) from samples collected using a high volume dichotomous virtual impactor (Solomon et al., 1983) that was modified by Fraser et al. (1997) for the collection of semi-volatile organic compounds along with particulate matter. Using this sampler fine particle mass is collected on a quartz fiber filter (102 mm diameter Tissuequartz 2500 AQO, Pallflex) and semi-volatile organic compounds are collected downstream of the quartz fiber filter on five consecutive polyurethane foam (PUF) cartridges (7.6 cm diameter by 2.5 cm long, density =  $0.022 \text{ g cm}^{-3}$ , ILD = 30, Atlas Foam).

The sample handling and extraction procedures employed to quantify semi-volatile vapor-phase and particle-phase organic compounds in atmospheric samples have been discussed previously (Fraser et al., 1997). Before the quartz fiber filters and PUF cartridges were extracted, they were spiked with deuterated internal recovery standards. Extracts were filtered, combined, and reduced in volume to approximately 250 ml, and were split into two separate fractions. One fraction was derivatized with diazomethane to convert organic acids to their methyl ester analogues which are amenable to GC/MS identification and quantification. Both the derivatized and underivatized sample fractions from all

of the sample substrates were analyzed by GC/MS. 1-Phenyldodecane was used as a co-injection standard for all sample extracts and standard runs. Hundreds of authentic standards have been prepared for the positive identification and quantification of the organic compounds found in the ambient samples.

The semi-volatile and fine particle hydrocarbons data from Fraser et al. (1997) are scaled upward across all non-aromatic compounds by a factor of 1.7 to correct an error in the reported air volumes sampled.

### **11.2.2 Source Samples**

Emissions from major urban air pollution sources were measured including gas-phase, semi-volatile, and particle-phase organic compounds, plus fine particle emission rates and fine particle elemental composition (Chapters 2-8). A dilution source sampler was employed to dilute hot exhaust emissions with HEPA-filtered and activated carbon-filtered dilution air to bring the source effluent to near ambient temperatures and pressures. The sampler was equipped with a residence time chamber that provides time for the cooled semi-volatile gases to equilibrate between the gas and particle phases under conditions similar to those in the plume downwind of the stack. The diluted exhaust was sampled from the residence time chamber by the same analytical techniques used for the ambient air pollutant measurements discussed above.

A detailed description of the dilution source sampler has been presented previously (Chapter 2). Using the dilution sampler, fine particle organic compound emissions were sampled by two simultaneous sampling trains, a denuder/filter/PUF system and a filter/PUF system. In both sampling trains, diluted exhaust was withdrawn from the residence time chamber of the source sampler through AIHL-design cyclone separators that are designed to remove coarse particles. The denuder/filter/PUF sampling train uses an XAD-coated annular denuder (4 channel, 400 mm long, URG) followed by three quartz fiber filters (47 mm diameter Tissuequartz 2500 QAO, Pallflex) operated in parallel followed by two PUF cartridges (5.7 cm diameter by 7.6 cm long; density =  $0.022 \text{ g cm}^{-3}$ , ILD = 30, Atlas Foam) operated in series. In the denuder/filter/PUF sampling train, semi-volatile organic compounds are collected on the XAD-coated denuder and particulate matter and particle-associated semi-volatile organic compounds are collected on the filter. The downstream PUF cartridges collect any particle-associated semi-volatile organic compounds that volatilize off of the quartz fiber filter. The filter/PUF sampling unit operates according to the same principle as the ambient filter/PUF samplers discussed above. Chemical analysis to quantify individual organic compounds in the source emissions was conducted by gas chromatography/mass spectrometry (GC/MS) as described previously for the ambient samples. As shown in Chapter 2 the total mass of semi-volatile and particle-phase organic compounds collected by the denuder/filter/PUF and filter/PUF sampling trains are in good agreement.

Also connected to the residence chamber of the dilution source sampler was a cyclone-based sampling unit for the collection of fine particulate matter and gas-phase hydrocarbons. In this sampling train, fine particulate matter collected on a quartz fiber filter (47 mm diameter, Pallflex Tissuequartz 2500 QAO) was used for EC/OC determination by the same method as described for the ambient samples. Fine particle samples collected on Teflon membrane filters (47 mm diameter, Gelman Teflo, 2  $\mu\text{m}$  pore size) were used for gravimetric determination of the fine particle mass emissions rate and for analysis of trace metals and inorganic ions by the same analytical techniques as used for the ambient samples. Downstream of one of the Teflon filters, the sample flow was divided and a small portion of the flow was used to fill a 6 liter polished stainless steel SUMA canister for the collection of non-methane volatile hydrocarbons ranging from  $\text{C}_1$  to  $\text{C}_{10}$ . The 6 liter SUMA canister was filled continuously at a constant flowrate set to fill the canister over the entire source test cycle. The analysis of the volatile hydrocarbons in the source emissions again were analyzed by the same analytical techniques as described for the ambient samples.

The composition of the emissions from gasoline-powered motor vehicle engines, diesel engines and meat cooking operations measured by the source sampling system just described form the basis for the organic chemical composition source profiles used for these sources by the organic tracer model. The gasoline-powered motor vehicle tests and the diesel-powered motor vehicle

tests were conducted in the summer of 1996 by Schauer et al. (Chapters 4 and 5) using commercial fuels and motor vehicles taken from the in-use fleet in Southern California. The diesel trucks tested in Chapter 4 were medium-duty diesel trucks which showed lower fine particle elemental carbon emission rates than the heavy-duty diesel trucks measured earlier by Hildemann et al. (1991). In the present receptor modeling study, organic compounds emitted from diesel trucks are represented by the diesel engine source profile of Chapter 5 but the elemental carbon content of diesel engine exhaust is increased to give the same EC/OC ratio as measured by Hildemann et al. (1991) for heavy duty diesel trucks. The meat charbroiling source profile is as described in Chapter 2.

In addition, several other source emissions profiles were required for use in the present receptor modeling study. The chemical composition of fine particle paved road dust was measured by resuspending road dust collected in the south coast region of Southern California into a cleaned glove box followed by sampling through AIHL-design cyclone separators to remove coarse particles and collection on quartz fiber filters and Teflon filters, with chemical analysis as described above for elemental composition and organic compound quantification. Gas-phase pollutant measurements were not made for the road dust sample as road dust is not a significant source of gas-phase pollutants. (Road dust emissions profiles are included in Appendix A.) Particulate emissions profiles for vegetative detritus and residential natural gas combustion were taken from Rogge et al. (1993a, 1993b). Gas-phase hydrocarbon and

VOC emissions data from these sources were not available, but these emissions are thought to be relatively small. Commercial diesel fuel obtained in Southern California in the summer of 1996 was analyzed by the same analytical techniques as used for semi-volatile and particle-phase organic compounds to obtain an emissions profile for whole diesel fuel vapors. The composition of a 1995 sample of Southern California gasoline, constructed as a market share weighted average of the product of the five largest gasoline retailers in Southern California, was used to define the organic compound distribution in whole gasoline vapors. The 1995 gasoline composition data were modified to match conditions during the summer 1993 atmospheric experiments; these changes reflect the reduction in benzene and the increase in MTBE content of gasoline that occurred between the summer of 1993 and the summer of 1995.

A gasoline headspace vapor profile corresponding to the estimated 1993 gasoline composition and a natural gas leakage profile also are needed for the present study. Conner et al. (1995) have shown that the composition of the headspace vapors above a liquid pool of gasoline can be accurately calculated from the liquid gasoline composition and the Raoult's law coefficients for the gasoline components in a gasoline mixture. The gasoline headspace vapor composition for this study was therefore calculated from the composition of the whole gasoline sample described above using Raoult's law coefficients calculated from the data collected by Aulich et al. (1994). (Whole gasoline and



gasoline headspace vapor emissions profiles are included in Appendix B). The natural gas leakage profile was taken from Harley et al. (1992).

## 11.3 Source/Receptor Reconciliation

### 11.3.1 Chemical Mass Balance Approach

Chemical mass balance (CMB) receptor models that use organic compounds as mass balance species have been demonstrated on several occasions (Harley et al., 1992; Scheff and Wadden, 1993; Fujita et al., 1994; Schauer et al., 1996, Chapter 10). In the CMB model, the source contributions are calculated by determining the linear combination of source fingerprints that best reconstruct the ambient concentration data set. The chemical mass balance model can be represented by a set of linear equations as follows:

$$c_{ik} = \sum_{j=1}^m a_{ij} s_{jk} \quad (1)$$

where  $c_{ik}$ , the concentration of chemical species  $i$  at receptor site  $k$ , equals the sum over  $m$  source types of the product of  $a_{ij}$ , the relative concentration of chemical constituent  $i$  in the emissions from source  $j$ , and  $s_{jk}$ , the increment to the total pollutant mass concentration at receptor site  $k$  originating from source  $j$ . The system of equations (1) states that the ambient concentration of each mass balance species must result only from the  $m$  sources included in the model and that no selective loss or gain occurs in transport from the source to the receptor

site. Therefore, the selection of mass balance compounds must be limited to: (1) species in which all major sources are included in the model, (2) species that do not undergo selective removal by chemical reaction or other mechanisms between the source and the receptor site, and (3) species which are not significantly formed by chemical reactions in the atmosphere.

In the present study, the system of equations (1) is solved using the CMB7 receptor modeling computer program (Watson et al., 1990). That algorithm employs an effective variance weighted least-squares solution to the problem of determining the unknown source contributions,  $s_{jk}$ , given the relative concentrations of the chemical substances in the emissions from the sources ( $a_{ij}$ ) and the atmospheric pollutant concentrations,  $c_{ik}$ .

### **11.3.2 Selection of Sources and Organic Compounds**

The selection criteria for the particle-phase organic compounds which are used as tracers in the current study are based on the previous work discussed in Chapters 9 and 10. Selection of the gas-phase hydrocarbon tracers used in the combined gas and particle phase tracer model is based on the criteria outlined by Harley et al. (1992). As previously indicated the motor vehicle source tests used in this analysis were conducted using commercially distributed fuels approximately 3 years after the atmospheric measurements were made. In this time period, no significant changes in diesel fuel formulation were reported but changes were made to the composition of gasoline. Changes in the benzene

and MTBE content of gasoline between 1993 and 1995 are well documented and corrections have been made to the emissions profiles used in this study for whole gasoline vapors and gasoline headspace vapors, but the effect of these fuel composition changes on tailpipe emissions are more difficult to address. Data from the 1993 Van Nuys tunnel study conducted by Fraser et al. (1998) also show methylcyclopentane and methylcyclohexane concentrations in tunnel air that are much lower in the 1993 than would be expected from the tailpipe exhaust and gasoline vapor profiles obtained in 1996 and 1995, respectively. The apparent increase in the methylcyclopentane and methylcyclohexane content of gasoline between 1993 and 1995 is likely due to the direct introduction of these compounds into gasoline accompanied by the removal of these compounds from the catalytic reformer feedstock in the petroleum refinery in order to prevent the formation of benzene from these methylcyloalkanes. For these reasons, methylcyclopentane, methylcyclohexane, benzene, and MTBE are not used as mass balance species in the model.

Methane is used to help trace the leakage of natural gas to the Southern California urban atmosphere. The background air entering the South Coast Air Basin of Southern California contains methane at a concentration of approximately 1700 ppb (Harley et al., 1992) which was subtracted from the measured methane values at each air monitoring site.

## **11.4 Results**

### **11.4.1 Comprehensive Apportionment of Organic Compounds in the Atmosphere**

The comprehensive source apportionment model calculates the contributions of individual air pollution source types to the sum of gas-phase plus particle-phase organic compounds in the atmosphere. The total organic compound concentration in the atmosphere studied here due to a given source is the sum of the volatile organic compounds (VOC) concentrations due to that source as measured by EPA method TO-12, plus the sum of all gas-phase semi-volatile organic compounds and fine particulate organic compounds from that source. Since the ratio of the VOC's, the semi-volatile organic compounds, and the fine particle organic compounds to the sum of these three categories of organic compounds is known in the source emissions, the separate contributions of each source type to the VOC, the semi-volatile organic compounds and the fine particle organic compounds concentrations in the atmosphere can be extracted from the CMB model results.

In the present study, the atmospheric contributions from ten primary sources of organic compounds are calculated. The ten sources which have been included in the model are gasoline-powered motor vehicle exhaust, diesel engine exhaust, whole gasoline vapors, gasoline headspace vapors, whole diesel fuel vapors, fine particulate paved road dust, tire wear debris, vegetative

detritus and meat cooking exhaust. Four additional sources, which have been previously included in organic compound-based CMB models, were not included either for lack of ambient data or because the contributions determined from the model were found not to be significantly different from zero using a 95% confidence interval. Cigarette smoke contributions could not be determined, since the anteiso- and iso-alkanes that are used to trace cigarette smoke particles were below detection limits in the summer 1993 ambient samples. Likewise, the contributions for wood smoke were too low to be determined on the days studied as the ambient sampling program was conducted during hot summer conditions when very little wood is burned. The minor mass contributions from residential natural gas combustion aerosol were not included in the model since the polycyclic aromatic compounds used to trace this source may not be sufficiently stable in the atmosphere during the extreme photochemical smog episode studied here. Sensitivity studies conducted with the model showed that when residential natural gas combustion was included in the model, the contribution from this source was found to be not significantly different from zero with 95% confidence. This inability to quantify the small contribution from residential natural gas combustion may be due to the decreased consumption of natural gas for home heating during this high temperature summer smog episode or may be due to the increased reactivity of the atmosphere which can destroy the PAH and oxy-PAH tracer species used to track the effluent from natural gas combustion. Emissions from paint spray

coating operations were not found in the atmosphere at a level significantly different from zero with greater than 95% confidence and likewise they were removed from the model.

The calculated concentrations of the mass balance species in the receptor model and the measured concentrations of these species showed very good agreement at all four air monitoring sites studied. An example of the degree of agreement between the predicted and measured values of the mass balance species is shown in Figure 11.1 for atmospheric pollutants measured at Azusa. The only compound used as a mass balance species that appears to fit poorly in Figure 11.1 is n-triacontane. Although a comparatively large difference in the measured and calculated concentrations for that compound is seen in Figure 11.1, the difference shown is not significantly different from zero. There is a high uncertainty attached to the calculated value for this compound due to the relatively high uncertainty in the quantification of this compound present at low levels in the emissions from several sources such as motor vehicle exhaust and paved road dust. The CMB model results for this source apportionment study produce a  $R^2$  value of greater than or equal to 0.94 at each of the four air quality monitoring sites studied.

#### **11.4.2 Apportionment of Volatile Organic Compound Concentrations**

Non-methane volatile organic compound concentrations are determined by EPA method TO-12. The TO-12 measurement is based on a flame ionization

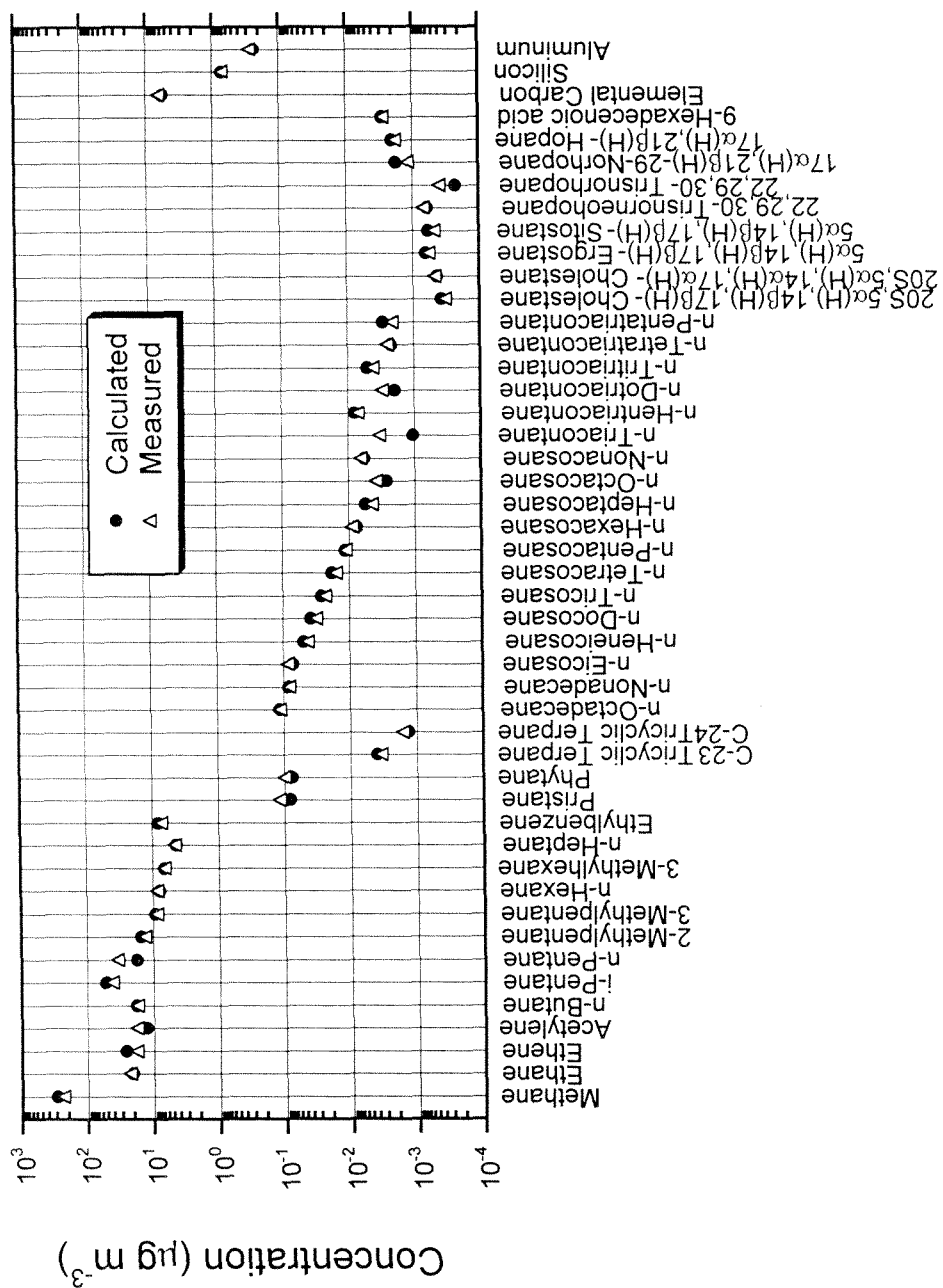


Figure 11.1. Comparison of the measured and calculated ambient concentrations of the mass balance species used in the fine particle CMB model at Azusa, California, September 8-9, 1993.

detection (FID) method which does not respond to all organic carbon in a completely quantitative fashion. For example a carbon atom in a carbonyl group does not respond to the FID analysis such that formaldehyde would give zero response and acetaldehyde would be counted as having half the number of carbon atoms that are actually present. In addition, some highly polar organic compounds such as glycols do not respond well to the TO-12 analysis as they tend to stick to the SUMA canister used for sample collection and to the TO-12 measurement apparatus. For these reasons, the TO-12 method does not truly measure all gas-phase organic carbon. Since all gas-phase organic compounds cannot readily be identified and quantified without exhaustive efforts, the VOC measurement used here still provides the best reproducible measure of the total gas-phase organic carbon present in an atmospheric sample. The fact that the TO-12 method does not respond to some of the oxidized products of gas phase photochemistry is noted since during the severe photochemical smog episode studied here the oxidation of hydrocarbons will tend to decrease the VOC concentration as measured by the EPA TO-12 method even if the total vapor-phase organic carbon content in the atmosphere has remained the same. For this reason, along with the fact that some gas-phase organic compounds will oxidize to form carbon monoxide as well as oxygenated semi-volatile and particle-phase organic compounds, the total quantity of VOC's apportioned from primary sources using non-reactive tracers is likely to be greater than that measured by method TO-12.



The source apportionment model results for volatile organic compounds are shown in Figure 11.2 and are listed in Table 11.1. Gasoline-powered motor vehicle exhaust is the largest single contributor making up over half of the VOC's at all sites. Gasoline vapors comprised of whole gasoline and gasoline headspace vapors are the next largest contributors to the VOC concentrations. At the Central Los Angeles site, the gasoline headspace vapors contribution was not found to be significantly different from zero, as was the whole gasoline vapor contribution at the Claremont site. Natural gas leakage also makes up a noticeable contribution to the ambient VOC concentrations. In addition, the small contributions to VOC's from meat cooking operations and diesel engine exhaust are quantified.

As can be seen in Table 11.1, the apportioned contributions of VOC's at Long Beach, at central Los Angeles, and at Azusa are not significantly different from the measured values at the sites at the 95% confidence level. Although the measured and modeled values are not statistically different from each other, the ratio of apportioned VOC's to measured VOC's increases from approximately 1.1 at Long Beach and Central Los Angeles where much of the pollutant concentrations are due to local sources to 1.2 at Asuza which is at a downwind location that receives air pollution transported from Central Los Angeles. At Claremont, which is even farther downwind than Asuza and where gas-phase emissions experience significant gas-phase chemical reaction prior to arriving at this site, the ratio of predicted to measured VOC concentrations rises

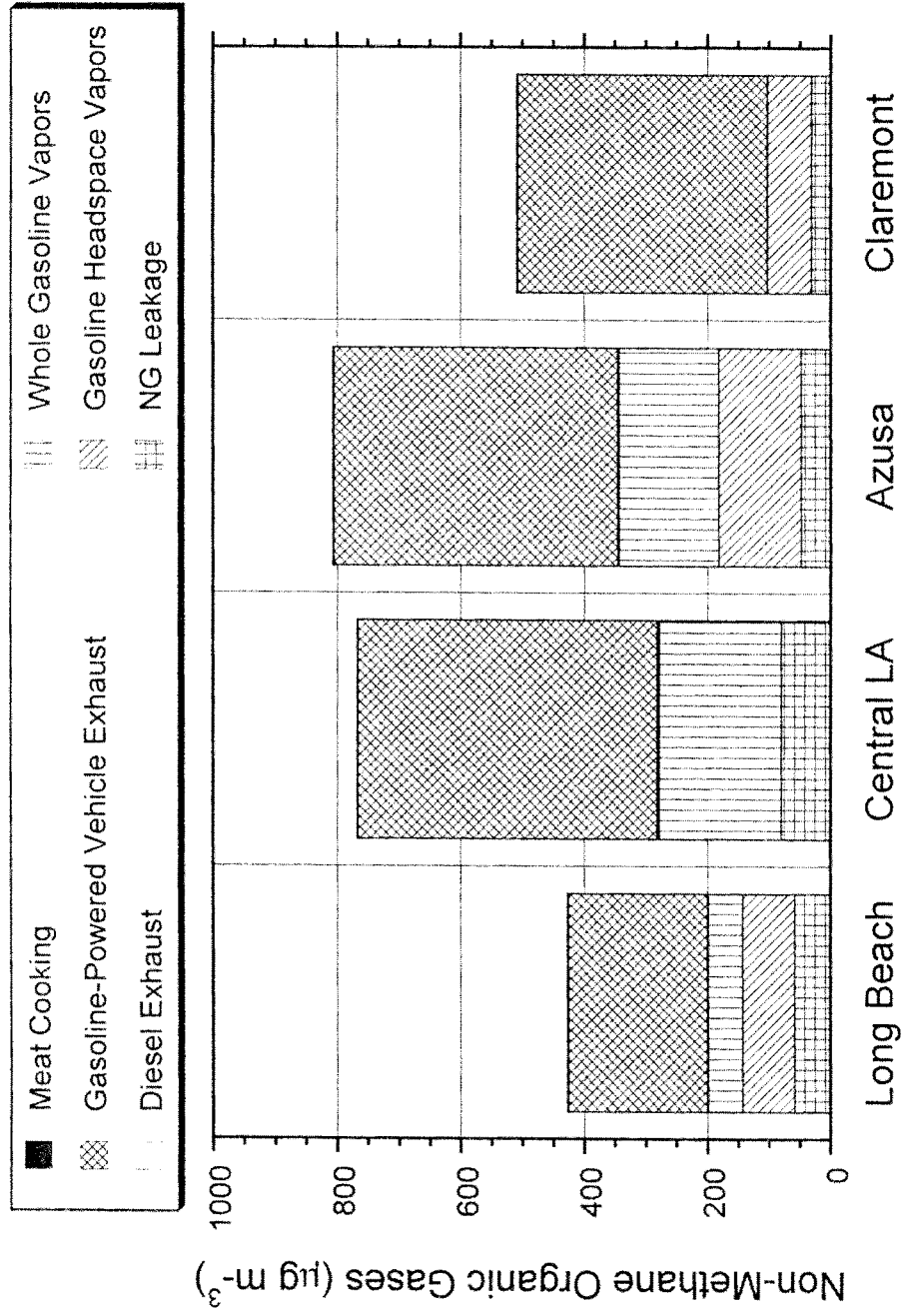


Figure 11.2. Source contributions to non-methane organic gases concentrations, September 8-9, 1993.

Table 11.1. Source apportionment of non-methane organic gas (TO-12) concentrations during the severe photochemical smog episode of September 8-9, 1993; determined by chemical mass balance

	Long Beach (avg $\pm$ std in $\mu\text{g m}^{-3}$ )	Downtown L.A. (avg $\pm$ std in $\mu\text{g m}^{-3}$ )	Azusa (avg $\pm$ std in $\mu\text{g m}^{-3}$ )	Claremont (avg $\pm$ std in $\mu\text{g m}^{-3}$ )
Gasoline-powered motor vehicle exhaust	226 $\pm$ 31.1	485 $\pm$ 64.6	459 $\pm$ 63.7	404 $\pm$ 35.6
Whole gasoline vapors	56 $\pm$ 20.4	198 $\pm$ 37.4	161 $\pm$ 40.1	<sup>a</sup>
Gasoline headspace vapors	84 $\pm$ 22.0	<sup>a</sup>	134 $\pm$ 33.2	71 $\pm$ 16.6
Diesel exhaust	1.4 $\pm$ 0.20	3.6 $\pm$ 0.39	2.7 $\pm$ 0.34	1.4 $\pm$ 0.35
Natural gas leakage	58.7 $\pm$ 8.1	80.8 $\pm$ 10.8	48.0 $\pm$ 8.0	31.9 $\pm$ 5.4
Meat cooking	1.5 $\pm$ 0.36	1.5 $\pm$ 0.45	1.4 $\pm$ 0.43	1.0 $\pm$ 0.34
Sum	428 $\pm$ 44.0	768 $\pm$ 75.4	807 $\pm$ 82.6	509 $\pm$ 39.6
Measured	401 $\pm$ 35.7	713 $\pm$ 76.0	666 <sup>b</sup> $\pm$ 66.8	342 <sup>b</sup> $\pm$ 27.0

<sup>a</sup> Not statistically different from zero with 95 percent confidence, and therefore removed from CMB model

<sup>b</sup> Note that the TO-12 method measurement underreports the VOC concentrations of oxygenated species such as carbonyls.

to 1.5. These trends are consistent with the characteristics of the TO-12 measurement method discussed above.

#### **11.4.3 Apportionment of Fine Particulate Organic Compound Mass and Fine Particulate Mass**

Source contributions to fine particle organic compound concentrations are shown in Figure 11.3 and are listed in Table 11.2. Of the primary sources, motor vehicle exhaust is the largest single contributor to fine particle organic compound mass at all sites followed by meat cooking and road dust. Smaller but quantifiable contributions from vegetative detritus and tire wear debris are observed at all the sites except Central Los Angeles where tire wear debris concentrations were not found to be significantly different from zero with 95% confidence. One of the most notable features of Figure 11.3 is the significant amount of organic compound mass that cannot be attributed to the primary sources. The quantity of other organics that cannot be attributed to primary sources is calculated by subtracting the apportioned fine particle organic compound mass from the total fine particle organic compound mass measured at these sites. The organic compound mass at the ambient monitoring sites is estimated by multiplying the fine particle organic carbon measured by thermal evolution and combustion analysis by a factor of 1.4 to account for the H, O, N, and S present in organic compounds. Since there are no other potentially large sources of primary particulate organic carbon that have not been addressed here, it is reasonable to assume that much of the “other” organic material is

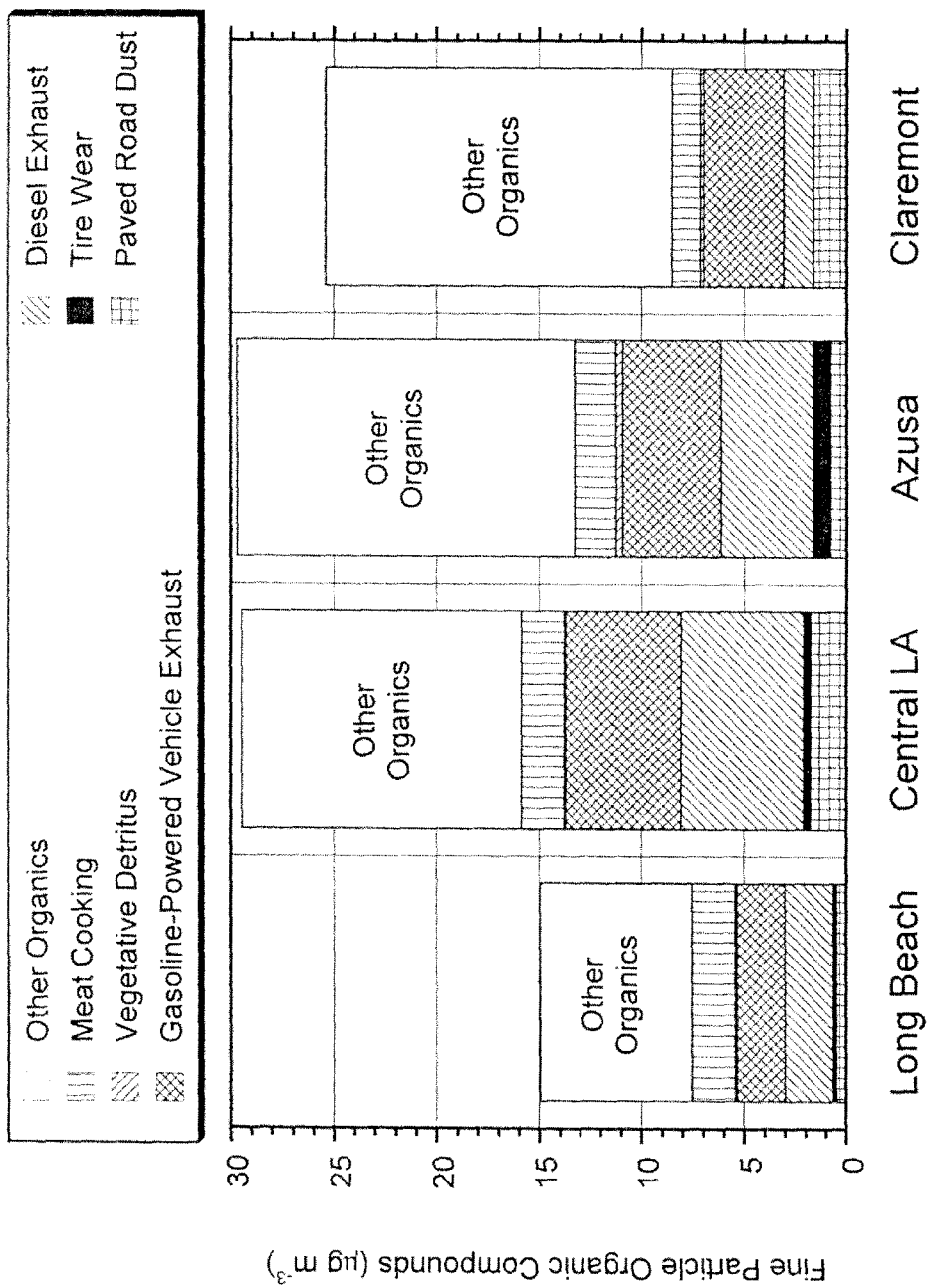


Figure 11.3. Source contributions to fine particulate organic carbon concentrations, September 8-9, 1993.

Table 11.2. Source apportionment of fine particulate organic compound concentrations during the severe photochemical smog episode of September 8-9, 1993: determined by chemical mass balance

	Long Beach (avg $\pm$ std in $\mu\text{g m}^{-3}$ )	Central LA (avg $\pm$ std in $\mu\text{g m}^{-3}$ )	Azusa (avg $\pm$ std in $\mu\text{g m}^{-3}$ )	Claremont (avg $\pm$ std in $\mu\text{g m}^{-3}$ )
Gasoline-powered motor vehicle exhaust	2.33 $\pm$ 0.27	5.62 $\pm$ 0.57	4.65 $\pm$ 0.54	3.90 $\pm$ 0.31
Diesel exhaust	2.36 $\pm$ 0.33	5.98 $\pm$ 0.66	4.51 $\pm$ 0.57	1.45 $\pm$ 0.36
Tire wear debris	0.17 $\pm$ 0.051	0.36 $\pm$ 0.11	0.87 $\pm$ 0.14	*
Paved road dust	0.48 $\pm$ 0.046	1.76 $\pm$ 0.055	0.78 $\pm$ 0.052	1.64 $\pm$ 0.057
Meat cooking	2.09 $\pm$ 0.50	2.07 $\pm$ 0.64	2.02 $\pm$ 0.60	1.39 $\pm$ 0.48
Vegetative detritus	0.10 $\pm$ 0.018	0.075 $\pm$ 0.024	0.33 $\pm$ 0.053	0.16 $\pm$ 0.028
Sum of identified primary sources	7.53 $\pm$ 0.66	15.9 $\pm$ 1.08	13.2 $\pm$ 1.00	8.54 $\pm$ 0.68
Measured	15.0 $\pm$ 1.50	29.5 $\pm$ 2.18	29.6 $\pm$ 2.02	25.4 $\pm$ 1.53

\* Not statistically different from zero with 95 percent confidence, and therefore removed from CMB model

secondary organic aerosol (SOA) formed from the low volatility reaction products of gas-phase chemical reactions. As seen in Figure 11.3, the fraction of organic carbon that is not attributed to the primary sources increases as the air masses move inland. The lowest proportions of presumed SOA are seen at Long Beach and Central Los Angeles, with a higher fraction of SOA at Azusa and an even a greater proportion at Claremont. This behavior is consistent with the increased time for chemical reaction experienced by the emissions that arrive at the downwind sites.

Since the ratio of organic compound mass to overall fine particle mass in the emissions from the primary sources is known, the source contributions to the overall atmospheric fine particle mass concentrations can be calculated. The contributions of the primary fine particle emissions sources to the ambient fine particle concentrations are shown in Figure 11.4 and listed in Table 11.3 along with the secondary sulfate ion, nitrate ion, and ammonium ion measured at the four sampling locations. The quantity of "other" (presumably secondary organics) is determined above. As can be seen in Figure 11.4 the contributions of secondary inorganic ions to atmospheric fine particle concentrations during this particular smog episode show a spatial trend that is the reverse of that observed for the secondary organic aerosol. The contribution from secondary inorganic ions decreases as a function of distance from the coast on this occasion. This is likely due to the larger influence of sulfate from fuel combustion by ships at the harbor and from refineries near the coast

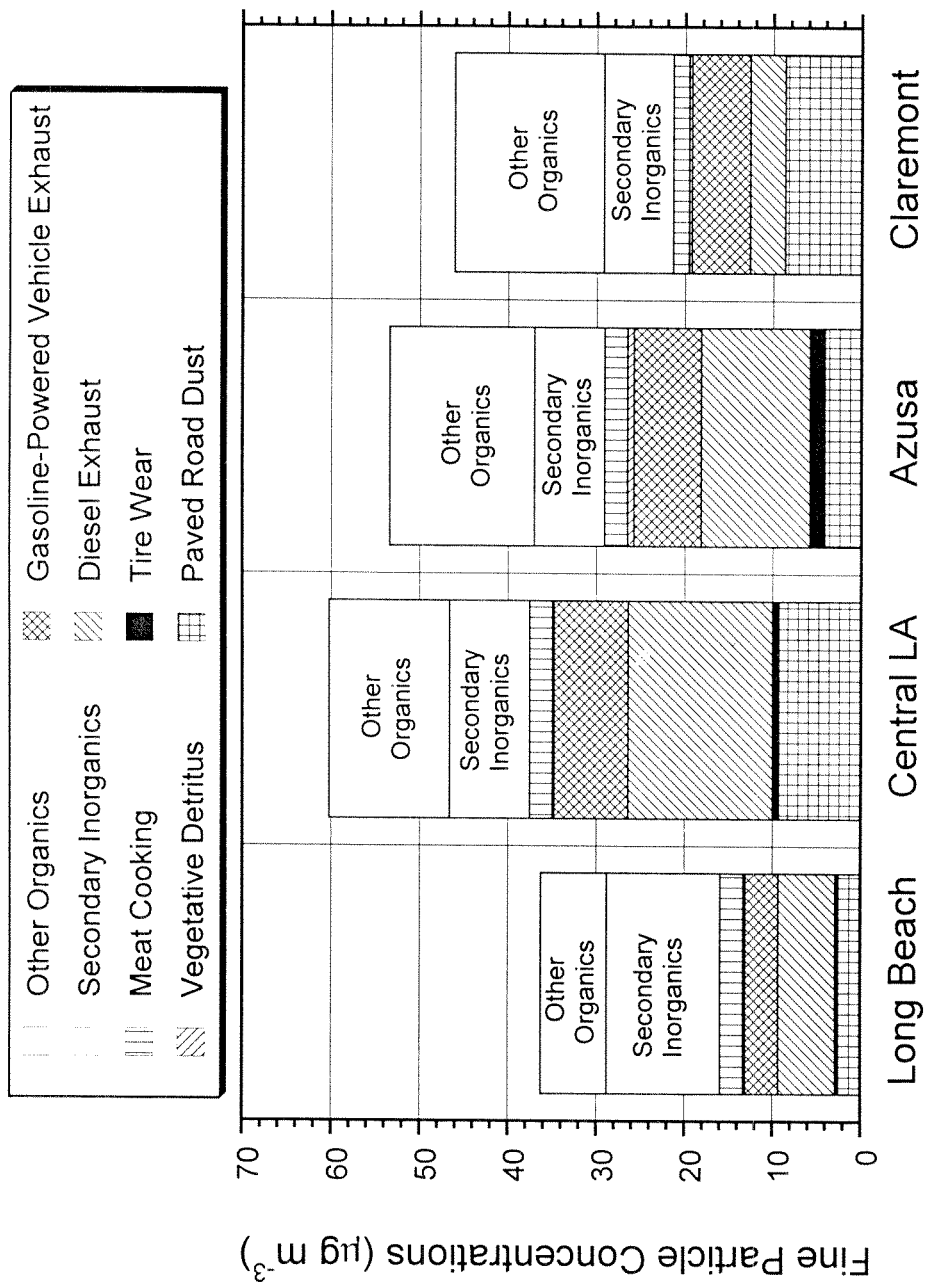


Figure 11.4. Source contributions to fine particle mass concentrations, September 8-9, 1993.



Table 11.3. Source apportionment of fine particle mass concentrations during the severe photochemical smog episode of September 8-9, 1993: determined by chemical mass balance

	Long Beach (avg $\pm$ std in $\mu\text{g m}^{-3}$ )	Central LA (avg $\pm$ std in $\mu\text{g m}^{-3}$ )	Azusa (avg $\pm$ std in $\mu\text{g m}^{-3}$ )	Claremont (avg $\pm$ std in $\mu\text{g m}^{-3}$ )
Gasoline-powered motor vehicle exhaust	3.75 $\pm$ 0.49	8.35 $\pm$ 1.02	7.59 $\pm$ 1.15	6.59 $\pm$ 0.66
Diesel exhaust	6.46 $\pm$ 0.91	16.4 $\pm$ 1.80	12.3 $\pm$ 1.56	3.97 $\pm$ 0.99
Tire wear debris	0.34 $\pm$ 0.10	0.71 $\pm$ 0.21	1.73 $\pm$ 0.27	
Paved road dust	2.53 $\pm$ 0.24	9.31 $\pm$ 0.29	4.13 $\pm$ 0.28	8.68 $\pm$ 0.30
Meat cooking	2.64 $\pm$ 0.63	2.61 $\pm$ 0.84	2.55 $\pm$ 0.76	1.76 $\pm$ 0.61
Vegetative detritus	0.22 $\pm$ 0.039	0.17 $\pm$ 0.052	0.73 $\pm$ 0.12	0.35 $\pm$ 0.062
Other organics	7.45 $\pm$ 1.64	13.6 $\pm$ 2.43	16.4 $\pm$ 2.25	16.9 $\pm$ 1.67
Sulfate ion (secondary plus background)	7.21 $\pm$ 0.72	4.89 $\pm$ 0.33	4.43 $\pm$ 0.29	4.23 $\pm$ 0.28
Secondary nitrate ion <sup>Δ</sup>	2.93 $\pm$ 0.75	2.41 $\pm$ 0.32	1.84 $\pm$ 0.39	2.10 $\pm$ 0.13
Secondary ammonium ion <sup>Δ</sup>	2.73 $\pm$ 0.35	1.77 $\pm$ 0.12	1.68 $\pm$ 0.14	1.53 $\pm$ 0.10
Sum	36.3 $\pm$ 2.33	60.2 $\pm$ 3.35	53.5 $\pm$ 3.08	46.1 $\pm$ 2.16
Measured <sup>Δ</sup>	38.4 $\pm$ 5.55	47.9 $\pm$ 5.72	46.6 $\pm$ 5.79	59.3 $\pm$ 5.07

\* Not statistically different from zero with 95 percent confidence, and therefore removed from CMB model

<sup>Δ</sup> Directly measured from fine particle Teflon filter

accompanied by a decrease in ammonium nitrate concentrations at inland locations due to the very high ambient temperatures during the smog episode (greater than 40 °C peak temperature) that can drive the ammonium nitrate into the gas-phase. At all of the locations studied, except Claremont, the apportioned primary fine particle mass plus secondary aerosol concentrations are not significantly different from the measured fine particle mass concentrations with greater than 95% confidence. The uncertainties in the measured fine particle mass concentrations are in part due to the fairly small quantities of fine particle mass collected for gravimetric determination during a four-hour sampling period. At Claremont, the apportioned fine particle mass plus secondary aerosol falls short of the measured concentration by approximately 22%.

#### **11.4.4 Apportionment of Semi-volatile Organic Compounds**

Table 11.4 shows the contributions to the ambient concentrations of gas-phase semi-volatile organic compounds determined by the source apportionment model. Motor vehicle exhaust from the gasoline-powered and the diesel-powered engines along with diesel fuel vapors make up virtually all of the ambient concentrations of gas-phase semi-volatile organic compounds with only a small fraction resulting from meat cooking operations. It should be noted that some or all of the unburned whole diesel fuel vapors may be from diesel exhaust emissions not represented by the hot-start dynamometer diesel emissions profile

Table 11.4. Source apportionment of gas-phase semi-volatile organic compound concentrations during the severe photochemical smog episode of September 8-9, 1993: determined by chemical mass balance

	Long Beach (avg $\pm$ std in $\mu\text{g m}^{-3}$ )	Central LA (avg $\pm$ std in $\mu\text{g m}^{-3}$ )	Azusa (avg $\pm$ std in $\mu\text{g m}^{-3}$ )	Claremont (avg $\pm$ std in $\mu\text{g m}^{-3}$ )
Gasoline-powered motor vehicle exhaust	3.41 $\pm$ 0.53	6.77 $\pm$ 1.09	7.02 $\pm$ 1.08	6.36 $\pm$ 0.60
Diesel exhaust	2.30 $\pm$ 0.32	5.84 $\pm$ 0.64	4.40 $\pm$ 0.56	1.41 $\pm$ 0.35
Diesel fuel vapors	6.89 $\pm$ 0.56	8.68 $\pm$ 0.83	7.69 $\pm$ 0.71	7.36 $\pm$ 0.61
Meat cooking	0.055 $\pm$ 0.013	0.054 $\pm$ 0.017	0.053 $\pm$ 0.016	0.036 $\pm$ 0.013
Sum	12.7 $\pm$ 0.83	21.3 $\pm$ 1.51	19.2 $\pm$ 1.41	15.4 $\pm$ 0.93

\* Not statistically different from zero with 95 percent confidence, and therefore removed from CMB model

used in this study (i.e., unburned diesel fuel may be emitted in much larger quantities during cold starts).

#### **11.4.5 Apportionment of Individual Organic Compounds**

An additional result that can be calculated from the source apportionment model used in this study is the relative contribution of each primary source to the atmospheric concentrations of individual organic compounds. Figure 11.5 shows the contribution of each source to the atmospheric concentration of the mass balance species at the Azusa air monitoring site.

#### **11.4.6 Comparison of Unapportioned Organic Compound Mass to Organic Acid Tracers**

1,2-Benzenedicarboxylic acid is found in noticeable quantities in the atmosphere (Rogge et al., 1993; Chapter 10; Fraser 1998) but has not been identified in the emissions from any of the major urban air pollution sources tested (Chapters 2-8). Therefore, it is likely that this non-volatile organic acid is formed in the atmosphere by gas-phase chemical reactions and is a secondary aerosol product. Shown in Figure 11.6 is the ambient concentration of 1,2-benzenedicarboxylic acid compared to the "other" organics category determined in the present study and in a wintertime fine particle source apportionment study conducted in California's San Joaquin Valley (Chapter 10). Data points are shown in Figure 11.6, only if the quantity of "other" organics determined from the source apportionment results were found to be significantly

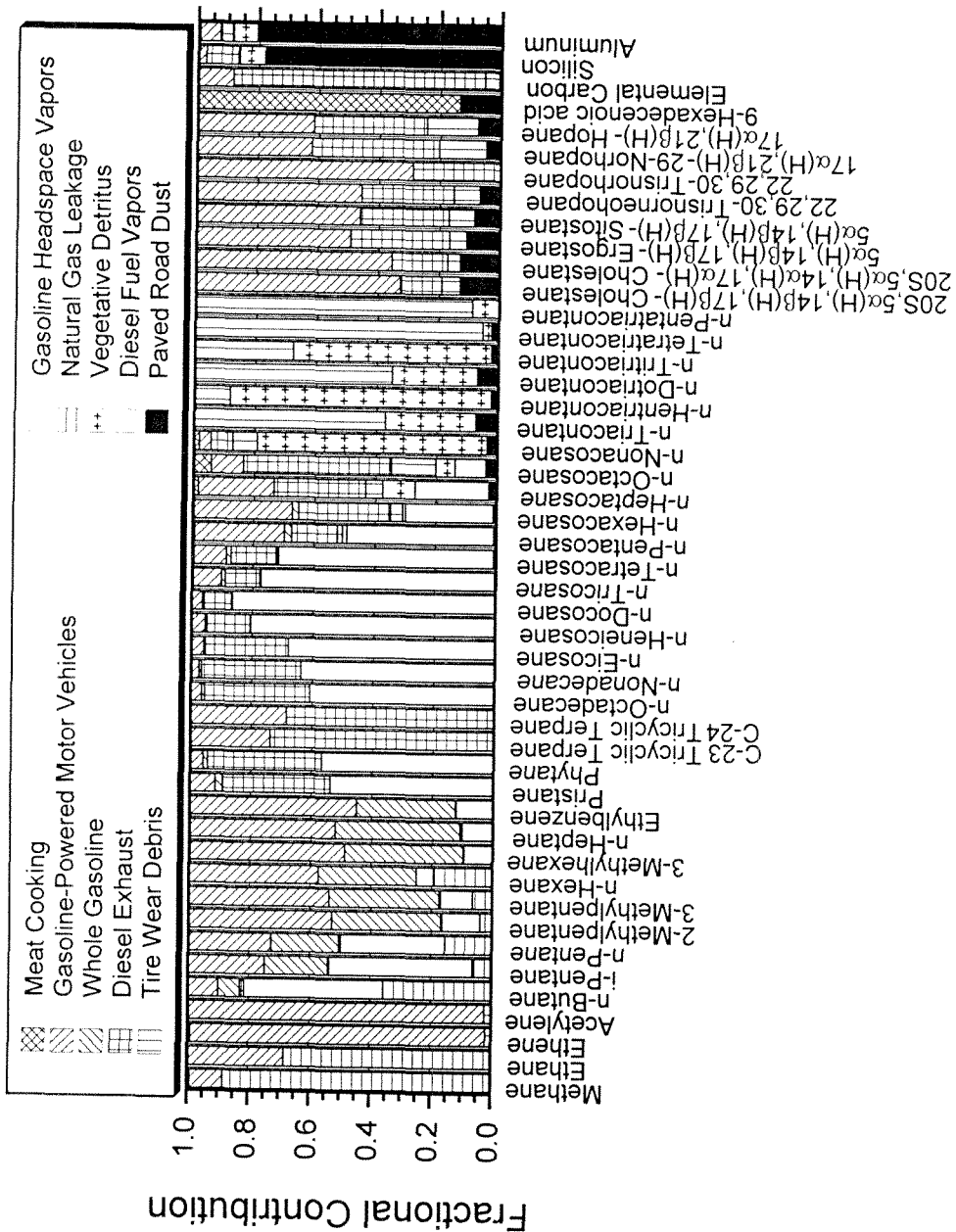


Figure 11.5. Source contributions to the atmospheric concentrations of the mass balance species used in the CMB model at Azusa, September 8-9, 1993.

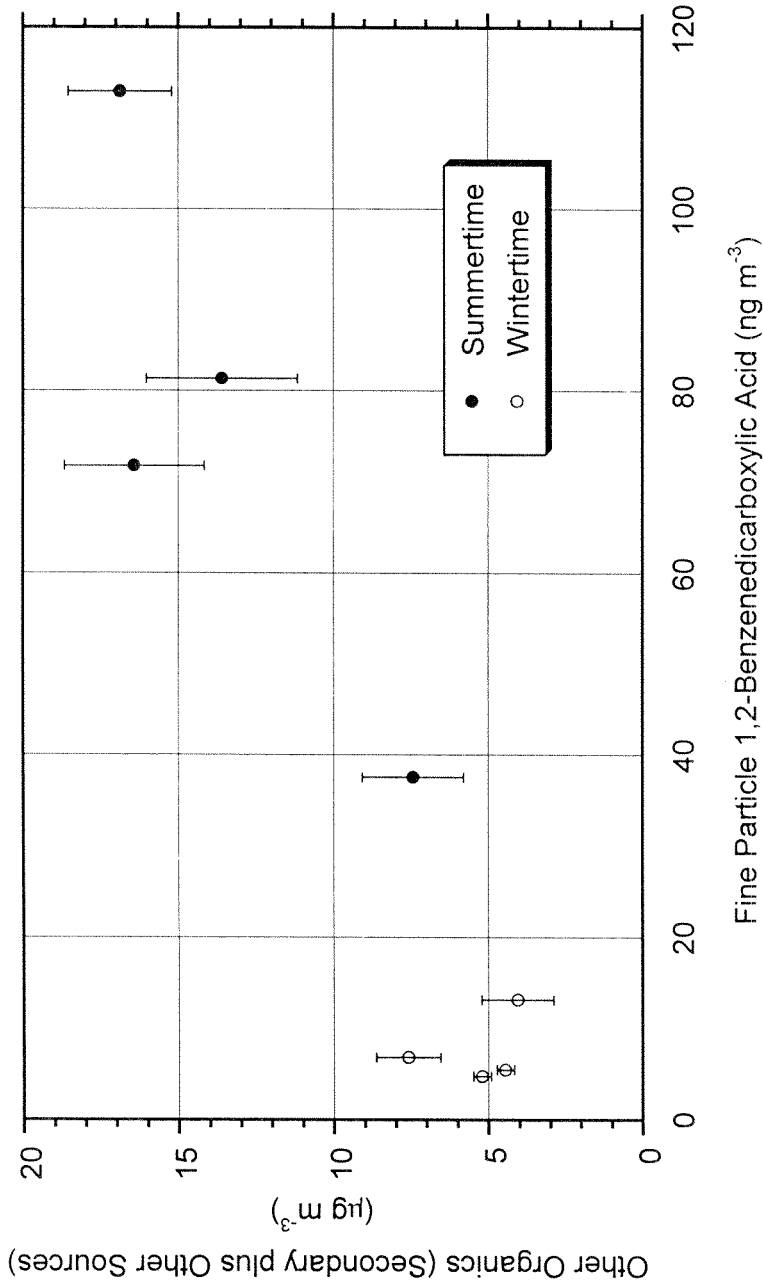


Figure 11.6. Comparison of the calculated "other" organics from the CMB model results and the fine particle 1,2-benzenedicarboxylic acid concentrations for the present summer study and from a fine particle source apportionment study of the wintertime aerosol in California's San Joaquin Valley (Chapter 10).

greater than zero with 95% confidence. The error bars shown in Figure 11.6 represent one standard deviation of the estimate of the quantity of “other” organics for the sampling events studied. As seen in Figure 11.6, the concentration of 1,2-benzenedicarboxylic acid present in the aerosol correlates fairly well with the calculated quantity of “other” organic compounds that cannot be assigned to a primary source and that thus are assumed to be largely due to secondary organic aerosol formation by atmospheric chemical reaction. The fact that a curve through the points in Figure 11.6 has an approximate intercept of about  $4 \mu\text{g m}^{-3}$  of “other” organics when the 1,2-benzenedicarboxylic acid concentration is zero roughly matches the levels of background organic aerosol seen at remote air monitoring sites. Other small sources of primary organics which are not included in the model may also exist.

## 11.5 References

- Aulich T. R., He X. M., Grisanti A. A. and Knudson, C. L. (1994) Gasoline evaporation-ethanol and nonethanol blends. *J. Air & Waste Manage. Assoc.* **44**, 1004-1009.
- Birch M. E. and Cary R. A. (1996) Elemental carbon-based method for monitoring occupational exposures to particulate diesel exhaust. *Aerosol. Sci. Technol.* **25**, 221-241.
- Cass G. R. and McRae G. J. (1983) Source-receptor reconciliation of routine air monitoring data for trace metals: An emissions inventory assisted approach. *Environ. Sci. Technol.* **17**, 129-139.
- Conner T. A., Lonneman W. A. and Seila R. L. (1995) Transportation-related volatile hydrocarbon source profiles measured in Atlanta. *J. Air & Waste Manage. Assoc.* **45**, 383-394.
- Fraser M. P., Grosjean D., Grosjean E., Rasmussen R. A. and Cass, G. R. (1996) Air quality model evaluation data for organics. 1. Bulk chemical composition and gas/particle distribution factors. *Environ. Sci. Technol.* **30**, 1731-1743.



- Fraser M. P., Simoneit B. R. T., Cass G. R. and Rasmussen R. (1997) Air quality model evaluation data for organics. 4. C<sub>2</sub>-C<sub>36</sub> nonaromatic hydrocarbons. *Environ. Sci. Technol.* **31**, 2356-2367.
- Fraser M. P. (1998) Measuring and modeling the concentrations of individual organic compounds in the urban environment, Ph.D. thesis, Calif. Inst. of Technol., Pasadena, CA.
- Fraser M. P., Simoneit B. R. T., Cass G. R. and Rasmussen R. (1998) Gas-phase and particle-phase organic compounds emitted from motor vehicle traffic in a Los Angeles roadway tunnel. Submitted to *Environ. Sci. Technol.*
- Friedlander S. K. (1973) Chemical element balances and identification of air pollution sources. *Environ. Sci. Technol.* **7**, 235-240.
- Fujita E. M., Watson J. G., Chow J. D. and Lu Z. (1994) Validation of the chemical mass balance receptor model applied to hydrocarbon source apportionment in the Southern California Air Quality Study. *Environ. Sci. Technol.* **28**, 1633-1649.
- Harley R. A., Hannigan M. P. and Cass G. R. (1992) Respeciation of organic gas emissions and the detection of excess unburned gasoline in the atmosphere. *Environ. Sci. Technol.* **26**, 2395-2408.

- Harrison R. M., Smith D. J. T. and Luhana L. (1996) Source apportionment of polyaromatic-hydrocarbons collected from an urban location in Birmingham, UK. *Environ. Sci. Technol.* **30**, 825-832.
- Hawthorne S. B., Miller D. J., Langenfeld J. J. and Krieger M. S. (1992) PM<sub>10</sub> high-volume collection and quantification of semi-volatile and non-volatile phenols, methoxylated phenols, alkanes, and polyaromatic-hydrocarbons from winter urban air and their relationship to woodsmoke emissions. *Environ. Sci. Technol.* **11**, 2251-2262.
- Hildemann L. M., Markowski G. R. and Cass G. R. (1991) Chemical composition of emissions from urban sources of fine organic aerosol. *Environ. Sci. Technol.* **25**, 744-759.
- John W. and Reischl G. (1980) A cyclone for size-selective sampling of ambient air. *JAPCA* **30**, 872-876.
- Khalil M. A. K., Edgerton S. A. and Rasmussen R. A. (1983) A gaseous tracer for air pollution from residential wood burning. *Environ. Sci. Technol.* **9**, 555-559.
- Miller M. S., Friedlander S. K. and Hidy G. M. (1972) A chemical element balance for the Pasadena aerosol. *J. Colloid Interface Sci.* **39**, 165-176.

- Rogge W. F., Hildemann L. M., Mazurek M. A., Cass G. R. and Simoneit B.R.T.  
(1993a) Sources of fine organic aerosol. 4. Particulate abrasion products from leaf surfaces of urban plants. *Environ. Sci. Technol.* **27**, 2700-2711.
- Rogge W. F., Hildemann L. M., Mazurek M. A., Cass G. R. and Simoneit B.R.T.  
(1993b) Sources of fine organic aerosol. 5. Natural gas home appliances. *Environ. Sci. Technol.* **27**, 2736-2744.
- Rogge W. F., Mazurek M. A., Hildemann L. M., Cass G. R. and Simoneit B.R.T.  
(1993c) Quantification of urban organic aerosols at a molecular level: Identification, abundance and seasonal variation. *Atmos. Environ.* **27**, 1309-1330.
- Schauer J. J., Rogge W. F., Hildemann L. M., Mazurek M. A., Cass G. R. and Simoneit B. R. T. (1996) Source apportionment of airborne particulate matter using organic compounds as tracers. *Atmos. Environ.* **30**, 3837-3855.
- Scheff P. A. and Wadden R. A. (1993) Receptor modeling of volatile organic compounds. 1. Emissions inventory and validation. *Environ. Sci. Technol.* **27**, 617-625.

Solomon P. A., Moyers J. L. and Fletcher R. A, (1984) High-volume dichotomous virtual impactor for the fractionation and collection of particles according to aerodynamic size. *Aerosol. Sci. Technol.* **4**, 455-464.

Watson J. G., Robinson N. F., Chow J. C., Henry R. C., Kim B. M., Pace T. G., Meyer E. I. and Nguyen Q. (1990) The USEPA/DRI chemical mass balance receptor model, CMB 7.0. *Environ. Softw.* **5**, 38-49.

## Chapter 12

### Conclusion

#### 12.1 Summary

Gas-phase volatile organic compounds, semi-volatile organic compounds and high molecular weight particle-phase organic compounds have been simultaneously quantified on a single compound basis in the emissions from major sources of urban air pollutants. These sources include catalyst-equipped gasoline-powered motor vehicles, noncatalyst gasoline-powered motor vehicles, medium duty diesel trucks, meat charbroiling, cooking operations that use seed oils, cigarette combustion, and spray coating operations. A dilution source sampling system was employed to dilute hot exhaust emissions with activated carbon-filtered and HEPA-filtered air which in the presence of sufficient residence time causes those organic vapors that will form particulate matter upon cooling in the atmosphere instead to condense onto pre-existing particles in the source exhaust within the dilution sampler itself. The emissions thus can be sampled at near atmospheric temperature and pressure in order to obtain data on the partitioning of organic compounds between the gas and particle phases. Advanced sampling techniques were used to characterize the gas/particle phase distribution of semi-volatile organic compounds in the diluted and cooled exhaust emissions.

The organic compound emissions profiles developed during the source testing program were used in receptor-based air pollution models to determine the primary source contributions to volatile organic gases, semi-volatile organic gases, fine particle organic compounds, fine particle mass and individual organic compound concentrations in the urban atmosphere. The model results also can be used to place an upper limit on the contribution of secondary organic aerosol to atmospheric fine particle concentrations. The models were used to help understand the source contributions to atmospheric pollutants under annual average, wintertime and summertime conditions.

### **12.1.1 Meat Charbroiling**

Emission rates of 120 organic compounds, spanning carbon numbers from C<sub>1</sub> to C<sub>29</sub> were quantified in the exhaust from meat charbroiling including n-alkanoic acids, n-alkenoic acids, carbonyls, lactones, alkanes, aromatics, polycyclic aromatic hydrocarbons, alkenes, and steroids. Ethylene, formaldehyde, and acetaldehyde were found to be the predominant light gas-phase organic compounds emitted from the charbroiling operations. n-Alkanoic acids, n-alkenoic acids, and carbonyls made up a significant fraction of the quantified semi-volatile and particle-phase organic compound emissions. Meat charbroiling is one of the few sources identified to date that contributes to the high molecular weight aldehydes measured in the urban atmosphere. Semi-volatile and particle-phase organic compounds were collected for quantification

by two simultaneous sampling protocols: (1) quartz fiber filters followed by polyurethane foam (PUF) cartridges, and (2) XAD-coated annular denuders followed by quartz fiber filters and PUF cartridges. Good agreement was observed for the total mass emissions collected by the two different sampling procedures; however, the partitioning of the semi-volatile organic compounds between the gas phase and particle phase, as measured by the two sampling procedures, showed significant differences for n-alkanoic acids, indicating that significant artifact adsorption of these compounds occurs to the filter in the filter/PUF sampling system.

### **12.1.2 Cooking Vegetables in Seed Oil**

Two cooking methods and three types of seed oils were examined: vegetables stir fried in soybean oil, vegetables stir fried in canola oil, and potatoes deep fried in hydrogenated soybean oil. The emission rates of 99 organic compounds were quantified, including n-alkanes, branched alkanes, alkenes, n-alkanoic acids, n-alkenoic acids, carbonyls, aromatics, polycyclic aromatic hydrocarbons (PAH), and lactones. Carbonyls and fatty acids (n-alkanoic and n-alkenoic acids) made up a significant portion of the organic compounds emitted from all three seed oil cooking procedures. The compositional differences in the organic compound emissions between the different cooking operations were consistent with the differences in the organic composition of the various cooking oils used. The distribution of the n-alkanoic

acids between the gas and particle phases was found to be in good agreement with gas/particle partitioning theory. The relative importance of emissions from commercial cooking operations that employ seed oils to the total emissions of C<sub>16</sub> and C<sub>18</sub> n-alkanoic acids in the Los Angeles urban area was estimated, and showed that cooking with seed oils accounted for approximately 12% of the total primary emissions of these acids. Estimates indicated that cooking with seed oils may make up a significant fraction of the emissions of the n-alkanoic acids in the molecular weight range of nonanoic acid.

### **12.1.3 Diesel Trucks**

Emissions from late-model medium-duty diesel trucks were quantified using a two-stage dilution source sampling system. The diesel trucks were driven through the hot-start Federal Test Procedure (FTP) urban driving cycle on a transient chassis dynamometer. Emission rates of 52 gas-phase volatile hydrocarbons, 67 semi-volatile and 28 particle-phase organic compounds, and 26 carbonyls, were quantified along with fine particle mass and chemical composition. It was found that all C<sub>1</sub>-C<sub>13</sub> carbonyls combined account for 63% of the gas-phase organic compound mass emitted from medium duty-diesel trucks. Fine particulate matter emission rates and chemical composition were quantified simultaneously by two methods: a denuder/filter/PUF sampler and a traditional filter sampler. Both sampling techniques yielded the same elemental carbon emission rate of 56 mg per km driven, but the particulate organic carbon



emission rate determined by the denuder-based sampling technique was found to be 35% lower than the organic carbon mass collected by the traditional filter-based sampling technique due to a positive vapor-phase sorption artifact that affects the traditional filter sampling technique. The distribution of organic compounds in the diesel fuel used in this study was compared to the distribution of these compounds in the vehicle exhaust. Significant enrichment in the ratio of unsubstituted polycyclic aromatic hydrocarbons (PAH) to their methyl and dimethyl substituted homologues was observed in the tailpipe emissions relative to the fuel. Isoprenoids and tricyclic terpanes were quantified in the semi-volatile organics emitted from diesel vehicles. When used in conjunction with data on the light gas-phase hydrocarbons and elemental carbon emitted, the isoprenoids and the tricyclic terpanes may help trace the presence of diesel exhaust in atmospheric samples.

#### **12.1.4 Gasoline-Powered Motor Vehicles**

Organic compounds present in the tailpipe emissions from an in-use fleet of gasoline-powered automobiles and light-duty trucks were quantified using a two stage dilution source sampling system. The vehicles were driven through the cold-start Federal Test Procedure (FTP) urban driving cycle on a transient dynamometer. Emission rates of gas-phase volatile hydrocarbons, semi-volatile and particle-phase organic compounds, carbonyls, and fine particle mass and chemical composition were quantified. Six isoprenoids and two tricyclic

terpanes, which were quantified using new source sampling techniques for semi-volatile organic compounds, have been identified as potential tracers for gasoline-powered motor vehicle effluent emissions. A composite sample of the commercially-distributed California Phase II Reformulated Gasoline used in these tests was analyzed by several analytical methods to quantify the organic compound distribution in the gasoline including some organic compounds that are found in the atmosphere as semi-volatile and particle-phase species. These results allowed a direct comparison of the semi-volatile and particle-phase organic compound emissions from gasoline-powered motor vehicles to the gasoline burned by these vehicles. The distribution of n-alkanes and isoprenoids emitted from the catalyst-equipped gasoline-powered vehicles was found to be the same as the distribution of these compounds in the gasoline used. In contrast, the distribution of polycyclic aromatic hydrocarbons (PAH) present in the gasoline was significantly different from the distribution of the PAH in the tailpipe emissions.

#### **12.1.5 Fireplace Combustion of Wood**

The emissions rates of volatile organic compounds (VOC), gas-phase semi-volatile organic compounds, and particle-phase organic compounds from residential fireplace combustion of wood were measured. Firewood from a conifer tree (pine) and from two deciduous trees (oak and eucalyptus) were burned to determine organic compound emissions profiles for each wood type

including the distribution of the alkanes, alkenes, aromatics, polycyclic aromatic hydrocarbons (PAH), phenol and substituted phenols, guaiacol and substituted guaiacols, syringol and substituted syringols, carbonyls, alkanolic acids, resin acids, and levoglucosan. Levoglucosan was the major constituent in the fine particulate emissions from all three wood types, contributing 18 to 30 percent of the fine particulate organic compound emissions. Guaiacol (2-methoxyphenol), guaiacols with an additional substituents at position 4 on the molecule, and resin acids were found to be emitted in significant quantities from pine wood combustion. Syringol (2,6-dimethoxyphenol) and syringols with additional substituents at position 4 on the molecule were emitted in large amounts from oak and eucalyptus firewood combustion but these compounds were not detected in the emissions from pine wood combustion. Syringol and most of the substituted syringols are found to be semi-volatile compounds that are present in both the gas and particle phases, but two substituted syringols which have not been previously quantified in wood smoke emissions, propionylsyringol and butyrylsyringol, were found exclusively in the particle-phase and can be used to help trace wood smoke particles in the atmosphere. Benzene, ethene, and acetylene are often used as tracers for motor vehicle exhaust in the urban atmosphere. Our measurements showed that the contribution of wood smoke to the ambient concentration of benzene, ethene, and acetylene is large enough in areas with substantial wood combustion that use of these compounds as if they

were vehicle tracers could lead to an overestimate of the contribution of motor vehicle tailpipe exhaust to atmospheric VOC concentrations.

### **12.1.6 Cigarette Smoke**

One hundred and thirty-seven gas-phase, semi-volatile, and particle-phase organic compounds including alkanes, olefins, aromatics, polycyclic aromatic hydrocarbons (PAH), fatty acids, carbonyls, nicotine and other nitrogen-containing organic compounds were quantified in the emissions from cigarette smoking. Six different brands of commercially-available cigarettes, representing four cigarette manufacturers, were smoked by a cigarette customer to obtain an average cigarette smoke emissions profile that combined both sidestream and exhaled mainstream smoke. Gas-phase emissions were found to have significant alkanes, olefins, aromatics, carbonyls and nicotine content. Quantified particle-phase emissions also contain nicotine accompanied by noticeable contributions from alkanes, phenols, and fatty acids. Nicotine was emitted at the highest rate of all of the individual non-methane organic compounds quantified in the emissions from cigarette smoke followed by isoprene and acetaldehyde. Olefins and carbonyls were the largest contributors to low molecular weight volatile gas-phase organic compound emissions followed next by alkanes and aromatic hydrocarbons. The distribution of light gas-phase hydrocarbons and carbonyls emitted from cigarette smoking was compared to the distribution of these compounds in wood smoke and meat charbroiling

emissions. The quantitative differences in these emission profiles provide one basis for distinguishing the contributions from different sources to air pollutant levels in environments that contain cigarette smoke that is mixed with the emissions from other domestic or commercial activities. In addition, the gas/particle phase-distribution and emission rates of semi-volatile organic compounds emitted in cigarette smoke, including nicotine, triacetin, menthol and neophytadiene, have been quantified. Carbonyls, cotinine, nicotinic acid and N-oxynicotine are identified as supplemental particle-phase tracers for cigarette smoke, which could be used along with the high molecular weight iso- and anteiso-alkanes to track cigarette smoke contributions to air pollutant concentrations.

### **12.1.7 Spray Coating Operations**

Gas-phase and particle-phase emissions from industrial-scale spray painting operations were measured. Both water-based paint and oil-based paint formulations were examined. The emissions rates of 35 organic compounds that included alkanes, aromatics, aldehydes, ketones, and esters were quantified, along with the fine particle mass emission rate and fine particle elemental composition. Total non-methane organic gas emissions from water-based spray coating operations were dominated by the emission of acetone and butanone. Total non-methane organic gas emissions from oil-based spray coating operations were found to contain alkanes, cycloalkanes, aromatics, and

aliphatic ketones. Fine particle and semi-volatile organic compound mass emissions from the use of both paint types were much lower than the mass emissions of gas-phase organic compounds. Texanol (2,2,4-trimethyl-1,3-pentanediol monoisobutyrate), a semi-volatile organic compound emitted from spray coating operations using water-based paints that can be measured by standard GC/MS techniques, was identified as a potentially useful tracer for the emissions from water-based spray coating operations. Organic carbon and titanium (presumably present as titanium dioxide) were the largest contributors to the fine particle mass emitted from both types of paint tested in the present study.

#### **12.1.8 Source Contributions to Atmospheric Fine Particle Concentrations**

A chemical mass balance receptor model based on organic compounds has been developed that relates source contributions to airborne fine particle mass concentrations. Source contributions to the concentrations of specific organic compounds are revealed as well. The model was applied to four air quality monitoring sites in Southern California using atmospheric organic compound concentration data and source test data collected specifically for the purpose of testing this model. The contributions of up to nine primary particle source types were separately identified in ambient samples based on this method, and approximately 85% of the organic fine aerosol was assigned to primary sources on an annual average basis. The model provided information

on source contributions to fine mass concentrations, fine organic aerosol concentrations and individual organic compound concentrations. The largest primary source contributors to fine particle mass concentrations in Los Angeles were found to include diesel engine exhaust, paved road dust, gasoline-powered vehicle exhaust, plus emissions from food cooking and wood smoke, with smaller contributions from tire dust, plant fragments, natural gas combustion aerosol, and cigarette smoke. Once these primary aerosol source contributions were added to the secondary sulfates, nitrates and organics present, virtually all of the annual average fine particle mass at Los Angeles area monitoring sites was assigned to its sources.

#### **12.1.9 Source Contributions to Wintertime Gaseous and Particulate Pollutant Concentrations**

Two chemical mass balance receptor models were developed which can determine the source contributions to atmospheric pollutant concentrations using organic compounds as tracers. The first model used particle-phase organic compounds to apportion the primary source contributions to atmospheric fine particulate organic compound concentrations and fine particle mass concentrations. This model can separately distinguish contributions from hardwood combustion and softwood combustion, in addition to the contributions from diesel engine exhaust, gasoline-powered motor vehicle exhaust, meat cooking operations, paved road dust, natural gas combustion, and vegetative detritus. The second receptor model simultaneously used both volatile gas-

phase hydrocarbons and particle-phase organic compounds as tracers to determine source contributions to the non-methane organic gases in the atmosphere. The non-methane organic gas apportionment model can distinguish contributions from gasoline-powered motor vehicles, diesel-powered motor vehicles, wood combustion, meat cooking operations, whole gasoline vapors, and gasoline headspace vapor emissions.

Both models were applied to data collected in California's San Joaquin Valley during two severe wintertime air pollution episodes. Source contributions to fine particle air quality were calculated for two urban sites, in Fresno and Bakersfield, and one background site, Kern Wildlife Refuge. Primary particle emissions from wood combustion, diesel engines, meat cooking, and gasoline-powered motor vehicles contributed on average 79% of the airborne fine particle organic compound mass at the urban sites during both episodes while these primary sources contributed less than 15% of the fine particle mass concentration at the background site. Fine particle organic compound mass which could not be attributed to any of these anthropogenic sources and that could not be attributed to vegetative detritus averages  $4.5 \mu\text{g m}^{-3}$  at the urban sites and  $4.6 \mu\text{g m}^{-3}$  at the background site, suggesting that the regional secondary organic aerosol concentration was as uniform across the valley as was also observed for the secondary inorganic ions: sulfate, nitrate, and ammonium. Contributions to non-methane organic gases were calculated only at Fresno as gas-phase hydrocarbon data were not available at the other sites



for the episodes studied. Gasoline-powered motor vehicle exhaust and whole gasoline vapors were found to be the largest contributors to non-methane organic gases concentrations followed by natural gas leakage. Smaller but statistically significant contributions to the ambient volatile organic compound concentrations from wood combustion, meat cooking, and diesel exhaust also were quantified.

#### **12.1.10 A Comprehensive Source Apportionment Model for Organic Compounds**

A comprehensive organic compound-based receptor model was developed to simultaneously apportion the source contributions to atmospheric gas-phase organic compounds, semi-volatile organic compounds, fine particle organic compounds, and fine particle mass concentrations. The model was applied to ambient data collected at four sites in the south coast region of California during a severe summertime photochemical smog episode, where the model was able to determine the direct primary contributions to atmospheric pollutant concentrations from ten distinct air pollution source types. The ten sources included in the model were gasoline-powered motor vehicle exhaust, diesel engine exhaust, whole gasoline vapors, gasoline headspace vapors, whole diesel fuel vapors, paved road dust, tire wear debris, meat cooking exhaust, natural gas leakage, and vegetative detritus. Gasoline engine exhaust plus gasoline vapors are the predominant sources of volatile organic gases, while gasoline and diesel engine exhaust plus diesel fuel vapors dominate the

emissions of semi-volatile organic compounds from these sources during the episode studied at all four sites. Fine particle organic compound mass on this occasion was made up of noticeable contributions from both gasoline-powered motor vehicles, diesel engines, meat cooking and paved road dust with smaller but quantifiable contributions from vegetative detritus and tire wear debris. In addition, secondary organic aerosol, which is formed from the low-vapor pressure products of gas-phase organic compound reactions, was found to be a major source of fine particle organic compound mass. The upper limit to the concentrations of secondary organic aerosol calculated both in the present study and in a previous study were shown to correlate fairly well with the concentrations of 1,2-benzenedicarboxylic acid in the atmospheric fine particle mass, indicating that this aromatic acid may be useful in tracing the presence of certain sources of secondary organic aerosol in the atmosphere.

## **12.2 Suggestions for Future Research**

The comprehensive organic compound emissions profiles reported here when used with the newly developed organic chemical tracer-based receptor models demonstrate the power of organic chemical tracer analysis. The further expansion of this work requires efforts in several key areas. First, the sources characterized here are the major emitters in California and in much of the western United States. Although many of the emissions profiles used in the current work are applicable to many other areas of the United States and the

world, additional emissions profiles are needed for those sources which are important in other locations. These sources include coal combustion, as well as residential and commercial fuel oil combustion. Characterization of the gas-phase emissions from residential natural gas combustion also is warranted.

In addition to expanding the emission profile data base, this work cannot be applied to other locations and different types of air pollution episodes without the proper collection of high quality ambient samples. Such samples must be collected according to protocols that prevent organic compound contamination, as used in the work presented here. Samples must be collected on properly prepared substrates with sampling equipment that is completely free of greases, coatings, and rubber parts. Likewise, the sampling equipment must be rigorously cleaned before use as was done in the study reported here.

Development of improved analytical techniques which can be used to quantify the ambient concentrations of highly polar organic compounds and high molecular weight polymeric compounds would allow a much larger fraction of the organic compound emissions to be identified and quantified on a single compound basis. The quantification of these compounds will not only enhance the ability of the receptor models reported here but also will provide valuable additional data that can be used in the future to assist in the evaluation of photochemical airshed models for prediction of the concentrations of organic compounds in the atmosphere.

## Appendix A

### Whole Gasoline Vapor and Gasoline Headspace Vapor Emissions Profiles

A 1995 gasoline sample was assembled as a market share weighted average of the gasoline products of the five largest gasoline retailers in Southern California. The 1995 sample was collected and analyzed to obtain a whole gasoline vapor emissions profile. In order to obtain a 1993 whole gasoline vapor emissions profile, the 1995 gasoline composition data were modified to match conditions during the summer 1993 atmospheric experiments; these changes reflect the reduction in benzene and the increase in MTBE content of gasoline that occurred between the summer of 1993 and the summer of 1995. The whole gasoline vapor profiles are provided in Table A.1.

Gasoline headspace vapor profiles which correspond to the associated whole gasoline emissions profiles were calculated. Conner et al. (1995) have shown that the composition of the headspace vapors above a liquid pool of gasoline can be accurately calculated from the liquid gasoline composition and the Raoult's law coefficients for the individual gasoline components in a gasoline mixture. The gasoline headspace vapor composition for this study was therefore calculated using Raoult's law coefficients from the data collected by Aulich et al. (1994). The gasoline headspace samples are also shown in Table A.1.

Table A.1. Whole Gasoline Vapor and Headspace Gasoline Vapor Emissions Profiles

Compound	1995 Southern California Market-Share Gasoline (Wt %)		1993 Southern California Market-Share Gasoline (Wt %)	
	Whole Gasoline	Headspace Gasoline	Whole Gasoline	Headspace Gasoline
n-Alkanes				
Propane	0.01	0.2	0.01	0.2
n-Butane	0.79	6.2	0.91	6.5
n-Pentane	2.19	4.1	2.46	4.3
n-Hexane	1.41	0.3	1.59	0.3
n-Heptane	1.01	0.3	1.14	0.3
n-Octane	0.46	0.2	0.52	0.2
n-Nonane	0.24	0.1	0.27	0.1
n-Decane	0.12	0.0	0.14	0.0
Branched alkanes				
i-Butane	0.15	1.7	0.17	1.8
2,2-Dimethylpropane	0.01	0.1	0.01	0.1
i-Pentane	6.12	16.9	6.89	17.9
2,2-Dimethylbutane	0.22	0.2	0.25	0.2
2,3-Dimethylbutane	0.98	1.0	1.10	1.1
2-Methylpentane	3.01	1.3	3.39	1.4
3-Methylpentane	1.86	0.7	2.09	0.7
2,4-Dimethylpentane	0.90	0.3	1.01	0.3
2-Methylhexane	1.44	0.5	2.00	0.6
2,3-Dimethylpentane	1.73	0.5	1.95	0.6
3-Methylhexane	1.44	0.4	1.62	0.5
2,2,4-Trimethylpentane	2.55	0.8	2.87	0.9
2,5-Dimethylhexane	0.50	0.2	0.56	0.2
2,4-Dimethylhexane	0.52	0.2	0.59	0.2
2,3,4-Trimethylpentane	1.18	0.4	1.33	0.4
2,3-Dimethylhexane	0.14	0.0	0.16	0.0
2-Methylheptane	0.75	0.2	0.84	0.2
n-Alkenes				
1-Butene	0.02	0.2	0.02	0.2
<i>trans</i> -2-Butene	0.08	0.6	0.09	0.7
<i>cis</i> -2-Butene	0.08	0.5	0.09	0.6
1-Pentene	0.22	0.6	0.25	0.6
<i>trans</i> -2-Pentene	0.51	0.9	0.57	1.0

Table A.1. (continued - page 2)

Compound	1995 Southern California Market-Share Gasoline (Wt %)		1993 Southern California Market-Share Gasoline (Wt %)	
	Whole	Headspace	Whole	Headspace
	Gasoline	Gasoline	Gasoline	Gasoline
n-Alkenes				
<i>cis</i> -2-Pentene	0.27	0.5	0.30	0.5
1-Hexene	0.12	0.1	0.14	0.1
<i>trans</i> -2-Hexene	0.24	0.1	0.27	0.1
<i>cis</i> -2-Hexene	0.16	0.1	0.18	0.1
Branched alkenes				
Isobutene	0.02	0.2	0.02	0.2
3-Methyl-1-butene	0.05	0.2	0.06	0.2
2-Methyl-1-butene	0.25	0.5	0.28	0.6
2-Methyl-2-butene	0.25	0.4	0.28	0.4
4-Methyl-1-pentene	0.15	0.2	0.17	0.2
2-Methyl-1-pentene	0.15	0.1	0.17	0.1
2-Methyl-2-pentene	0.33	0.4	0.37	0.4
Saturated cycloalkanes				
Cyclopentane	0.34	0.3	0.38	0.4
Methylcyclopentane	2.46	0.7	2.77	0.8
Cyclohexane	0.75	0.5	1.99	0.6
Methylcyclohexane	1.14	0.3	1.28	0.4
Unsaturated cycloalkenes				
Cyclopentene	0.13	0.2	0.15	0.2
Aromatic hydrocarbons				
Benzene	0.84	0.7	2.00	1.7
Toluene	6.67	1.9	7.50	2.0
Ethylbenzene	1.46	0.7	1.64	0.7
m & p-Xylene	6.17	2.4	6.94	2.5
o-Xylene	2.29	1.3	2.58	1.4
i-Propylbenzene	0.10	0.1	0.11	0.1
n-Propylbenzene	0.54	0.4	0.61	0.4
p-Ethyltoluene	0.73	0.6	0.82	0.6
m-Ethyltoluene	1.67	1.3	1.88	1.3
1,3,5-Trimethylbenzene	0.84	0.7	0.95	0.7
o-Ethyltoluene	0.58	0.4	0.65	0.4
1,2,4-Trimethylbenzene	2.90	2.7	3.26	2.7
Ethers				
MTBE	10.57	*	1.10	*

Notes: \* Not Calculated

## A1.1 References

Conner, T. A., Lonneman, W. A. and Seila, R. L. (1995) Transportation-related volatile hydrocarbon source profiles measured in Atlanta. *J. Air & Waste Manage. Assoc.* **45**, 383-394.

## Appendix B

### Paved Road Dust Emissions Profiles

Fine particle road dust emissions profiles were generated by separately resuspending a road dust sample and then introducing the road dust/air mixture into the residence time chamber of the dilution source sampler. Samples were drawn through AIHL-design cyclone separators to remove coarse particles larger than 1.8  $\mu\text{m}$  in diameter and were collected on quartz fiber filters and Teflon filters and then analyzed chemically as described for the other sources tested. Gas-phase measurements were not made for the road dust sample as road dust is not thought to be a significant source of gas-phase pollutants. Paved road dust emissions profiles are shown in Table B.1.



Table B.1. Emissions Profiles for Paved Road Dust Fine Particulate Mass

Compound	Fresno*	Bakersfield*	Kern Wildlife Refuge*	Long Beach	Central LA	Rubidoux
	$\mu\text{g g}^{-1}$	$\mu\text{g g}^{-1}$	$\mu\text{g g}^{-1}$	$\mu\text{g g}^{-1}$	$\mu\text{g g}^{-1}$	$\mu\text{g g}^{-1}$
<b>n-Alkanes</b>						
n-Tricosane	18.6	18.6	18.6	5.86	8.81	5.06
n-Tetracosane	18.9	18.9	18.9	4.76	9.53	4.40
n-Pentacosane	22.0	22.0	22.0	14.3	11.1	5.62
n-Hexacosane	23.7	23.7	23.7	8.62	13.9	6.15
n-Heptacosane	28.5	28.5	28.5	35.3	15.2	10.7
n-Octacosane	18.9	18.9	18.9	11.5	14.2	7.16
n-Nonacosane	54.6	54.6	54.6	53.1	13.2	20.4
n-Triacontane	15.4	15.4	15.4	11.4	10.8	6.01
n-Hentriacontane	16.7	16.7	16.7	42.4	11.2	15.7
n-Dotriacontane	6.28	6.28	6.28	9.26	9.00	3.16
n-Tritriacontane	6.03	6.03	6.03	28.0	10.3	5.37
n-Tetatriacontane				6.42		
n-Pentatriacontane				11.9		
<b>Polycyclic aromatic hydrocarbons</b>						
Fluoranthene	3.05	3.05	3.05	0.93	1.79	1.25
Pyrene				0.71	0.94	0.98
Benz[a]anthracene				0.73	0.98	1.41
<b>n-Alkanoic acids</b>						
n-Dodecanoic acid	91.5	91.5	91.5	30.8	66.4	78.2
n-Tridecanoic acid	16.2	16.2	16.2	5.18	6.57	6.44
n-Tetradecanoic acid	236	236	236	58.9	124	82.1
n-Pentadecanoic acid	135	135	135	21.0	61.7	27.5
n-Hexadecanoic acid	1180	1180	1180	351	486	328
n-Heptadecanoic acid	50.1	50.1	50.1	11.8	20.1	12.7
n-Octadecanoic acid	516	516	516	156	173	143
n-Nonadecanoic acid	24.7	24.7	24.7	4.90	5.28	3.42
n-Eicosanoic acid	17.7	17.7	17.7	36.9	10.7	10.4
n-Heneicosanoic acid	6.85	6.85	6.85	6.35	1.69	2.62
n-Docosanoic acid	35.4	35.4	35.4	33.7	7.59	11.9
n-Tricosanoic acid	15.9	15.9	15.9	9.27	3.48	4.54
n-Tetracosanoic acid				53.4	18.2	21.0
n-Pentacosanoic acid				9.63		3.61
n-Hexacosanoic acid				50.9	8.60	18.6
n-Heptacosanoic acid				5.38		6.94
n-Octacosanoic acid				30.0		14.3
n-Triacontanoic acid				21.9		6.56

Notes: \* IMS95 paved road dust samples were composited for organic compound analysis due to limited fine particle mass. Inorganic species were analyzed separately in each IMS95 fine particle sample.

Table B.1. (continued - page 2)

Compound	Fresno*	Bakersfield*	Kern Wildlife Refuge*	Long Beach	Central LA	Rubidoux
	$\mu\text{g g}^{-1}$	$\mu\text{g g}^{-1}$	$\mu\text{g g}^{-1}$	$\mu\text{g g}^{-1}$	$\mu\text{g g}^{-1}$	$\mu\text{g g}^{-1}$
n-Alkenoic acids						
n-9-Hexadecenoic acid	297	297	297	39.1	193.4	55.5
n-9-Octadecenoic acid	450	450	450	178	643	122
n-9,12-Octadecadienoic acid	198	198	198	36.9	70.8	28.2
Resin acids						
Dehydroabietic acid	44.7	44.7	44.7	15.6	14.7	44.7
Other compounds						
Squalene	178	178	178	25.7	303	23.4
Elemental composition						
Aluminum	21100	41700	42900	40100	41200	50200
Silicon	61500	125000	118000	142000	138000	155000
Organic carbon	99000	149000	129000	153000	151000	103000
Elemental Carbon	4000	10000	15000	18000	9000	3700

---

Notes: \* IMS95 paved road dust samples were composited for organic compound analysis due to limited fine particle mass. Inorganic species were analyzed separately in each IMS95 fine particle sample.